frontiers | Research Topics

Use of computerized gait analysis in neurological pathologies

Edited by
Simone Carozzo, Carmelo Chisari and Marco Iosa

Published in
Frontiers in Human Neuroscience

ISSN 1664-8714
ISBN 978-2-83251-110-7
DOI 10.3389/978-2-83251-110-7

About Frontiers

Frontiers is more than just an open access publisher of scholarly articles: it is a pioneering approach to the world of academia, radically improving the way scholarly research is managed. The grand vision of Frontiers is a world where all people have an equal opportunity to seek, share and generate knowledge. Frontiers provides immediate and permanent online open access to all its publications, but this alone is not enough to realize our grand goals.

Frontiers journal series

The Frontiers journal series is a multi-tier and interdisciplinary set of open-access, online journals, promising a paradigm shift from the current review, selection and dissemination processes in academic publishing. All Frontiers journals are driven by researchers for researchers; therefore, they constitute a service to the scholarly community. At the same time, the *Frontiers journal series* operates on a revolutionary invention, the tiered publishing system, initially addressing specific communities of scholars, and gradually climbing up to broader public understanding, thus serving the interests of the lay society, too.

Dedication to quality

Each Frontiers article is a landmark of the highest quality, thanks to genuinely collaborative interactions between authors and review editors, who include some of the world's best academicians. Research must be certified by peers before entering a stream of knowledge that may eventually reach the public - and shape society; therefore, Frontiers only applies the most rigorous and unbiased reviews. Frontiers revolutionizes research publishing by freely delivering the most outstanding research, evaluated with no bias from both the academic and social point of view. By applying the most advanced information technologies, Frontiers is catapulting scholarly publishing into a new generation.

What are Frontiers Research Topics?

Frontiers Research Topics are very popular trademarks of the *Frontiers journals series*: they are collections of at least ten articles, all centered on a particular subject. With their unique mix of varied contributions from Original Research to Review Articles, Frontiers Research Topics unify the most influential researchers, the latest key findings and historical advances in a hot research area.

Find out more on how to host your own Frontiers Research Topic or contribute to one as an author by contacting the Frontiers editorial office: frontiersin.org/about/contact

Use of computerized gait analysis in neurological pathologies

Topic editors

Simone Carozzo — Sant'Anna Crotone Institute, Italy
Carmelo Chisari — Pisana University Hospital, Italy
Marco Iosa — Sapienza University of Rome, Italy

Citation

Carozzo, S., Chisari, C., Iosa, M., eds. (2023). *Use of Computerized Gait Analysis in Neurological Pathologies*. Lausanne: Frontiers Media SA.
doi: 10.3389/978-2-83251-110-7

Table of contents

frontiers | Frontiers in Human Neuroscience

TYPE Editorial
PUBLISHED 07 December 2022
DOI 10.3389/fnhum.2022.1078539

OPEN ACCESS

EDITED AND REVIEWED BY
Julie Duque,
Université Catholique de Louvain, Belgium

*CORRESPONDENCE
Simone Carozzo
simone.carozzo@gmail.com

SPECIALTY SECTION
This article was submitted to Motor Neuroscience, a section of the journal Frontiers in Human Neuroscience

RECEIVED 24 October 2022
ACCEPTED 16 November 2022
PUBLISHED 07 December 2022

CITATION
Carozzo S, Chisari C and Iosa M (2022) Editorial: Use of computerized gait analysis in neurological pathologies. *Front. Hum. Neurosci.* 16:1078539. doi: 10.3389/fnhum.2022.1078539

Editorial: Use of computerized gait analysis in neurological pathologies

Simone Carozzo[1]*, Carmelo Chisari[2] and Marco Iosa[3,4]

[1]Research in Advanced Neurorehabilitation (RAN), Sant'Anna Crotone Institute, Crotone, Italy, [2]Department of Translational Research and New Technology in Medicine and Surgery, University of Pisa, Pisa, Italy, [3]Department of Psychology, Faculty of Medicine and Psychology, Sapienza University of Rome, Rome, Italy, [4]IRCCS Santa Lucia Foundation, Rome, Italy

KEYWORDS

gait analysis, neurological pathologies, computerized gait analysis, machine learning, rehab

Editorial on the Research Topic
Use of computerized gait analysis in neurological pathologies

The interest in computer-assisted quantitative gait evaluation sharply increased sharply in recent years (Figure 1). Its widespread use provides evidence of applicability to obtain objective and comparable measures supplementing clinical scales and subjective judgments.

The aim of this Research Topic was to collect papers exploring the utility of computerized gait analysis for exploring the impact of neurological diseases on gait functions. We have selected 13 articles that have been found to be of high quality for publication in this Research Topic. These papers covered different aspects related to protocols and technologies, and many different pathologies (stroke, cerebral palsy, Parkinson's disease, multiple sclerosis, spinal cord injury, Charcot Marie Tooth disease, Duchenne muscular dystrophy).

Systematic research has implemented procedures and paradigms generating a large number of potential variables for kinematic analysis; some debate on their relevance and proper selection is going on; several algorithms and equipment configurations to automatically identify the timing of gait events are being tested to comply with the clinician's needs. Whether individual markers of combinations of markers and their position on different body districts can influence the accuracy of the algorithms and therefore, the clinical and scientific findings remain unclear (Visscher et al.).

Usual gait analysis often reports the kinematics of hip, knee and ankle, but the influence of the pelvis as a biomechanical constraint during gait also needs to be deeply investigated (Favetta et al.).

Multiple Sclerosis has been systematically studied by means of kinematic analysis, partly due to its being characterized by the fatigue progressing with the disease worsening. This fatigue in walking can be studied through an antiphase pattern of limbs coordination while seated when movements of lower are performed leg as quickly as possible (Goetschalckx et al.). Over the years, thanks to the increasing collaboration between clinicians and complex systems analysts, individual "indices' have

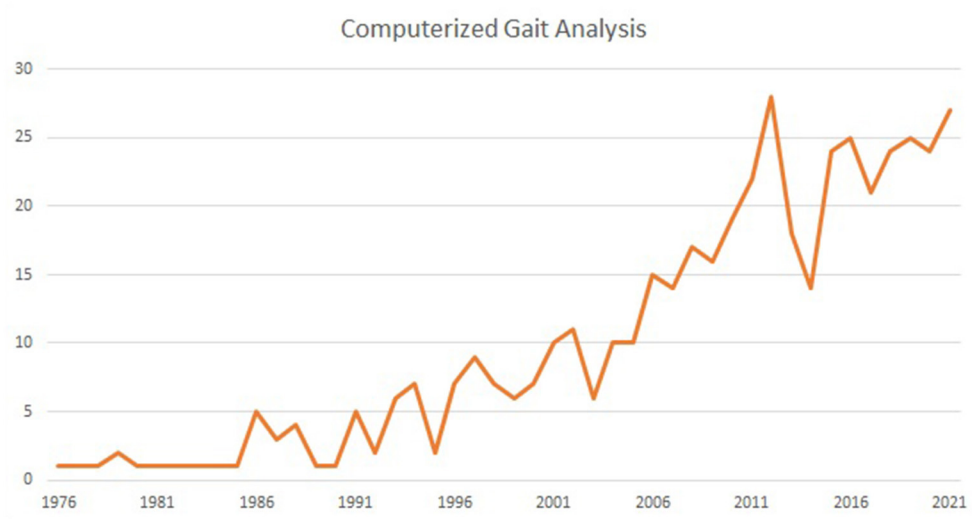

FIGURE 1
The increment of publications related to "computerized gait analysis" as reported on Pubmed at November 2022.

been identified to characterize the evolution of various diseases and to quantify and monitor the patients; motor recovery, in order to verify the effectiveness of medical and physiotherapic treatments.

In the study of chronic post-stroke hemiparetic patients, for instance, the range of motion of the ankle, spasticity of the triceps sural, walking speed, the scales related to assistance and the limitation in the subjects; social participation have been taken in to consideration (Mazzoli et al.). Or again for post-stroke subjects a set of kinematic variables that are sufficient to evaluate gait, thus being able to substantially facilitate future diagnosis and monitoring of rehabilitation progress (Nedergård et al.).

One of the main developers and computerized systems analysts; challenge in the analysis of gait kinematics is to create indicators as reliable as the clinical scales in use. The main options are basically two:

1- to create analysis procedures and verify their compatibility with existing scales; or 2- to identify indicators able to replace the same scales with comparable or better reliability. An example in this regard is the attempt to provide objective interpretations of the observational gait assessment based on the Wisconsin Gait Scale (WGS) used to assess walking quality in post-stroke hemiplegic subjects. Computer-assisted investigations proved able to provide useful, low-cost and timely feedback to monitor treatments and the evolution of the disease (Guzik et al.).

For a long time, especially in Europe, the gait of subjects with infantile cerebral palsy have been examined by assessing the clinical relevance of fluctuations in the regularity of gait patterns between repetitive cycles. The approach is congruent with sensorimotor system organization, with gait fluctuation and regularity influenced by factors such as age and pathology, and supports the interpretation of clinical gait analysis and therapeutic decision making (Tabard-Fougère et al.).

3D gait analysis allows compare systematically and without human error the gait patterns of different neuromotor conditions: normal gait, cerebral palsy (CP), Charcot Marie's tooth (CMT) and Duchenne muscular dystrophy (DMD). These comparisons can be of use in the correct interpretation of gait clinical pattern (Minosse et al.).

The Gait Deviation Index (GDI), a multivariate measure of the overall gait pathology based on 15 gait characteristics derived from three-dimensional kinematic data, proved an indicator most suitable of application with good efficacy in the evaluation of cerebral (CP), post-stroke hemiparetic gait, Duchenne muscular dystrophy and Parkinson's disease, and its clinical significance also in other pathologies such as spinal cord injury (SCI) is being tested (Sinovas-Alonso et al.). But also, an identification of a core set of gait features could be helpful for clinicians to support treatment decision-making processes related to children with CP (van der Krogt et al.).

The use of machine learning algorithms is increasingly frequent in instrumental diagnostics and evaluation, even in the field of computerized motion analysis. Its purpose is to treat variables and indices extrapolated from the various tools; it allows to classify and evaluate patients in remote and help doctors in making decisions and monitor treatment and follow-up, without depending on the administration of scales or on personal clinical experience. For example, to classify patients with Parkinson's disease in a useful and accurate way, they use low-cost portable devices (Muñoz-Ospina et al.). Also,

children with cerebral palsy could benefit from a machine learning approach for identifying the intertwine between motor control and gait kinematics after orthopedic surgery (Steele and Schwartz).

Three-dimensional gait analysis can provide parameters to study the effectiveness of clinical trials aimed at preserving walking, as data can be recorded covering the entire walking period, by performing a so-called mixed cross-sectional longitudinal study, without possible variations in evaluations due to the change of the test administrator or clinical evaluator. As in treatment in children with Duchenne muscular dystrophy (DMD) (Vandekerckhove et al.).

Author contributions

SC chose the other two guest editors and the specialists to send the proposal to participate in the Research Topic, carried out the task of accepting some works after the reviews of the reviewers, and wrote editorial. CC and MI accepted some jobs after the reviews and editorial revisions. All authors contributed to the article and approved the submitted version.

Acknowledgments

As editor of this Research Topic, and authors of this editorial, we would like to thank all the reviewers who spent their time evaluating and improving the submitted manuscripts. We would also like to thank the authors of these manuscripts for having contributed to the success of this Research Topic.

Conflict of interest

The authors declare that the research was conducted in the absence of any commercial or financial relationships that could be construed as a potential conflict of interest.

Publisher's note

frontiers in Human Neuroscience

BRIEF RESEARCH REPORT
published: 13 September 2021
doi: 10.3389/fnhum.2021.720699

Impact of the Marker Set Configuration on the Accuracy of Gait Event Detection in Healthy and Pathological Subjects

Rosa M. S. Visscher[1,2], Marie Freslier[3], Florent Moissenet[4], Sailee Sansgiri[5], Navrag B. Singh[1], Elke Viehweger[2,3], William R. Taylor[1] and Reinald Brunner[2,3]*

[1] Laboratory for Movement Biomechanics, Department of Health Science and Technology, Institute for Biomechanics, ETH Zürich, Zurich, Switzerland, [2] Biomechanics of Movement Group, Department of Biomedical Engineering, University of Basel, Basel, Switzerland, [3] Laboratory for Movement Analysis, Department of Orthopedics, University Children's Hospital Basel, Basel, Switzerland, [4] Laboratory for Kinesiology, University of Geneva and Geneva University Hospitals, Geneva, Switzerland, [5] Department of Biomedical Engineering, Faculty of Mechanical, Maritime, and Materials Engineering, Delft University of Technology, Delft, Netherlands

OPEN ACCESS

Edited by:
Marco Iosa, Sapienza University of Rome, Italy

Reviewed by:
Leonardo Gizzi, University of Stuttgart, Germany
Yushin Kim, National Institutes of Health (NIH), United States

***Correspondence:**
Rosa M. S. Visscher
rosa.visscher@hest.ethz.ch

Specialty section:
This article was submitted to Motor Neuroscience, a section of the journal Frontiers in Human Neuroscience

Received: *04 June 2021*
Accepted: *24 August 2021*
Published: *13 September 2021*

Citation:
Visscher RMS, Freslier M, Moissenet F, Sansgiri S, Singh NB, Viehweger E, Taylor WR and Brunner R (2021) Impact of the Marker Set Configuration on the Accuracy of Gait Event Detection in Healthy and Pathological Subjects. Front. Hum. Neurosci. 15:720699. doi: 10.3389/fnhum.2021.720699

For interpreting outcomes of clinical gait analysis, an accurate estimation of gait events, such as initial contact (IC) and toe-off (TO), is essential. Numerous algorithms to automatically identify timing of gait events have been developed based on various marker set configurations as input. However, a systematic overview of the effect of the marker selection on the accuracy of estimating gait event timing is lacking. Therefore, we aim to evaluate (1) if the marker selection influences the accuracy of kinematic algorithms for estimating gait event timings and (2) what the best marker location is to ensure the highest event timing accuracy across various gait patterns. 104 individuals with cerebral palsy (16.0 ± 8.6 years) and 31 typically developing controls (age 20.6 ± 7.8) performed clinical gait analysis, and were divided into two out of eight groups based on the orientation of their foot, in sagittal and frontal plane at mid-stance. 3D marker trajectories of 11 foot/ankle markers were used to estimate the gait event timings (IC, TO) using five commonly used kinematic algorithms. Heatmaps, for IC and TO timing per group were created showing the median detection error, compared to detection using vertical ground reaction forces, for each marker. Our findings indicate that median detection errors can be kept within 7 ms for IC and 13 ms for TO when optimizing the choice of marker and detection algorithm toward foot orientation in midstance. Our results highlight that the use of markers located on the midfoot is robust for detecting gait events across different gait patterns.

Keywords: gait analysis, pathological gait, cerebral palsy, gait event detection, motion capture

INTRODUCTION

3D Clinical Gait Analysis (CGA) is increasingly used for quantifying gait deviations, informing clinical decision making, and monitoring the effectiveness of therapy in movement disorders (Cimolin and Galli, 2014; Armand et al., 2016). Accurate estimation of gait events, such as initial contact (IC) and toe-off (TO), is essential for interpreting CGA outcomes, as incorrect identification

of gait events could lead to errors in normalization of kinematic and kinetic data and its ensemble-averaging, as well as to inaccurate spatio-temporal parameters. The gold standard for estimating gait event timing is the use of vertical ground reaction forces (vGRFs), during which a threshold is set, when the vGRF crossed the force threshold a gait event is detected (Bruening and Ridge, 2014). However, for this method to work in an automatic manner, clean force plate hits (during which only one foot contacts a force plate) are necessary. These clean hits are often limited due to use of assistive devices, short step lengths or partial contact with the plate, which limits the number of strides that can be used for analysis. As an alternative to vGRFs, kinematics-based algorithms have been introduced. These algorithms use the position, velocity, or acceleration of IMU sensor(s) (placed on the hip, shank, or feet) or a set of reflective cutaneous markers (placed on bone-landmarks of the foot/ankle) to estimate gait event timing. Over the years, numerous algorithms have been developed, based on various marker sets as input (Stanhope et al., 1990; Bruening and Ridge, 2014). Here, previous work has shown that adaptation of the markers' locations could improve the estimation of gait event timing, especially in pathological populations such as children with cerebral palsy (CP) (Visscher et al., 2021). Within the CP population, multiple types of pathological gait patterns are present such as True equinus, Jump knee, Apparent equinus, and Crouch gait (Rodda and Graham, 2001). Per gait pattern, the part of the foot used for IC and TO can differ. It might therefore be of interest to evaluate how different marker locations perform when different parts of the foot are initially contacting or leaving the ground. However, a systematic overview of the effect of the markers' locations on the accuracy of estimating gait event timing is lacking.

With the aim to guide the choice of markers for optimal estimation of gait event timing, the goal of this study was to present a detection error map (with vGRFs as the reference), examining the effect of the markers' locations on estimation of gait event timing, based on a set of commonly used kinematics-based algorithms.

METHODS

Participants

104 individuals with CP and 31 typically developing (TD) controls were retrospectively included in this study (**Table 1**). All participants underwent CGA in a local hospital between August 2016 and May 2019. Each subject was categorized into 1 of 4 groups for IC estimations depending on the orientation of their foot in the sagittal plane (ankle dorsiflexion/plantarflexion) at midstance (Criteria were set based on the mean values of the TD group with thresholds chosen to allow for homogeneous distribution of patients between groups, Group IC1: >mean + 2SD n_{TD} = 62 median dosiflexion angle = 17.8° n_{CP} = 51, 9.8°; Group IC2: mean-2SD ≤ mean + 2SD n_{TD} = 0, n_{CP} = 25, -0.2°; Group IC3: mean-10SD ≤ mean-2SD n_{TD} = 0, n_{CP} = 42, -5.6°; Group IC4: <mean-10SD n_{TD} = 0, n_{CP} = 39, -15.5°; **Supplementary Table 1**), and into 1 of 4 groups for TO estimations depending on the orientation of their foot in the frontal plane (ankle eversion/inversion) at midstance (criteria were set based on the mean values of the TD group with thresholds chosen to allow for homogeneous distribution of participants between groups, Group TO1: >mean + 2SD n_{TD} = 0, n_{CP} = 15, 17.0°; Group TO2: mean-2SD ≤ mean + 2SD n_{TD} = 11, 4.3°, n_{CP} = 55, 5.6°; Group TO3: mean-4SD ≤ mean-2SD n_{TD} = 30, -2.4°, n_{CP} = 36, -1.8°; Group TO4: <mean-4SD n_{TD} = 21, -9.7°, n_{CP} = 50, -12.5°; **Supplementary Table 1**). Further information on grouping and calculation of the foot orientation can be found in **Supplementary Table 1** and on our GitLab page.[1] All participants or their guardians, gave their written informed consent prior to inclusion in the study, which as approved by the local ethical committee (2018-01449). All measurements were conducted according to the Declaration of Helsinki.

TABLE 1 | Descriptive statistics of the participants (independent samples *T*-test, chi-square test for gender).

	TD (*n* = 31)	CP (*n* = 104)	*p*-value
Age (years)	20.6 (7.8)	16.0 (8.6)	**0.008**
Gender	15 males 16 females	66 males 38 females	0.133
Height (m)	1.64 (0.17)	1.52 (0.20)	**0.002**
Weight (kg)	55.0 (15.6)	45.9 (18.1)	0.012
BMI (kg/m^2)	20.0 (2.80)	19.0 (4.0)	0.232
Legs evaluated (*n*)	62	156	NA
Types of CP	NA	52 Hemiplegic 52 Diplegic	NA
GMFCS	NA	I: 73 II: 31	NA

All parameters reported as mean (SD). TD, typically developing controls; CP, cerebral palsy; SD, standard deviation; BMI, body mass index; NA, not applicable. Bold values indicate significant difference between TD and CP groups.

Measurement Procedure

All participants walked barefoot on an instrumented walkway at their self-selected walking speed for six trials, one trial per participant was selected for analysis. Out of a total of 64 markers (9.5 mm diameter), which were attached to the participants according to the modified Conventional Gait Model (CGM1.0) model (Kadaba et al., 1990) (**Supplementary Presentation 1**), 11 markers located on the foot/ankle were selected for analysis (hallux, HLX; distal metatarsal I, DMT1; distal metatarsal II, DMT2; distal metatarsal V, DMT5; proximal metatarsal I, PMT1; cuneiform, CUN; proximal metatarsal V, PMT5; sinus tarsi, SITA; lateral malleolus, ANK; below ANK on calcaneus, TPR; calcaneus, HEE; **Figures 1**, **2**). Marker trajectories were collected at a sampling frequency of 150 Hz using a 12-camera optoelectronic motion capture system (MTX20, VICON, Oxford, United Kingdom).

Data Processing

Data pre-processing was performed within the VICON-NEXUS software (v1.8.5), filtering was done using the built-in Woltring

[1]https://github.com/Roosje95/HEAT_gait-event-detection

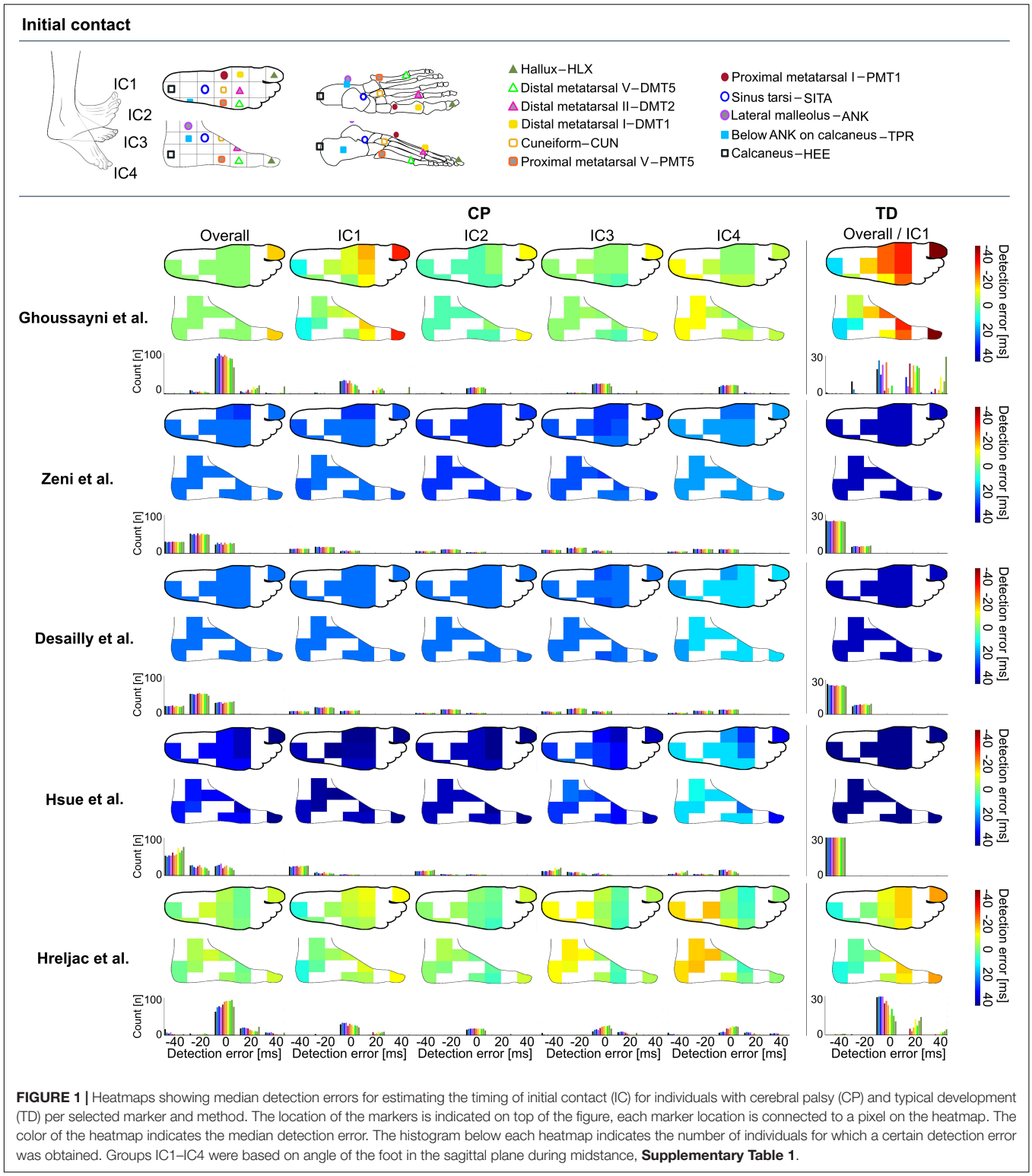

FIGURE 1 | Heatmaps showing median detection errors for estimating the timing of initial contact (IC) for individuals with cerebral palsy (CP) and typical development (TD) per selected marker and method. The location of the markers is indicated on top of the figure, each marker location is connected to a pixel on the heatmap. The color of the heatmap indicates the median detection error. The histogram below each heatmap indicates the number of individuals for which a certain detection error was obtained. Groups IC1–IC4 were based on angle of the foot in the sagittal plane during midstance, **Supplementary Table 1**.

filter (mean squared error set to 10 mm^2), marker gaps smaller than five frames were filled using the built-in gap filling functions. To extract gait events (IC, TO) using vGRFs, a force threshold of 20 N was applied to the vertical component of the ground reaction force signal collected through the force plates (Kistler, Switzerland, sampling frequency 1,500 Hz) embedded in the walkway (Visscher et al., 2021). Post-processing analyses were performed in MATLAB (R2019a, The Mathworks, Natick, United States) using the open-source Biomechanical ToolKit package (BTK) (Barre and Armand, 2014). Trials with excessive

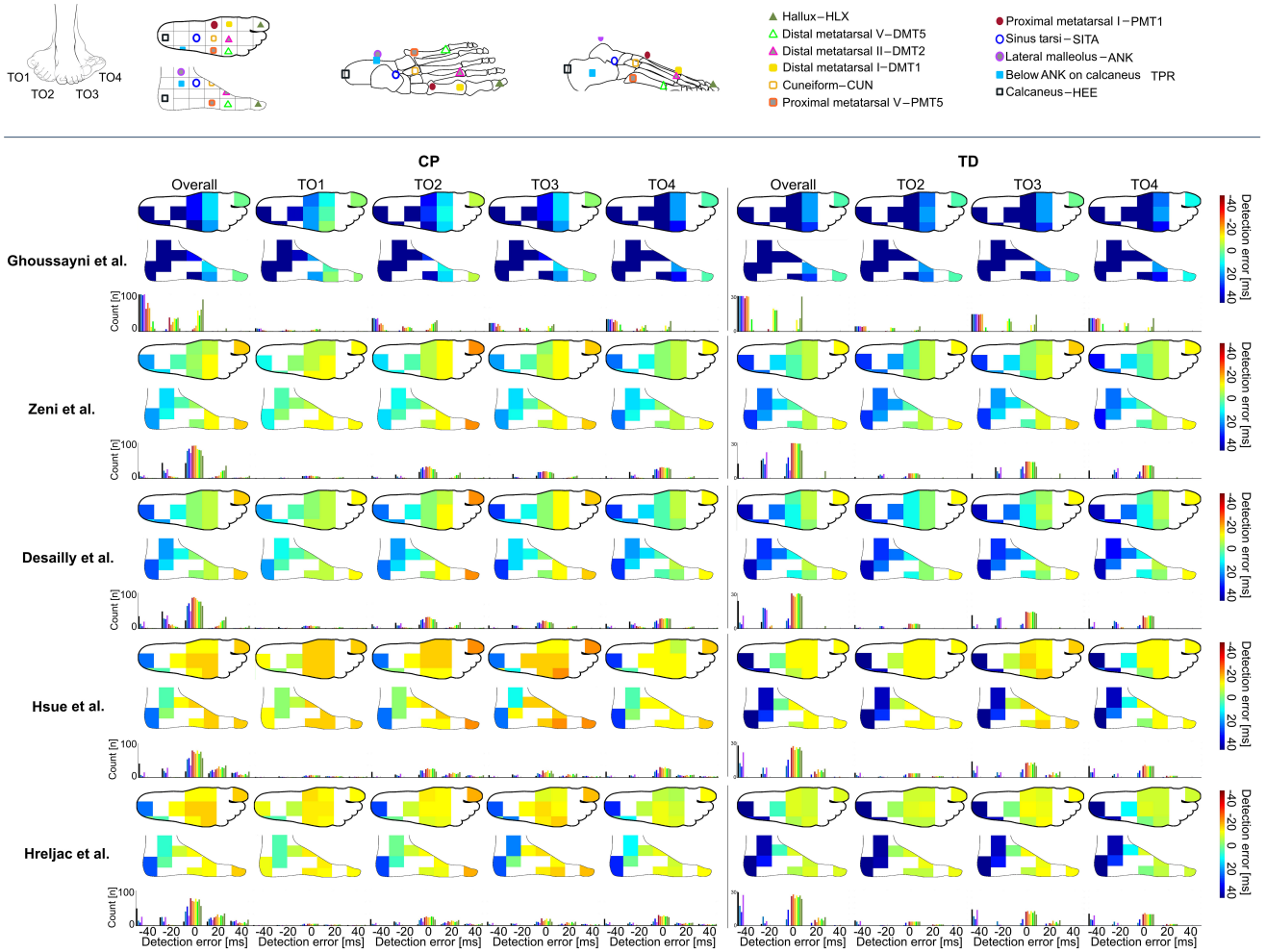

FIGURE 2 | Heatmaps showing median detection errors for estimating the timing of toe-off (TO) for individuals with CP and TD. The location of the markers is indicated on top of the figure, each marker location is connected to a pixel on the heatmap. The color of the heatmap indicates the median detection error. The histogram below each heatmap indicates the number of individuals for which a certain detection error was obtained. Groups TO1–TO4 were based on angle of the foot in the sagittal plane during midstance, **Supplementary Table 1**.

soft tissue artifacts, poor consistency, or signs of inaccurate marker placement were excluded after visual inspection. One valid gait cycle (GC) of each limb per participant was used in further analyses. Only the paretic side was included for hemiplegic patients.

The 3D marker trajectories of 1 of the following 11 foot/ankle markers (HLX, DMT1, DMT2, DMT5, PMT1, CUN, PMT5, SITA, ANK, TPR, and HEE, **Figures 1**, **2**) were used to calculate the gait event timings (IC, TO) according to five previously published kinematics-based algorithms: Zeni et al. (2008), Desailly et al. (2009), Ghoussayni et al. (2004), Hsue et al. (2007), and Hreljac and Marshall (2000), **Table 2** and all available on a published repository (see text footnote 1). The choice of these algorithms was guided by a previous review article that evaluated automated event detection algorithms in pathological gait (Bruening and Ridge, 2014). To reduce the chance of false positives, a time window of ±30 frames (0.2 s, as we measured at 150 Hz) around the estimated event timing by Zeni et al. (2008) was used for applying the other algorithms. The differences (in ms) in gait event timings obtained using vGRFs vs kinematics-based algorithms were defined as the detection error.

Statistical Analysis

As errors were not normally distributed, the median detection error and the 95 percentile confidence interval lower and upper boundaries (95%CI) were calculated for each event (IC and TO), method (Ghoussayni et al., 2004; Zeni et al., 2008; Desailly et al., 2009; Hsue et al., 2007; Hreljac and Marshall, 2000), group (IC1–IC4 and TO1–TO4), and marker (HLX, TOE/DMT1, DMT5, PMT1, CUN, PMT5, SITA, ANK, TPR, and HEE). Median detection errors were used to create a heatmap of the top and side views of the foot for each event, method, and group. In

TABLE 2 | Definition of gait events (IC, TO) according to included algorithms.

Authors	Description of IC	Description of TO	Markers used for IC and TO determination
Zeni et al., 2008	Maximum horizontal marker position relative to sacrum	Minimum horizontal marker position relative to sacrum	HLX, DMT5, DMT2, DMT1, CUN, PMT5, PMT1, SITA, ANK, TPR, and HEE
Desailly et al., 2009	High pass filtered maximum horizontal marker position (Cut-off frequency set at 0.5* cadence)	High pass filtered minimum horizontal marker position (Cut-off frequency set at 0.5* cadence)	HLX, DMT5, DMT2, DMT1, CUN, PMT5, PMT1, SITA, ANK, TPR, and HEE
Ghoussayni et al., 2004	IC occurs when the sagittal velocity of the marker falls below a threshold of 500 m/s	TO occurs when the sagittal velocity of the marker crosses a threshold of 500 m/s	HLX, DMT5, DMT2, DMT1, CUN, PMT5, PMT1, SITA, ANK, TPR, and HEE
Hsue et al., 2007	Minimum of the horizontal acceleration of the marker	Maximum of the horizontal acceleration of the marker	HLX, DMT5, DMT2, DMT1, CUN, PMT5, PMT1, SITA, ANK, TPR, and HEE
Hrejac et al., 2000	IC occurs at the local maxima in the vertical acceleration of the marker and the point of zero-crossing of the jerk (as it decreases)	TO occurs at the local maxima in the horizontal acceleration of the marker and the point of zero-crossing of the jerk (as it increases)	HLX, DMT5, DMT2, DMT1, CUN, PMT5, PMT1, SITA, ANK, TPR, and HEE

For convenience, the algorithms have been listed according to the primary author's last names.
HLX, hallux marker; DMT5, distal metatarsal V; DMT2, distal metatarsal II; DMT1, distal metatarsal I; CUN, cuneiform; PMT5, proximal metatarsal V; PMT1, proximal metatarsal I; SITA, Sinus tarsi; ANK, lateral malleolus; TPR, below ANK on calcaneus; HEE, Calcaneus.

addition, histograms were generated to indicate the number of individuals for which a certain detection error was obtained.

RESULTS

Initial Contact

Depending on the choice of algorithm and marker, differences for detecting IC timings were up to 147 ms in TD and 80 ms in CP (**Supplementary Data Sheet 1**). For estimating the timing of IC across groups, the best estimations were obtained when using the algorithm proposed by Hreljac et al. with SITA marker for TD (median detection error: -1 ms, 95%CI: -12 to 16 ms, ±3 frames, **Figure 1**), and the algorithm proposed by Ghoussayni et al. with SITA or PMT5 marker for CP (median detection error: 0 ms, 95%CI: -27 to 31 ms, ± 5 frames, **Figure 1**). Outcomes for IC1 were most sensitive toward the marker selected for analyses when the Ghoussayni et al. approach was used, yielding differences of up to Δ80 ms in TD and Δ20 ms in CP (**Figure 1**, **Supplementary Data Sheet 1**). While in IC1 best results were achieved with rare- or mid-foot markers (HEE/TPR/ANK/SITA/PMT5), in IC4 best results were achieved with fore-foot markers (PMT1/CUN/DMT1/DMT2/DMT5/HLX). As indicated by the green pixels in **Figure 1**, median detection errors could be kept below 7 ms for IC for all groups when using the approaches from Ghoussayni et al. or Hreljac et al. with PMT1, CUN, or PMT5 marker (**Supplementary Data Sheet 1**).

Toe-Off

Similar to the detection of IC timings, differences for detecting TO timings were up to 153 ms in TD and 143 ms in CP (**Supplementary Data Sheet 1**), depending on the algorithm and marker selected for analysis. For estimating the timing of TO across groups, best estimations were obtained when using the algorithm proposed by Desailly et al. with DMT5 marker in TD (median detection error: 0 ms, 95%CI: -13 to 13 ms, ±2 frames, **Figure 2**) and with CUN marker in CP (median detection error: 0 ms, 95%CI: -33 to 27 ms, ±6 frames, **Figure 2**). As indicated by the dark blue to orange heatmap pixels in **Figure 2**, outcomes for all groups and methods showed to be sensitive toward marker selection (**Supplementary Data Sheet 1**) (Δ 37–133 ms in TD, Δ 10–120 ms in CP). For TO estimation, the green pixels in **Figure 2** indicate median detection errors could be kept below 13 ms for all groups when using the approaches from Zeni et al. or Desailly et al. with PMT1, CUN, or PMT5 marker (**Supplementary Data Sheet 1**).

DISCUSSION

The aim of this manuscript was to provide a systematic overview of the effects that marker selection has on the accuracy of gait event timing estimation. Our results present a median detection error map (with vGRFs as reference) according to the markers used as inputs for a set of common kinematics-based algorithms for gait event timing estimation. This map allows for ease in visualization and can be used by researchers and clinicians to optimize their choice for algorithm and marker selection depending on their participant's gait patterns.

To our knowledge, this is the first study that has evaluated the impact of marker location on the accuracy of gait event timing estimation. Our results support the hypothesis in Visscher et al. (2021) that event detection in pathologies could be improved through optimal selection of the marker set according to the study cohort pathology. For example, generally the HEE-marker with Hreljac approach is used for estimating IC. In a TD child who presents a clear heel strike this leads to a small under estimation with a median detection error of -12 ms compared to force plate detection, however, in a spastic CP patient who presents equinus gait and uses the fore-foot for IC this could lead to an over estimation with a median detection error of +18 ms. When for both subjects the ideal method and marker is used according to the provided heatmaps and the position of their foot during midstance, the detection error can stay below 7 ms in both cases. The results of our study show that the use of markers on the midfoot (PMT1, PMT5, and CUN) is generally robust for detecting gait events across different gait patterns when

using the Hreljac approach as errors for all groups stayed below 20 ms. Indicating, that clinical gait laboratories that measure a lot of different types of gait patterns and want to keep the amount of adaptations needed per case to a minimum, might benefit from including mid-foot markers to their marker model for estimating IC and TO. However, many of the frequently used marker sets in clinical practice do not include markers on the midfoot (Deschamps et al., 2011).

We acknowledge our study had some limitations. First, as the study is conducted retrospectively it has an inferior level of evidence compared to a prospective study design. Second, significant differences were observed between TD and CP cohorts for age and height, these differences might have interfered with the results. However, as the results for subgroups in TD (IC1, TO2, TO3, and TO4) are very similar to the results from the subgroups with CP, we expect the interference to be minimal. In addition, the generalizability of the study is limited as only individuals with one specific pathology (spastic cerebral palsy), walking barefoot, were included, while severely affected individuals were excluded. Further investigations should certainly expand this analysis to different pathologies and severities in order to present more global recommendations on marker selection. To support others to apply our method to their datasets, we have shared all our analysis codes and metadata on a published repository (see text footnote 1).

Overall, our study showed that gait event timing estimation can be improved by optimizing the marker set and the detection algorithm toward specific gait patterns. Our heatmaps presented in this work can be used to guide researchers and clinicians toward which marker set would be most beneficial for their intended use. Further research can expand the current approach toward other gait patterns and walking conditions.

DATA AVAILABILITY STATEMENT

The datasets presented in this study can be found in online repositories. The names of the repository/repositories can be found in the article/**Supplementary Material**.

ETHICS STATEMENT

The studies involving human participants were reviewed and approved by KEK - Local ethical committee canton Zurich, Zurich, Switzerland. Written informed consent to participate in this study was provided by the participants' legal guardian/next of kin.

AUTHOR CONTRIBUTIONS

RV, MF, FM, and RB contributed the conception and design of the study. RV, MF, FM, and SS developed the codes for data analysis. MF and SS processed and organized the data. RV and MF performed the statistical analysis. RV wrote the first draft of the manuscript. MF wrote sections of the manuscript. All authors contributed to manuscript revision, read, and approved the submitted version.

FUNDING

This work was financially supported by the Ralf-Loddenkemper Foundation.

ACKNOWLEDGMENTS

We would like to thank the gait lab staff from the Movement Analysis Laboratory of the University Children's Hospital Basel for their continuous support throughout the project.

SUPPLEMENTARY MATERIAL

The Supplementary Material for this article can be found online at: https://www.frontiersin.org/articles/10.3389/fnhum.2021.720699/full#supplementary-material

REFERENCES

Armand, S., Decoulon, G., and Bonnefoy-Mazure, A. (2016). Gait analysis in children with cerebral palsy. *EFORT Open Rev.* 1, 448–460.

Barre, A., and Armand, S. (2014). Biomechanical ToolKit: open-source framework to visualize and process biomechanical data. *Comput. Methods Programs Biomed.* 114, 80–87. doi: 10.1016/j.cmpb.2014.01.012

Bruening, D. A., and Ridge, S. T. (2014). Automated event detection algorithms in pathological gait. *Gait Posture* 39, 472–477. doi: 10.1016/j.gaitpost.2013.08.023

Cimolin, V., and Galli, M. (2014). Summary measures for clinical gait analysis: a literature review. *Gait Posture* 39, 1005–1010. doi: 10.1016/j.gaitpost.2014.02.001

Desailly, E., Daniel, Y., Sardain, P., and Lacouture, P. (2009). Foot contact event detection using kinematic data in cerebral palsy children and normal adults gait. *Gait Posture* 29, 76–80. doi: 10.1016/j.gaitpost.2008.06.009

Deschamps, K., Staes, F., Roosen, P., Nobels, F., Desloovere, K., Bruyninckx, H., et al. (2011). Body of evidence supporting the clinical use of 3D multisegment foot models: a systematic review. *Gait Posture* 33, 338–349. doi: 10.1016/j.gaitpost.2010.12.018

Ghoussayni, S., Stevens, C., Durham, S., and Ewins, D. (2004). Assessment and validation of a simple automated method for the detection of gait events and intervals. *Gait Posture* 20, 266–272. doi: 10.1016/j.gaitpost.2003.10.001

Hreljac, A., and Marshall, R. N. (2000). Algorithms to determine event timing during normal walking using kinematic data. *J. Biomech.* 33, 783–786. doi: 10.1016/s0021-9290(00)00014-2

Hsue, B., Miller, F., Su, F., Henley, J., and Church, C. (2007). Gait timing event determination using kinematic data for the toe walking children with cerebreal palsy. *J. Biomech.* 40:S529.

Kadaba, M. P., Ramakrishnan, H. K., and Wootten, M. E. (1990). Measurement of lower extremity kinematics during level walking. *J. Orthop. Res.* 8, 383–392. doi: 10.1002/jor.1100080310

Rodda, J., and Graham, H. K. (2001). Classification of gait patterns in spastic hemiplegia and spastic diplegia: a basis for a management algorithm. *Eur. J. Neurol.* 8(Suppl. 5), 98–108. doi: 10.1046/j.1468-1331.2001.00042.x

Stanhope, S. J., Kepple, T. M., McGuire, D. A., and Roman, N. L. (1990). Kinematic-based technique for event time determination during gait. *Med. Biol. Eng. Comput.* 28, 355–360. doi: 10.1007/bf02446154

Visscher, R. M. S., Sansgiri, S., Freslier, M., Harlaar, J., Brunner, R., Taylor, W. R., et al. (2021). Towards validation and standardization of automatic gait event identification algorithms for use in paediatric pathological populations. *Gait Posture* 86, 64–69. doi: 10.1016/j.gaitpost.2021.02.031

Zeni, J. Jr., Richards, J., and Higginson, J. (2008). Two simple methods for determining gait events during treadmill and overground walking using kinematic data. *Gait Posture* 27, 710–714. doi: 10.1016/j.gaitpost.2007.07.007

Conflict of Interest: The authors declare that the research was conducted in the absence of any commercial or financial relationships that could be construed as a potential conflict of interest.

frontiers in Human Neuroscience

ORIGINAL RESEARCH
published: 20 October 2021
doi: 10.3389/fnhum.2021.765254

Interlimb Coordination Performance in Seated Position in Persons With Multiple Sclerosis: Reduced Amplitude Over 6 min and Higher Coordination Variability in Persons With Walking Fatigability

Mieke Goetschalckx[1†‡], Fanny Van Geel[1,2*†‡], Raf Meesen[1†], Lisa Tedesco Triccas[1†], Marc Geraerts[1†], Lousin Moumdjian[1,2,3†] and Peter Feys[1,2†]*

[1] REVAL Rehabilitation Research Center, Faculty of Rehabilitation Sciences, Hasselt University, Hasselt, Belgium, [2] Universitair Multiple Sclerosis Centrum (UMSC), Hasselt-Pelt, Hasselt, Belgium, [3] Faculty of Art and Philosophy, IPEM, Institute of Psychoacoustic and Electronic Music, Ghent University, Ghent, Belgium

Background: Walking fatigability is prevalent in MS and can be measured by a percentage distance decline during a 6-min walking test. Walking is characterized by an accurate and consistent interlimb antiphase coordination pattern. A decline in coordination each minute during a 6-min walking test is observed in persons with MS (pwMS). Measuring coordination during a 6-min seated coordination task with minimized balance and strength requirements, is assumed to examine a more fundamental interlimb antiphase coordination pattern in pwMS. This research aimed to answer the following research question: How does interlimb antiphase coordination pattern change during a seated coordination task in pwMS with walking fatigability (WF), non-walking fatigability (NWF) and Healthy Controls (HC)?

Methods: Thirty-five pwMS and 13 HC participated. Interlimb coordination was assessed by a seated 6-min coordination task (6MCT) with the instruction to perform antiphase lower leg movements as fast as possible. Outcomes were Phase Coordination Index (PCI) and movement parameters (amplitude, frequency).

Results: Mixed models revealed a significant effect of time for the the variability of generating interlimb movements, with a difference in mean values between WF and HC. A significant group*time interaction effect was found for movement amplitude, represented by a significant decrease in movement amplitude in the WF group from minute 1 to the end of the task.

Conclusion: The higher variability in interlimb coordination and decrease in movement amplitude over time during the 6MCT in the WF group could be an indicator

OPEN ACCESS

Edited by:
Marco Iosa,
Sapienza University of Rome, Italy

Reviewed by:
Maria Grazia Grasso,
Santa Lucia Foundation, Scientific Institute for Research, Hospitalization and Healthcare (IRCCS), Italy
Thorsten Rudroff,
The University of Iowa, United States

****Correspondence:***
Mieke Goetschalckx
mieke.goetschalckx@uhasselt.be
Fanny Van Geel
fanny.vangeel@uhasselt.be

†ORCID:
Mieke Goetschalckx
orcid.org/0000-0003-1633-1448
Fanny Van Geel
orcid.org/0000-0002-7518-7899
Raf Meesen
orcid.org/0000-0002-7938-3758
Lisa Tedesco Triccas
orcid.org/0000-0001-9097-9352
Marc Geraerts
orcid.org/0000-0002-3108-0432
Lousin Moumdjian
orcid.org/0000-0003-4973-5190
Peter Feys
orcid.org/0000-0002-5680-5495

‡These authors share first authorship

Specialty section:
This article was submitted to Motor Neuroscience, a section of the journal Frontiers in Human Neuroscience

Received: *26 August 2021*
Accepted: *29 September 2021*
Published: *20 October 2021*

of decreased control of fundamental antiphase coordination pattern in pwMS with walking fatigability.

Clinical Trial Registration: www.clinicaltrials.gov, identifier NCT04142853 (registration date: October 29, 2019) and NCT03938558 (registration date: May 6, 2019).

Keywords: multiple sclerosis, phase coordination index, seated coordination task, coordination, fatigability

INTRODUCTION

Fatigue is highly reported in people with MS (pwMS), with a prevalence up to 80%, showing a high impact on quality of life (Kluger et al., 2013; Filippi et al., 2018). Recent taxonomies have indicated two types of fatigue: trait fatigue and state fatigue. Trait fatigue is referred to as an overall perception of fatigue over a longer time which is frequently assessed by questionnaires such as the modified fatigue impact scale (MFIS). State fatigue is activity dependent. State fatigue can be either assessed by asking the perceived fatigue by a visual analog scale (VAS), or assessed objectively by performance decline during, for example, maximal strength contractions or walking (Kluger et al., 2013; Van Geel et al., 2019). So far, research on motor fatigability has often been based on evaluation of the capacity to maintain maximal isometric muscle force measured on the body function level of International Classification of Functioning, disability and health (ICF); or the susceptibility to muscle fatigue (Severijns et al., 2017). With the use of the twitch interpolation technique, it has shown that motor fatigability in MS is mainly influenced by central factors such as reduced voluntary central drive. These theories assume a larger contribution of central than peripheral neural activation to motor fatigability (Steens et al., 2012; Bachinger et al., 2019; Severijns et al., 2019).

In recent years the focus of the assessment of motor fatigability have been changed from body function level of ICF to walking at ICF activity level. Walking-related fatigability has been quantified in pwMS by comparing walking velocity during different paradigms (Phan-Ba et al., 2012), and more recently, by comparing the last vs. the first minute of the 6 min walking test (6MWT), quantified by a "distance walked index" (Leone et al., 2016; Van Geel et al., 2020). Walking-related fatigability limits the mobility of pwMS in daily life, and is prevalent in up to half of pwMS with moderate to severe impairments (Leone et al., 2016). During the 6MWT, pwMS perceive more balance problems and gait impairments, and report overall higher state fatigue levels across minutes (Van Geel et al., 2021).

Walking requires accurate and consistent antiphase interlimb coordination pattern, to ensure safe ambulatory functions. Interlimb coordination involves a distributed network at both supraspinal and spinal level (Swinnen, 2002). It has been suggested that defaults in the central nervous system (Debaere et al., 2001; Swinnen, 2002; Swinnen and Carson, 2002), such as muscle firing timing, slowed motor nerve conduction time and reduced voluntary drive by the motor cortex (Swinnen and Carson, 2002; Wurdeman et al., 2011; Swanson and Fling, 2018) may contribute to the impaired coordination. When walking at self-selected and fast speed, pwMS with mild to moderate disability shows a worse interlimb coordination pattern than healthy controls (HC) (Richmond et al., 2020). Moreover, when performing a 6-min walking task, interlimb coordination pattern deteriorates each minute (Plotnik et al., 2020). Interlimb coordination in pwMS may be impacted by the presence of heterogenous symptoms, ranging from impaired dynamical balance, decreased muscle strength, asymmetric gait, compensatory movements, or perception of fatigue or performance fatigability. Therefore, a seated 6-min coordination task (6MCT) was designed to mimic the 6-min walking test (6MWT) but with minimalized balance requirements or major muscular effort, which are required during a regular walking task. Our main hypothesis is that a change in coordination pattern would be observed during the seated 6MCT, by the end of the task as a result of fatigability. This change is hypothesized to be more present in a group with walking-related performance fatigability, as both walking fatigability and coordination are assumed to be mostly (but not exclusively) influenced by central neural activation mechanisms.

The aim of this study was consequently to examine more fundamental antiphase interlimb coordination pattern while seated in pwMS, with and without walking fatigability in comparison to healthy controls.

MATERIALS AND METHODS

Participants

The present study reports on exploratory observational baseline data of the clinical trials registered at www.clinicaltrials.gov: NCT04142853 (MS n = 27, HC n = 13) and NCT03938558 (MS n = 18). Seven pwMS participated in both studies and therefore, data of their first participation (NCT03938558) was included. PwMS and healthy controls (HC) were tested at the REVAL Rehabilitation Research Centre of Hasselt University, and recruited via REVAL, Rehabilitation, the MS Centre Overpelt and the non-for-profit organization Move To Sport. The ethical committee of Hasselt University, MS Centre Overpelt and Hospitalo-Facultaire Universitaire de Liège approved the protocols (B707201835771 and B9115201836892) and written informed consent was obtained from all participants. Participants were aged between 18 and 70 years, and had to be able to walk for 6 min with or without support (bilateral or unilateral). PwMS were diagnosed according to the McDonald criteria (Thompson et al., 2018). Three pwMS

were excluded as they could not perform the 6MWT or the 6MCT safely.

Descriptive Data

Age, gender, EDSS, Type MS, years since diagnosis, Timed 25 foot walk test (T25FW), Paced Auditory Serial Addition test (PASAT), Single Digit Modalities test (SDMT), Modified Fatigue Impact Scale (MFIS), and Multiple Sclerosis Walking Scale (MSWS-12), were collected in pwMS.

To divide patients into groups with or without walking fatigability, subjects performed the 6-min walking test (6MWT) according to the script of Goldman et al. (2008) in a 30-m corridor, where participants were asked to walk as fast as possible and cover as much distance as possible, making them challenge their maximal effort. Distance walked each minute was collected. The Distance Walked Index (DWI_{6-1}) (Leone et al., 2016) was used to allocate pwMS into a walking fatigability (WF) and a non-walking fatigability group (NWF), according to the rounded cut-off value of −10% (Van Geel et al., 2020): [(distance walked in min 6 - distance walked in min 1)/distance walked in min 1]*100. Before the start of the test (baseline), and after each minute of the 6MWT and 6-min coordination test (6MCT), participants were asked to rate their subjective perception of fatigue on a VAS scale, where 0 is no fatigue and 10 is extremely fatigued. Change in perceived fatigue was calculated as followed: (perceived fatigue VAS score in minute 6 - perceived fatigue VAS score at baseline) × 10.

Apparatus Interlimb Coordination Test

To assess antiphase interlimb coordination of the lower limbs, participants performed a seated 6 min coordination task. Subjects were seated on a steel chair covered with foam, to which two levers were attached. To ensure a stable posture,

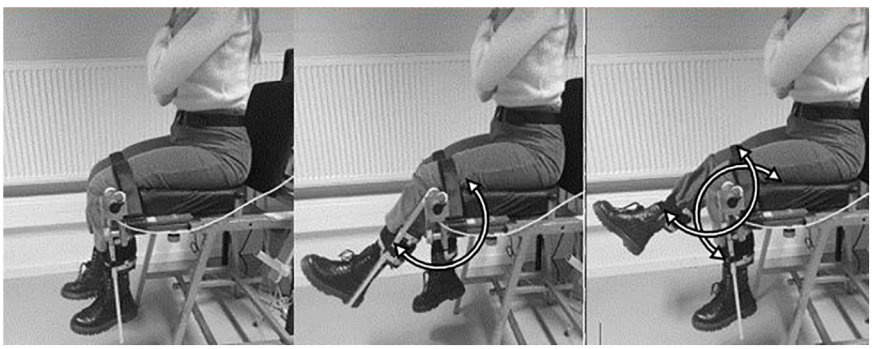

FIGURE 1 | Representation of the seated antiphase interlimb coordination task. Subjects make simultaneous left and right knee flexion and extension antiphase movements.

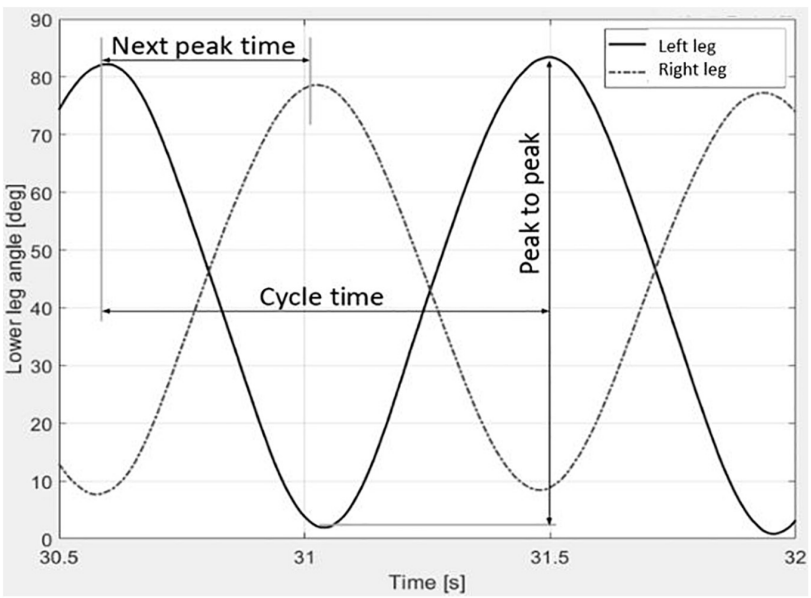

FIGURE 2 | Visualization of movement cycles of left and right leg of a person with MS.

TABLE 1 | Descriptive, demographic characteristics and interlimb coordination outcomes (mean, standard deviation) in HC and pwMS (WF-NWF).

	MS			HC	
	Total (*n* = 35)	**WF (*n* = 13)**	**NWF (*n* = 22)**	**HC (*n* = 13)**	***p*-value**
Descriptive variables					
Age (years)					
Mean+SD 95%CI	48.9 ± 9.3 [45.8; 52.1]	49.8 ± 6.4 [45.9; 53.6]	48.5 ± 10.7 [43.7; 53.2]	51.7 ± 16.5 [41.7; 61.7]	NS[b]
Gender: female					
(n; %)	29; 82.9%	12; 92.3%	17; 77.3%	8; 61.5%	NS[c]
EDSS (0–10)					
Mean+SD 95%CI Missing data	3.3 ± 1.5 [2.7; 3.9] *n* = 9	3.7 ± 1.2 [2.9; 4.5] *n* = 3	3.0 ± 1.7 [2.1; 3.9] *n* = 6	NA	NS[a]
Type of MS (RR/PP/SP)					
Mean+SD Missing data	25/2/2 *n* = 6	10/0/0 *n* = 3	15/2/2 *n* = 3	NA	NS[c]
Years since diagnosis					
Mean+SD 95%CI Missing data	13.1 ± 6.0 [10.9; 15.3] *n* = 4	13.0 ± 6.4 [8.7; 17.3] *n* = 2	13.1 ± 5.9 [10.3; 15.9] *n* = 2	NA	NS[a]
Motor outcomes					
T25FW (s)					
Mean+SD 95%CI	5.1 ± 1.5 [4.5; 5.6]	5.4 ± 1.3 [4.7; 6.2]	4.9 ± 1.7 [4.1; 5.6]	3.3 ± 0.4 [3.1; 3.6]	**<0.0001[b]** **WF – HC(0.0014)** **NWF – HC(< 0.0001)**
Walking fatigability (DWI %)					
Mean+SD 95%CI Missing data	−8.0 ± 8.0 [−10.7; −5.2]	−16.2 ± 5.8 [−19.8; −12.7]	−3.1 ± 4.0 [−4.9; −1.3]	−2.3 ± 2.7 [−3.98; −0.5] *n* = 1	**<0.0001[a]** **WF – HC(< 0.0001)** **WF – NWF(< 0.0001)**
6MWT (m)					
Mean+SD 95%CI Missing data	474 ± 118 [433; 514]	414 ± 115 [345; 484]	509 ± 108 [461; 556]	608 ± 53 [574; 642] *n* = 1	**<0.0001[a]** **WF – HC(< 0.0001)** **NWF – HC(0.0079)** **WF – NWF(0.0094)**
Cognitive outcomes					
PASAT (./60)					
Mean+SD 95%CI	47 ± 9 [44; 50]	49 ± 7 [45; 54]	46 ± 10 [41; 50]	49 ± 9 [43; 55]	NS[a]
SDMT (./110)					
Mean+SD 95%CI	55 ± 13b [51; 60]	52 ± 13 [44; 60]	57 ± 13 [51; 63]	62 ± 12 [55; 70]	NS[a]
Questionnaires					
MFIS (./84)					
Mean+SD 95%CI Missing data	39 ± 16 [33; 45] *n* = 6	45 ± 12 [36; 55] *n* = 4	36 ± 16 [28; 43] *n* = 2	NA	NS[a]
MSWS-12 (./60)					
Mean+SD 95%CI Missing data	32 ± 14 [27; 38] *n* = 6	42 ± 8 [36; 49] *n* = 4	28 ± 14 [21; 34] *n* = 2	NA	**0.013[b] WF – NWF**
Interlimb coordination outcomes (6MCT)					
PCI					
Mean+SD 95%CI	15.9 ± 9.5 [12.6; 19.2]	17.7 ± 8.8 [12.4; 23.0]	14.8 ± 10 [10.4; 19.3]	10.3 ± 4.7 [7.4; 13.1]	**0.028[b] WF – HC**
Coefficient of variation (CV) φ					
Mean+SD 95%CI	8.1 ± 6.1 [6.0; 10.1]	8.6 ± 4.2 [6.0; 11.1]	7.8 ± 7.0 [4.7; 10.9]	5.1 ± 1.6 [4.1; 6.0]	**0.011[b] WF – HC**
Absolute error (ABS) φ					
Mean+SD 95%CI	7.8 ± 5.1 [6.1; 9.6]	9.1 ± 5.7 [5.6; 12.6]	7.1 ± 4.7 [5.0; 9.2]	5.2 ± 4.7 [2.4; 8.1]	NS[b]

(Continued)

TABLE 1 | (Continued)

	MS			HC	
	Total (*n* = 35)	**WF (*n* = 13)**	**NWF (*n* = 22)**	**HC (*n* = 13)**	***p*-value**
Movement amplitude					
Mean+SD 95%CI	70.0 ± 21.9 [62.4; 77.4]	61.3 ± 21.1 [48.5; 74.0]	75.1 ± 21.1 [65.7; 84.4]	77.7 ± 24.9 [62.7; 92.8]	NS[a]
Movement frequency					
Mean+SD 95%CI	72.4 ± 13.7 [67.7; 77.1]	72.3 ± 16.0 [62.6; 81.9]	72.4 ± 12.5 [66.9; 78.0]	81.5 ± 22.7 [67.8; 95.2]	NS[b]

MS, Multiple sclerosis; WF, walking fatigability group; NWF, non-walking fatigability group; HC, Healthy controls; EDSS, Expanded Disability Status Scale; RR, relapsing remitting MS; PP, primary progressive MS; SP, secondary progressive MS; T25FW, Timed 25-foot walk test; DWI, Distance walked index; 6MWT, 6 min walking test; PASAT, Paced auditory serial addition test; SDMT, Symbol digit modality test; MFIS, Modified fatigue impact scale; MSWS-12, Multiple sclerosis walking scale; PCI, Phase coordination index; ns, not significant; NA, not applicable.

Bold: significant effect $p \leq 0.05$, NA, Not applicable, NS, not significant ($p > 0.05$), [a]Independent t-test or ANOVA (post hoc Tukey HSD), [b]Wilcoxon or Kruskal-Wallis test (post hoc using Steel-Dwass method), [c]Chi^2 test, n, Number, 95% CI, 95% Confidence interval [lower 95%; upper 95%], SD, Standard deviation.

subjects were strapped into the chair with a belt at the upper legs (**Figure 1**). The back was supported, but not fixed, so that participants could sit in the most comfortable position for them to perform the task. Participants were asked to keep their arm crossed by the shoulders throughout the 6MCT. The lower limbs were attached to levers to allow the lower legs to perform knee flexion and extension movements. The lateral joint line of the knee was aligned with the axis of rotation of the levers. At full knee extension, the mass of the each lever was 540 grams. Joint angles were registered by means of 2 incremental shaft encoders (Hengstler®, 1,000 bits per revolution, accuracy = 0.36°, sampling frequency = 100 Hz; Romsey, United Kingdom) mounted at the axis of rotation of each lever.

Methodology Interlimb Coordination Test

Participants were asked to perform flexion and extension movements at the knee joints in a coordinated antiphase pendulum movement. The movements had to be as fast or as many as possible for 6 min. For individualization purpose, no limits for range of motion were set. Participants performed antiphase interlimb movement for approximately 5 times, to ensure understanding and correct execution. The first 10 s of the test were excluded for data processing due to start-up movements. MATLAB (version R2019a) was used for data processing. An upsample rate of 10 was used for sample frequency. **Figure 2** visualizes one movement cycle. Consequently, interlimb coordination parameters were analyzed and averaged per minute.

Outcomes Interlimb Coordination Task

Originally, the phase coordination index (PCI) measures the consistency and accuracy in generating antiphase left-right leg movements while walking (Plotnik et al., 2007). The PCI was used to analyze interlimb coordination of the lower limbs during the seated 6MCT. Similar relative phase coordination outcomes were used previously, using a similar apparatus (Swinnen et al., 1997; Serrien, 1998; Serrien and Stelmach, 2000; Goetschalckx et al., 2021). Relative phase φ expressed the relative timing between the contralateral peaks [360*(next peak time/cycle time)]. The accuracy in generating antiphase left-right leg movements is expressed by absolute error ABS(φ) = ((mean $|\varphi i - 180|$)/180) × 100. The coefficient of variation (CV φ) was used to express the consistency in generating antiphase left-right leg movements CV(φ) = (Standard deviation φ/mean φ) × 100.

The PCI is the sum of the absolute error (ABS φ) and coefficient of variation (CV) of the relative phase (φ), expressed as a percentage. A lower PCI indicates a higher phase control and coordination.

The movement amplitude, seen as the spatial measure, consists of the peak-to-peak amplitude for each individual cycle (Serrien and Stelmach, 2000). Movement frequency, seen as the temporal measure, is expressed by the number of cycles per minute. One cycle was defined between two successive peak extension positions. The average movement amplitude and movement frequency for each leg were calculated for each minute.

Data and Statistical Analysis

Data analysis was performed using SAS JMP®Pro 14.10. (SAS Institute Inc., Cary, NC, United States). Linear mixed models were used to analyze the effect of group and time on interlimb coordination and spatiotemporal parameters, after checking the conditional residuals plots. To assess asymmetry between legs, mean values of movement amplitude and movement frequency of left and right leg were compared. Comparison of the mean values over 6MCT between left and right legs revealed no significant difference in any groups. Therefore, the analysis for spatiotemporal parameters during the 6MCT was performed with the mean value of both legs, per minute. Fixed effects were included in the mixed model which were group (WF, NWF, HC), time (minute 1, 2, 3, 4, 5, 6) and the interaction group*time, using a Bonferroni correction for significance ($p = 0.05/3$). Participants were included as random factor. To compare factors between groups (HC, WF, NWF) a ANOVA was used, after normality was confirmed by Shapiro-Wilk test. For non-normal distributed data, the non-parametric Wilcoxon/Kruskal-Wallis test (Rank sums) was used. Two-sided *p*-values were set at alpha level of 0.05. If a significant effect existed, multiple comparison Tukey HSD was used for

normal distributed data and Steel-Dwass method for non-normal distributed data. The Chi^2 test was used to compare groups for nominal data.

RESULTS

Demographics and Walking Fatigability

In total, 35 pwMS and 13 HC could be included in data analysis of 6MCT. Data of the 6MWT of one HC was excluded from descriptive analysis because the participant started to jog. In our study sample, 13 pwMS showed walking fatigability (WF = 37.15%). **Figure 3** represents the distance walked each minute during the 6MWT (mean ± CI) for the different groups.

Descriptive and demographic outcomes are shown in **Table 1**. Significant differences between three groups were found for TF25W, DWI, 6MWT, and MSWS-12.

Figure 4 represents the median (quartiles) of the change in perceived fatigue for each test and group. No significant differences were found between change in perceived fatigue during the 6MWT and 6MCT in HC and NWF group. However, in pwMS with WF, the 6MWT led to a significant higher change in perceived fatigue compared to the 6MCT [$t(23.44) = 2.23$; $p = 0.036$]. Additionally, a significant difference was found between WF-NWF ($MD = 8.51$; $SE = 3.53$; $z = 2.41$; $p = 0.042$) for the change in perceived fatigue for the 6MCT.

Interlimb Coordination

Mean values of all interlimb coordination outcomes measures are shown in **Table 1**. **Figures 5A–C** visualize, respectively, the course of the ABS φ, CV φ, and PCI during each minute of the 6MCT (mean ± CI). A main effect of time was observed for the CV φ (variability in generating antiphase left-right leg movements) [$F(5, 225) = 3.20$; $p < 0.01$]. After *post hoc* multiple comparison significant differences were seen in CV φ from minute 2–5 [$t(225) = -3.26$; $p = 0.0161$] and 2–6 [$t(225) = -3.57$; $p < 0.01$] (see **Figure 5**). Mixed model analysis revealed no significant main effect of time, group, nor an interaction effect of group*time for PCI and ABS φ.

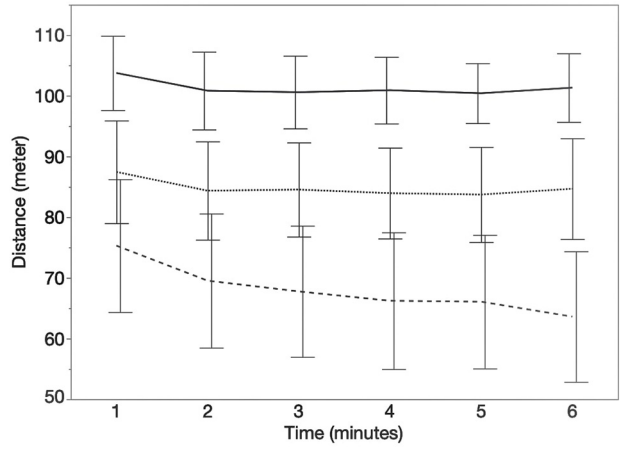

FIGURE 3 | Course of the distance (meters) walked each minute during the 6MWT. Error bars represents 95% confidence intervals. Stripe pattern line represents persons with MS with walking fatigability (WF), dotted line represents persons with MS without walking fatigability (NWF) and solid line represents healthy controls (HC).

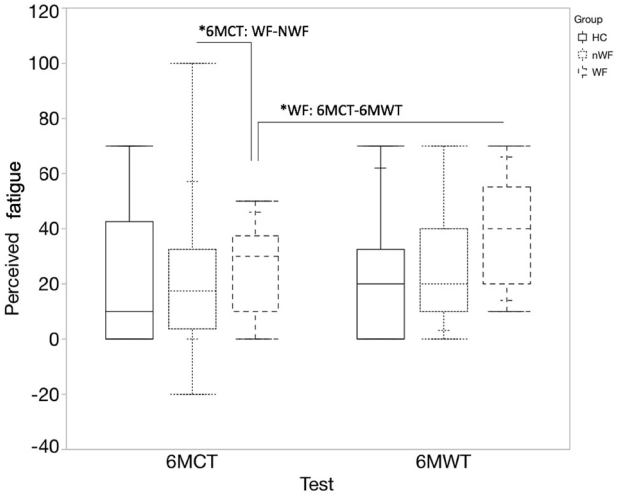

FIGURE 4 | Median change in perceived fatigue (quartiles) during 6MWT and 6MCT. Full blocks represent data of healthy controls (HC); block with stripes pattern represents persons with MS with walking fatigability (WF), block with dot pattern represents persons with MS without walking fatigability (NWF). *6MCT: WF-NWF: significant difference in change in perceived fatigue between the WF and NWF group for the 6MCT ($p = 0.042$). *WF: 6MCT-6MWT: significant difference in change in perceived fatigue between 6MCT and 6MWT in persons with WF ($p = 0.036$).

The mean values of most interlimb coordination parameters differed significantly between HC and PwMS with WF (PCI_{mean}: $MD = 7.69$; $SE = 3.00$; $z = 2.56$; $p = 0.028$; CV_{mean}: $MD = 8.61$; $SE = 3.00$; $z = 2.87$; $p = 0.011$). **Supplementary Table 1** displays mean ± standard deviation (SD) of the interlimb coordination outcomes each minute.

Figures 6A,B visualize, respectively, the course of the movement amplitude and movement frequency during each minute of the 6MCT (mean ± CI). A significant interaction effect of group*time was found for movement amplitude [$F(10, 225) = 4.57$; $p < 0.001$]. *Post-hoc* multiple comparison showed that pwMS with WF decreased their movement amplitude significantly from minute 1 to both minute 5 [$t(225) = 4.40$; $p < 0.01$] and 6 [$t(225) = 4.89$; $p < 0.001$]. In contrast to the movement amplitude, no significant main time effect, nor an interaction effect was observed for movement frequency, suggesting that no group significantly changed their movement frequency over the 6MCT. **Supplementary Table 2** displays the spatiotemporal movement parameters of each group by time (mean ± SD).

DISCUSSION

This is the first study that investigates an antiphase coordination pattern of the lower limbs during a seated 6 min coordination task (6MCT) in pwMS and changes over time. The seated

6MCT was designed to examine more fundamental interlimb coordination of the lower limbs, assuming minimized balance and strength demands, which are required during walking. Our main hypothesis was that a change in coordination pattern over time, due to performance fatigability, would be observed during seated 6MCT in pwMS with WF, by means of change in antiphase coordination movements (ABS, CV, PCI), and decrease in spatial and temporal movement parameters (movement amplitude, movement frequency). We hypothesized this change, as a similar trend of deterioration in coordination pattern over each minute have been observed in pwMS while performing a 6-min walking task (Plotnik et al., 2020).

The exploratory results of this study showed that interlimb coordination changes over time, observed by an increase in their variability in generating antiphase left-right movement CV(φ), toward the end of the task. As expected, this change in variability was greatest in pwMS with WF. Besides the observed change over time, the mean values of CV(φ) and PCI differed significantly between HC and pwMS with WF, with worse values in pwMS with WF. Noteworthy is that ABS(φ) in antiphase generation did not differ between group and did not changed significantly over time. These results suggest that pwMS with WF have more difficulties in the control of seated antiphase coordination of the lower limbs compared to HC.

Regarding the temporal and spatial movement parameters during the 6MCT, we expected to observe a similar trend of decline in performance in movement frequency or amplitude in pwMS with WF, as they show a decrease in walking distance during the 6MWT. As the 6MWT requires not only a consistent and accurate antiphase coordination pattern, but also balance and strength, the 6MCT was designed to minimalize balance requirements or major muscular effort, and therefore in theory stresses more central neural mechanism. This 6MCT was based on a similar test in previous research

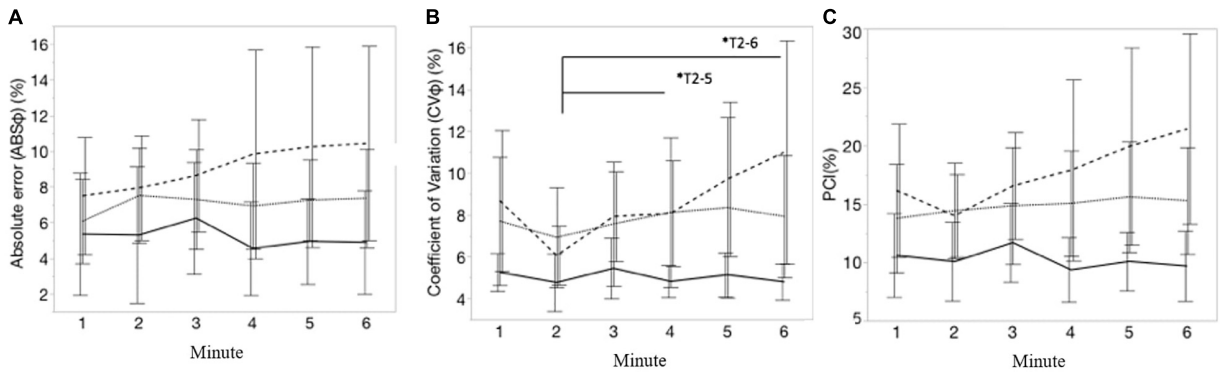

FIGURE 5 | (A–C) Represents, respectively, the course of absolute error of the relative phase (ABS φ, %), coefficient of variation of relative phase (CV φ; %) and the phase coordination index (PCI, %), during each minute of the 6MCT. Error bars represents 95% confidence intervals. Stripe pattern line represents persons with MS with walking fatigability (WF), dotted line represents persons with MS without walking fatigability (NWF) and solid line represents healthy controls (HC). *T2–5, *T2–6: significant main effect of time for CV(φ) from minute 2 to 5 ($p = 0.0161$) and minute 2 to 6 ($p < 0.01$).

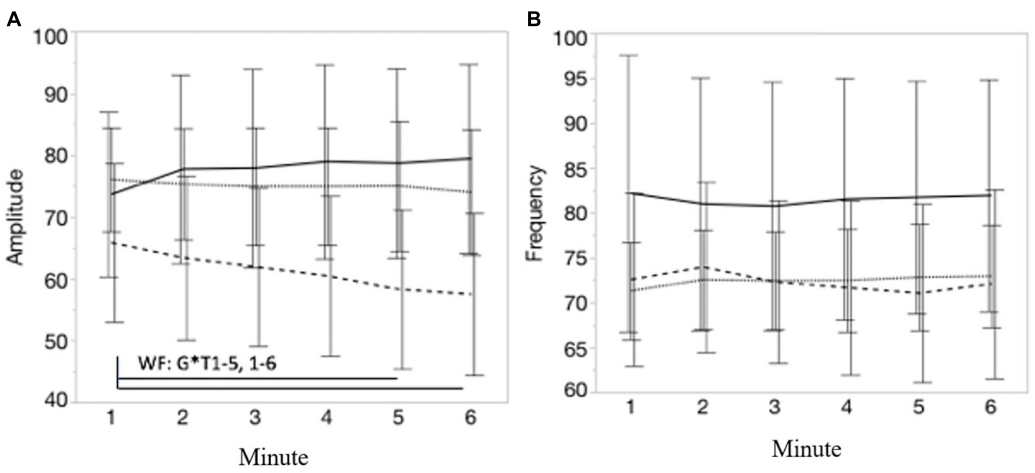

FIGURE 6 | (A,B) Represents, respectively, the course of the movement amplitude and movement frequency during each minute of the 6MCT. Error bars represents 95% confidence intervals. Stripe pattern line represents persons with MS with walking fatigability (WF), dotted line represents persons with MS without walking fatigability (NWF) and solid line represents healthy controls (HC). *WF: G*T1–5, 1–6: significant interaction effect of group*time: pwMS with WF decreased their movement amplitude significantly from minute 1 to 5 ($p < 0.01$) and minute 6 ($p < 0.00$).

to measure phase coordination deficits, in stroke, elderly and Parkinson (Swinnen et al., 1997; Serrien, 1998; Serrien and Stelmach, 2000). We found that only in pwMS with WF, the movement amplitude significantly decreased over time, and not movement frequency. One of the first studies that used this interlimb seated coordination task in Parkinson disease found significant differences in movement amplitude compared to HC. Temporal measure (cycle duration) and absolute error (ABS) did not significantly differ between patients and HC. Together, these results suggest that during a seated coordination task, the temporal movement parameter is less influenced by neurological diseases, like pwMS and Parkinson disease, than spatial movement parameters. However, direct comparison is not possible due to difference in population, but also in length of the task (24 trials of 15 s vs. sustained 6 min) and performing the task while listening to a metronome (1 Hz) (Swinnen et al., 1997).

In the WF group, the change in perceived state fatigue during the 6MCT was lower than during the 6MWT, indicating that the seated task was perceived less fatiguing than walking. However, despite low levels of perceived state fatigue, the test detected differences in antiphase interlimb coordination pattern between groups. These results suggest that the 6MCT can be used as an alternative for patients who are not able to perform the 6MWT due to extreme fatigue or having severe motor disabilities. This assumption should, however, be further investigated, as the 6MCT cannot be directly compared to walking, as explained further. We note that, although pwMS without walking fatigability did show walking impairments assessed by the T25FWT and 6MWT, no significant differences were found in seated interlimb coordination performance, nor in change in perceived state fatigue, between pwMS in the NWF group and HC. Besides, we note that abnormal trait fatigue was present in many pwMS with WF (see **Table 1**, mean MFIS = 45), assessed by the MFIS. However, no significant difference in trait fatigue was found in pwMS with or without walking-related performance fatigability, and thus trait fatigue seems to be rather a general MS characteristic. This result may suggest that trait fatigue do not directly relates to walking-related performance fatigability. These results highlight the importance of interlimb coordination in walking-related performance fatigability.

In contrast to 6MCT, walking is for example characterized by different sensory-motor interactions, different and higher muscle activity, higher dynamic balance needs, metabolic cost, higher automaticity, etc., which all seems to be different in the 6MCT. Moreover, Meesen et al. (2005) found that movement with the head is a contributing factor for disturbance of coordination. Serrien and Stelmach (2000) confirms that movements integrating different limbs show more coordination effort in elderly. Future research could investigate these perturbations and multi-limb coordination patterns during the seated coordination test, to increase the ecologically validity of the 6MCT toward walking. The 6MCT should therefore be considered as a model that allows (in theory) isolation of the central neural drive mechanisms, taking lower limbs into account.

Future studies, should take the following limitation of this study into account. This research instructed participants to perform as many movements as possible, so move as fast as possible during 6 min, similar to the instructions of the 6MWT, where patients are instructed to walk as fast as possible, and cover as much distance as they can. Therefore, movement frequency could have been prioritized and the main focus of the participants over the 6 min instead of movement amplitude. The decrease in amplitude might have been a compensation strategy to keep the frequency equal, and perform as many movements as possible. Future studies could focus on different instructions and look at the possible influence of prioritization of amplitude or frequency. However, movement frequency is often prioritized in other tasks of the locomotor system, wherefore we do not think that the instruction has exclusively influenced our results (Malone et al., 2012; Motl et al., 2012; Comber et al., 2017).

Methodological considerations apply. The small sample size, especially in subgroups, and no *a priori* power analysis, should be considered when interpreting the results. A power analysis could not be made given it was the first time that the task was used in persons with MS. Besides, no one-to-one matching was performed between HC and MS groups. Next, we cannot exclude the impact of the relative weight of the levers, muscle strength asymmetries, accuracy of axis alignment of the device during the task, the liberty of comfortable range of motion of the legs and optional use of back support on differences in task performance between participants. Because of individualization purpose, participants were not restricted in their movement amplitude, nor externally paced in their movement frequency, similar to 6MWT were the step length and cadence are not standardized. One may argue that muscle strength asymmetries may have impacted the results. In this research, maximal lower limb strength was unfortunately not recorded given strength requirements in the seated coordination task were limited and likely not importantly affecting interlimb coordination control. Still, future research is advised to include maximal lower leg muscle strength as strength asymmetry might be present in pwMS (Farrell et al., 2021) and can then be included as factor in statistical analyses. Further research should also elaborate on more standardized task constraints regarding movement amplitude or correct for variability in movement amplitude to avoid that variability expressed in absolute values could influence group comparisons.

CONCLUSION

Our exploratory results suggest that the antiphase coordination of the lower limbs change over time while performing a seated 6-min coordination task. These changes were apparent by an average higher coordination variability and a decrease in movement amplitude. The observed changes where more prominent in pwMS with walking-related performance fatigability. Results suggest indirectly the influence of central mechanism contributing to coordination patterns in the walking-related performance fatigability group. Further studies in a powered sample size with new methodological considerations are warranted to determine the relative contribution of centrally driven interlimb coordination and walking fatigability.

DATA AVAILABILITY STATEMENT

The raw data supporting the conclusions of this article will be made available by the authors after request.

ETHICS STATEMENT

The studies involving human participants were reviewed and approved by the Ethical Committee of Hasselt University, MS Centre Overpelt and Hospitalo-Facultaire Universitaire de Liège approved the protocols (B707201835771 and B9115201836892). The patients/participants provided their written informed consent to participate in this study.

AUTHOR CONTRIBUTIONS

FV was responsible for study conceptualization, data collection, data processing, and writing of the manuscript. MGo was responsible for data analyzing, data interpretation, and writing of the manuscript. MGe was responsible for data processing. RM was responsible for equipment conceptualization, data processing, and data interpretation. LT and LM were responsible for data interpretation and writing of the manuscript. PF was responsible for study conceptualization, data interpretation, and writing of the manuscript. All authors contributed to the article and approved the submitted version.

FUNDING

This study was supported by the Special Research Fund (BOF) of Hasselt University (19DOC50BOF).

ACKNOWLEDGMENTS

We acknowledge all participants for volunteering to be part of this study. Besides we thank the master thesis students of the University of Hasselt for their assistance in testing and data curation.

SUPPLEMENTARY MATERIAL

The Supplementary Material for this article can be found online at: https://www.frontiersin.org/articles/10.3389/fnhum.2021.765254/full#supplementary-material

REFERENCES

Bachinger, M., Lehner, R., Thomas, F., Hanimann, S., Balsters, J., and Wenderoth, N. (2019). Human motor fatigability as evoked by repetitive movements results from a gradual breakdown of surround inhibition. *Elife* 8:e46750.

Comber, L., Galvin, R., and Coote, S. (2017). Gait deficits in people with multiple sclerosis: a systematic review and meta-analysis. *Gait Posture* 51, 25–35. doi: 10.1016/j.gaitpost.2016.09.026

Debaere, F., Van Assche, D., Kiekens, C., Verschueren, S. M., and Swinnen, S. P. (2001). Coordination of upper and lower limb segments: deficits on the ipsilesional side after unilateral stroke. *Exp. Brain Res.* 141, 519–529. doi: 10.1007/s002210100891

Farrell, J. W. III, Motl, R. W., Learmonth, Y. C., and Pilutti, L. A. (2021). Persons with multiple sclerosis exhibit strength asymmetries in both upper and lower extremities. *Physiotherapy* 111, 83–91. doi: 10.1016/j.physio.2020.07.006

Filippi, M., Bar-Or, A., Piehl, F., Preziosa, P., Solari, A., Vukusic, S., et al. (2018). Multiple sclerosis. *Nat. Rev. Dis. Primers.* 4:43.

Goetschalckx, M. V. G. F., Meesen, R., Moumdjian, L., Geraerts, M., and Feys, P. (2021). Rhythmic interlimb coordination of the lower limbs in multiple sclerosis during auditory pacing to three different frequencies. *Gait Posture* 86, 334–340. doi: 10.1016/j.gaitpost.2021.04.001

Goldman, M. D., Marrie, R. A., and Cohen, J. A. (2008). Evaluation of the six-minute walk in multiple sclerosis subjects and healthy controls. *Mult. Scler.* 14, 383–390. doi: 10.1177/1352458507082607

Kluger, B. M., Krupp, L. B., and Enoka, R. M. (2013). Fatigue and fatigability in neurologic illnesses: proposal for a unified taxonomy. *Neurology* 80, 409–416. doi: 10.1212/wnl.0b013e31827f07be

Leone, C., Severijns, D., Dolezalova, V., Baert, I., Dalgas, U., Romberg, A., et al. (2016). Prevalence of walking-related motor fatigue in persons with multiple sclerosis: decline in walking distance induced by the 6-minute walk test. *Neurorehabil. Neural Repair* 30, 373–383. doi: 10.1177/1545968315597070

Malone, L. A., Bastian, A. J., and Torres-Oviedo, G. (2012). How does the motor system correct for errors in time and space during locomotor adaptation? *J. Neurophysiol.* 108, 672–683. doi: 10.1152/jn.00391.2011

Meesen, R. L., Wenderoth, N., and Swinnen, S. P. (2005). The role of directional compatibility in assembling coordination patterns involving the upper and lower limb girdles and the head. *Behav. Brain Res.* 165, 262–270. doi: 10.1016/j.bbr.2005.07.029

Motl, R. W., Suh, Y., Balantrapu, S., Sandroff, B. M., Sosnoff, J. J., Pula, J., et al. (2012). Evidence for the different physiological significance of the 6- and 2-minute walk tests in multiple sclerosis. *BMC Neurol.* 12:6.

Phan-Ba, R., Calay, P., Grodent, P., Delrue, G., Lommers, E., Delvaux, V., et al. (2012). Motor fatigue measurement by distance-induced slow down of walking speed in multiple sclerosis. *PLoS One* 7:e34744. doi: 10.1371/journal.pone.0034744

Plotnik, M., Giladi, N., and Hausdorff, J. M. (2007). A new measure for quantifying the bilateral coordination of human gait: effects of aging and Parkinson's disease. *Exp. Brain Res.* 181, 561–570. doi: 10.1007/s00221-007-0955-7

Plotnik, M., Wagner, J. M., Adusumilli, G., Gottlieb, A., and Naismith, R. T. (2020). Gait asymmetry, and bilateral coordination of gait during a six-minute walk test in persons with multiple sclerosis. *Sci. Rep.* 10:12382.

Richmond, S. B., Swanson, C. W., Peterson, D. S., and Fling, B. W. (2020). A temporal analysis of bilateral gait coordination in people with multiple sclerosis. *Mult. Scler. Relat. Disord.* 45:102445. doi: 10.1016/j.msard.2020.102445

Serrien, D. J. S. S. P. (1998). Interactive processes during interlimb coordination: combining movement patterns with different frequency ratios. *Psychol. Res.* 61, 191–203. doi: 10.1007/s004260050024

Serrien, D. J. S. S. P., and Stelmach, G. E. (2000). Age-related deterioration of coordinated interlimb behavior. *J. Gerontol. Psychol. Sci.* 55B, 295–303.

Severijns, D., Cuypers, K., Meesen, R., Feys, P., and Zijdewind, I. (2019). Force decline after low and high intensity contractions in persons with multiple sclerosis. *Clin. Neurophysiol.* 130, 359–367. doi: 10.1016/j.clinph.2018.11.027

Severijns, D., Zijdewind, I., Dalgas, U., Lamers, I., Lismont, C., and Feys, P. (2017). The assessment of motor fatigability in persons with multiple sclerosis: a systematic review. *Neurorehabil. Neural. Repair* 31, 413–431. doi: 10.1177/1545968317690831

Steens, A., Heersema, D. J., Maurits, N. M., Renken, R. J., and Zijdewind, I. (2012). Mechanisms underlying muscle fatigue differ between multiple sclerosis patients and controls: a combined electrophysiological and neuroimaging study. *Neuroimage* 59, 3110–3118. doi: 10.1016/j.neuroimage.2011.11.038

Swanson, C. W., and Fling, B. W. (2018). Associations between gait coordination, variability and motor cortex inhibition in young and older adults. *Exp. Gerontol.* 113, 163–172. doi: 10.1016/j.exger.2018.10.002

Swinnen, S. P. (2002). Intermanual coordination: from behavioural principles to neural-network interactions. *Nat. Rev. Neurosci.* 3, 348–359. doi: 10.1038/nrn807

Swinnen, S. P., Carson, R. G. (2002). The control and learning of patterns of interlimb coordination: past and present issues in normal and disordered control. *Acta Psychol.* 110, 129–137. doi: 10.1016/s0001-6918(02)00030-6

Swinnen, S. P., Van Langendonk, L., Verschueren, S., Peeters, G., Dom, R., De Weerdt, W. (1997). Interlimb coordination deficits in patients with Parkinson' s disease during the production of two-joint oscillations in the sagittal plane. *Movement Dis.* 12, 958–968. doi: 10.1002/mds.870120619

Thompson, A. J., Banwell, B. L., Barkhof, F., Carroll, W. M., Coetzee, T., Comi, G., et al. (2018). Diagnosis of multiple sclerosis: 2017 revisions of the McDonald criteria. *Lancet Neurol.* 17, 162–173.

Van Geel, F., Bielen, H., Theunissen, K., Moumdjian, L., Van Nieuwenhoven, J., Van Wijmeersch, B., et al. (2021). Clinical manifestation and perceived symptoms of walking-related performance fatigability in persons with multiple sclerosis. *Int. J. Rehabil. Res.* 44, 118–125. doi: 10.1097/mrr.0000000000000457

Van Geel, F., Moumdjian, L., Lamers, I., Bielen, H., and Feys, P. (2019). Measuring walking-related performance fatigability in clinical practice: a systematic review. *Eur. J. Phys. Rehabil. Med.* 56, 88–103.

Van Geel, F., Veldkamp, R., Severijns, D., Dalgas, U., and Feys, P. (2020). Day-to-day reliability, agreement and discriminative validity of measuring walking-related performance fatigability in persons with multiple sclerosis. *Mult. Scler.* 26, 1785–1789.

Wurdeman, S. R., Huisinga, J. M., Filipi, M., and Stergiou, N. (2011). Multiple sclerosis affects the frequency content in the vertical ground reaction forces during walking. *Clin. Biomech.* 26, 207–212.

Conflict of Interest: PF was steering committee member of Neurocompass, participated to advisory board meetings of BIOGEN IDEC, and received teaching honoraria for EXCEMED and PARADIGMS.

The remaining authors declare that the research was conducted in the absence of any commercial or financial relationships that could be construed as a potential conflict of interest.

Citation: Goetschalckx M, Van Geel F, Meesen R, Triccas LT, Geraerts M, Moumdjian L and Feys P (2021) Interlimb Coordination Performance in Seated Position in Persons With Multiple Sclerosis: Reduced Amplitude Over 6 min and Higher Coordination Variability in Persons With Walking Fatigability. Front. Hum. Neurosci. 15:765254. doi: 10.3389/fnhum.2021.765254

frontiers in Human Neuroscience

BRIEF RESEARCH REPORT
published: 14 January 2022
doi: 10.3389/fnhum.2021.771392

Indices of Loading and Propulsive Ability in the Gait of Patients With Chronic Stroke With Equinus Foot Deviation: A Correlation Study

*Davide Mazzoli[1], Giacomo Basini[1], Paolo Prati[1], Martina Galletti[1], Francesca Mascioli[1], Chiara Rambelli[1,2], Paolo Zerbinati[3], Isabella Campanini[4] and Andrea Merlo[1]**

[1] Gait and Motion Analysis Laboratory, Sol et Salus Hospital, Rimini, Italy, [2] Section of Rehabilitation, Department of Neuroscience, University of Padova, Padova, Italy, [3] Neuro-Orthopedic Unit, Sol et Salus Hospital, Rimini, Italy, [4] LAM-Motion Analysis Laboratory, Department of Neuromotor and Rehabilitation, Azienda USL-IRCCS di Reggio Emilia, S. Sebastiano Hospital, Correggio, Italy

In literature, indices of overall walking ability that are based on ground reaction forces have been proposed because of their ease of administration with patients. In this study, we analyzed the correlation between the indices of dynamic loading and propulsion ability of 40 chronic hemiparetic post-stroke patients with equinus foot deviation and a set of clinical assessments of ankle joint deviations and walking ability. Ankle passive and active range of motion (ROM) and triceps surae spasticity were considered, along with walking speed and three complementary scales of walking ability focusing respectively on the need for assistance on functional mobility, including balance and transfers, and the limitation in social participation. The correlation between the ground reaction force-based indices and both clinical and functional variables was carried out using the non-parametric Spearman correlation coefficient. Both indices were correlated to 8 of the 10 investigated variables, thus supporting their use. In particular, the dynamic propulsive ability was correlated with all functional scales (rho = 0.5, $p < 0.01$), and has the advantage of being a continuous variable. Among clinical assessments, limited ankle ROM affected walking ability the most, while spasticity did not. Since the acquisition of ground reaction forces does not require any patient prepping, the derived indices can be used during the rehabilitation period to quickly detect small improvements that, over time, might lead to the broad changes detectable by clinical scales, as well as to immediately highlight the lack of these improvements, thus suggesting adjustments to the ongoing rehabilitation approach.

Keywords: gait, stroke, equinus foot deviation, ground reaction force, rehabilitation, physiotherapy

OPEN ACCESS

Edited by:
Marco Iosa,
Sapienza University of Rome, Italy

Reviewed by:
Kishor Lakshminarayanan,
Vellore Institute of Technology (VIT), India
Giovanni Morone,
Santa Lucia Foundation (IRCCS), Italy

***Correspondence:**
Andrea Merlo
ingmerlo@me.com

Specialty section:
This article was submitted to Motor Neuroscience, a section of the journal Frontiers in Human Neuroscience

Received: *06 September 2021*
Accepted: *06 December 2021*
Published: *14 January 2022*

Citation:
Mazzoli D, Basini G, Prati P, Galletti M, Mascioli F, Rambelli C, Zerbinati P, Campanini I and Merlo A (2022) Indices of Loading and Propulsive Ability in the Gait of Patients With Chronic Stroke With Equinus Foot Deviation: A Correlation Study. Front. Hum. Neurosci. 15:771392. doi: 10.3389/fnhum.2021.771392

INTRODUCTION

Stroke is a major cause of disability worldwide. The number of subjects facing a post-stroke condition continues to rise due to the increase and aging of the global population and to the decrease in mortality associated with acute vascular events (Patrick and Keenan, 2007; Katan and Luft, 2018) People who survive this acute event can develop pathological gait patterns,

which eventually lead to a decreased deambulatory performance in terms of walking speed, energy expenditure, safety, and pain (Kesar et al., 2011). An impaired walking ability strongly contributes to the reduction of the independence of a patient and leads to a decrease in social participation (Perry et al., 1995).

Pathological walking patterns originate from a combination of factors, including the loss in muscle strength, inappropriate muscle activation, altered exteroceptive or proprioceptive perception, and the development of joint deformities. Focusing on the lower limb, the equinus and equinovarus foot deviations (EVD, EVFD) are the most common lower limb deformity in stroke survivors (Giannotti et al., 2018) along with the limitation in knee flexion referred to as stiff knee gait (SKG) (Merlo and Campanini, 2019).

In clinical practice, the assessment of pathophysiological conditions underlying joint deviations and altered motor function typically rely on a clinical evaluation at the bedside [e.g., range of motion (ROM), force, and spasticity], on visual assessment when walking and on the use of a set of walking-related clinical scales and functional tests that are used to assess the walking ability of a patient in different settings (e.g., indoor/outdoor) with or without assistance.

When designing the rehabilitation plan for a patient, the instrumental assessment of gait can be used to answer specific questions that arise from the clinical assessment, and which cannot be answered by the clinical investigation itself (Baude et al., 2019; Campanini et al., 2020). Furthermore, in patients with stroke, the presence or absence of specific muscle activation patterns (e.g., spasticity) at the bedside evaluation, does not necessarily predict the presence or absence of the same patterns while standing and walking (Gracies, 2005; Baude et al., 2019; Merlo and Campanini, 2019; Campanini et al., 2020).

While being used in the decision-making process, a comprehensive clinical and instrumental assessment cannot be performed to monitor the patient evolution throughout the whole treatment period, due to its time requirements and costs. In literature, instrumental indices computed from ground reaction force (GRF) data, such as the dynamic loading ability (DLA) and the peak or mean dynamic propulsive ability (DPA), have been suggested to overcome this issue (Morita and Yamamoto, 1995; Turns et al., 2007; Campanini and Merlo, 2009; Raja et al., 2012; Roelker et al., 2019). Since the GRF acquisition does not require any patient prepping (e.g., markers, electrodes), this instrumental assessment can be completed in a few minutes and could be reasonably used during the rehabilitation period to complement the information provided by clinical assessments and walking speed. Moreover, the indices can be obtained even with patients wearing orthoses or using walking aids thus providing a quick tool to compare the effect of different orthoses (Bowden et al., 2006; Campanini and Merlo, 2009).

Because of the potential usefulness of DLA and DPA in the assessment of the recovery of walking ability in patients and developed EVFD, in this study, we analyzed the correlation between the clinical assessment of EVFD and walking ability and the instrumental assessment of walking provided by the indices.

MATERIALS AND METHODS

Study Design and Setting

In this correlation study, we retrospectively analyzed data from patients with stroke with chronic hemiparesis who were referred to our laboratory for the detailed identification of the causes of their joint deviations to support treatment selection.

Participants

Patients were included in this study based upon the following criteria: (1) ischemic or hemorrhagic stroke; (2) right or left hemiparesis; (3) time elapsed since the stroke >6 months; (4) ability to walk barefoot and without assistance at a self-selected speed for 10 meters; (5) available clinical and GRF data; (6) available signed informed consent of data collection and usage for clinical research purposes. The exclusion criteria were: (1) any other neurological or orthopedic disease that could limit their ability to walk; (2) any previous lower limb surgical intervention; (3) any focal inhibition on the lower limb muscles during the 6 months prior to evaluation.

This study was approved by the Local Ethics Committee (CEROM, protocol 5953/2017).

Clinical Assessment

Based on the clinical assessment we extracted the following variables from the records of the patients: age, sex, affected side, the time elapsed from stroke and its etiology, the maximum passive ankle dorsiflexion measured with the knee both extended and flexed at 90°, the plantar flexor muscles spasticity assessed by the Modified Tardieu Scale (MTS) and with the knee in both positions, and the strength of plantar and flexor muscles assessed using the Medical Research Council (MRC) scale.

Walking ability was assessed by three complementary scales: the Functional Ambulation Category (FAC), the Rivermead Mobility Index (RMI), and the Walking Handicap Scale (WHS). FAC is a quick visual measurement of walking ability (Mehrholz et al., 2007). It ranges between 0 (non-walking patient) and 5 (independent ambulator or any surface), with intermediate scores indicating the amount of assistance needed to walk. RMI ranges between 0 and 15 and covers a clinically relevant range of activities from the ability to turn in bed, to sit, to stand, walking inside and outside with and without help, up to running (Collen et al., 1991). For WHS, a range of 0–6 is used to distinguish between housebound patients and walkers with community potential (Perry et al., 1995). Direct measurement of walking speed was also recorded.

Instrumental Assessment

Force plate data, which are the focus of this study, were acquired by means of four force plates (Infinity-T, BTS Bioengineering, Milan, Italy) at a sampling frequency of 400 Hz and off-line analyzed by means of custom-made software to obtain the GRF-derived indices. During gait assessments, the patients walked barefoot at a speed they considered comfortable for spontaneous walking and no further instructions were given to them.

TABLE 1 | Demographic and clinical characteristics of the sample patients.

Characteristic	*N* = 40
Age	51 (12); 22–77
Sex, M/F	20/20
Affected side, Left/Right	20/20
Stroke onset, years	5.6 (7.0); 0.7–34.5
pADF Knee_0, deg	−6 (11); −40–10
pADF Knee_90, deg	+6 (11); −40–20
aADF Knee_0, deg	−25 (14); −55–5
aADF Knee_90, deg	−8 (12); −40–15
MTS PF Knee_0	3; 0–4
MTS PF Knee_90	3; 0–4
FAC	4; 2 – 5
RMI	12; 8–15
WHS	5; 3–6
Used orthoses	20 None; 12 AFO; 2 Peromed; 1 Dictus; 1 Foot-up; 4 other/customized

Data are reported as mean (std) and range for age, angles, and years from stroke onset, as median and range for clinical scale scores, and as count for sex, affected side, and used orthoses.

As described in a previous study by Campanini and Merlo (Campanini and Merlo, 2009), DLA was computed as the mean value of the vertical component of the ground reaction force. It refers to the weight-bearing ability over the stance foot. DPA was computed as the mean value of the positive portion (forward direction) of the fore-aft component of the ground reaction force. DPA refers to the ability to get propulsion from the stance foot (Campanini and Merlo, 2009). Both DLA and DPA are expressed as percentages of body weight (%BW). At least three trials per patient were used in this study and the indices' median values were computed and used for further analyses.

Statistical Analysis

First, descriptive statistics were used to analyze the data. Age, sex, clinical scores, and the values of instrumental indices were reported either by count or by the mean, standard deviation (SD), and range. Next, according to the aim of the study, a correlation analysis was carried out between DLA, DPA, and the structure- (RoMs, MTS) and activity-related (FAC, RMI, WHS, walking speed) variables. The non-parametric Spearman correlation index was used for all correlations because of the presence of ordinal variables and non-Gaussian distributed continuous variables. The statistical significance was set at 5%.

RESULTS

Data from 40 subjects were used in the study. There were 20 men and 20 women, with a mean age of 51 (12) years. The complete demographic and clinical data of the sample patients are reported in **Table 1**.

In the sample, walking speed was on average 0.45 (0.20) m/s, which is approximately one-third of the normal reference, and ranged between 0.1 and 1.1 m/s, indicating a level of impairment ranging from very severe to very mild (Bowden et al., 2008). Once normalized, the walking speed was, on average, 27 (12) %height/s and ranged between 5 and 68 % height/s. Despite their slowness, the sample patients exhibited—on average—moderate walking ability when assessed by clinical scales (see **Table 1**). Actually, out of 40 patients, 34 walked independently on level ground (FAC $\geq$ 4), 24 were community walkers (WHS $\geq$ 5), and 22 were able to walk on grass and uneven surfaces (RMI $\geq$ 12). These characteristics are common for post-stroke walking patients who are referred to rehabilitation services, thus supporting the external validity of the following results.

The DLA was on average 63 (12) %BW and ranged between 27 and 83 %BW. The DPA was, on average, 2.2 (1.7) %BW and ranged between 0 and 6.4 %BW. The DPA and DLA distributions are shown in **Figure 1**.

The correlation between the investigated clinical and instrumental variables is reported in **Table 2**. The scatterplots between walking speed, normalized by height, and both DLA and DPA are presented in **Figure 2**, along with the line of robust regression and the linear relationship between the indices and gait velocity.

DISCUSSION

In this study, we examined the relationship between the instrumental indices of loading and propulsive ability during gait and a set of clinical assessments associated with walking ability in a sample of patients with chronic stroke. The main finding is that DLA and DPA are correlated with all clinical variables; the only exception being passive ankle dorsiflexion measured with the extended knee. In most cases, correlations were significant at the 0.01 level.

Among all investigated variables, the strongest correlation with DLA and DPA was found when measuring walking velocity, with *rho* values similar to those reported by Campanini and Merlo (Campanini and Merlo, 2009). An increase in propulsion resulted in increased walking velocity (rho $= 0.7$, $p < 0.01$). The increase in velocity resulted in an increase in both the rising front and the peaks of the vertical GRF, which are detected by DLA (rho $= 0.8$, $p < 0.01$).

The correlation between indices and both ankle RoMs and ankle spasticity was in the order of 0.4 (see **Table 2**). This indicates a moderate association between the impairment assessed at the bedside and the weight-bearing and propulsive ability of the patient. No relationship was found between the assessment of triceps surae spasticity at the bedside and any of the scales assessing either activity or participation. As pointed out in recent literature, this confirms that the amount of triceps spasticity assessed at the bedside is not the primary cause of walking impairment in patients with acquired lower limb deformities including EVD, EVFD, and SKG (Gracies, 2005; Baude et al., 2019; Merlo and Campanini, 2019).

When focusing on clinical scales, the findings outline the difference in correlation strength among walking speed, FAC, RMI, and WHS, as can be seen both in **Table 2** and in **Figure 2**.

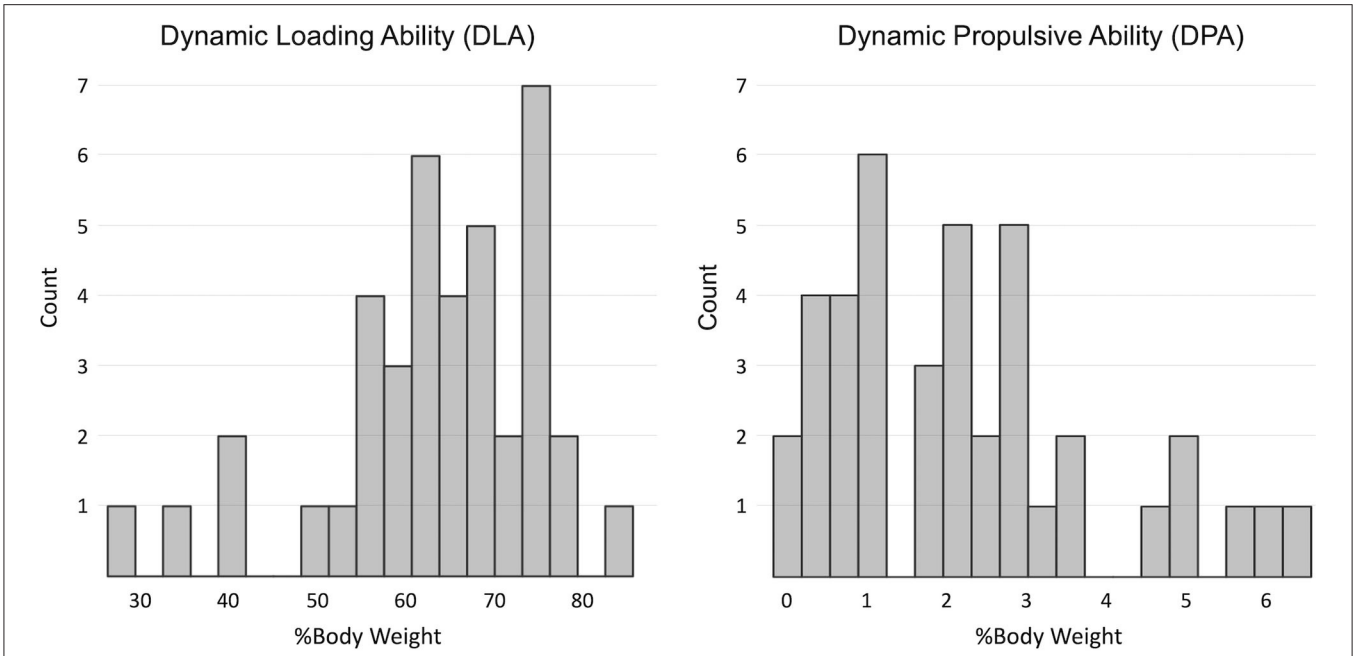

FIGURE 1 | Distribution of indices of dynamic loading ability (DLA) and dynamic propulsive ability (DPA) in the sample.

TABLE 2 | Spearman's correlation between variables typically assessed during clinical evaluation of patients with chronic stroke, related to both *Body Structures and Function* and *Activity* domains of the International Classification of Functioning, Disability and Health, and GRF-based indices of dynamic loading ability (DLA) and dynamic propulsive ability (DPA) during walking at spontaneous speed.

	Vel (%height/s)	pADF Knee_0, deg	pADF Knee_90, deg	aADF Knee_0, deg	aADF Knee_90, deg	MTS PF Knee_0, deg	MTS PF Knee_90, deg	FAC	RMI	WHS
DLA, %BW	0.796***	0.131	0.389*	0.458**	0.380*	−0.436**	−0.480**	0.296	0.328*	0.361*
DPA; %BW	0.696***	0.239	0.443**	0.460**	0.380*	−0.272	−0.478**	0.473**	0.440**	0.474**
FAC	0.275	0.221	0.274	0.342*	0.359*	0.003	−0.229	—		
RMI	0.515***	0.324*	0.356*	0.332*	0.308	−0.037	−0.189	0.770***	—	
WHS	0.395*	0.163	0.255	0.329*	0.286	0.050	−0.109	0.832***	0.838***	—

** $p < 0.05$, ** $p < 0.01$, *** $p < 0.001$.*

Vel: height normalized walking velocity; pADF Knee_0: maximum passive Ankle DorsiFlexion, with the knee extended; pADF Knee_90: maximum passive Ankle DorsiFlexion, with the knee flexed; aADF Knee_0: maximum active Ankle DorsiFlexion, with the knee extended; aADF Knee_90: maximum active Ankle DorsiFlexion, with the knee flexed; MTS PF Knee_0: Modified Tardieu Scale at the Plantar Flexor muscles, with the knee extended; MTS PF Knee_90: Modified Tardieu Scala at the Plantar Flexor muscles, with the knee flexed; FAC: Functional Ambulatory Categories; RMI: Rivermead Mobility Index; WHS: Walking handicap Scale; %BW: percentage of the Body Weight.

The covariation is especially evident for RMI, which focuses more on function rather than on the amount of assistance (FAC) and the type of surroundings needed for walking (WHS). Propulsion of the paretic limb is key in the daily life of the patients, as can be observed in **Table 2**, where DPA proved to be correlated with FAC, RMI, and WHS at the 0.01 level with *rho* approaching 0.5. Moreover, previous investigations have shown that changes in paretic propulsion correlate with the amount of lower limb muscle activity (Turns et al., 2007), walking speed (Raja et al., 2012) and walking endurance when assessed with the 6 min walking test (Awad et al., 2015).

In patients with stroke, the impairment at the gastro-soleus complex due to muscle shortening increases muscle stiffness and, in some cases, muscle overactivity affects both foot placement and balance during the stance phase, thus limiting the ability to bear the weight over the stance foot, as measured by DLA. Conversely, an extensible triceps surae allows for better foot support during stance and the forward rotation of the tibia over the stance foot (i.e., the second rocker). This results in a forward tilted GRF, which in turn generates forward propulsion, as assessed by DPA (Campanini et al., 2013). DLA and DPA encompass many different features related to body structures and body functions (e.g., ankle RoMs) that result in weight-bearing and propulsive abilities, which are essential to walking efficiency and speed.

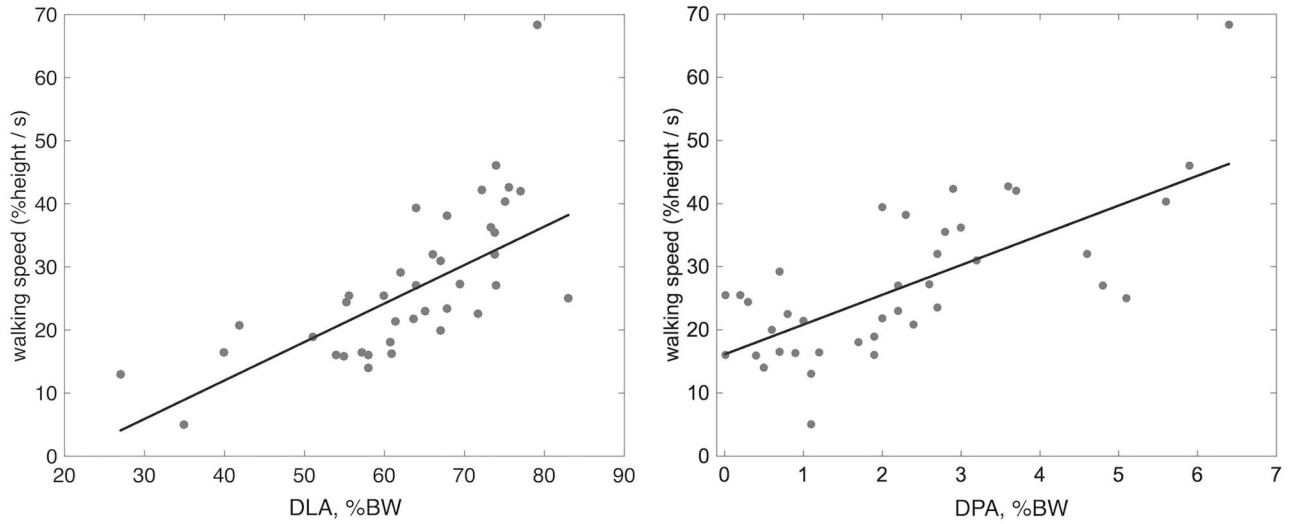

FIGURE 2 | Scatter plot with robust regression line between height normalized walking speed and the indices of DLA and DPA.

Use of DLA and DPA in Clinical Routine Assessments

The value of GRF-based indices lies in the extreme ease of this instrumental examination and in the ability to also evaluate patients who wear orthoses or use walking aids. Normative values for DPA and DLA are available in the literature and can be used when assessing patients (Campanini and Merlo, 2009).

The ability of the paretic limb to generate propulsion during walking is a critical determinant of long-distance walking function after a stroke (Awad et al., 2015).

During the rehabilitation period, DLA and DPA can be used to test whether the increased speed of the gait of the patient is due to a real recovery in the propulsion of the affected and treated limb, or due to an increase in compensation of the contralateral limb (Morita and Yamamoto, 1995). Particularly, in hemiparetic patients, the same increase in walking speed can be obtained either through the recovery of the impaired limb—as targeted by the rehabilitative intervention—or through compensatory mechanisms with greater propulsion from the contralateral limb. These two opposite behaviors can be easily recognized by the GRF-based indices, thus providing valuable feedback on the effectiveness (or lack thereof) of the ongoing rehabilitation. Although an increase in walking speed is a positive result, regardless of how it is achieved, quantitative feedback on the treatment effectiveness in terms of propulsion would allow practitioners to corroborate or modify the ongoing rehabilitative treatment. GRF-based indices further provide clinical cues, such as highlighting the presence of a braking mechanism of the lower limbs. When walking speed remains limited despite adequate propulsion, a brake must exist. This typically occurs at the knee, where flexion is stopped by the reflex activation of the quadriceps prompted precisely by the rapid knee flexion consequent to propulsion (Campanini et al., 2013; Merlo and Campanini, 2019).

Study Limitations

Univariate analysis of variable correlations was conducted for this study in line with the limited sample size ($n = 40$). However, to estimate the extent of these correlations, when the set of variables analyzed is mutually related, a multivariate approach would be more appropriate. Future studies based on larger samples could address this topic.

Conclusions

Our results support the use of DLA and DPA when measuring the overall walking ability in patients with chronic stroke. Thanks to the ease in obtaining these indices, their validity, and the availability in the literature of both their normal values and minimal detectable change, professionals could use them to quantify and monitor the motor recovery of patients with stroke during their rehabilitation.

DATA AVAILABILITY STATEMENT

The raw data supporting the conclusions of this article will be made available by the authors, without undue reservation.

ETHICS STATEMENT

This study was reviewed and approved by CEROM, protocol 5953/2017. The patients provided their written informed consent to participate in this study.

AUTHOR CONTRIBUTIONS

DM and AM: conceptualization, methodology, and supervision. GB, PP, MG, FM, CR, and PZ: data curation. AM, DM, and GB: formal analysis and writing–original draft. AM, DM, IC, and GB: writing–review and editing. All authors contributed to the article and approved the submitted version.

REFERENCES

Awad, L. N., Binder-Macleod, S. A., Pohlig, R. T., and Reisman, D. S. (2015). Paretic propulsion and trailing limb angle are key determinants of long-distance walking function after stroke. *Neurorehabil. Neural. Repair*. 29, 499–508. doi: 10.1177/1545968314554625

Baude, M., Nielsen, J. B., and Gracies, J. M. (2019). The neurophysiology of deforming spastic paresis: A revised taxonomy. *Ann Phys Rehabil Med*. 62, 426–430. doi: 10.1016/j.rehab.2018.10.004

Bowden, M. G., Balasubramanian, C. K., Behrman, A. L., and Kautz, S. A. (2008). Validation of a speed-based classification system using quantitative measures of walking performance poststroke. *Neurorehabil. Neural. Repair*. 22, 672–675. doi: 10.1177/1545968308318837

Bowden, M. G., Balasubramanian, C. K., Neptune, R. R., and Kautz, S. A. (2006). Anterior-posterior ground reaction forces as a measure of paretic leg contribution in hemiparetic walking. *Stroke*. 37, 872–876. doi: 10.1161/01.STR.0000204063.75779.8d

Campanini, I., Cosma, M., Manca, M., and Merlo, A. (2020). Added value of dynamic EMG in the assessment of the equinus and the equinovarus foot deviation in stroke patients and barriers limiting its usage. *Front. Neurol*. 11, 583399. doi: 10.3389/fneur.2020.583399

Campanini, I., and Merlo, A. (2009). Reliabilty, smallest real difference and concurrent validity of indices computed from GRF components in gait of stroke patients. *Gait Posture*. 30, 127–131. doi: 10.1016/j.gaitpost.2009.03.011

Campanini, I., Merlo, A., and Damiano, B. (2013). A method to differentiate the causes of stiff-knee gait in stroke patients. *Gait Posture*. 38, 165–169. doi: 10.1016/j.gaitpost.2013.05.003

Collen, F. M., Wade, D. T., Robb, G. F., and Bradshaw, C. M. (1991). The rivermead mobility index: A further development of the rivermead motor assessment. *Disabil. Rehabil*. 13, 50–54. doi: 10.3109/03790799109166684

Giannotti, E., Merlo, A., Zerbinati, P., Prati, P., Masiero, S., and Mazzoli, D. (2018). Safety and long term effects on gait of hemiplegic patients in equino varus foot deformity surgical correction followed by immediate rehabilitation. A prospective observational study. *Eur. J. Phys Rehabil Med*. 55, 169–175. doi: 10.23736/S1973-9087.18.05290-5

Gracies, J. M. (2005). Pathophysiology of spastic paresis II: Emergence of muscle overactivity. *Muscle Nerve*. 31, 552–571. doi: 10.1002/mus.20285

Katan, M., and Luft, A. (2018). Global Burden of Stroke. *Semin. Neurol*. 38, 208–211. doi: 10.1055/s-0038-1649503

Kesar, T. M., Binder-Macleod, S. A., Hicks, G. E., and Reisman, D. S. (2011). Minimal detectable change for gait variables collected during treadmill walking in individuals post-stroke. *Gait Posture*. 33, 314–317. doi: 10.1016/j.gaitpost.2010.11.024

Mehrholz, J., Wagner, K., Rutte, K., Meißner, D., and Pohl, M. (2007). Predictive validity and responsiveness of the functional ambulation category in hemiparetic patients after stroke. *Arch. Phys. Med. Rehabil*. 88, 1314–1319. doi: 10.1016/j.apmr.2007.06.764

Merlo, A., and Campanini, I. (2019). Impact of instrumental analysis of stiff knee gait on treatment appropriateness and associated costs in stroke patients. *Gait Posture*. 72, 195–201. doi: 10.1016/j.gaitpost.2019.06.009

Morita, S., and Yamamoto, H. F. K. G. (1995). analysis of hemiplegic patients by measurement of ground reaction force. *J Rehabil Med*. 27, 37–42. doi: 10.2340/1650197795273742

Patrick, J. H., and Keenan, M. A. E. (2007). Gait analysis to assist walking after stroke. *Lancet*. 369, 256–257. doi: 10.1016/S0140-6736(07)60124-X

Perry, J., Garrett, M., Gronley, J. K., and Mulroy, S. J. (1995). Classification of walking handicap in the stroke population. *Stroke*. 26, 982–989. doi: 10.1161/01.STR.26.6.982

Raja, B., Neptune, R. R., and Kautz, S. A. (2012). Coordination of the non-paretic leg during hemiparetic gait: Expected and novel compensatory patterns. *Clin. Biomech*. 27, 1023–1030. doi: 10.1016/j.clinbiomech.2012.08.005

Roelker, S. A., Bowden, M. G., Kautz, S. A., and Neptune, R. R. (2019). Paretic propulsion as a measure of walking performance and functional motor recovery post-stroke: A review. *Gait Posture*. 68, 6–14. doi: 10.1016/j.gaitpost.2018.10.027

Turns, L. J., Neptune, R. R., and Kautz, S. A. (2007). Relationships Between Muscle Activity and Anteroposterior Ground Reaction Forces in Hemiparetic Walking. *Arch. Phys. Med. Rehabil*. 88, 1127–1135. doi: 10.1016/j.apmr.2007.05.027

Conflict of Interest: The authors declare that the research was conducted in the absence of any commercial or financial relationships that could be construed as a potential conflict of interest.

frontiers in Human Neuroscience

ORIGINAL RESEARCH
published: 03 February 2022
doi: 10.3389/fnhum.2022.775261

Assessment of Agreement Between a New Application to Compute the Wisconsin Gait Score and 3-Dimensional Gait Analysis, and Reliability of the Application in Stroke Patients

Agnieszka Guzik, Andżelina Wolan-Nieroda and Mariusz Drużbicki*

Department of Physiotherapy, Institute of Health Sciences, Medical College, University of Rzeszów, Rzeszów, Poland

Currently, there are no computerized tools enabling objective interpretation of observational gait assessment based on Wisconsin Gait Scale (WGS), which is a reliable and well-tested tool. The solution envisaged by us may provide a practical tool for assessing gait deviations in patients with hemiparesis after stroke. The present study assessed agreement between a new application software for computerized WGS and 3-dimensional gait analysis (3DGA), and reliability of the application. The study involved 33 individuals with hemiparesis after stroke. The software was developed based on a model designed taking into account components of the WGS and incorporating auxiliary lines passing through the relevant anthropometric points on the patient's body, as well as measurements of angular values, distances and duration of the specific gait phases, which make it possible to substantiate assessment based on this scale. Series of videos were made to record gait of the qualified patients. After the gait evaluation was carried out using the app, the data were retrieved from the software. The gait assessment was performed separately by three independent examiners who reviewed the video recording using the new app twice (two weeks apart). Additionally, 3DGA was carried out for all the subjects, and the results of the app-aided assessment were compared to those acquired using 3DGA. The findings show statistically significant correlations ($p < 0.05$) between majority of the WGS items measured using the new app, and the relevant spatiotemporal and kinematic parameters identified by 3DGA. Agreement between the scores reported by the three examiners was high in both measurements, as reflected by Cronbach's alpha exceeding 0.8. The findings reflect very good intra-observer reliability (as reflected by kappa coefficients from 0.847 to 1) and inter-observer reliability (as reflected by kappa coefficients from 0.634 to 1) of the new application software for computerized WGS. The opportunities offered by the observational gait scale objectified through our new software for computerized WGS result from the fact that the tool provides a useful low-cost and time-effective feedback to monitor ongoing treatments or formulate hypotheses.

Keywords: gait analysis, observational gait analysis, 3D gait analysis, hemiparetic gait, stroke, application software

OPEN ACCESS

Edited by:
Marco Iosa,
Sapienza University of Rome, Italy

Reviewed by:
Elena Bergamini,
Foro Italico University of Rome, Italy
Adérito Ricardo Duarte Seixas,
Escola Superior de Saúde Fernando Pessoa, Portugal

****Correspondence:***
Agnieszka Guzik
agnieszkadepa2@wp.pl

Specialty section:
This article was submitted to Motor Neuroscience, a section of the journal Frontiers in Human Neuroscience

Received: *13 September 2021*
Accepted: *13 January 2022*
Published: *03 February 2022*

Citation:
Guzik A, Wolan-Nieroda A and Drużbicki M (2022) Assessment of Agreement Between a New Application to Compute the Wisconsin Gait Score and 3-Dimensional Gait Analysis, and Reliability of the Application in Stroke Patients. Front. Hum. Neurosci. 16:775261. doi: 10.3389/fnhum.2022.775261

INTRODUCTION

Given the fact that the ability to walk is crucial for personal autonomy and the quality of life, hemiparetic gait analysis is of great importance from the viewpoint of stroke rehabilitation. During the entire process, clinicians must regularly evaluate improvements in the gait of patients with stroke to assess effectiveness of treatments or therapies (Li et al., 2018; Marin et al., 2020; Sánchez and Winstein, 2021).

Objective 3-dimensional gait analysis (3DGA) is a gold standard in gait assessment since it provides a combination of kinematics, kinetic and electromyography (EMG) data, and as a result is useful in treatment selection and in clinical decision-making. Indeed, instrumental gait analysis and EMG are considered among the fundamental sources of information to drive treatment selection (McGinley et al., 2009; Campanini et al., 2020). However, 3DGA is rather costly, and the related measurements provide a large body of data to be interpreted, which may be inconvenient in the clinical setting. Due to these drawbacks, many researchers worldwide are looking for new solutions specifically enabling gait analysis in patients after stroke (Ferrarello et al., 2013; Begg et al., 2014; Solanki and Lahiri, 2018; Li et al., 2019; Tian et al., 2019; Seo et al., 2020; Iosa et al., 2021; Mohan et al., 2021; Wang et al., 2021). As an example, Seo et al. proposed an assessment method referred to as clinometric gait analysis and applying a smart insoles technology. In a pilot study, they examined twenty-two gait parameters in relation to selected stroke severity data, including scores in Fugl-Meyer Assessment (FMA) related to lower and upper limbs, the Mini–Mental State Examination as well as the Modified Barthel Index. Ten out of the 22 parameters presented significant correlations (difference in stance and swing duration, sound-side stance and swing duration, hemiplegic-side stance duration, single support time, cadence, walking speed). The researchers reported the strongest correlations between the FMA lower-extremity scores and the differences between the unaffected and hemiplegic sides in stance duration (Seo et al., 2020). Generally, however, many of these novel approaches, based on advanced technologies, may present similar practical challenges as far as their everyday use in clinical settings. Due to this, simple and affordable observational methods are still commonly used since they allow clinicians to quickly perform quantitative evaluation of deviations from normal gait patterns (Allen and Neptune, 2012; Gor-García-Fogeda et al., 2016; Estrada-Barranco et al., 2021). On the other hand, observational scales or tests apply subjective methods, naturally associated with a certain margin of error. Furthermore, since there are no consistent standards applicable to observational gait analyses, it is difficult to compare findings reported by various researchers. In view of the above, there is a need for a highly specific and accurate tool enabling both detailed evaluation of visible motor changes and effective monitoring of progress achieved in the course of rehabilitation.

The available tools for visual gait assessment include the simple Observational Gait Analysis Checklist adapted from a checklist developed by the Professional Staff Association of Rancho Los Amigos Medical Center; the former tool is based on a short list of gait deficits and the examiner is required to make yes/no decisions about their presence (Downey, 1989). Scales demonstrating a higher methodological quality and designed for use in assessing patients with central nervous system disorders include the Visual Gait Assessment Scale, Salford Gait Tool, Edinburgh Visual Gait Score (Rathinam et al., 2014; Ridao-Fernández et al., 2019) as well as Gait Assessment and Intervention Tool (Gor-García-Fogeda et al., 2016). Conversely, the Wisconsin Gait Scale (WGS), proposed in 1996 by Rodriquez et al. (1996) was specifically intended for individuals with hemiparesis after stroke. It was designed to enable quick assessment of fourteen visible gait parameters, and consequently to facilitate evaluation of progress achieved in course of rehabilitation programs specifically by patients with hemiparesis after stroke. The factors assessed using WGS include hip, knee and ankle kinematics during specific gait phases (stance and swing), spatiotemporal gait parameters (e.g., length of step, duration of stance phase on the specific sides), symmetry between the affected and unaffected sides of the body, postural balance, as well as the need for orthopedic devices (Rodriquez et al., 1996; Estrada-Barranco et al., 2021). A number of studies have demonstrated reliability and validity of WGS for gait analysis in subjects with hemiparesis after stroke (Rodriquez et al., 1996; Turani et al., 2004; Pizzi et al., 2007; Yaliman et al., 2014; Lu et al., 2015; Wellmon et al., 2015; Guzik et al., 2016; Estrada-Barranco et al., 2019, 2021; Murciano Casas et al., 2020). It has also been shown to correlate well with 3DGA and with tools assessing performance, balance, and independence at different stages of evolution post-stroke (Rodriquez et al., 1996; Turani et al., 2004; Pizzi et al., 2007; Yaliman et al., 2014; Lu et al., 2015; Wellmon et al., 2015; Guzik et al., 2016; Estrada-Barranco et al., 2019, 2021; Murciano Casas et al., 2020). Obviously, in addition to the positive metric properties, the WGS also presents a limitation as regards the final score because to sum up arbitrary ordinal item scores into a total score and treating this score as a number is methodologically wrong (Boateng et al., 2018).

Currently, no computerized tools are available to facilitate the use and objective interpretation of observational gait assessment performed using WGS, which is a reliable and well-tested tool (Rodriquez et al., 1996; Turani et al., 2004; Pizzi et al., 2007; Yaliman et al., 2014; Lu et al., 2015; Wellmon et al., 2015; Guzik et al., 2016; Estrada-Barranco et al., 2019, 2021). The solution envisaged by us may provide a fast, simple and useful tool for assessing gait deviations in patients with hemiparesis after stroke. Hence, the study presents an innovative approach in the area of clinimetrics, since no attempts have previously been made to objectify the descriptive WGS whose high biometric value (psychometric properties) has been demonstrated by a number of studies (Rodriquez et al., 1996; Turani et al., 2004; Pizzi et al., 2007; Yaliman et al., 2014; Lu et al., 2015; Wellmon et al., 2015; Guzik et al., 2016; Estrada-Barranco et al., 2019, 2021; Murciano Casas et al., 2020). The gains of this novel approach are linked with the fact that the new application software, taking into account analysis of a given person's gait pattern, will create a quantitative representation of gait and will make it possible to record the results using a standardized template. The ultimate objective of the project was to develop a computer-aided observational assessment tool which may be helpful for

clinicians in formulating hypotheses on clinical outcomes, and in monitoring the effectiveness of the ongoing rehabilitative treatments for patients with hemiparetic gait.

The present study aimed to test the agreement between the data collected by the new application software for computerized WGS and the data acquired using 3DGA; it also assessed the intrarater and interrater reliability of the data collected by the application.

METHODS

Sample Size

The minimum sample size for the population investigated was determined using sample size calculator ("PLUS module" from Statistica 13.3 software), taking into account the number of individuals with stroke receiving treatment in the rehabilitation clinic in one year, and with the following parameters specified: a fraction size 0.9, a maximum error of 6%, and a 95% confidence level. Ultimately, a sample size of 31 patients was determined.

The following formula was used for the sample size calculation:

$$\mathrm{N\,min} = \frac{\mathrm{NP}[\alpha 2 \cdot \mathrm{f}(1-\mathrm{f})]}{\mathrm{NP} \cdot \mathrm{e}2 + \alpha 2 \cdot \mathrm{f}(1-\mathrm{f})}$$

*N*min – minimum sample size
NP – size of the population from which the sample is drawn
α – level of confidence for the results
f - fraction size
e – expected maximum error

Participants

The study group consisted of thirty-three individuals (24 males, 9 females; aged 42–79 years) after a single ischemic stroke, at least 6 months from the incident (46.3 ± 44.14 months post-stroke), diagnosed with post-stroke hemiparesis, and able to walk a distance of 10 meters without assistance of another person. Ambulatory assistive devices were permitted during the trials (see **Table 1** for the characteristics of the study participants). Patients unable to follow instructions and those with walking skills impaired due to orthopedic or other neurologic conditions were excluded from the study. The study protocol was reviewed and accepted by the local Bioethics Commission at University of Rzeszow's Medical Faculty. The study design complied with the Declaration of Helsinki. All the study participants gave their informed consent in writing.

Measures

The newly developed application software, dedicated to WGS, comprises 14 items related to assessment of the specific gait phases: stance phase, toe off, swing phase, and heel strike. All these items are rated on a 3-point scale, except for Item 1 which is rated on a 5-point scale, and Item 11 rated on a 4-point scale. The subjects can obtain a maximum score of 42 points and a minimum score of 13.35, a lower score reflecting higher quality of the gait pattern (Rodriquez et al., 1996). We developed the code, and a system comprising a module for analysis of images, a database making it possible to process the data collected by the image analysis module, as well as a module for reporting the data from the conducted examinations. The software implements the Model-View-Controller (MVC) design pattern and was executed using technologies and solutions that enable running applications in a standard PC environment (web browser). The system uses a relational database as well as object-oriented programming and scripting languages. Data analysis and data processing take place in a dedicated reporting module which makes it possible to export data to an Excel format. The software, based on a developed model utilizing the components of WGS, was additionally provided with auxiliary lines passing through the relevant anthropometric points on the patient's body, as well as measurements of angular values, distances and duration of the specific gait phases, which make it possible to substantiate assessment based on this scale. The assessments were carried out on selected frames matching specific WGS items (auxiliary lines and angles were marked on the specific freeze frames matched to the WGS items). A detailed description of the method applied in drawing the auxiliary lines and angles for the specific items assessed by the app is presented in **Supplementary Table 1**. Sample assessment of selected gait parameters are shown in **Figure 1**.

Series of videos were made to record gait of the patients enrolled in the study. The video recording and the 3D recording were done simultaneously, with two video cameras (BTS Vixta, BTS Bioengineering Corp., Brooklyn, NY, United States) working in synchronicity, and the recording was done in both the sagittal and the frontal plane. The walking distance of 10 meters was defined. A minimum of 6 walks were recorded, including 3 walks involving the affected and 3 walks involving the unaffected side. During the trials the participants walked at a comfortable (self-selected) speed, and were permitted to use their orthopedic aids. After the gait analysis was carried out using the app, the data were retrieved from the software. The gait analysis was performed separately by three independent examiners who reviewed the video recording using the new app twice (two weeks apart). Finally, the results of the app-aided assessment were compared to those obtained using 3DGA.

The 3DGAs were performed with a motion capture system (BTS SMART-DX 700, 250 Hz) comprising two force-plates, six

TABLE 1 | Characteristics of the study participants.

Subject (*N* = 33)	
Gender (females/males), *N*	9/24
Hemiparesis (left/right), *N*	12/21
Age (years), Mean (SD)	60.75 (9.7)
Mass (kg), Mean (SD)	73 (8.3)
Height (m), Mean (SD)	1.71 (0.9)
Time since stroke (months), Mean (SD)	46.3 (44.14)
Gait speed (m/s), Mean (SD)	0.75 (0.24)
Fugl-Meyer (lower limb) score, Mean (SD)	23.4 (3.6)

N, number of subjects; SD, standard deviation.

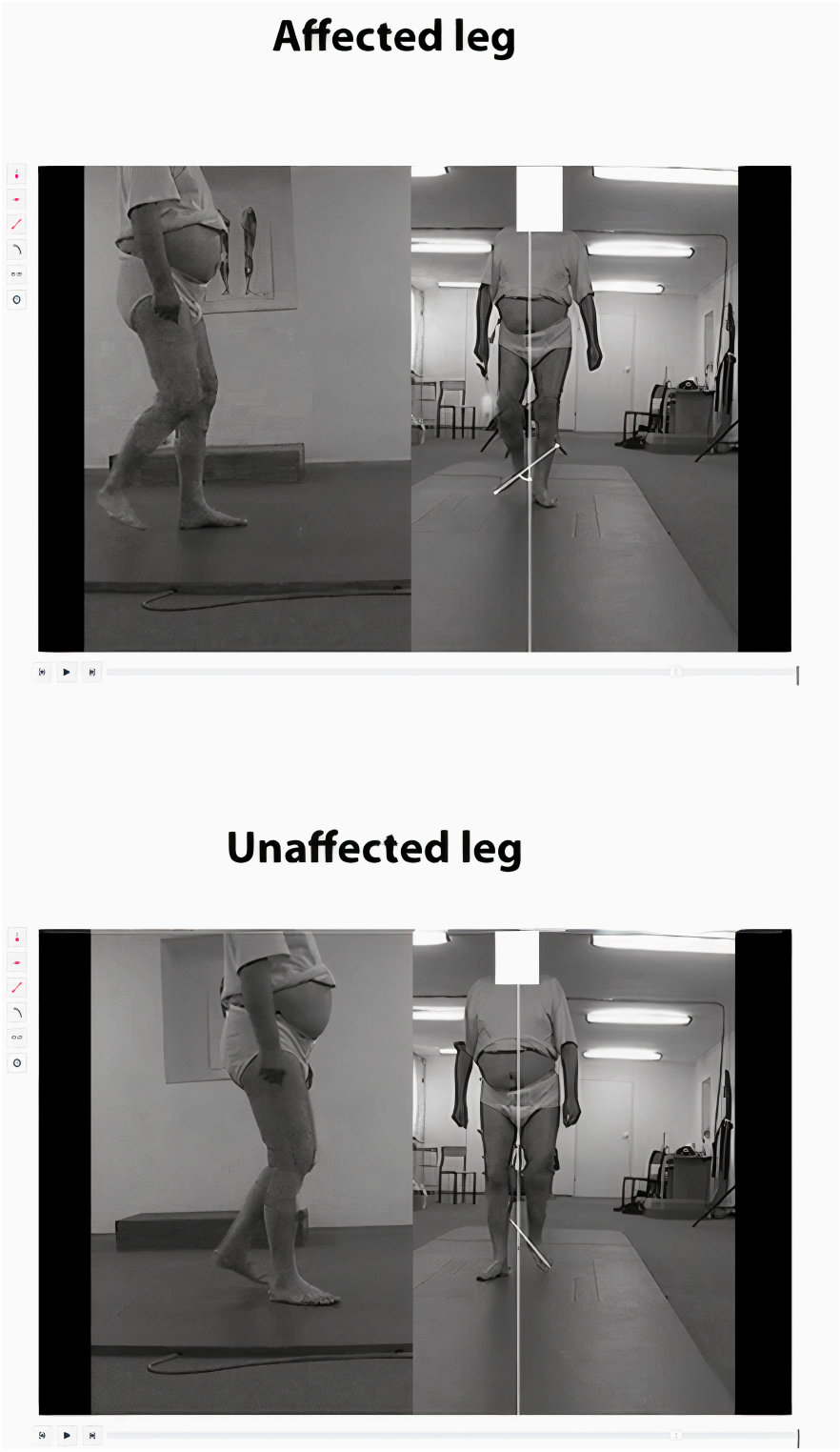

FIGURE 1 | A new application for computerized gait analysis. Subject with right hemiparesis after stroke. Sample assessment of a selected gait parameter in WGS. Swing phase of the affected leg - external rotation during initial swing. On the freeze frame showing the frontal view, we draw two auxiliary straight lines and measure the angle between them. One line shows the direction of gait and runs in the middle of the distance between the medial malleoli, and the other line marks the long axis of the foot (in the middle of the distance between the heads of the first and the fifth metatarsal bones or between the calcaneal tuber and the second toe). The result is compared to the healthy leg. The examiner checks the angles measured and determines the rating (the same angles in both legs, reflecting a normal condition - 1 point; greater angle on the paretic side, but lower than 45 degrees - 2 points; angle exceeding 45 degrees on the paretic side - 3 points).

cameras as well as the related software, with SMART Capture, Tracker and Analyzer functions. Passive markers were placed on the participants' skin, in compliance with Davis Marker Placement system (Davis et al., 1991). During the examination, six or more passages over a distance of 10 meters were recorded for each subject. The participants were instructed to walk at a pace that felt natural to them. Tracker and Analyzer programs (BTS Bioengineering) were applied to compute the mean values of spatiotemporal and kinematic measures based on complete records. Further analyses took into account the following parameters: (1) spatiotemporal: stance time, step length, step width, and (2) kinematic parameters of hip in sagittal, frontal and transverse planes, knee in sagittal plane, and ankle joints as well as pelvis in frontal and transverse planes.

Data Analysis

The acquired materials were subjected to statistical analyses using Statistica 13.3. Distributions of the investigated variables were examined for normality using Shapiro—Wilk W-test. The descriptive statistics computed for the numerical variables (parameters from computerized WSG and 3DGA) included the mean, median, minimum, and maximum values, the first and third quartile, as well as standard deviation.

Data Analysis Strategy to Test the Agreement Between Data Collected by the Application for Computerized WSG and Data From 3-Dimensional Gait Analysis

Correlation of two variables failing to meet the criterion of normality of distribution was determined using Spearman's rank correlation coefficient ($0.3 \leq |R| < 0.5$ low correlation; $0.5 \leq |R| < 0.7$ moderate correlation; $0.7 \leq |R| < 0.9$ strong correlation; $0.9 \leq |R| < 1$ very strong correlation) (Mukaka, 2012). Analyses were carried out to examine the potential correlations between the matching pairs of variables assessed using the WGS App and 3D Gait Analysis, i.e., we investigated whether the results in the specific items of gait assessment in the WGS App correlated with the results for the corresponding spatiotemporal and kinematic parameters in 3DGA. Statistical significance was assumed if $p < 0.05$. The following matching pairs of variables were defined:

- App stance time on affected side versus 3DGA stance time [s] on affected side (it was assumed that longer 3DGA stance time [s] on affected side was better, corresponding to a lower score (better result) in App stance time on affected side) (Patterson et al., 2008; Mukaino et al., 2016).
- App step length on unaffected side versus 3DGA step length [m] on unaffected side (it was assumed that greater 3DGA step length [m] on unaffected side was better, corresponding to a lower score (better result) in App step length on unaffected side) (Oken and Yavuzer, 2008; Patterson et al., 2008; Lauzière et al., 2014).
- App weight shift to affected side versus 3DGA pelvic oblique range of motion (ROM) on affected side (it was assumed that higher value of 3DGA pelvic oblique range of motion (ROM) on affected side was better, corresponding to a lower score (better result) in App weight shift to affected side)
- App stance width versus 3DGA step width [m] (it was assumed that lower value of 3DGA step width [m] was better, corresponding to a lower score (better result) in App stance width) (Mukaino et al., 2016).
- App guardedness (pause prior to advancing affected leg) versus 3DGA stance time [s] on unaffected side (it was assumed that shorter 3DGA stance time [s] on unaffected side was better, corresponding to a lower score (better result) in App guardedness) (Mukaino et al., 2018).
- App hip extension on affected side versus 3DGA hip flexion/extension (FE) ROM on affected side (it was assumed that higher value of 3DGA hip FE ROM on affected side was better, corresponding to a lower score (better result) in App hip extension on affected side) (Kim and Eng, 2004; Boudarham et al., 2013).
- App external rotation during initial swing on affected side versus 3DGA hip internal/external rotation (IE) ROM on affected side (it was assumed that lower value of 3DGA hip IE ROM on affected side was better, corresponding to a lower score (better result) in App external rotation during initial swing of affected side).
- App circumduction at mid swing on affected side versus 3DGA hip abduction/adduction (AA) ROM on affected side (it was assumed that lower value of 3DGA hip AA ROM on affected side was better, corresponding to a lower score (better result) in App circumduction at mid swing on affected side).
- App hip hiking at mid swing on affected side versus 3DGA hip FE ROM and pelvic oblique ROM on affected side (it was assumed that higher value of 3DGA hip FE ROM on affected side and lower value of 3DGA pelvic oblique ROM on affected side were better, corresponding to a lower score (better result) in App hip hiking at mid swing on affected side) (Mukaino et al., 2018).
- App knee flexion from toe off to mid swing on affected side versus 3DGA knee FE ROM on affected side (it was assumed that higher value of 3DGA knee FE ROM on affected side was better, corresponding to a lower score (better result) in App knee flexion from toe off to mid swing on affected side) (Matsuda et al., 2016; Mukaino et al., 2018; Haruyama et al., 2021).
- App toe clearance on affected side versus 3DGA total between ankle flex in initial contact phase (IC) and ankle flex in toe off phase (TO) on affected side (it was assumed that higher 3DGA total between ankle flex IC and ankle flex TO on affected side was better; patient more effectively controls the foot, and during the swing phase there is a lower risk of toe catch, while the ankle remains in dorsiflexion until it reaches the natural position; this corresponds to a lower score (better result) in App toe clearance on affected side) (Matsuda et al., 2016; Haruyama et al., 2021).
- App pelvic rotation at terminal swing on affected side versus 3DGA pelvic rotation ROM on affected side (it was assumed that higher value of 3DGA pelvic rotation ROM

on affected side was better, corresponding to a lower score (better result) in App pelvic rotation at terminal swing on affected side).
- App initial foot contact on affected side versus 3DGA ankle flex IC on affected side (it was assumed that the value of 3DGA ankle flex IC on affected side closer to zero was better, corresponding to a lower score (better result) in App initial foot contact on affected side).

The Data Analysis Strategy to Test the Agreement of the Data Collected by the Application for Computerized WSG (Reliability)

The differences in the median levels of a numerical characteristic were assessed using Kruskal—Wallis ANOVA, which was applied to compare the results obtained by the three independent examiners during measurement 1 and measurement 2. On the other hand, Wilcoxon signed-rank test was applied to compare results identified by the same examiner in measurement 1 and measurement 2. Internal reliability of the tool was measured using Cronbach's alpha. Inter- and intrarater reliability for qualitative variables was assessed with kappa coefficient. Cohen's version was used for two measurements whereas Fleiss' version was applied for more than two measurements. Significance level for all statistical tests was set to 0.05.

RESULTS

Descriptive statistics summarizing the trends in all the measures of computerized WSG and 3DGA are shown in **Supplementary Tables 2, 3**, respectively (**Supplementary Materials**).

Agreement Between the Data Collected by the Application for Computerized WGS and the 3-Dimensional Gait Analysis Data

Statistically significant correlations were identified between majority of the scores in gait assessment carried out using the newly developed application software and the matching spatiotemporal or kinematic parameters measured with 3DGA. Strong correlations ($0.7 \leq |R| < 0.9$) were found between the following pairs: WGS App external rotation during initial swing affected side versus 3DGA hip IE ROM affected side, as well as WGS App circumduction at mid swing affected side versus 3DGA hip AA ROM affected side. Moderate correlations ($0.5 \leq |R| < 0.7$) were found in the case of: WGS App step length unaffected side versus 3DGA stride length unaffected side, WGS App hip extension affected side versus 3DGA hip FE ROM affected side, WGS App external rotation during initial swing affected side versus 3DGA hip IE ROM affected side, WGS App circumduction at mid swing affected side versus 3DGA hip AA ROM affected side, WGS App hip hiking at mid swing affected side versus 3DGA hip FE ROM affected side, WGS App knee flexion from toe off to mid swing affected side versus 3DGA knee FE ROM affected side, WGS App toe clearance affected side versus 3DGA total ankle flex IC and ankle flex TO affected side, as well as WGS App initial foot contact affected side versus 3DGA ankle flex IC affected side. Low correlations ($0.3 \leq |R| < 0.5$) were identified between the pairs: WGS App stance time affected side versus 3DGA stance time affected side, WGS App step length unaffected side versus 3DGA step length [m] unaffected side, WGS App stance width versus 3DGA step width, WGS App hip extension affected side versus 3DGA hip FE ROM affected side, WGS App circumduction at mid swing affected side versus 3DGA hip AA ROM affected side, as well as WGS App pelvic rotation at terminal swing affected side versus 3DGA pelvic rotation ROM affected side. Statistically significant correlations were identified in both assessments performed by all three examiners (**Supplementary Table 4**).

The findings show no statistically significant correlations only in the case of three pairs of variables: WGS App weight shift to affected side versus 3DGA pelvic oblique ROM affected side, WGS App guardedness versus 3DGA stance time affected side, and WGS App hip hiking at mid swing affected side versus 3DGA pelvic oblique ROM affected side (**Supplementary Table 5**).

Agreement of the Data Collected by the Application for Computerized WSG (Reliability)

Reliability of Computerized WGS Values as Assessed by the Therapists

The results obtained by the three examiners did not differ significantly in measurements 1 and 2 (**Table 2**). At the next stage the results obtained by the specific therapists were examined for correlations. It was shown that there were no statistically significant differences between the results obtained in measurement 1 and 2 by the specific examiners.

Intrarater and Interrater Reliability

Intrarater reliability was measured using Cronbach's alpha. Agreement between the scores reported by the three examiners was high in both measurements, as reflected by Cronbach's alpha exceeding 0.8 (**Table 3**). Inter- and intrarater reliability was assessed with kappa coefficient. Comparative analysis of two measurements performed by the same examiner (intrarater reliability), showed very high and in some cases perfect agreement for all three examiners, as reflected by kappa coefficients ranging from 0.847 to 1 (from 91.92% to 100% agreement) – **Table 4**. Comparison of measurements performed by three examiners (interrater reliability), in both measurements showed moderate to perfect agreement, as reflected by kappa coefficients from 0.634 to 1 (from 72.73% to 100% agreement) – **Table 5**.

DISCUSSION

This study investigated agreement between data collected by a new application software for computerized WGS and 3DGA data, and reliability of the data collected by the application. We initiated the related research since the qualitative and quantitative methods most commonly used to evaluate walking ability in patients, in addition to certain advantages also present serious

TABLE 2 | Comparison of the results obtained by three independent examiners in measurement 1 and measurements 2.

Items of computerized WGS	Comparison of the results obtained by three independent examiners in measurement 1 p	Comparison of the results obtained by three independent examiners in measurement 2 p
STANCE PHASE AFFECTED LEG use of hand-held gait aid	1.000	1.000
stance time on affected side	0.991	0.916
step length on unaffected side	0.656	0.555
weight shift to affected side	0.960	0.943
stance width	0.820	0.994
TOE OFF AFFECTED LEG guardedness (pause prior to advancing affected leg)	0.643	0.633
hip extension on affected side	0.635	0.480
SWING PHASE AFFECTED LEG external rotation during initial swing	0.922	0.864
circumduction at mid swing	0.807	0.689
hip hiking at mid swing	0.970	0.884
knee flexion from toe off to mid swing	1.000	1.000
toe clearance	1.000	1.000
pelvic rotation at terminal swing	1.000	1.000
HEEL STRIKE AFFECTED LEG initial foot contact	1.000	1.000
points – final score	0.970	0.964

p, probability index in Kruskal—Wallis ANOVA.

TABLE 3 | Agreement between measurements 1 and 2 performed by examiners 1,2 and 3.

Cronbach's alpha	Examiner 1		Examiner 2		Examiner 3	
	1	2	1	2	1	2
	0.84	0.83	0.81	0.81	0.81	0.81
STANCE PHASE AFFECTED LEG use of handheld gait aid	0.83	0.82	0.80	0.80	0.81	0.80
stance time on affected side	0.83	0.82	0.80	0.80	0.80	0.79
step length on unaffected side	0.82	0.80	0.79	0.80	0.80	0.80
weight shift to affected side	0.86	0.85	0.84	0.83	0.83	0.83
stance width	0.85	0.83	0.81	0.81	0.82	0.81
TOE OFF AFFECTED LEG guardedness (pause prior to advancing affected leg)	0.83	0.82	0.81	0.80	0.81	0.80
hip extension on affected side	0.83	0.81	0.80	0.80	0.80	0.80
SWING PHASE AFFECTED LEG external rotation during initial swing	0.83	0.80	0.79	0.80	0.80	0.79
circumduction at mid swing	0.82	0.80	0.77	0.77	0.80	0.79
hip hiking at mid swing	0.82	0.80	0.79	0.79	0.80	0.79
knee flexion from toe off to mid swing	0.81	0.79	0.77	077	0.78	0.77
toe clearance	0.84	0.82	0.80	0.80	0.81	0.80
pelvic rotation at terminal swing	0.82	0.80	0.77	0.77	0.79	0.78
HEEL STRIKE AFFECTED LEG initial foot contact	0.81	0.79	0.76	0.76	0.78	0.77

drawbacks, and due to this there is a need to objectify the descriptive gait analysis.

The results of the app-aided assessment were compared to those obtained using 3DGA. We examined the correlations with fourteen 3D gait parameters, which included spatiotemporal and kinematic measures. We matched the corresponding 3D parameters with the specific items of gait assessment performed using the application software dedicated to the WGS, which is designed to evaluate a variety of factors, including spatial (step length, stance width), temporal (stance time) as well as kinematic (pelvic, hip, knee, ankle ROM) parameters of gait. The latter aspect explains the value of WSG and the advantages it presents

TABLE 4 | Comparison of two measurements performed by the same examiner (intrarater reliability), for all three examiners.

Items of computerized WGS	Kappa coefficient	95% Confidence Interval		Agreement	Interpretation
STANCE PHASE AFFECTED LEG use of hand-held gait aid	1.000	1.000	1.000	100.00%	Perfect
stance time on affected side	0.921	0.847	0.996	95.6%	Nearly perfect
step length on unaffected side	0.902	0.810	0.995	95.6%	Nearly perfect
weight shift to affected side	0.896	0.816	0.977	93.4%	Strong
stance width	0.895	0.806	0.984	94.5%	Strong
TOE OFF AFFECTED LEG guardedness (pause prior to advancing affected leg)	0.847	0.750	0.944	91.2%	Strong
hip extension on affected side	0.898	0.813	0.984	94.5%	Strong
SWING PHASE AFFECTED LEG external rotation during initial swing	0.981	0.945	1.000	98.9%	Nearly perfect
circumduction at mid swing	0.965	0.916	1.000	97.8%	Nearly perfect
hip hiking at mid swing	0.983	0.948	1.000	98.9%	Nearly perfect
knee flexion from toe off to mid swing	1.000	1.000	1.000	100.00%	Perfect
toe clearance	1.000	1.000	1.000	100.00%	Perfect
pelvic rotation at terminal swing	1.000	1.000	1.000	100.00%	Perfect
HEEL STRIKE AFFECTED LEG initial foot contact	1.000	1.000	1.000	100.00%	Perfect

TABLE 5 | Comparison of measurements performed by three different examiners (interrater reliability), in both examinations.

Items of computerized WGS	Kappa coefficient	95% Confidence Interval		Agreement	Interpretation
STANCE PHASE AFFECTED LEG use of hand-held gait aid	1.000	1.000	1.000	100.00%	Perfect
stance time on affected side	0.902	0.816	0.980	92.42%	Nearly perfect
step length on unaffected side	0.634	0.458	0.783	77.27%	Moderate
weight shift to affected side	0.706	0.578	0.822	74.24%	Moderate
stance width	0.789	0.664	0.895	84.85%	Moderate
TOE OFF AFFECTED LEG guardedness (pause prior to advancing affected leg)	0.655	0.512	0.778	72.73%	Moderate
hip extension on affected side	0.715	0.589	0.845	78.79%	Moderate
SWING PHASE AFFECTED LEG external rotation during initial swing	0.794	0.670	0.900	83.33%	Moderate
circumduction at mid swing	0.859	0.750	0.947	87.88%	Strong
hip hiking at mid swing	0.948	0.878	1.000	95.45%	Nearly perfect
knee flexion from toe off to mid swing	1.000	1.000	1.000	100.00%	Perfect
toe clearance	1.000	1.000	1.000	100.00%	Perfect
pelvic rotation at terminal swing	1.000	1.000	1.000	100.00%	Perfect
HEEL STRIKE AFFECTED LEG initial foot contact	1.000	1.000	1.000	100.00%	Perfect

over other scales as regards evaluation of gait in individuals with hemiparesis post-stroke (Gor-García-Fogeda et al., 2016; Estrada-Barranco et al., 2019, 2021). Of the fourteen spatiotemporal and kinematic 3D gait parameters, eleven showed significant correlations. This means that both the kinematic measures related to lower limb joints (hip, knee, and ankle) and the spatial measures of gait determined using the newly developed application software are highly consistent with the results of 3DGA, which is the most objective method enabling evaluation of walking ability. This suggests that the proposed application software dedicated to the WGS is a promising tool for gait analysis. We should also point out, however, that Rathinam et al. performed a systematic review of observational gait assessment tools, in terms of their validity and consistency relative to instrumented gait analysis methods. They reported that none of the observational tools were as reliable as the instrumented methods, even though the Edinburgh Visual Gait Score was found to achieve a greater level of consistency, compared to the other tools. The authors also point out that there are very few studies investigating these specific observational tools, hence there is insufficient evidence to determine their clinical validity (Rathinam et al., 2014).

In the present study, no statistically significant correlations were identified only in the case of three matching pairs of

variables: WGS App weight shift to affected side versus 3DGA pelvic oblique ROM affected side; WGS App hip hiking at mid swing affected side versus 3DGA pelvic oblique ROM affected side; and WGS App guardedness versus 3DGA stance time affected side. The only 3D kinematic parameter which did not correlate with the matching measure of gait determined using the WGS App was pelvic oblique ROM on affected side. We believe this may be linked to the fact that in order to calculate pelvic oblique ROM in 3DGA in line with Davis Marker Placement system, the passive markers are positioned on the pelvis on the anterior and posterior iliac spine (Davis et al., 1991), which may be problematic in the case of patients after stroke, frequently presenting with obesity. It is very difficult to find the accurate place and to position the marker in the required anthropometric point on the pelvis of a patient with obesity because the marker moves with a skin fold or it is frequently partly covered up by the abdominal walls; this may adversely affect accurate recording of pelvic oblique ROM. On the other hand, the lack of statistically significant correlations between WGS App guardedness (pause prior to advancing affected leg) and 3DGA stance time affected side possibly reflects the fact that matching the former measure with the corresponding 3DGA parameter was problematic. Basically, no 3DGA parameter corresponds to guardedness options described in the WGS as "good forward momentum with no hesitancy noted, or slight/marked hesitation." Because of this we hypothesized that greater hesitancy or guardedness before advancing affected leg would correspond to longer stance time in seconds. However, the findings do not support this assumption. It is likely that guardedness, i.e., pause prior to advancing affected leg, may be related to a number of factors, such as fear of falling, and due to this we are unable to select one corresponding 3DGA parameter matching the measure of guardedness.

The findings show very good intra- and inter-observer reliability of the new application software. The gait assessment was performed separately by three independent examiners who reviewed the video recording using the new app twice (two weeks apart). Pasqual Marques et al. investigated inter- and intra-observer reliability of hip flexion and abduction measurements performed using computerized photogrammetry and universal goniometer. In that study two independent examiners conducted the measurements twice (one week apart). The authors also concluded that assessments performed using computerized photogrammetry and universal goniometer were highly reliable, while the correlations between measurements of flexion and abduction based on the two methods were either excellent or very good, meaning that both methods were valid (Pasqual Marques et al., 2017). Notably, some free tools available today make it possible to assess some kinematic characteristics, based on good quality videos. One of these is Kinovea, a free open-source tool intended for sport analysis, and making it possible to record, slow down, compare, annotate as well as measure motion in videos. In fact, research has shown that Kinovea software is a valid and reliable tool (Puig-Diví et al., 2019).

In summary, the analyses based on Spearman's rank correlation coefficient provided evidence that the results of computerized WGS and 3DGA were similar. This could lead us to a conclusion that an examiner using computerized WGS would be able to see and describe gait with similar accuracy to that achieved by a 3D system. Generally, the findings suggest that this is a tool which will make it possible to clarify disputable situations during assessments based on the WGS. In fact, we have aimed to develop a tool which will make it easier to take decisions, and will facilitate interpretation of observations during the rating process performed with the WGS, based on an optical tool. The WGS is the essential component of the tool, whereas the processing and viewing of the video recording enabled by the app is intended to facilitate accurate scoring in that scale. Our study has demonstrated very good intra- and inter-observer reliability of the new application software which means that owing to the support of the app, WGS-based measurements performed twice by three examiners provide highly consistent information. Generally, the tool which we developed was not intended to replace the existing and available instruments but rather it was designed to facilitate and improve objectivity of assessments performed with the reliable and valid WGS (Rodriquez et al., 1996; Turani et al., 2004; Pizzi et al., 2007; Yaliman et al., 2014; Lu et al., 2015; Wellmon et al., 2015; Guzik et al., 2016; Estrada-Barranco et al., 2019, 2021; Murciano Casas et al., 2020). If the ability of the App to identify changes promoted by treatments (sensitivity of the tool) can be demonstrated, the tool may prove to be useful in the daily practice of clinical professionals.

Limitations

The first limitation is related to the Davis protocol applied in the study, and in particular to assessment of ankle kinematics, since the equinovarus foot deformity is the most common deviation in stroke survivors, but unfortunately this is not measured by the Davis protocol. We applied the Davis Protocol because it is the most commonly used gait analysis procedure (Tenore et al., 2006), however we are aware of the limitations related to that protocol. Furthermore, no control group was included in the study and the simultaneous very good intra- and inter-observer reliability of the new application software has only been confirmed for patients at a chronic phase of recovery after stroke. It would be justified to carry out another study with a similar design in a group of patients at an early phase of recovery post-stroke, in order to evaluate the ability of the proposed software to discriminate between different levels of motor ability/pathology severity. Moreover, it is necessary to carry out further research to investigate the sensitivity of the tool to changes resulting from treatments applied and rehabilitation programs implemented. Another limitation is related to the fact that, in line with the EU regulation 2017/745 the proposed app is a medical device. This means that it requires a certification procedure before being used with patients and before being proposed to other users.

CONCLUSION

The findings show very good intra- and inter-observer reliability of the new application software enabling computerized WGS

evaluation of gait in individuals with post-stroke hemiparesis. The opportunities offered by the observational gait scale objectified through our new software for computerized WGS result from the fact that the tool provides a useful low-cost and time-effective feedback to monitor ongoing treatments or formulate hypotheses. It is necessary to carry out further research to assess the sensitivity of the tool to changes produced by treatments and rehabilitation programs.

DATA AVAILABILITY STATEMENT

The raw data supporting the conclusions of this article will be made available by the authors, without undue reservation.

ETHICS STATEMENT

The studies involving human participants were reviewed and approved by Bioethics Committee of the University of Rzeszów. The patients/participants provided their written informed consent to participate in this study.

AUTHOR CONTRIBUTIONS

AG: conceptualization, methodology, investigation, formal analysis, and writing—original draft preparation. MD and AW-N: investigation, data curation, and writing—review and editing. All authors contributed to the article and approved the submitted version.

FUNDING

This research project receives grant from the Operational Program of the Podkarpackie Region, Poland. The research project is entitled: "Development of an innovative gait assessment method for the needs of medical rehabilitation, with the use of application software enabling image analysis" RPPK.01.02.00-18-0041/18.

SUPPLEMENTARY MATERIAL

The Supplementary Material for this article can be found online at: https://www.frontiersin.org/articles/10.3389/fnhum.2022.775261/full#supplementary-material

REFERENCES

Allen, J. L., and Neptune, R. R. (2012). Three-dimensional modular control of human walking. *J. Biomech.* 45, 2157–2163. doi: 10.1016/j.jbiomech.2012.05.037

Begg, R. K., Tirosh, O., Said, C. M., Sparrow, W. A., Steinberg, N., Levinger, P., et al. (2014). Gait training with real-time augmented toe-ground clearance information decreases tripping risk in older adults and a person with chronic stroke. *Front. Hum. Neurosci.* 8:243. doi: 10.3389/fnhum.2014.00243

Boateng, G. O., Neilands, T. B., Frongillo, E. A., Melgar-Quiñonez, H. R., and Young, S. L. (2018). Best Practices for Developing and Validating Scales for Health. *Soc. Behav. Res.* 11:149. doi: 10.3389/fpubh.2018.00149

Boudarham, J., Roche, N., Pradon, D., Bonnyaud, C., Bensmail, D., and Zory, R. (2013). Variations in kinematics during clinical gait analysis in stroke patients. *PLoS One* 8:e66421. doi: 10.1371/journal.pone.0066421

Campanini, I., Disselhorst-Klug, C., Rymer, W. Z., and Merletti, R. (2020). Surface EMG in Clinical Assessment and Neurorehabilitation: barriers Limiting Its Use. *Front. Neurol.* 2:934. doi: 10.3389/fneur.2020.00934

Davis, R. B., Õunpuu, S., Tyburski, D., and Gage, J. R. (1991). A gait analysis data collection and reduction technique. *Hum. Mov. Sci.* 10, 575–587.

Downey, C. A. (1989). *Observational gait analysis handbook. Professional Staff Association.* Washington: Rancho Los Amigos Medical Center Press.

Estrada-Barranco, C., Abuín-Porras, V., López-Ruiz, J., Sanz-Esteban, I., Molina-Rueda, F., and Cano-de-la-Cuerda, R. (2021). Spanish Cross-Cultural Adaptation of the Wisconsin Gait Scale. *Int. J. Environ. Res. Public Health* 18:6903. doi: 10.3390/ijerph18136903

Estrada-Barranco, C., Cano-De-La-Cuerda, R., and Molina-Rueda, F. (2019). Construct validity of the Wisconsin Gait Scale in acute, subacute and chronic stroke. *Gait Posture.* 68, 363–368. doi: 10.1016/j.gaitpost.2018.12.020

Ferrarello, F., Bianchi, V. A., Baccini, M., Rubbieri, G., Mossello, E., Cavallini, M. C., et al. (2013). Tools for observational gait analysis in patients with stroke: a systematic review. *Phys. Ther.* 93, 1673–1685. doi: 10.2522/ptj.20120344

Gor-García-Fogeda, M. D., de la Cuerda, R., Tejada, M. C., Diego, I. M. A., and Rueda, F. M. (2016). Observational gait as-sessments in people with neurological disorders: a systematic review. *Arch. Phys. Med. Rehabil.* 97, 131–140. doi: 10.1016/j.apmr.2015.07.018

Guzik, A., Drużbicki, M., Przysada, G., Kwolek, A., Brzozowska-Magoń, A., Wyszyńska, J., et al. (2016). Assessment of test-retest reliability and internal consistency of the Wisconsin Gait Scale in hemiparetic post-stroke patients. *Postep. Rehabil.* 30, 41–53. doi: 10.1515/rehab-2015-0048

Haruyama, K., Kawakami, M., Okada, K., Okuyama, K., Tsuzuki, K., and Liu, M. (2021). Pelvis-Toe Distance: 3-Dimensional Gait Characteristics of Functional Limb Shortening in Hemiparetic Stroke. *Sensors* 21:5417. doi: 10.3390/s21165417

Iosa, M., Capodaglio, E., Pelà, S., Persechino, B., Morone, G., Antonucci, G., et al. (2021). Artificial Neural Network analyzing wearable device gait data for identifying patients with stroke unable to return to work. *Front. Neurol.* 12:561. doi: 10.3389/fneur.2021.650542

Kim, C. M., and Eng, J. J. (2004). Magnitude and pattern of 3D kinematic and kinetic gait profiles in persons with stroke: relationship to walking speed. *Gait Posture* 20, 140–146. doi: 10.1016/j.gaitpost.2003.07.002

Lauzière, S., Betschart, M., Aissaoui, R., and Nadeau, S. (2014). Understanding spatial and temporal gait asymmetries in individuals post stroke. *Int. J. Phys. Med. Rehabil.* 2:3. doi: 10.4172/2329-9096.1000201

Li, M., Tian, S., Sun, L., and Chen, X. (2019). Gait Analysis for Post-Stroke Hemiparetic Patient by Multi-Features Fusion Method. *Sensors* 19:1737. doi: 10.3390/s19071737

Li, S., Francisco, G. E., and Zhou, P. (2018). Post-stroke Hemiplegic Gait: new Perspective and Insights. *Front. Physiol.* 9:1021. doi: 10.3389/fphys.2018.01021

Lu, X., Hu, N., Deng, S., Li, J., Qi, S., and Bi, S. (2015). The reliability, validity and correlation of two observational gait scales assessed by video tape for Chinese subjects with hemiplegia. *J. Phys. Ther. Sci.* 27, 3717–3721. doi: 10.1589/jpts.27.3717

Marin, J., Marin, J. J., Blanco, T., de la Torre, J., Salcedo, I., and Martitegui, E. (2020). Is My Patient Improving? Individualized Gait Analysis in Rehabilitation. *Appl. Sci.* 10:8558. doi: 10.3390/app10238558

Matsuda, F., Mukaino, M., Ohtsuka, K., Tanikawa, H., Tsuchiyama, K., and Teranishi, T. (2016). Biomechanical factors behind toe clearance during the swing phase in hemiparetic patients. *Top Stroke Rehabil.* 24, 177–182. doi: 10.1080/10749357.2016.1234192

McGinley, J. L., Baker, R., Wolfe, R., and Morris, M. E. (2009). The reliability of three-dimensional kinematic gait measurements: a systematic review. *Gait Posture.* 29, 360–369. doi: 10.1016/j.gaitpost.2008.09.003

Mohan, D. M., Khandoker, A. H., Wasti, S. A., Ismail, S., Ibrahim, Ismail Alali, S., et al. (2021). Assessment Methods of Post-stroke Gait: a Scoping Review of Technology-Driven Approaches to Gait Characterization and Analysis. *Front. Neurol.* 12:650024. doi: 10.3389/fneur.2021.650024

Mukaino, M., Ohtsuka, K., Tanikawa, H., Matsuda, F., Yamada, J., Itoh, N., et al. (2018). Clinical-oriented Three-dimensional Gait Analysis Method for Evaluating Gait Disorder. *J. Vis. Exp.* 133:57063. doi: 10.3791/57063

Mukaino, M., Ohtsuka, K., Tsuchiyama, K., Matsuda, F., Inagaki, K., Yamada, J., et al. (2016). Feasibility of a Simplified, Clinically Oriented, Three-dimensional Gait Analysis System for the Gait Evaluation of Stroke Patients. *Prog. Rehabil. Med.* 15:20160001. doi: 10.2490/prm.20160001

Mukaka, M. M. (2012). A guide to appropriate use of Correlation coefficient in medical research. *Malawi Med. J.* 24, 69–71.

Murciano Casas, M. P., Zarco Periñán, M. J., Corral López, I., Álamo Vera, V., Ferrand Ferri, P., and Barrera Chacón, J. M. (2020). Development of the Spanish version of the Wisconsin Gait Scale. Reliability and consistency analysis of spatial and temporal parameters with gait assessment in stroke patients. *Rehabilitacion* doi: 10.1016/j.rh.2020.10.003 [Epub Online ahead of print]

Oken, O., and Yavuzer, G. (2008). Spatio-temporal and kinematic asymmetry ratio in subgroups of patients with stroke. *Eur. J. Phys. Rehabil. Med.* 44, 127–132.

Pasqual Marques, A., Oshima Marcolan, J. N., Nucci Nogueira, Prado, J., Nogueira Burke, T., Alves Gonçalves, et al. (2017). Inter- and intra-rater reliability of computerized photogrammetry and universal goniometer in the measurement of hip flexion and abduction. *Fisioter Pesqui.* 24, 22–28. doi: 10.1590/1809-2950/15886624012017

Patterson, K. K., Parafianowicz, I., Danells, C. J., Closson, V., Verrier, M. C., Staines, W. R., et al. (2008). Gait asymmetry in community-ambulating stroke survivors. *Arch. Phys. Med. Rehab.* 89, 304–310. doi: 10.1016/j.apmr.2007.08.142

Pizzi, A., Carlucci, G., Falsini, C., Lunghi, F., Verdesca, S., and Grippo, A. (2007). Gait in hemiplegia: evaluation of clinical features with the wisconsin gait scale. *Acta. Derm. Venereol.* 39, 170–174. doi: 10.2340/16501977-0026

Puig-Diví, A., Escalona-Marfil, C., Padullés-Riu, J. M., Busquets, A., Padullés-Chando, X., and Marcos-Ruiz, D. (2019). Validity and reliability of the Kinovea program in obtaining angles and distances using coordinates in 4 perspectives. *PLoS One.* 14:e0216448. doi: 10.1371/journal.pone.0216448

Rathinam, C., Bateman, A., Peirson, J., and Skinner, J. (2014). Observational gait assessment tools in paediatrics–a systematic review. *Gait Posture* 40, 279–285. doi: 10.1016/j.gaitpost.2014.04.187

Ridao-Fernández, C., Pinero-Pinto, E., and Chamorro-Moriana, G. (2019). Observational Gait Assessment Scales in Patients with Walking Disorders: systematic Review. *Biomed. Res. Int.* 31:2085039. doi: 10.1155/2019/2085039

Rodriquez, A. A., Black, P. O., Kile, K. A., Sherman, J., Stellberg, B., McCormnick, J., et al. (1996). Gait training efficacy using a home-based practice model in chronic hemiplegia. *Arch. Phys. Med. Rehabil.* 77, 801–805.

Sánchez, N., and Winstein, C. J. (2021). Lost in Translation: simple Steps in Experimental Design of Neurorehabilitation-Based Research Interventions to Promote Motor Recovery Post-Stroke. *Front. Hum. Neurosci.* 15:644335. doi: 10.3389/fnhum.2021.644335

Seo, M., Shin, M. J., Park, T. S., and Park, J. H. (2020). Clinometric Gait Analysis Using Smart Insoles in Patients With Hemiplegia After Stroke: pilot Study. *JMIR mHealth uHealth* 8:e22208. doi: 10.2196/22208

Solanki, D., and Lahiri, U. (2018). Design of instrumented shoes for gait characterization: a usability study with healthy and post-stroke hemiplegic individuals. *Front. Neurosci.* 12:459. doi: 10.3389/fnins.2018.00459

Tenore, N., Fortugno, F., Viola, F., Galli, M., and Giaquinto, S. (2006). Gait analysis as a reliable tool for rehabilitation of chronic hemiplegic patients. *Clin. Exp. Hypertens.* 28, 349–355. doi: 10.1080/10641960600549504

Tian, S., Li, M., Wang, Y., and Chen, X. (2019). Application of an Improved Correlation Method in Electrostatic Gait Recognition of Hemiparetic Patients. *Sensors* 19:2529. doi: 10.3390/s19112529

Turani, N., Kemiksizog, A., and Karatas, M. (2004). Assessment of hemiplegic gait using the Wisconsin Gait Scale. *Scand. J. Caring. Sci.* 18, 103–108. doi: 10.1111/j.1471

Wang, F. C., Chen, S. F., Lin, C. H., Shih, C. J., Lin, A. C., Yuan, W., et al. (2021). Detection and Classification of Stroke Gaits by Deep Neural Networks Employing Inertial Measurement Units. *Sensors* 21:1864.

Wellmon, R., Degano, A., Rubertone, J. A., Campbell, S., and Russo, K. A. (2015). Interrater and intrarater reliability and minimal detectable change of the Wisconsin Gait Scale when used to examine videotaped gait in individuals post-stroke. *Arch. Phys.* 5:11. doi: 10.1186/s40945-015-0011-z

Yaliman, A., Kesiktas, N., Ozkaya, M., Eskiyurt, N., Erkan, O., and Yilmaz, E. (2014). Evaluation of intrarater and interrater reliability of the Wisconsin Gait Scale with using the video taped stroke patients in a Turkish sample. *Neurorehabilitation* 34, 253–258. doi: 10.3233/NRE-131033

Conflict of Interest: The authors declare that the research was conducted in the absence of any commercial or financial relationships that could be construed as a potential conflict of interest.

Publisher's Note: All claims expressed in this article are solely those of the authors and do not necessarily represent those of their affiliated organizations, or those of the publisher, the editors and the reviewers. Any product that may be evaluated in this article, or claim that may be made by its manufacturer, is not guaranteed or endorsed by the publisher.

frontiers in Human Neuroscience

ORIGINAL RESEARCH
published: 24 February 2022
doi: 10.3389/fnhum.2021.820104

Core Sets of Kinematic Variables to Consider for Evaluation of Gait Post-stroke

Heidi Nedergård[1], Lina Schelin[2], Dario G. Liebermann[3], Gudrun M. Johansson[1] and Charlotte K. Häger[1]*

[1] Department of Community Medicine and Rehabilitation, Physiotherapy, Umeå University, Umeå, Sweden, [2] Department of Statistics, Umeå School of Business, Economics and Statistics, Umeå University, Umeå, Sweden, [3] Department of Physical Therapy, Sackler Faculty of Medicine, Stanley Steyer School of Health Professions, Tel Aviv University, Tel Aviv, Israel

Background: Instrumented gait analysis post-stroke is becoming increasingly more common in research and clinics. Although overall standardized procedures are proposed, an almost infinite number of potential variables for kinematic analysis is generated and there remains a lack of consensus regarding which are the most important for sufficient evaluation. The current aim was to identify a discriminative core set of kinematic variables for gait post-stroke.

Methods: We applied a three-step process of statistical analysis on commonly used kinematic gait variables comprising the whole body, derived from 3D motion data on 31 persons post-stroke and 41 non-disabled controls. The process of identifying relevant core sets involved: (1) exclusion of variables for which there were no significant group differences; (2) systematic investigation of one, or combinations of either two, three, or four significant variables whereby each core set was evaluated using a leave-one-out cross-validation combined with logistic regression to estimate a misclassification rate (MR).

Results: The best MR for one single variable was shown for the *Duration of single-support* (MR 0.10) or *Duration of 2nd double-support* (MR 0.11) *phase*, corresponding to an 89–90% probability of correctly classifying a person as post-stroke/control. Adding *Pelvis sagittal ROM* to either of the variables *Self-selected gait speed* or *Stride length,* alternatively adding *Ankle sagittal ROM* to the *Duration of single-stance phase,* increased the probability of correctly classifying individuals to 93–94% (MR 0.06). Combining three variables decreased the MR further to 0.04, suggesting a probability of 96% for correct classification. These core sets contained: (1) a spatial (*Stride/Step length*) or a temporal variable (*Self-selected gait speed/Stance time/Swing time* or *Duration of 2nd double-support),* (2) *Pelvis sagittal ROM* or *Ankle plantarflexion during push-off,* and (3) *Arm Posture Score* or *Cadence* or a knee/shoulder joint angle variable. Adding a fourth variable did not further improve the MR.

OPEN ACCESS

Edited by:
Marco Iosa,
Sapienza University of Rome, Italy

Reviewed by:
Stefano Filippo Castiglia,
Sapienza University of Rome, Italy
Noureddin Nakhostin Ansari,
Tehran University of Medical Sciences, Iran

****Correspondence:***
Heidi Nedergård
heidi.nedergard@umu.se

Specialty section:
This article was submitted to Motor Neuroscience, a section of the journal Frontiers in Human Neuroscience

Received: *22 November 2021*
Accepted: *28 December 2021*
Published: *24 February 2022*

Citation:
Nedergård H, Schelin L, Liebermann DG, Johansson GM and Häger CK (2022) Core Sets of Kinematic Variables to Consider for Evaluation of Gait Post-stroke. Front. Hum. Neurosci. 15:820104. doi: 10.3389/fnhum.2021.820104

Conclusion: A core set combining a few crucial kinematic variables may sufficiently evaluate post-stroke gait and should receive more attention in rehabilitation. Our results may contribute toward a consensus on gait evaluation post-stroke, which could substantially facilitate future diagnosis and monitoring of rehabilitation progress.

Keywords: gait analysis, walking, stroke, biomechanical evaluation, instrumented gait analysis

INTRODUCTION

Instrumented motion analysis is increasingly used to evaluate movement patterns during gait post-stroke (Baker et al., 2016). It serves to identify specific gait deviations based on objective information to guide clinical decision-making, individual treatment and rehabilitation. Different forms of instrumented measurement techniques, such as timing devices, pressure-sensitive walkways, sensor systems, and 3D motion capture systems, have become popular and are today often available in clinics. However, the resulting raw data is vast and may yield almost endless biomechanical descriptors. Therefore, the need for a consensus regarding which variables to focus on in evaluation and rehabilitation as the most relevant and informative descriptors of gait post-stroke has thus been pointed out repeatedly (Krasovsky and Levin, 2010; Wikström et al., 2014; Wonsetler and Bowden, 2017; Sharifi far et al., 2019; Nedergård et al., 2021).

The focus of gait analysis is commonly on the lower limbs. Recent studies nevertheless emphasize the importance of incorporating also the trunk and upper limbs, particularly in post-stroke gait analyses, since this information adds to the understanding of balance control, energy expenditure and functional ability (Verheyden et al., 2006; Stephenson et al., 2010; Punt et al., 2015; Van Criekinge et al., 2017). In addition, post-stroke gait analyses that include more than the lower limbs can identify deviations in other body parts and their possible underlying causes or consequences (Kahn et al., 2019). That kind of information is important when assessing gait function, tailoring exercises that aim to improve gait post-stroke, and evaluating the effects of treatment. There is however a lack of consensus concerning which standard variables to incorporate in whole-body analyses for evaluation of gait post-stroke. This lack of agreement aggravates comparisons between research studies and may detriment the process of evaluating gait rehabilitation post-stroke (Sharifi far et al., 2019; Nedergård et al., 2021). The aim of this study was hence to contribute toward such a consensus by identifying a core set of a few kinematic variables to discriminate post-stroke gait from the gait of non-disabled controls. For this purpose, we used a statistical process including leave-one-out cross-validation combined with logistic regression. Similar methods have previously been applied to other populations, e.g., in proposing a test battery for individuals with rupture of the anterior cruciate ligament (Schelin et al., 2017). In our analysis, we included the most common kinematic gait variables obtained from the literature that have been used to evaluate gait post-stroke, as well as information of the upper limb (Johansson et al., 2014) and the coordination of the upper and lower body (Nedergård et al., 2020).

MATERIALS AND METHODS

Participants

This cross-sectional study involved 31 persons post-stroke and 41 non-disabled controls. Characteristics of the participants are presented in **Table 1**. The stroke group was recruited from two clinics in Umeå, Sweden. Inclusion criteria were: 35–85 years of age; > 3 months since stroke onset; unilateral hemiparesis following ischemic or hemorrhagic stroke; ability to walk indoors without aids; comprehension of written and verbal information. Exclusion criteria were impairments or diseases other than stroke which could influence gait. The post-stroke participants were assessed as having an average of moderate motor impairments (Duncan et al., 1992) with a total score of 77 ± 18 (100 maximum) on the Fugl-Meyer Assessment (Fugl-Meyer et al., 1975). The controls were recruited among colleagues, acquaintances and through a local organization for retired persons. Individuals with musculoskeletal or neurological movement impairments were excluded from the control group. Some of the participants were also included in a previous study addressing arm swing during post-stroke gait (Johansson et al., 2014). The study was approved by the Regional Ethical Review Board in Umeå, Sweden (Dnr. 2011-199-31). All participants signed a written informed consent form before participation in accordance with the Declaration of Helsinki.

Procedures

Gait analyses were performed in the U-Motion Laboratory at Umeå University, Sweden. Seventy-two reflective markers were attached to anatomical locations according to a full-body model described in detail previously (Frykberg et al., 2014). Markers were placed according to a strict protocol by three

TABLE 1 | Participant characteristics (including summary information for the three explanatory variables for the first step of the analysis).

Background variables	Persons post-stroke	Controls	*p*-value
Sex (male/female)	18/13	21/20	0.74
Age, years	67.3 (10.5)	64.9 (11.5)	0.36
Body mass index*	27.6 (3.9)	24.9 (2.3)	0.00
Height, cm	171.1 (8.2)	173.9 (8.8)	0.64
Time since stroke, months	25.7 (22.1)	N/A	N/A
Brain lesion side R/L (n)	15/16	N/A	N/A
Gait speed*	0.9 (0.3)	1.3 (0.1)	0.00

**Significant differences between groups ($p < 0.05$). Means (standard deviations) are presented together with p-values from the respective t-test. The number of males/females is presented with a p-value from a Chi-squared test.*

physiotherapists. Participants were instructed to walk barefoot at a self-selected speed on a 10 m walkway for a minimum of six trials. Kinematics were captured by an eight-camera three-dimensional motion capture system (240 Hz; Oqus®, Qualisys Gothenburg, Sweden). Data were recorded from the middle 3 m of the walkway and included 2–4 gait cycles for each trial. The data were analyzed using the Qualisys Track Manager software (QTM; Qualisys), filtered (15 Hz, fourth-order bidirectional low-pass Butterworth digital filter) and processed in Visual 3D (C-motion, Germantown, MD, United States).

Variables and Stepwise Data Analyses

Included kinematic variables are presented in **Table 2**. Range of motion (ROM) was defined as the difference between the highest and lowest values of the angular joint motion curve, and the maximum (MAX) joint angle was defined as the highest value of the angular joint motion. ROM Index (ROMI) represents the ratio value of ROM, comparing the affected and non-affected side (A/NA) in persons post-stroke, and the non-dominant and dominant side (ND/D) in controls. Upper and lower body inclination angles were defined as the highest value of the inclination angle between the ankle and COM, and the head and COM, respectively (Nedergård et al., 2020). If not specified otherwise, all variables were represented by extracted discrete values based on information from the entire GC. Data from the affected side were depicted for all unilateral outcomes with the one exception of hip abduction during the stance phase. The deviation scores: Gait Profile Score, (Baker et al., 2009), Gait Deviation Index (Schwartz and Rozumalski, 2008) and the Arm Posture Score (Riad et al., 2011; Frykberg et al., 2014), represented the root mean square deviation between the lower and upper limb joint angles of each participant of the post-stroke group and the average of the controls. For further descriptions of the variables, including descriptive statistics (see **Supplementary Appendix A: Tables A–C**).

The statistical approach consisting of three steps, briefly presented below, followed the main setup in Schelin et al. (2017). For all outcome variables presented in **Supplementary Appendix A: Table A**, we used a linear regression model to test whether there was a difference between persons post-stroke and non-disabled persons while controlling for age, sex and BMI (Step I). Descriptive statistics for the background variables age, sex and BMI are presented in **Table 1**. Variables with non-significant group differences were excluded from the subsequent analyses (**Table 2**).

In order to identify one or several potential core sets of variables, we systematically investigated all combinations consisting of 1–4 variables obtained from the complete set of all those variables that were significantly different between groups. Each core set was evaluated using leave-one-out cross-validation in combination with logistic regression to estimate the different models' misclassification rate (MR) (Step II). For each core set, a logistic regression model based on the variables in the core set, with no interaction terms, was used to model the probability that the person (that was left out) belonged to the group of persons post-stroke. The default threshold of 0.5 was used for classification, implying that for an estimated probability above 0.5, the person was classified as post-stroke. The MR was estimated as the proportion of wrongly classified individuals. Confusion matrices that identified the rates of true positive, true negative, false positive, and false negative classifications were also considered. To add information about potential relationships between the variables, Spearman's rank correlation was used to estimate the pair-wise correlations between the variables of interest. All analyses were performed in R (R Core Team, 2014).

RESULTS

The first step in the analysis process identified which variables that were significantly different between persons post-stroke and non-disabled controls (see **Table 2**, and with further details reported in **Supplementary Appendix A: Tables A–C**).

In the second step, we calculated the MR for single variables, as well as for the combination of different variables. When using only one variable, the MR ranged from 0.10 to 0.42. The lowest, hence also the best, MR (0.10) was shown for the *Duration of single-support* phase in the affected side (**Table 3**). This corresponds to a 90% probability of correctly classifying a person as post-stroke or control based on this specific variable. *Duration of 2nd double-support* phase classified 89% (MR 0.11), and *Stride length* 87% (MR 0.13) of the persons correctly. A core set of two variables resulted in MRs ranging from 0.06 to 0.42. The lowest rate (MR 0.06) was shown for *Step length/Stride length* in combination with *Pelvis sagittal ROM* (pelvis anterior/posterior tilt). These two combinations of variables classified 94% of persons correctly. Combining three variables decreased the MR further to 0.04 (range: 0.04–0.42). Each core set of three variables correctly classified 96% of persons. A spatial (*Stride length/Step length*) or temporal variable (*Self-selected gait speed/Stance time/Swing time/Duration of 2nd double-support*) was combined with either *Pelvis sagittal ROM or Ankle plantarflexion, terminal stance* (during push-off). In addition, these variables were combined with either *Arm Posture Score, Cadence,* or a knee or shoulder joint angle variable, to generate the best possible MR based on our populations. Adding yet another variable did not decrease the MR further, nor did it change the types of variables included in the core sets (all core sets still included at least one variable describing joint angle motions, most often *Pelvis sagittal ROM*). The combination of exclusively spatial and temporal gait variables (i.e., not including joint angle data) that most correctly classified persons post-stroke was *Stride width, Cadence, Duration of stance* phase and *Duration of 2nd double-support* phase (**Table 3**). This combination correctly classified 93% of persons (MR 0.07).

Since the MR does not include information about whether the different models are better at classifying post-stroke persons or controls, this was addressed with confusion matrices to identify the rates for true positive (0.39), true negative (0.57), false positive (0.00), and false negative (0.04) classifications. These values are valid for all core sets of size three with MR equal to 0.04. The results showed that persons post-stroke and controls were classified correctly to a similar extent in the models with low MRs.

When investigating potential relationships between the variables, correlation analyses were performed based on pooled data from both groups but also calculated separately for

TABLE 2 | Variables included in Step I of the analysis.

	Spatial and temporal gait variables	ROM joint angles	MAX joint angles	ROM Index	Lower and upper body inclination angles	Gait deviation scores	Stroke-specific gait variables
Included	Step length	Pelvis X	Hip Z	Hip X	A-CoMIA, stance	GPS GDI	Hip extension, swing
	Stride length	Hip X	knee X	Hip Y	A-CoMIA, swing	APS	
	Step width	Hip Y	Shoulder Y	Knee X	A-CoMIA, stance		Knee flexion, swing
	Self-selected gait speed	Hip Z		Ankle X			
	Cadence	Knee X		Shoulder X			
	Stance phase duration	Ankle X	Elbow X				Ankle plantarflexion, terminal stance
	Stance phase duration	Thorax Y					
	Duration of 1st double-support	Thorax Z					
	Duration of 2nd double-support	Shoulder X					
	Step time	Shoulder Y					
	Support	Shoulder Z					
	Swing time	Elbow X					
	Stride time						
	Temporal symmetry						
	Spatial symmetry						
Excluded		Thorax X	Pelvis X	Pelvis X	H-CoMIA, swing		Hip abduction, swing
		Pelvis Z	Pelvis Z	Hip Z			
		Pelvis Y	Pelvis Y	Shoulder Y			Ankle dorsiflexion, swing
			Hip X	Shoulder Z			
			Hip y				
			Ankle X				
			Shoulder X				
			Shoulder Z				Hip abduction in the non-affected side, stance
			Eibow X				Knee extension, single stance

Spatial and temporal gait variables ROM joint angles. The variables that differed significantly between persons post-stroke and controls were included in the subsequent analysis (Step II).
A-CoMIA = ankle-center of mass inclination angle; APS = arm posture score; GDI = Gait Deviation Index; GPS = gait profile score; H-CoMIA = head-center of mass inclination angle MAX = maximum = sagittal plane; ROM = Range of motion; X = sagittal plane; Y= frontal plane; Z = transversal plane. If not specified, data from the affected side are depicted for all unilateral outcomes.

each group (**Supplementary Appendix B: Figures A–C**). The correlation matrices revealed both similarities and differences in the correlations between variables when comparing persons post-stroke and controls. In both groups, the spatial and temporal variables were generally significantly correlated, although with some exceptions (see **Supplementary Appendix B: Figures B,C**). Correlations for joint angle data were fewer among non-disabled controls than in persons post-stroke.

DISCUSSION

The stepwise analysis demonstrated that using only a single variable correctly discriminated persons post-stroke from controls with a 60–90% probability (MR 0.10-0-42) (**Table 3**). The most sensitive stand-alone variable was the *Duration of single-support* (MR 0.10) followed by the *Duration of 2nd double-support* (MR 0.11). Adding *Pelvis sagittal ROM* to the specific temporal or spatial variables (see **Table 3**) generated core sets that increased the probability of correctly classifying individuals to as high as 93–94%. Adding yet another kinematic variable to the core sets increased the probability even further to 96%.

Several of the gait variables represented in the core sets, such as the *Duration of single-* or *2nd double-stance* (longer in persons post-stroke), *Self-selected gait speed* and *Stride/Step length* (slower and shorter, respectively, in persons post-stroke), are common, well-established variables used for evaluation of gait in persons post-stroke (Balaban and Tok, 2014; Sheffler and Chae, 2015; Baker et al., 2016). As confirmed by our correlation matrices (**Supplementary Appendix B: Figures A–C**) and in agreement with previous research (Olney and Richards, 1996; Nadeau et al., 2013; Sharififar et al., 2019), these variables were highly interrelated and also generated similar MRs. Note, however, that *Cadence* alone received the highest MR of the spatial and temporal gait variables and only classified persons correctly with a 68% probability (MR 0.32).

TABLE 3 | The five lowest misclassification rates (MR) for one variable alone, or for core sets of 2–3 variables in combination.

	Variables					MR
One variable	*Duration of single-support*					0.10
	Duration of 2nd double-support					0.11
	Stride length					0.13
	Self-selected gait speed					0.15
	Step length					0.17
Two variables	*Step/stride length*	+	*Pelvis sagittal ROM*			0.06
	Self-selected gait speed	+	*Pelvis sagittal ROM*			0.07
	Duration of single-support	+	*Ankle sagittal ROM*			
	Duration of single-support	+	*Ankle plantarflexion, terminal stance*			
	Duration of 2nd double-support	+	*Knee flexion, swing*			
Three variables	*Stride/Step length*	+	*Pelvis sagittal ROM*	+	*Shoulder sagittal ROM Index/Knee sagittal ROM*	0.04
	Self-selected gait speed	+	*Pelvis sagittal ROM*	+	*Shoulder sagittal ROM Index/Knee flexion MAX/Arm Posture Score/Cadence*	
	Stance/Swing time	+	*Pelvis sagittal ROM*	+	*Knee flexion MAX*	
	Duration of 2nd double-support	+	*Ankle plantarflexion, terminal stance*	+	*Shoulder abduction MAX*	
Spatial and temporal gait parameters	*Stride width + Cadence + Duration of stance phase + Duration of 2nd double-support*					0.07
	Self-selected gait speed + Swing time/Temporal asymmetry					0.09

MAX, maximum; ROM, range of motion.

Our results indicate that for improved sensitivity, spatial and temporal variables should be analyzed in combination with variables such as the *Pelvis sagittal ROM* or knee/shoulder kinematics. When used independently, several variables had a higher probability of correctly differentiating persons post-stroke from controls than *Pelvis sagittal ROM*. But when *Pelvis sagittal ROM* was used in combination with other variables, it generated improved MRs and thus seems highly relevant for post-stroke gait analysis. Indeed, two-thirds of the here presented core sets combining 2–3 variables included this specific variable. The pelvis connects the trunk to the lower limbs, and muscular control at the pelvis has been suggested to be crucial for dynamic balance and weight transmission during walking (Karthikbabu et al., 2016). Data from our post-stroke population confirm earlier observed increased ROM regarding pelvis anterior/posterior tilt among persons post-stroke (Verheyden et al., 2014; Karthikbabu et al., 2017). This is presumed to be a consequence of impaired trunk control as well as due to adaptations following lower limb impairments (Van Criekinge et al., 2017). The range of sagittal motion of the pelvis is, however, relatively small especially compared to the range of sagittal motion in the lower limbs (Chen et al., 2003). This makes pelvic tilt more difficult to observe or measure in clinical settings without any technological devices. Furthermore, the constitution and attire of an individual may complicate assessing the pelvic tilt during gait. Nevertheless, the pelvic function should be considered when evaluating and treating gait post-stroke. Selective pelvic exercises, for instance, seems to have a beneficial effect on trunk function, standing balance, and mobility after stroke (Haruyama et al., 2016).

Altered knee movement patterns, such as greater or lesser knee flexion during the early stance phase followed by knee hyperextension in the late stance phase, have been reported post-stroke (Woolley, 2001; Baker et al., 2016). For the swing phase, previous studies have shown that the most common knee joint angle deviation is a generally decreased knee flexion and/or decreased knee extension prior to initial contact (Olney and Richards, 1996; Balaban and Tok, 2014; Baker et al., 2016). In 3D gait analysis, the knee sagittal kinematics are considered as reliable variables that also are suggested to predict gait function post-stroke (Guzik et al., 2020). In agreement with that, our results suggest that sagittal knee angle motions (represented by *Knee flexion MAX* and *Knee sagittal ROM*) are of particular importance when classifying gait post-stroke. These two variables were represented in several emerging core sets. For the *Knee sagittal ROM*, estimates of the minimal detectable change and the minimal clinically important difference have been established for persons post-stroke (Geiger et al., 2019; Guzik et al., 2020) and these estimated values are useful when interpreting changes of knee flexion/extension observed in persons who have undergone gait interventions post-stroke.

In contrast to the focus on the lower limbs, kinematics of the upper limbs during gait post-stroke has been far from as extensively investigated (Carmo et al., 2012). A few recent studies have, however, emphasized the importance of incorporating the trunk (i.e., the thorax) and arm movements in post-stroke gait analyses (Stephenson et al., 2010; Carmo et al., 2012). Stroke affects upper limb function in 50–70% of persons in the subacute phase post-stroke (Krakauer, 2005) and may have

a clear influence on gait (Johansson et al., 2014). In the long term, around 40% experience disabilities of the upper limbs (Alt Murphy and Häger, 2015), whereas a lower percentage present with disabilities for functions of the lower limbs. It thus becomes clear that the inclusion of upper limb kinematic variables is of importance for ensuring comprehensive gait analyses. In the current study, upper limb motions (*Shoulder abduction MAX, Arm Posture Score* and *Shoulder sagittal ROM Index)* were represented in several suggested core sets of variables, providing further evidence that the upper limbs influence post-stroke gait movement pattern. An increased shoulder abduction angle among persons post-stroke (*Shoulder abduction MAX)* seems characteristic for post-stroke gait and has been assumed to be part of a compensatory strategy to help improve body weight distribution and balance (Carmo et al., 2012). In addition, an earlier reported variation in shoulder movement deviations in the sagittal plane (Kahn et al., 2019) was also observed among our persons post-stroke. While some persons display excessive movements (large ROM), others employ a more fixed joint posture (small ROM) during walking. Another interesting aspect was the generally greater number of associations between joint position variables among persons post-stroke when compared with controls (see the correlation matrices, **Supplementary Appendix A: Tables B,C**). Even though the absence of impairments would theoretically allow for greater variation, walking on an even surface without any obstacles and in a controlled fashion seems to generate a stable movement pattern. The fewer correlations between several variables among non-disabled controls when compared to persons post-stroke may hence be explained, at least partly, by lesser variability.

The potential for assessing the core set variables in a clinical context differs. The spatial and temporal variables are most accessible in clinics today since this data can be gathered relatively efficiently with the use of, e.g., pressure-sensitive walkways or timing devices. Self-selected gait speed is one of the most commonly used outcome measures. By combining *Self-selected gait speed* (MR 0.15) in the present study with another temporal variable, such as *Duration of swing* or *Temporal asymmetry*, the MR improved to 0.09. The combination of spatial and temporal variables that most correctly seems to classify persons post-stroke and controls included *Stride width, Cadence, Duration of stance* and *Duration of 2nd double-support*. Together these four variables classified persons correctly with a 93% probability.

Gathering joint position data, compared with spatial and temporal variables, generally requires more time, equipment and data processing. For example, calculation of the *Arm Posture Score* is currently based on comprehensive 3D upper limb joint position data, whereas estimating the *Sagittal ROM Shoulder Index* requires bilateral shoulder flexion/extension data. Low-cost webcam technology has, however, shown potential for real-time tracking of joint kinematics, particularly in the sagittal plane and if performed following specific recommendations related to data collection setup and camera and analysis software (Michelini et al., 2020). Such technology opens up new, more accessible possibilities for kinematic assessments during gait which may be more easily utilized in a clinical setting compared to laboratory-based data collection with 3D motion capture systems. Data collection of *Pelvis sagittal ROM* or *Knee flexion MAX/Knee sagittal ROM*, for instance, can also be made with 2D data-collecting systems. The use of portable inertial sensors to capture kinematic information over an extended space and time and in real-life conditions has also been described by Petraglia et al. (2019) and van Schaik and Dominici (2020).

Methodological Considerations

The purpose of Step II of the current analytical approach was to identify potential core sets of variables for discussion and future research toward a consensus on crucial variables for the kinematic evaluation of gait post-stroke. The focus of the current paper was not on checking model assumptions, interpreting parameter estimates, or comparing models in other ways than their classification ability. If identified core sets are to be used further in similar analyses, these assumptions should be checked. One specific assumption relates to the lack of multicollinearity, i.e., that the variables included in the model are not highly correlated. Note that gait speed and cadence were identified in the same core set and that these variables seem significantly correlated both in our analyses (see correlation matrices, **Supplementary Appendix B: Figures A–C**) and in previous research (Sharififar et al., 2019). Combining these two variables may therefore not be advisable if they represent the same underlying central nervous networks in the motor control process related to gait. While we have not *a priori* eliminated collinear variables based on conceptual conjectures, we are aware that this could result in redundancy in the discrimination process (one could potentially use various combinations that provide similar results).

Analyzing individuals walking at a self-selected speed as opposed to at their fastest possible gait speed or at a predetermined pace, will likely influence the results. Earlier research suggests, for instance, that gait speed affects the pelvic motions of non-disabled individuals (Lewis et al., 2017), while knee kinematics in the sagittal plane, on the other hand, seems not to be speed dependent when comparing persons post-stroke with non-disabled persons walking with matched gait speed (Chen et al., 2005). Due to close relationships between gait speed and other temporal and spatial variables, while persons post-stroke walked slower than non-disabled controls in our study, the core sets presented may be influenced either by the pathology *per se* or by gait speed, or both.

The generalizability of this study is limited to a population in a long-term phase post-stroke and with mainly relatively mild impairments. Previous studies have shown that e.g., pelvic tilt may vary depending on stroke onset (Van Criekinge et al., 2017) and severity level (Chen et al., 2003). Although our stroke sample does not fully represent the whole range of stroke severity, it is an important subpopulation as the individuals included may have treatable gait deficits that are not easily or clearly identified without instrumented motion analysis. Furthermore, the analysis has not considered the possible impact of the localization of injury which may affect functional outcomes and movement strategies post-stroke.

Only significant variables were included in the latter step of the analysis. Some variables could nonetheless still be important but were perhaps not significant due to lack of power. If altering

the default threshold of 0.5 that was used for classification, the MR, as well as the rate of true positive/negative, might change. However, since persons post-stroke and controls both were correctly classified, and the MR was low for many models, we see only a limited gain of finding and using an optimal threshold.

Finally, almost an endless number of variables are available from instrumented gait analysis. We chose to initially include those that were considered relevant from a clinical perspective as well as the ones most commonly used, based on the literature in the field. The identified core sets contain spatiotemporal gait variables and joint motion variables in the sagittal plane, several of which are considered highly reliable in persons post-stroke and where previous analyses include estimates of minimal detectable change (Geiger et al., 2019).

CONCLUSION

Our results contribute toward a consensus on which kinematic variables should be included in the evaluation of gait post-stroke. This may substantially facilitate future diagnostics and treatment planning regarding specific gait deficits post-stroke, as well as the monitoring and evaluation of rehabilitation progress in the clinics. It would also be of great value for comparisons across studies and in meta-analysis contexts if the same variables are to be used in research.

DATA AVAILABILITY STATEMENT

The raw data supporting the conclusions of this article will be made available by the authors, without undue reservation.

ETHICS STATEMENT

The studies involving human participants were reviewed and approved by the Regional Ethical Review Board in Umeå, Sweden (Dnr. 2011-199-31). The patients/participants provided their written informed consent to participate in this study.

AUTHOR CONTRIBUTIONS

HN, DL, CH, and GJ formulated the research question. CH and LS obtained the funding. HN and GJ performed the data collection and data preparations. LS performed the quantitative data analysis. HN drafted the preliminary manuscript. All authors helped in further writing and critical reviewing of the manuscript, read, and approved the final manuscript.

FUNDING

This study was supported by the Swedish Brain Foundation (FO2016-0289), The Swedish Research Council (2016-02763), the Umeå University Foundation for Medical Research (FS 2.1.6-1870-16), the Umeå University Strategic research Area Health Care Science SFOV, the Region Vasterbotten, the Foundation for Stroke Research in Norrland, and King Gustaf V and Queen Victoria's Foundation of Freemasons.

ACKNOWLEDGMENTS

Jonas Selling, Andrew Strong, and Gunilla E Frykberg are gratefully acknowledged for their assistive role and support of the work. Content of the manuscript in a preliminary version has been included in a doctoral thesis by Nedergård (2021), Umeå university: "Taking the next step: Whole-body biomechanical gait analysis, and user-perspectives on robotic-assisted gait training post-stroke."

SUPPLEMENTARY MATERIAL

The Supplementary Material for this article can be found online at: https://www.frontiersin.org/articles/10.3389/fnhum.2021.820104/full#supplementary-material

REFERENCES

Alt Murphy, M., and Häger, C. K. (2015). Kinematic analysis of the upper extremity after stroke – how far have we reached and what have we grasped? *Phys. Ther. Rev.* 20, 137–155. doi: 10.1179/1743288X15Y.0000000002

Baker, R., Esquenazi, A., Benedetti, M. G., and Desloovere, K. (2016). Gait analysis: clinical facts. *Eur. J. Phys. Rehabil. Med.* 52, 560–574.

Baker, R., McGinley, J. L., Schwartz, M. H., Beynon, S., Rozumalski, A., Graham, H. K., et al. (2009). The gait profile score and movement analysis profile. *Gait Posture* 30, 265–269. doi: 10.1016/j.gaitpost.2009.05.020

Balaban, B., and Tok, F. (2014). Gait disturbances in patients with stroke. *PM R* 6, 635–642. doi: 10.1016/j.pmrj.2013.12.017

Carmo, A. A., Kleiner, A. F., Costa, P. H., and Barros, R. M. L. (2012). Three-dimensional kinematic analysis of upper and lower limb motion during gait of post-stroke patients. *Braz. J. Med. Biol. Res.* 45, 537–545. doi: 10.1590/s0100-879x2012007500051

Chen, C.-L., Chen, H.-C., Tang, S. F.-T., Wu, C. Y., Cheng, P. T., and Hong, W. H. (2003). Gait performance with compensatory adaptations in stroke patients with different degrees of motor recovery. *Am. J. Phys. Med. Rehabil.* 82, 925–935. doi: 10.1097/01.Phm.0000098040.13355.B5

Chen, G., Patten, C., Kothari, D. H., and Zajac, F. E. (2005). Gait differences between individuals with post-stroke hemiparesis and non-disabled controls at matched speeds. *Gait Posture* 22, 51–56. doi: 10.1016/j.gaitpost.2004.06.009

Duncan, P. W., Goldstein, L. B., Matchar, D., Divine, G. W., and Feussner, J. (1992). Measurement of motor recovery after stroke. Outcome assessment and sample size requirements. *Stroke* 23, 1084–1089. doi: 10.1161/01.str.23.8.1084

Frykberg, G. E., Johansson, G. M., Schelin, L., and Häger, C. K. (2014). The Arm Posture Score for assessing arm swing during gait: an evaluation of adding rotational components and the effect of different gait speeds. *Gait Posture* 40, 64–69. doi: 10.1016/j.gaitpost.2014.02.006

Fugl-Meyer, A. R., Jääskö, L., Leyman, I., Olsson, S., and Steglind, S. (1975). The post-stroke hemiplegic patient. 1. a method for evaluation of physical performance. *Scand. J. Rehabil. Med.* 7, 13–31.

Geiger, M., Supiot, A., Pradon, D., Do, M. C., Zory, R., and Roche, N. (2019). Minimal detectable change of kinematic and spatiotemporal parameters in

patients with chronic stroke across three sessions of gait analysis. *Hum. Mov. Sci.* 64, 101–107. doi: 10.1016/j.humov.2019.01.011

Guzik, A., Drużbicki, M., Wolan-Nieroda, A., Turolla, A., and Kiper, P. (2020). Estimating minimal clinically important differences for knee range of motion after stroke. *J. Clin. Med.* 9:3305.

Haruyama, K., Kawakami, M., and Otsuka, T. (2016). Effect of core stability training on trunk function, standing balance, and mobility in stroke patients: a randomized controlled trial. *Neurorehabil. Neural Repair.* 31, 240–249. doi: 10.1177/1545968316675431

Johansson, G. M., Frykberg, G. E., Grip, H., Broström, E. W., and Häger, C. K. (2014). Assessment of arm movements during gait in stroke - the arm posture score. *Gait Posture* 40, 549–555. doi: 10.1016/j.gaitpost.2014.06.014

Kahn, M. B., Clark, R. A., Williams, G., Bower, K. J., Banky, M., Olver, J., et al. (2019). The nature and extent of upper limb associated reactions during walking in people with acquired brain injury. *J. Neuroeng. Rehabil.* 16:160. doi: 10.1186/s12984-019-0637-2

Karthikbabu, S., Chakrapani, M., Ganesan, S., and Ellajosyla, R. (2017). Pelvic alignment in standing, and its relationship with trunk control and motor recovery of lower limb after stroke. *Neurol. Clin. Neurosci.* 5, 22–28. doi: 10.1111/ncn3.12092

Karthikbabu, S., Chakrapani, M., Ganesan, S., and Ellajosyula, R. (2016). Relationship between pelvic alignment and weight-bearing asymmetry in community-dwelling chronic stroke survivors. *J. Neurosci. Rural Pract.* 7(Suppl. 1), S37–S40. doi: 10.4103/0976-3147.196460

Krakauer, J. W. (2005). Arm function after stroke: from physiology to recovery. *Semin. Neurol.* 25, 384–395. doi: 10.1055/s-2005-923533

Krasovsky, T., and Levin, M. F. (2010). Review: toward a better understanding of coordination in healthy and poststroke gait. *Neurorehabil. Neural Repair* 24, 213–224. doi: 10.1177/1545968309348509

Lewis, C. L., Laudicina, N. M., Khuu, A., and Loverro, K. L. (2017). The human pelvis: variation in structure and function during gait. *Anatom. Rec.* 300, 633–642. doi: 10.1002/ar.23552

Michelini, A., Eshraghi, A., and Andrysek, J. (2020). Two-dimensional video gait analysis: a systematic review of reliability, validity, and best practice considerations. *Prosthet. Orthot. Int.* 44, 245–262. doi: 10.1177/0309364620921290

Nadeau, S., Betschart, M., and Bethoux, F. (2013). Gait analysis for poststroke rehabilitation: the relevance of biomechanical analysis and the impact of gait speed. *Phys. Med. Rehabil. Clin. N. Am.* 24, 265–276. doi: 10.1016/j.pmr.2012.11.007

Nedergård H.(2021). *'Taking the Next Step': Whole-body Biomechanical Gait Analysis, and User-perspectives on Robotic Assisted Gait Training Post-stroke.* Ph.D. dissertation, Umeå University, Faculty of Medicine, Umeå. Available online at: http://urn.kb.se/resolve?urn=urn:nbn:se:umu:diva-187069

Nedergård, H., Arumugam, A., Sandlund, M., Brändal, A., and Häger, C. K. (2021). Effect of robotic-assisted gait training on objective biomechanical measures of gait in persons post-stroke: a systematic review and meta-analysis. *J. Neuroeng. Rehabil.* 18:64. doi: 10.1186/s12984-021-00857-9

Nedergård, H., Schelin, L., Frykberg, G. E., and Häger, C. K. (2020). Inclination angles of the ankle and head relative to the centre of mass identify gait deviations post-stroke. *Gait Posture* 82, 181–188. doi: 10.1016/j.gaitpost.2020.08.115

Olney, S. J., and Richards, C. (1996). Hemiparetic gait following stroke. Part I: characteristics. *Gait Posture* 4, 136–148. doi: 10.1016/0966-6362(96)01063-6

Petraglia, F., Scarcella, L., Pedrazzi, G., Brancato, L., Puers, R., and Costantino, C. (2019). Inertial sensors versus standard systems in gait analysis: a systematic review and meta-analysis. *Eur. J. Phys. Rehabil. Med.* 55, 265–280. doi: 10.23736/s1973-9087.18.05306-6

Punt, M., Bruijn, S. M., Wittink, H., and van Dieën, J. H. (2015). Effect of arm swing strategy on local dynamic stability of human gait. *Gait Posture* 41, 504–509. doi: 10.1016/j.gaitpost.2014.12.002

R Core Team (2014). *R: A Language and Environment for Statistical Computing.* Vienna: R Foundation for Statistical Computing.

Riad, J., Coleman, S., Lundh, D., and Broström, E. (2011). Arm posture score and arm movement during walking: a comprehensive assessment in spastic hemiplegic cerebral palsy. *Gait Posture* 33, 48–53. doi: 10.1016/j.gaitpost.2010.09.022

Schelin, L., Tengman, E., Ryden, P., and Häger, C. (2017). A statistically compiled test battery for feasible evaluation of knee function after rupture of the Anterior Cruciate Ligament - derived from long-term follow-up data. *PLoS One* 12:e0176247. doi: 10.1371/journal.pone.0176247

Schwartz, M. H., and Rozumalski, A. (2008). The Gait Deviation Index: a new comprehensive index of gait pathology. *Gait Posture* 28, 351–357. doi: 10.1016/j.gaitpost.2008.05.001

Sharififar, S., Vincent, H. K., Shuster, J., and Bishop, M. (2019). Quantifying poststroke gait deviations: a meta-analysis of observational and cross-sectional experimental trials. *J. Stroke Med.* 2, 23–31. doi: 10.1177/2516608519856246

Sheffler, L. R., and Chae, J. (2015). Hemiparetic gait. *Phys. Med. Rehabil. Clin. N. Am.* 26, 611–623. doi: 10.1016/j.pmr.2015.06.006

Stephenson, J. L., De Serres, S. J., and Lamontagne, A. (2010). The effect of arm movements on the lower limb during gait after a stroke. *Gait Posture* 31, 109–115. doi: 10.1016/j.gaitpost.2009.09.008

Van Criekinge, T., Saeys, W., Hallemans, A., Velghe, S., Viskens, P. J., Vereeck, L., et al. (2017). Trunk biomechanics during hemiplegic gait after stroke: a systematic review. *Gait Posture* 54, 133–143. doi: 10.1016/j.gaitpost.2017.03.004

van Schaik, J. E., and Dominici, N. (2020). Motion tracking in developmental research: methods, considerations, and applications. *Prog. Brain Res.* 254, 89–111. doi: 10.1016/bs.pbr.2020.06.007

Verheyden, G., Ruesen, C., Gorissen, M., Brumby, V., Moran, R., Burnett, M., et al. (2014). Postural alignment is altered in people with chronic stroke and related to motor and functional performance. *J. Neurol. Phys. Ther.* 38, 239–245. doi: 10.1097/npt.0000000000000054

Verheyden, G., Vereeck, L., Truijen, S., Troch, M., Herregodts, I., Lafosse, C., et al. (2006). Trunk performance after stroke and the relationship with balance, gait and functional ability. *Clin. Rehabil.* 20, 451–458. doi: 10.1191/0269215505cr955oa

Wikström, J., Georgoulas, G., Moutsopoulos, T., and Seferiadis, A. (2014). Intelligent data analysis of instrumented gait data in stroke patients-a systematic review. *Comput. Biol. Med.* 51, 61–72. doi: 10.1016/j.compbiomed.2014.04.004

Wonsetler, E. C., and Bowden, M. G. (2017). A systematic review of mechanisms of gait speed change post-stroke. Part 2: exercise capacity, muscle activation, kinetics, and kinematics. *Top Stroke Rehabil.* 24, 394–403. doi: 10.1080/10749357.2017.1282413

Woolley, S. M. (2001). Characteristics of gait in hemiplegia. *Top Stroke Rehabil.* 7, 1–18. doi: 10.1310/JB16-V04F-JAL5-H1UV

Conflict of Interest: The authors declare that the research was conducted in the absence of any commercial or financial relationships that could be construed as a potential conflict of interest.

frontiers in Human Neuroscience

ORIGINAL RESEARCH
published: 02 March 2022
doi: 10.3389/fnhum.2022.816088

Are Clinical Impairments Related to Kinematic Gait Variability in Children and Young Adults With Cerebral Palsy?

Anne Tabard-Fougère[1], Dionys Rutz[2], Annie Pouliot-Laforte[1], Geraldo De Coulon[3], Christopher J. Newman[4], Stéphane Armand[1] and Jennifer Wegrzyk[5]*

[1] Willy Taillard Laboratory of Kinesiology, Geneva University Hospitals and Geneva University, Geneva, Switzerland, [2] Physical Therapy Unit, Department of Clinical Neurosciences, Lausanne University Hospital, Lausanne, Switzerland, [3] Pediatric Orthopaedic Surgery Unit, Geneva University Hospitals, University of Geneva, Geneva, Switzerland, [4] Pediatric Neurology and Neurorehabilitation Unit, Department of Pediatrics, Lausanne University Hospital, University of Lausanne, Lausanne, Switzerland, [5] School of Health Sciences (HESAV), University of Applied Sciences and Arts Western Switzerland (HES-SO), Lausanne, Switzerland

Intrinsic gait variability (GV), i.e., fluctuations in the regularity of gait patterns between repetitive cycles, is inherent to the sensorimotor system and influenced by factors such as age and pathology. Increased GV is associated with gait impairments in individuals with cerebral palsy (CP) and has been mainly studied based on spatiotemporal parameters. The present study aimed to describe kinematic GV in young people with CP and its associations with clinical impairments [i.e., passive range of motion (pROM), muscle weakness, reduced selective motor control (selectivity), and spasticity]. This retrospective study included 177 participants with CP (age range 5–25 years; Gross Motor Function Classification System I-III) representing 289 clinical gait analyses [n = 172 for unilateral CP (uCP) vs. 117 for bilateral CP (bCP)]. As variability metrics, Root Mean Square Deviation (RMSD) for nine lower-limb kinematic parameters and Gait Standard Deviation (GaitSD) – as composite score of the kinematic parameters – were computed for the affected (unilateral = uCP) and most affected side (bilateral = bCP), respectively, as defined by clinical scores. GaitSD was then computed for the non/less-affected side for between leg comparisons. Uni- and multivariate linear regressions were subsequently performed on GaitSD of the affected/most affected side with all clinical impairments (composite scores) as independent variables. Highest RMSD were found in the transverse plane (hip, pelvis), for distal joints in the sagittal plane (knee, ankle) and for foot progression. GaitSD was not different between uCP and bCP (affected/most affected side) but higher in the non-affected vs. affected side in uCP. GaitSD was associated with age ($p < 0.001$), gait deviation index (GDI) ($p < 0.05$), muscle weakness ($p < 0.001$), selectivity ($p < 0.05$), and pROM ($p < 0.001$). After adjustment for age and GDI, GaitSD remained associated with muscle weakness (uCP: $p = 0.003$, bCP: $p < 0.001$) and selectivity (bCP: $p = 0.024$). Kinematic GV can be expressed as global indicator of variability (GaitSD) in young people with CP given the strong correlation of RMSD for lower-limb kinematic parameters. In terms of asymmetry, increased variability of the non-affected vs. affected side may indicate contralateral

OPEN ACCESS

Edited by:
Carmelo Chisari, Pisana University Hospital, Italy

Reviewed by:
Prue Elizabeth Morgan, Monash University, Australia
Ailish Malone, Royal College of Surgeons in Ireland, Ireland

***Correspondence:**
Anne Tabard-Fougère
anne.tabard@hcuge.ch

Specialty section:
This article was submitted to Motor Neuroscience, a section of the journal Frontiers in Human Neuroscience

Received: *16 November 2021*
Accepted: *02 February 2022*
Published: *02 March 2022*

Citation:
Tabard-Fougère A, Rutz D, Pouliot-Laforte A, De Coulon G, Newman CJ, Armand S and Wegrzyk J (2022) Are Clinical Impairments Related to Kinematic Gait Variability in Children and Young Adults With Cerebral Palsy? Front. Hum. Neurosci. 16:816088. doi: 10.3389/fnhum.2022.816088

compensation mechanisms in uCP. Notably muscle weakness (uCP, bCP) and selectivity (bCP) – but not spasticity – were associated with GaitSD. Further studies need to explore the clinical relevance of kinematic GV in CP to support the interpretation of clinical gait analyses and therapeutic decision-making.

Keywords: cerebral palsy, gait, variability, kinematic, clinical impairments

INTRODUCTION

Clinical Gait Analysis (CGA) is fundamental for the clinical management of pathological gait deviations. Intrinsic variability (i.e., cycle-to-cycle, within subject variability) occurring during one single testing session can be quantified using CGA. These temporal fluctuations in the regularity of gait patterns between repetitive cycles are inherent to the sensorimotor system and independent of error sources (extrinsic variability) (Schwartz et al., 2004). Intrinsic variability represents an important indicator of overall walking function (Stergiou et al., 2006) and can be a relevant parameter when interpreting CGA. Intrinsic variability depends on the neurological integration of multiple sensory inputs and the coordination of motor outputs (Wu et al., 2014; Pekny et al., 2015), and is influenced by factors such as age, walking speed, pathological and environmental conditions. In stable experimental environments (in which motor redundancy is reduced), low GV is usually considered as consistent and healthy, while increased GV is usually considered as less stable and pathological (Hausdorff, 2005). In contrast to simple variability measures (such as standard deviation and coefficient of variation) used to quantify data dispersion at specific instances of the gait cycle, more advanced variability metrics – such as the RMSD (Picerno et al., 2008) for unidimensional parameters, and GaitSD (Sangeux et al., 2016) as an overall index of kinematic GV – can characterize whole within-stride variability to quantify the similarity of curve patterns along the whole gait cycle (Di Marco et al., 2018). Association of these curve based metrics with clinical impairments could facilitate the interpretation of treatment efficacy on an individual basis.

Cerebral palsy (CP) represents a permanent, non-progressive "[. . .] disorder of movement and posture due to a defect or lesion of the immature brain" (Bax, 2008) and is the most frequent cause of motor disability in childhood (Pakula et al., 2009). Gait impairment in individuals with CP is complex and associated with clinical impairments such as spasticity, muscle weakness and reduced selective motor control. These sensorimotor deficits limit functional capacities within the locomotor system and may result in increased variability of kinematic and spatiotemporal parameters (Õunpuu et al., 2015). Heterogeneity in GV outcomes during the early stages of walking in young people with CP can also be explained by the degree of maturation associated with learning and neuroplasticity processes, rendering its interpretation challenging (Prosser et al., 2010).

In CGA, kinematic data are usually visualized as continuous data in the form of single-cycle curves for each joint, representing a time-varying value over one gait cycle (with stride-to-stride variability expressed as a set of curves over-plotted in the same graph). The mean curves of all gait cycles are visually inspected for each articulation/segment/plane and interpreted based on summary scores such as the gait deviation index (GDI) and the gait profile score (GPS) with regards to normative values of healthy control subjects. However, limited functional capacity (such as low walking speed) and compensation strategies of young people with CP impede a direct group comparison. Additionally, Oudenhoven et al. (2019) reported that even in typically developing (TD) children (especially at a young age), a substantial number of strides can be classified as abnormal with regards to stride-to-stride variability. Consequently, they concluded that a comparison of the mean curve of all gait cycles within one CGA session to that of an age-matched control group might lead to misinterpretation of gait deviations.

Given the particularly high intra-subject variability in neurodevelopmental disorders, mean values of discrete (spatiotemporal) parameters do not properly reflect individual gait characteristics (Sangeux et al., 2016). In contrast to spatiotemporal parameters, the variability of kinematic parameters remains largely unexplored in CP.

Objectives

The aims of this study were to investigate kinematic GV in children and young adults with unilateral and bilateral spastic CP while (1) describing the pathology specific GV patterns of nine lower limbs kinematic variables and (2) identifying the explanatory variables of the variability pattern observed based on clinical impairment scores.

MATERIALS AND METHODS

Participants

This retrospective study included young people with CP who underwent a CGA in the Kinesiology Laboratory of a tertiary hospital between 1994 and 2020. The local Ethics Committee approved this study (CER no. 2018-00229), i.e., permission to use and further process retrospective data recorded during CGA after anonymization. Informed consent was obtained from all participants and their respective legal guardians since this approval (March 2018). The local Ethics Committee granted a consent exemption for CGA performed prior to this date.

The inclusion criteria were: age between 5 and 25 years, diagnosis of unilateral or bilateral spastic CP (levels I to III on the Gross Motor Function Classification System-GMFCS) and the ability to walk 10 m without external support. The exclusion criteria were: lower limb surgery 12 months prior to the CGA, botulinum toxin injection (BTX) 6 months prior to the CGA, in case of multiple CGA time between each CGA < 1 year, and less than 5 valid kinematic gait cycles.

Data Collection

Please refer to **Table 1** for demographic and clinical participants' characteristics.

To limit bias due to age and sex on the interpretation of body mass index (BMI) in a pediatric population, the BMI-for-age was computed as z-score (z) (de Onis et al., 2007) and weight status categories were defined using cut-offs recommended by the World Health Organization (de Onis and Lobstein, 2010).

Gait Analysis

Participants were instructed to walk barefoot at a comfortable self-selected speed along a 10 m walkway. Kinematic parameters were measured using a 12-camera motion analysis system (model Oqus 7+, Qualisys, Göteborg, Sweden) between 2015 and 2019, a 12-camera motion analysis system (Vicon MX3+, Vicon Peak, Oxford, United Kingdom) between 2007 and 2015 and a 6-camera motion analysis system (Vicon 460, Vicon Peak, Oxford, United Kingdom) before 2007. The marker trajectories were recorded at 100 Hz and filtered using the predicted mean-squared error filter MSE10 in the Nexus software before 2015 and high-pass 4th order Butterworth filter (10 Hz) after. Participants were equipped with 35 reflective markers placed on the skin at defined anatomical and technical landmarks according to the full-body Plug-in-Gait model (Davis et al., 1991).

Clinical Examination

The same day as CGA, an experienced physiotherapist clinically assessed the lower limbs including spasticity, selectivity, muscle

TABLE 1 | Differences of demographic, clinical and gait outcomes between participants with unilateral cerebral palsy (uCP, *n* = 105, 172 CGA) and bilateral cerebral palsy (bCP, *n* = 72, 117 CGA).

	uCP (172 CGA)	bCP (117 CGA)	Groups comparison		
			P	**ES**	**95% CI**
Demographic and clinical characteristics					
Age, years old	12.4 (4.8)	13.1 (5.1)	0.240	0.143	−1.9 to 0.5
Female, n (%)	79 (46%)	42 (36%)	0.115	0.146	−2 to 22%
Body weight status	–	–	0.361	–	–
Underweight, n (%)	18 (10%)	14 (12%)	0.835	0.003	−10 to 7%
Normal weight, n (%)	104 (60%)	80 (68%)	0.212	0.092	−20 to 4%
Overweight, n (%)	36 (21%)	19 (16%)	0.398	0.042	−5 to 14%
Obese, n (%)	12 (7%)	4 (3%)	0.300	0.063	−2 to 9%
GMFCS Level	–	–	<0.001*	–	–
I, n (%)	155 (90%)	73 (62%)	<0.001*	1.794	17–38%
II, n (%)	14 (8%)	37 (32%)	<0.001*	1.461	−34 to −13%
III, n (%)	0 (0.0%)	7 (6%)	0.004*	0.480	−11 to −1%
Previous treatments					
BTX > 6 months before, n (%)	72 (42%)	40 (34%)	0.234	0.083	−4 to 20%
Surgery > 1 year before, n (%)	62 (36%)	37 (32%)	0.515	0.025	−7 to 16%
Composite impairment scores					
Spasticity composite score, 0–16	1.1 (1.6)	3.0 (2.8)	<0.001*	0.902	1.4–2.5
Weakness composite score, 0–30	22.6 (4.0)	23.0 (5.1)	0.422	0.102	−1.6 to 0.7
Selectivity composite score, 0–12	9.5 (2.2)	9.4 (2.7)	0.751	0.039	−0.5 to 0.7
pROM composite score, 0–9	2.9 (1.7)	2.2 (1.7)	0.002*	0.387	0.3–1.0
General gait characteristics					
Walking speed, m/s	1.11 (0.15)	1.02 (0.25)	<0.001*	0.451	0.04–0.14
Normalized walking speed, (m/s)/LL	1.45 (0.30)	1.37 (0.39)	0.060	0.240	−0.01 to 0.17
Gait deviation index (GDI)	85.0 (11.3)	81.2 (12.1)	0.008*	0.331	1.1–6.6
Gait asymmetry					
Step time asymmetry, %	13.9 (7.7)	6.5 (6.6)	<0.001*	1.015	5.7–9.0
Step length asymmetry, %	8.7 (8.1)	8.3 (7.2)	0.665	0.051	−1.4 to 2.2
Gait variability					
GaitSD, degrees	2.5 (0.8)	2.5 (0.9)	0.970	0.005	−0.3 to 0.2
Step time CV, %	3.2 (1.9)	4.0 (2.3)	0.007*	0.365	−1.3 to −0.2
Step length CV, %	3.6 (2.1)	4.5 (3.1)	0.002*	0.432	−1.8 to −0.4

Statistical tests used were the student t-tests for continuous outcomes presented as mean [standard deviation (SD)] and Pearson chi-2 test for dichotomous outcomes presented as n (%). Significant differences between groups were considered at $p < 0.05$ (*).

LL, leg length; CGA, clinical gait analysis; GDI, Gait deviation index; pROM, passive range of motion; GMFCS, gross motor function classification scale (Palisano et al., 2008); CV is coefficient of variation (SD/mean); BTX is botulinum toxin type A treatments; Spasticity composite score concerned the hip flexors, the knee flexors and extensors and the ankle plantar flexors; Weakness and selectivity composite score concerned the hip flexors and extensors, the knee flexors and extensors and the ankle plantar and dorsiflexors; pROM composite score concerned the hip extensors, the knee popliteal angle and the ankle dorsiflexors.

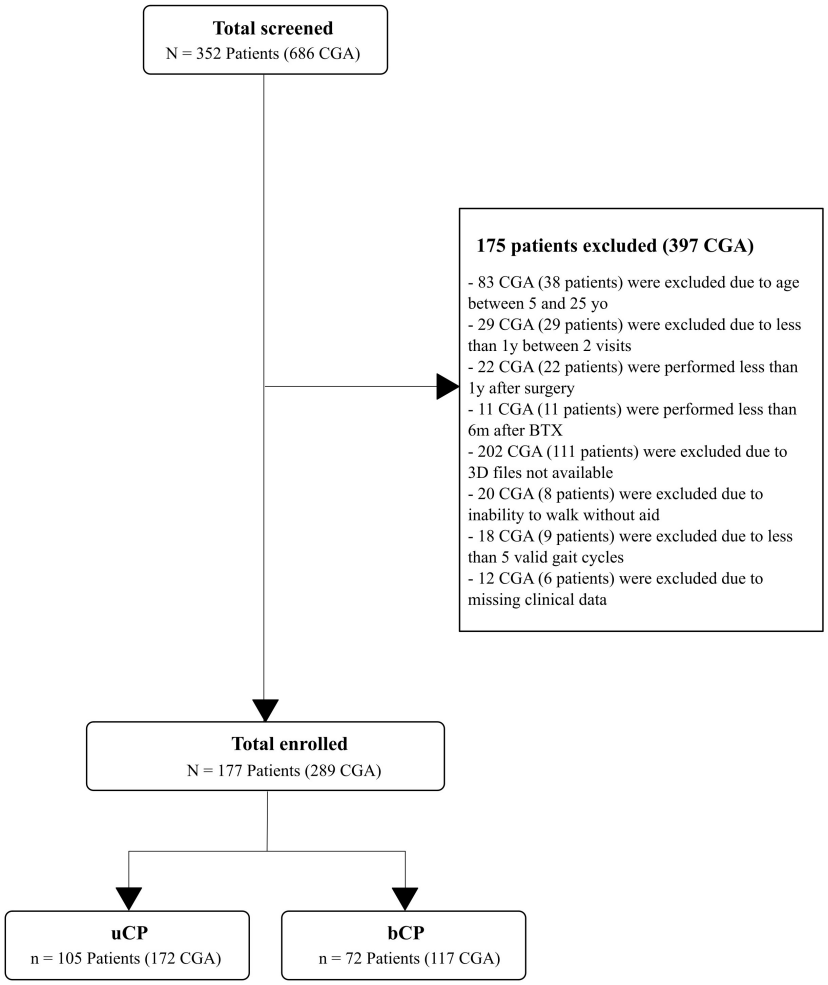

FIGURE 1 | Flow chart of the inclusion and exclusion criteria leading to the selection of the 105 subjects with unilateral cerebral palsy (uCP) and 72 subjects with bilateral cerebral palsy (bCP). According to the inclusion and exclusion criteria, multiple visits were included resulting in a total of 172 clinical gait analysis (CGA) in the uCP and 117 CGA in the bCP group. 3D file available means gait records computed with the custom-made software developed by Moveck® (https://moveck.com/). BTX is Botulinum toxin injection; yo, years old; y, year; m, months.

weakness, and passive range of motion (pROM; Viehweger et al., 2007). In this retrospective study, several physiotherapists were involved in the clinical examination over time. Spasticity was evaluated using the Modified Ashworth scale (MAS), ranging from 0 the 4 where a 0 score is no spasticity (Bohannon and Smith, 1987). Selective motor control was evaluated using the selective control assessment of the lower extremity (SCALE) on a scale ranging from 0 to 2 where 0 is no selective control (Fowler et al., 2009). Muscle weakness was assessed by the manual muscle testing (MMT), ranging from 0 to 5 where 5 is no weakness (Hislop et al., 2014). The pROM was measured using a goniometer to the nearest 5°.

Data Analysis

The affected and the most affected lower limb, respectively, were determined on the basis of higher clinical impairment composite scores (selectivity, spasticity, pROM, and muscle weakness, cf. section "Composite Clinical Score Analysis") scaled from 0 to 1 each.

General Gait Parameters Analysis

The gait cycle was defined by the time between two foot strikes of the same foot and event detection was computed from the trajectory of markers placed on the pelvis and feet (Zeni et al., 2008) and checked manually. For each participant, five randomly selected gait cycles were included in the analysis. Walking speed (m/s), cadence (steps/min), step time (s), and step length (cm) were computed for all included gait cycles. In order to reduce bias related to the participants' characteristics, both absolute and normalized (divided by leg length) walking speeds were reported (Hof, 1996).

The asymmetry of step time and step length were computed as abs[ln(left/right)] × 100% where 0% means perfect symmetry (Brændvik et al., 2020). The variability of step time and step length of the affected side/most affected lower-limb was

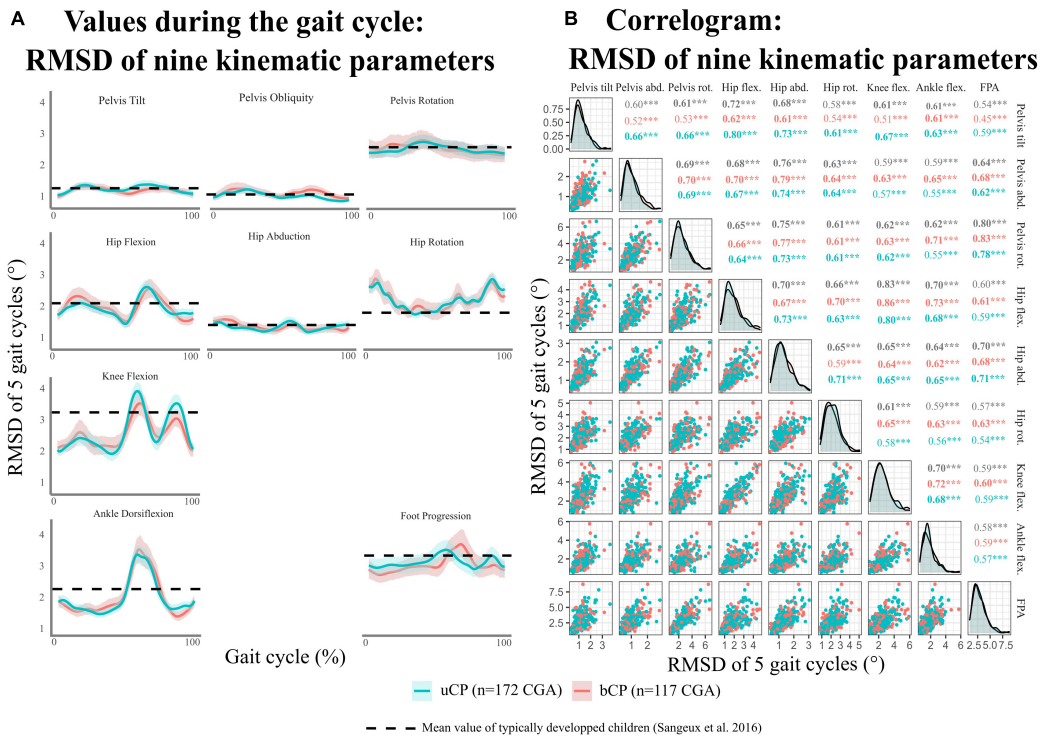

FIGURE 2 | (A) Distribution of kinematic intrinsic variability [evaluated using root mean square deviation (RMSD) for five gait cycles of the same visit] during gait cycle per kinematic parameters. **(B)** Correlogram of the mean RMSD for kinematic parameters. uCP, participants with unilateral cerebral palsy; bCP, participants with bilateral cerebral palsy; CGA, clinical gait analysis. Level of significance of Pearson correlations $^{*}p < 0.05$; $^{**}p < 0.01$; $^{***}p < 0.001$.

computed with the coefficient of variation (CV) defined as the ratio between the standard deviation and the mean (calculated as SD/mean × 100%) of the included gait cycles (Brændvik et al., 2020).

Kinematic Variability Analysis

Lower limb kinematic parameters were computed according to a replication of the conventional gait model (Davis et al., 1991) using a custom-made software developed by Moveck®[1]. The quality of gait kinematic parameters was checked for artifacts and outliers based on the visual inspection of each curve.

A total of nine kinematic variables were used for the affected limb: pelvic tilt, pelvic obliquity, pelvic rotation, hip flexion, hip abduction, hip rotation, knee flexion, ankle dorsiflexion, and foot progression angle. For each of those kinematic parameters, the RMSD was computed based on five randomly included gait cycles (Picerno et al., 2008).

Additionally, the GaitSD was computed based on the five randomly included cycles for each limb to compare the variability of both legs. For all other analysis, GaitSD concerned the affected/most affected side. The GaitSD – a composite score of the kinematic variability – has previously shown satisfying (1) precision for a low number of gait cycles and (2) sensitivity to changes with age in typically developing children (Sangeux et al., 2016).

[1]https://moveck.com/

Finally, the GDI was computed based on the same five included cycles (Schwartz and Rozumalski, 2008).

Composite Clinical Score Analysis

Based on Papageorgiou et al. (2019), individual joint scores (hip, knee, and ankle) per impairment (spasticity, selectivity, weakness, and pROM) were calculated and then combined into a composite score for the affected/most affected limb.

More specifically, spasticity scores were: "ankle spasticity" (median scores of the gastrocnemius and soleus muscles, from 0 to 4), "knee spasticity" (sum of the knee flexor and extensor scores, from 0 to 8), and "hip spasticity" (scores of the hip flexors, from 0 to 4). The composite spasticity score was computed as the sum of all muscle groups, from 0 to 16.

Similarly, the composite weakness score (from 0 to 30) was computed as the sum of all weakness scores: "ankle weakness" (median score of the dorsiflexors with knee flexed and extended, summed up with ankle plantar flexors, from 0 to 10), "knee weakness" (sum of knee flexors and knee extensors scores, from 0 to 10), and "hip weakness" (sum of hip flexors and extensors scores, from 0 to 10).

The composite selectivity score was calculated as the sum of the joint selectivity scores according to the muscles associated via the SCALE (from 0 to 12).

Finally, the composite pROM score was calculated based on the "hip pROM" (Thomas test score, from 0 to 3), "knee pROM" (median of knee flexors and knee extensors, from 0

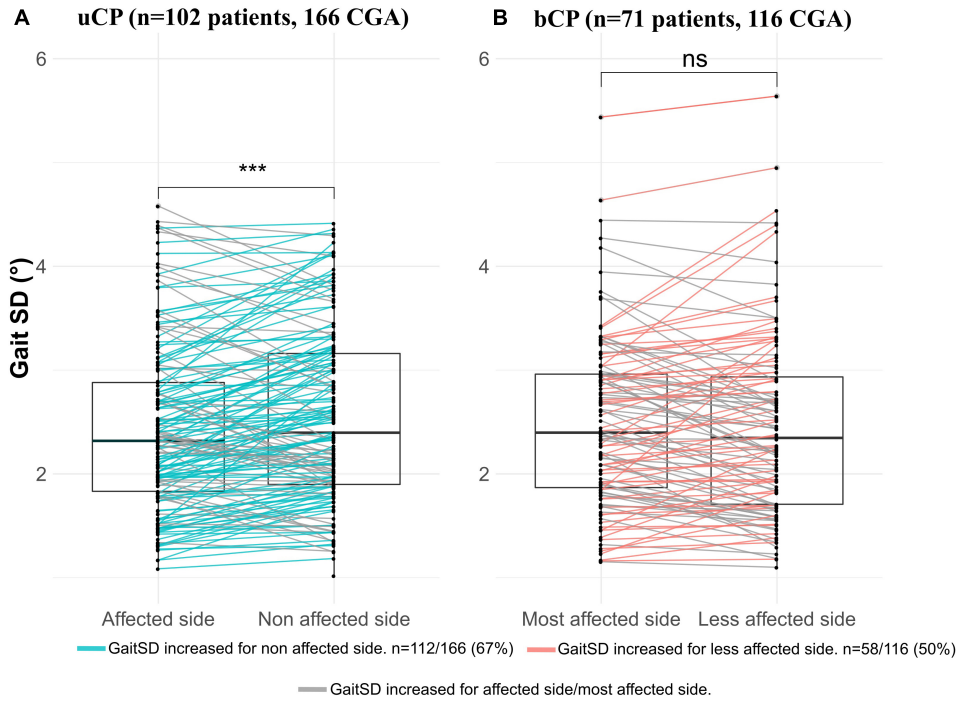

FIGURE 3 | Comparison of gait standard deviation (GaitSD) between: **(A)** Affected vs. non-affected side in participants with unilateral cerebral palsy (uCP); **(B)** Most affected side vs. less affected side in participants with bilateral cerebral palsy (bCP). Due to absence of minimum five valid gait cycles in both sides, six CGA (three patients) were excluded in uCP and one CGA (one patient) in bCP. Level of significance of paired Student *t*-tests $^{*}p < 0.05$; $^{**}p < 0.01$; $^{***}p < 0.001$.

to 3), and "ankle pROM" (median score of triceps flexion and plantar flexion, from 0 to 3) with a total score from 0 to 9. All pROM scores were coded based on aged-gender normal dataset of Soucie et al. (2011) with code 0 for values inferior to 5th percentile (severe impairments), 1 for values between 5th and 50th percentile (moderate impairments); 2 for values between 50th and 75th percentile (low impairments), and 3 for values superior to 75th percentile (no or slight contractures).

Statistical Analysis

Statistical analysis was performed using R (version v.3.6.1) with the RStudio interface (version 1.2.5033). To describe demographic and clinical data, descriptive statistics were used and reported as the mean (SD = standard deviation) for continuous variables and as n (%) for dichotomous variables. Additionally, normality distribution of continuous outcomes was tested with the Shapiro–Wilk test. Differences between groups were tested with the Student *t*-test, differences between frequency distributions with the Chi-square test (χ^2). Differences between groups were considered significant at $p < 0.05$.

Correlations between sets of the RMSD of all kinematic parameters were investigated using the R function "ggpairs" from the package GGally (version 1.5.0). Univariate linear regressions were performed on GaitSD with clinical composite scores as independent variables. Multivariate linear regressions were used to adjust for age and the gait deviation index (GDI). For each linear model, the linear regression coefficient β with the 95% confident interval (95% CI) and the adjusted R^2 (Adj. R^2) were reported. Adj. R^2 was adjusted by the number of predictors in the model. Significant associations were considered at $p < 0.05$.

Finally, for young people with uCP, the GaitSD of the affected side was compared with the non-affected side using a paired Student *t*-test. Accordingly, the most affected side (side with the higher sum of scaled composite scores of clinical impairments) was compared with the less affected side in bCP.

RESULTS

Participants

In total, 352 participants (686 CGA) with CP were screened: 41 (145 CGA) did not meet the following inclusion criteria: age between 5 and 25 years old, (>1 year between 2 CGA, >1 year after surgery, >6 m after BTX); 119 (222 CGA) did not have available 3D data (kinematics processed with Moveck) or walked with external aids; 9 (18 CGA) did not have > = 5 valid gait cycles and 6 (12 CGA) had missing clinical data (**Figure 1**). A total of 105 participants with uCP [172 CGA, 12.4 (4.8) years old, GMFCS: I (90%), II (10%)] and 72 participants with bCP [117 CGA, 13.1 (5.1) years old, GMFCS: I (62%), II (32%), III (6%)] were included (**Figure 1**).

As reported in **Table 1**, there were no significant differences between groups (uCP and bCP) for age, body weight status and previous treatments (BTX > 6 m before, Surgery > 1 year before), selectivity and weakness composite scores. They differed, however, with regard to GMFCS levels ($p < 0.001$), spasticity

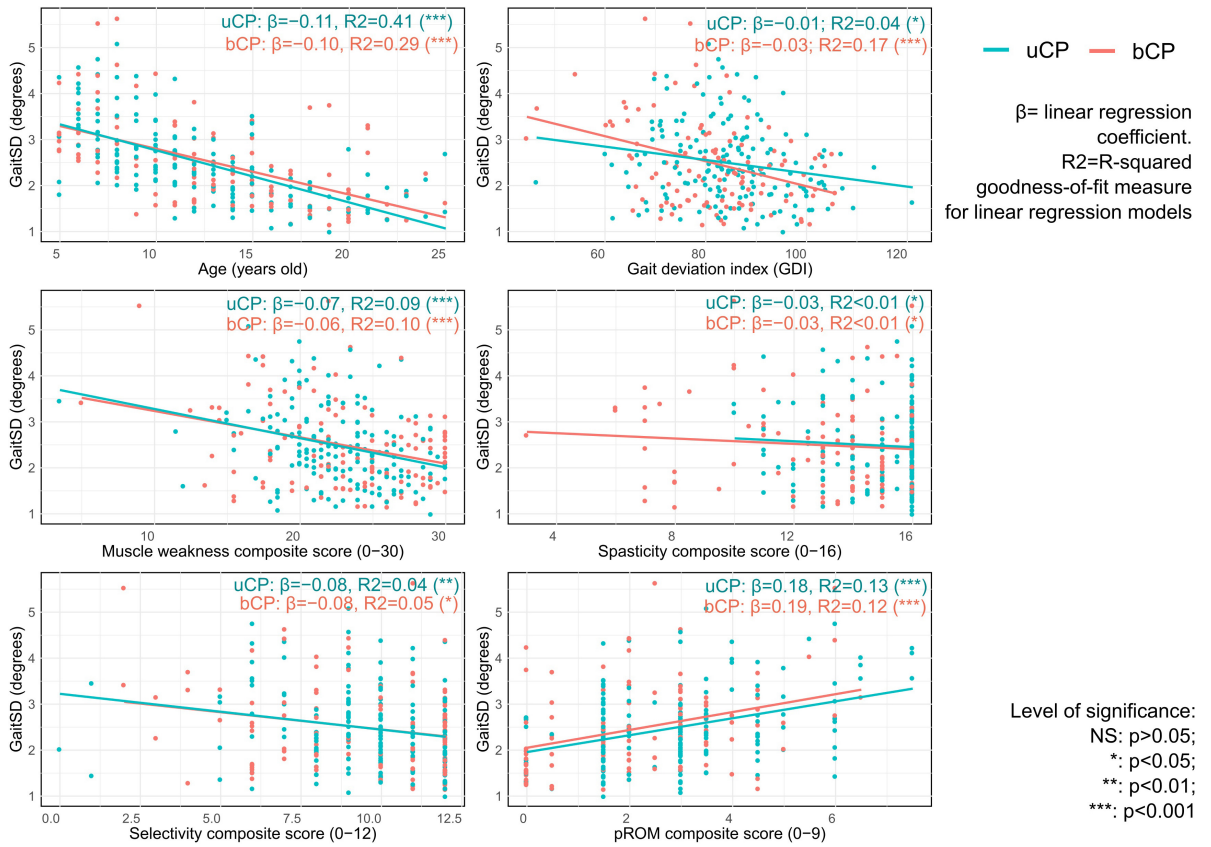

FIGURE 4 | Univariable linear regression results with scatterplot of gait standard deviation (GaitSD in degrees) for age, gait deviation index and composite scores of clinical impairments [spasticity, selectivity, muscle weakness, and passive range of motion (pROM)] of 105 subjects with unilateral cerebral palsy [uCP, 172 clinical gait analysis (CGA)] and 72 subjects with bilateral cerebral palsy (bCP, 117 CGA).

($p < 0.001$, 95% CI: 1.4–2.5) and pROM ($p < 0.001$, 95% CI: 0.3–1.0) composite scores.

Gait Characteristics

Compared to uCP, the bCP group had a significantly lower absolute walking speed ($p < 0.001$, 95% CI: 0.04–0.14), lower GDI ($p = 0.008$, 95% CI: 1.1–6.6), step time CV ($p < 0.007$, 95% CI: −1.3 to −0.2), and step length CV ($p < 0.002$, 95% CI: −1.8 to −0.4). In contrast, participants with bCP had a significantly lower step time asymmetry ($p < 0.001$, 95% CI: 5.7–9.0), but step length asymmetry was not significantly different between the groups ($p = 0.665$). Normalized walking speed, in contrast with absolute walking speed was not significantly different ($p = 0.06$) between uCP and bCP.

In uCP, step time was significantly higher ($p < 0.001$) on the affected side compared to the non-affected side [0.54 (0.07) vs. 0.47 (0.05) s] whereas step length was significantly reduced ($p = 0.012$) on the affected side compared to the non-affected side [0.55 (0.08) vs. 0.56 (0.08) m].

Kinematic Variability

As reported in **Figure 2A**, the highest values of RMSD (>2°) were found in the transverse plane and distal joints (knee, ankle). The RMSD of all nine kinematic variables were significantly correlated ($r > 0.50$, $p < 0.05$) (**Figure 2B**).

Gait Standard Deviation was not significantly different between the uCP and bCP groups (**Table 1**) and it was significantly higher on the non-affected side compared to the affected side in uCP (**Figure 3A**). On the contrary, GaitSD was not significantly higher in the most affected lower-limb compared to the less affected limb in bCP (**Figure 3B**). GaitSD was increased in the non-affected side compared to the affected side in 67% of all CGA in the uCP group (112 out of 166 CGA). This proportion was significantly higher ($p = 0.005$) than that of CGA performed by participants with bCP for which no increased GaitSD could be observed in the less affected side compared to the most affected side (50%; 58 out of 116 CGA).

Relation Between Age, Gait Deviation Index, Composite Impairment Scores and Gait Standard Deviation

As reported in **Figure 4**, univariate linear regression showed that GaitSD was significantly associated with age (uCP: $R^2 = 0.41$, $p < 0.001$, bCP: $R^2 = 0.29$, $p < 0.001$), GDI (uCP: $R^2 = 0.04$, $p = 0.012$, bCP: $R^2 = 0.17$, $p < 0.001$), muscle weakness (uCP:

TABLE 2 | Multiple-linear regression analysis of cycle-to-cycle gait kinematic variability (GaitSD) and clinical composite scores [weakness, spasticity, selectivity, and passive range of motion (pROM)] in subjects with unilateral cerebral palsy (uCP, *n* = 105, 172 CGA) and bilateral cerebral palsy (bCP, *n* = 72, 117 CGA).

	uCP (*n* = 172 CGA)			bCP (*n* = 117 CGA)		
Outcome	**β (95% CI)**	***p*-value**	**Adj. R^2**	**β (95% CI)**	***p*-value**	**Adj. R^2**
Weakness composite score						
Unadjusted	−0.06 (−0.10, −0.03)	<0.001*	0.086	−0.06 (−0.09, −0.02)	<0.001*	0.092
Age adjusted	−0.04 (−0.06, −0.01)	0.003*	0.433	−0.06 (−0.08, −0.03)	<0.001*	0.371
GDI adjusted	−0.06 (−0.09, −0.03)	<0.001*	0.098	−0.03 (−0.07, 0.01)	0.061	0.139
Age + GDI adjusted	−0.03 (−0.06, −0.01)	0.011*	0.443	−0.04 (−0.07, −0.01)	0.009*	0.387
Spasticity composite score						
Unadjusted	−0.03 (−0.11, 0.05)	0.489	0.003	−0.03 (−0.09, 0.03)	0.353	0.001
Age adjusted	−0.05 (−0.11, 0.01)	0.127	0.411	−0.05 (−0.10, 0.01)	0.077	0.297
GDI adjusted	−0.02 (−0.10, 0.06)	0.558	0.030	0.01 (−0.05, 0.07)	0.726	0.111
Age + GDI adjusted	−0.04 (−0.11, 0.02)	0.154	0.428	−0.02 (−0.07, 0.04)	0.534	0.350
Selectivity composite score						
Unadjusted	−0.08 (−0.14, −0.02)	0.007*	0.037	−0.08 (−0.14, −0.01)	0.021*	0.039
Age adjusted	−0.04 (−0.09, 0.01)	0.057	0.416	−0.08 (−0.14, −0.03)	0.036*	0.330
GDI adjusted	−0.07 (−0.13, −0.01)	0.017*	0.061	−0.03 (−0.09, 0.04)	0.469	0.115
Age + GDI adjusted	−0.04 (−0.08, 0.01)	0.109	0.430	−0.05 (−0.10, −0.01)	0.024*	0.361
pROM composite score						
Unadjusted	0.19 (0.12, 0.26)	<0.001*	0.134	0.19 (0.10, 0.029)	<0.001*	0.112
Age adjusted	0.07 (−0.04, 0.13)	0.065	0.415	0.05 (−0.06, 0.15)	0.384	0.281
GDI adjusted	0.19 (0.12, 0.26)	<0.001*	0.170	0.22 (0.14, 0.32)	<0.001*	0.269
Age + GDI adjusted	0.06 (−0.01, 0.12)	0.055	0.434	0.10 (−0.01, 0.20)	0.058	0.369

Univariate and multivariate linear regression were used. β is the linear regression coefficient; 95% CI is the 95 confident interval; R^2 is the proportion of the variance accounted for the dependent variable. Adj. R^2 has been adjusted for the number of predictors in the model. Significant associations were considered at $p < 0.05$ (*). CGA is clinical gait analysis; pROM is passive range of motion; GDI is Gait Deviation index; Spasticity composite score concerned the hip flexors, the knee flexors and extensors and the ankle plantar flexors; Weakness and selectivity composite score concerned the hip flexors and extensors, the knee flexors and extensors and the ankle plantar and dorsiflexors; pROM composite score concerned the hip extensors, the knee popliteal angle and the ankle dorsiflexors.

$R^2 = 0.09$, $p < 0.001$, bCP: $R^2 = 0.10$, $p < 0.001$), selectivity (uCP: $R^2 = 0.04$, $p = 0.007$, bCP: $R^2 = 0.05$, $p = 0.021$), and pROM (uCP: $R^2 = 0.13$, $p < 0.001$, bCP: $R^2 = 0.12$, $p < 0.001$). As reported in **Table 2**, only muscle weakness (uCP: $R^2 = 0.443$, $p = 0.011$, bCP: $R^2 = 0.387$, $p = 0.009$) and selectivity (bCP: $R^2 = 0.361$, $p = 0.024$) remained significantly correlated with GaitSD after adjustment for age and GDI.

DISCUSSION

The aim of this study was to investigate kinematic GV in children and young adults with unilateral and bilateral spastic CP while (1) describing pathology specific GV patterns of nine lower-limb kinematic variables and (2) identifying the explanatory variables of the variability pattern observed based on clinical impairment (composite scores). Results are interpreted separately for uCP and bCP as evidence suggests that lower-limb motor functioning differs based on the topographical classification of CP (Meyns et al., 2016).

For both groups (uCP and bCP), kinematic variability was highest for distal joints (knee, ankle) in the sagittal plane, for proximal joints (hip and pelvis) in the transverse plane, and for the foot progression angle. These results agree with those of Sangeux et al. (2016) showing increased stride to stride variability (GV SD > 3) for identical planes and joints in TD children of similar age (6–17 years). Consequently, kinematic variability characteristics per joint location and planes observed in participants with uCP and bCP do not seem to be related to pathological variability. Future studies including a matched control group would need to confirm this finding.

Moreover, the present results show no joint/segment specific kinematic GV pattern in young people with CP highlighted by the correlation of all nine RMSD parameters of the affected/most-affected limb in uCP and bCP. Consequently, the use of the GaitSD as a composite score – sensitive to changes with age and suggested for TD children (Sangeux et al., 2016) – can be applied in youngsters with CP. The inclusion of the GaitSD, allowing for intra-individual evaluation in clinical interpretation of CGA, might complement gait deviation scores [such as the gait profile score (GPS) and GDI] that refer to a norm (inter-individual comparison). As recently shown, even young TD children show high stride-to-stride variability with many strides classified as "abnormal" when compared to group averaged normalized curves (Oudenhoven et al., 2019). Thus, an interpretation of CGA based on the comparison of the mean curve of repetitive cycles within one session to normative values ignores both physiological and pathology-related intra-individual variability that can be a relevant clinical information for the understanding of gait deviations.

Another result of the present study is that the GaitSD and RMSD outcomes of the affected/most affected side were not

significantly different between participants with uCP and bCP. This finding was contrary to our hypothesis that kinematic variability would be increased on the most affected side in bCP compared to the affected side in uCP due to more severe clinical impairments. Indeed, we observed higher levels of spasticity, pROM, (overall) GFMCS and lower GDI in bCP compared to uCP, in agreement with previous research stating higher clinical impairments in bCP (Prosser et al., 2010; Meyns et al., 2016) even if the between group difference in GDI was not clinically significant (<10°). In previous literature, the comparison between variability characteristics in individuals with uCP vs. bCP has only been performed on spatiotemporal parameters without considering the implication of each lower limb. In agreement with Brændvik et al. (2020), we observed significantly higher step time variability and step length variability in bCP compared to uCP suggesting that adjustability of foot placement and timing is less affected in uCP.

Consequently, we investigated asymmetry characteristics of kinematic variability by comparing the affected/more affected side with the non/less affected side in both groups. Interestingly, GaitSD was increased on the non-affected side compared to the affected side in uCP. No inter-limb asymmetry based on the GaitSD comparison was found in bCP. Higher variability in the non-affected limb might be associated with the significantly shorter step time and higher step length observed in the non-affected vs. the affected limb in our population with uCP. Performing a longer distance during a shorter amount of time might suggest less refined motor skills inducing higher kinematic variability, however, this hypothesis requires further investigation. Alternatively, increased variability in the non-affected limb might reflect compensation via non-damaged cortical areas leading to higher motor capacity (through a broader motor repertoire allowing adjustment to motor deficits of the affected side). Such "good" variability might be associated with increased connectivity of the non-affected side as shown for stroke patients (Bajaj et al., 2015) and could explain the increased overall functional capacity in young people with uCP compared to bCP. Future studies would need to confirm the presence and origin of contralateral compensation patterns through increased variability and investigate underlying mechanisms. In terms of coordination of neural control across legs, Bulea et al. (2017) reported preserved control circuits in children with uCP allowing each leg to adapt independently to reduce gait asymmetry in response to external perturbations. This finding complements our finding of variability and asymmetries in the uCP group. Common research and practice that currently focuses on the affected side in uCP (Sangeux et al., 2013) should therefore not neglect the influence of the unaffected leg on gait patterns.

Concerning the second objective of this study, GaitSD was significantly associated with age, GDI and all composite scores (except spasticity) in both groups. The absence of association between GaitSD and the spasticity composite score could be explained by the relatively low level of spasticity in our sample compared to a previously investigated population (Papageorgiou et al., 2019).

The significant association between GaitSD and age is in line with the results reported by Sangeux et al. (2016) and Oudenhoven et al. (2019) in TD children showing high gait variability at a young age. The impact of gait maturity on kinematic GV should be considered in the clinical context to better support the interpretation of gait deviations in children with CP. To our knowledge, our study is the first to report a significant association between GaitSD and GDI in young people with uCP and bCP. Even though overall GaitSD level was similar to values reported in TD children, GaitSD was increased in participants with higher gait deviations, especially in bCP.

Concerning clinical composite scores, GaitSD remained significantly associated with muscle weakness in both groups after adjustment for age and GDI. These results are in line with Chang et al. (2013) who reported for patients with chronic stroke that weakness (rather than spasticity) affects voluntary force control and leads to higher force variability in isometric muscle contractions. However, even though muscle strength has been reported to be correlated with gait function in CP (Desloovere et al., 2006; Ross and Engsberg, 2007), the association between static isometric muscle contractions and complex gait is not straightforward in individuals with CP (Dallmeijer et al., 2011) and requires further investigation. Moreover, increased GaitSD was associated with reduced selective motor control after correction for age and GDI in bCP. In individuals with CP, the motor cortex and/or tracts are damaged which may affect volitional control of movement (Fowler, 2010) and spinal mechanisms responsible for the automatic control of gait (Clowry, 2007). Chruscikowski et al. (2017) observed a negative correlation between selectivity and the gait profile score (as an indicator of gait abnormality) in young people with bCP and hypothesized less complex control strategies during gait as the underlying neurological cause (Chruscikowski et al., 2017).

The present study has several limitations. First, the included participants with CP globally had mild to moderate clinical impairments. Our findings would need to be confirmed in young people with CP with more severe clinical impairments. Second, low to moderate inter-operator reliability of clinical evaluation (spasticity, selectivity, muscle weakness, and pROM) (Fosang et al., 2003) could have influenced the results with regards to the second objective of the present study. Another limitation is the fact that data acquisition (including technology) and processing have evolved over the years and unfortunately quality assurance was not uniform/standardized the same way over time. Finally, the calculation of the GaitSD is only based on five randomly selected cycles. According to Sangeux et al. (2016), a minimum of six strides is recommended for healthy subjects and up to 10 strides in pathological populations due to increased GV baseline values. In practice, however, 10 strides considerably increase the number of walking trials having the risk of inducing fatigue in populations with neuromotor disorders.

The presented metrics evaluating kinematic GV (i.e., RMSD and GaitSD) detect variations in amplitude and shape of the curve and are sensitive to time-shift between the curves (Di Marco et al., 2018). Temporal alignment could be achieved using existing techniques such as dynamic time warping (Helwig et al., 2011). Future studies could additionally investigate non-linear measures to assess gait variability (such as Largest Lyapunov Exponent), and gait regularity (such as approximate Entropy) (Stergiou et al., 2004).

Finally, gait at a self-selected speed in laboratory conditions does not reflect the complexity of gait in daily life. Investigations on the impact of cognitive load, walking surface and gait speed variations, would complement our findings of GV in individuals with CP.

CONCLUSION

Kinematic GV can be expressed as global indicator (GaitSD) in children and young adults with CP due to the strong correlation of the RMSD for the investigated lower-limb kinematic parameters. Increased variability on the non-affected side suggests contralateral compensation patterns in participants with uCP. After correction for age and GDI, GaitSD remained significantly associated with pathology-specific muscle weakness for the uCP and bCP groups and selectivity for the bCP group. Further studies need to explore the clinical relevance of kinematic GV in individuals with CP to support the interpretation of clinical gait analysis and therapeutic decision-making.

DATA AVAILABILITY STATEMENT

The data analyzed in this study is subject to the following licenses/restrictions: clinical data. Requests to access these datasets should be directed to the corresponding author.

ETHICS STATEMENT

The studies involving human participants were reviewed and approved by the Regional Research Ethics Committee (CCER) Geneva. Written informed consent to participate in this study was provided by the participants' legal guardian/next of kin.

AUTHOR CONTRIBUTIONS

AT-F, DR, AP-L, GD, CN, SA, and JW made substantial contributions to the conception or design of the work, the acquisition, analysis, or interpretation of data for the work, drafting the work or critically revising it for important intellectual content, and final approval of the version to be submitted for publication. All authors further agreed to be accountable for all aspects of the work in ensuring that questions related to the accuracy or integrity of any part of the work are appropriately investigated and resolved.

FUNDING

This work was part of a project supported by the Swiss National Science Foundation CRSII5_177179 (https://p3.snf.ch/project-177179). The funding source was not involved in the collection, analysis and interpretation of data, in writing of the report, and in the decision to submit the article for publication.

ACKNOWLEDGMENTS

We want to thank Marys Franco Carvalho (Kinesiology Laboratory of the University of Geneva, Switzerland) for her technical support.

REFERENCES

Bajaj, S., Butler, A. J., Drake, D., and Dhamala, M. (2015). Functional organization and restoration of the brain motor-execution network after stroke and rehabilitation. *Front. Hum. Neurosci.* 9:173. doi: 10.3389/fnhum.2015.00173

Bax, M. C. (2008). Terminology and classification of cerebral palsy. *Dev. Med. Child Neurol.* 6, 295–297.

Bohannon, R. W., and Smith, M. B. (1987). Interrater reliability of a modified Ashworth scale of muscle spasticity. *Phys. Ther.* 67, 206–207. doi: 10.1093/PTJ/67.2.206

Brændvik, S. M., Goihl, T., Braaten, R. S., and Vereijken, B. (2020). The Effect of Increased Gait Speed on Asymmetry and Variability in Children With Cerebral Palsy. *Front. Neurol.* 10:1399. doi: 10.3389/fneur.2019.01399

Bulea, T. C., Stanley, C. J., and Damiano, D. L. (2017). Part 2: adaptation of gait kinematics in unilateral cerebral palsy demonstrates preserved independent neural control of each limb. *Front. Hum. Neurosci.* 11:50. doi: 10.3389/fnhum.2017.00050

Chang, S. H., Francisco, G. E., Zhou, P., Rymer, W. Z., and Li, S. (2013). Spasticity, weakness, force variability, and sustained spontaneous motor unit discharges of resting spastic-paretic biceps brachii muscles in chronic stroke. *Muscle Nerve* 48, 85–92. doi: 10.1002/mus.23699

Chruscikowski, E., Fry, N. R. D., Noble, J. J., Gough, M., and Shortland, A. P. (2017). Selective motor control correlates with gait abnormality in children with cerebral palsy. *Gait Posture* 52, 107–109. doi: 10.1016/j.gaitpost.2016.11.031

Clowry, G. J. (2007). The dependence of spinal cord development on corticospinal input and its significance in understanding and treating spastic cerebral palsy. *Neurosci. Biobehav. Rev.* 31, 1114–1124. doi: 10.1016/j.neubiorev.2007.04.007

Dallmeijer, A. J., Baker, R., Dodd, K. J., and Taylor, N. F. (2011). Association between isometric muscle strength and gait joint kinetics in adolescents and young adults with cerebral palsy. *Gait Posture* 33, 326–332. doi: 10.1016/j.gaitpost.2010.10.092

Davis, R. B., Õunpuu, S., Tyburski, D., and Gage, J. R. (1991). A gait analysis data collection and reduction technique. *Hum. Mov. Sci.* 10, 575–587.

de Onis, M., and Lobstein, T. (2010). Defining obesity risk status in the general childhood population: which cut-offs should we use? *Int. J. Pediatr. Obes.* 5, 458–460. doi: 10.3109/17477161003615583

de Onis, M., Onyango, A. W., Borghi, E., Siyam, A., Nishida, C., and Siekmann, J. (2007). Development of a WHO growth reference for school-aged children and adolescents. *Bull. World Health Organ.* 85, 661–668. doi: 10.2471/blt.07.043497

Desloovere, K., Molenaers, G., Feys, H., Huenaerts, C., Callewaert, B., and Van de Walle, P. (2006). Do dynamic and static clinical measurements correlate with gait analysis parameters in children with cerebral palsy? *Gait Posture* 24, 302–313. doi: 10.1016/j.gaitpost.2005.10.008

Di Marco, R., Scalona, E., Pacilli, A., Cappa, P., Mazzà, C., and Rossi, S. (2018). How to choose and interpret similarity indices to quantify the variability in gait joint kinematics. *Int. Biomech.* 5, 1–8.

Fosang, A. L., Galea, M. P., McCoy, A. T., Reddihough, D. S., and Story, I. (2003). Measures of muscle and joint performance in the lower limb of children with cerebral palsy. *Dev. Med. Child Neurol.* 45, 664–670. doi: 10.1017/s0012162203001245

Fowler, S. P. (2010). Paraparesis secondary to intramedullary conus tuberculoma: a case report. *PMR* 2, S182–S183. doi: 10.1016/j.pmrj.2010.07.450

Fowler, E. G., Staudt, L. A., Greenberg, M. B., and Oppenheim, W. L. (2009). Selective Control Assessment of the Lower Extremity (SCALE): development, validation, and interrater reliability of a clinical tool for patients with cerebral

palsy. *Dev. Med. Child Neurol.* 51, 607–614. doi: 10.1111/J.1469-8749.2008.03186.X

Hausdorff, J. M. (2005). Gait variability?: methods, Modeling and Meaning. Example of Increased Stride Time Variability in Elderly Fallers Quantification of Stride-to-Stride Fluctuations. *J. Neuroeng. Rehabil.* 9, 1–9.

Helwig, N. E., Hong, S., Hsiao-Wecksler, E. T., and Polk, J. D. (2011). Methods to temporally align gait cycle data. *J. Biomech.* 44, 561–566. doi: 10.1016/j.jbiomech.2010.09.015

Hislop, H. J., Montgomery, J., and Brown, M. (2014). *Daniels and Worthingham's, Muscle Testing, Techniques of manual examination*, 9th Edn. United States: Elsevier .

Hof, A. L. (1996). Scaling gait data to body size. *Gait Posture* 4, 222–223. doi: 10.1016/s0966-6362(01)00097-2

Meyns, P., Van Gestel, L., Leunissen, I., De Cock, P., Sunaert, S., Feys, H., et al. (2016). Macrostructural and Microstructural Brain Lesions Relate to Gait Pathology in Children with Cerebral Palsy. *Neurorehabil. Neural Repair* 30, 817–833. doi: 10.1177/1545968315624782

Oudenhoven, L. M., Booth, A. T. C., Buizer, A. I., Harlaar, J., and van der Krogt, M. M. (2019). How normal is normal: consequences of stride to stride variability, treadmill walking and age when using normative paediatric gait data. *Gait Posture* 70, 289–297. doi: 10.1016/j.gaitpost.2019.03.011

Õunpuu, S., Gorton, G., Bagley, A., Sison-Williamson, M., Hassani, S., Johnson, B., et al. (2015). Variation in kinematic and spatiotemporal gait parameters by Gross Motor Function Classification System level in children and adolescents with cerebral palsy. *Dev. Med. Child Neurol.* 57, 955–962. doi: 10.1111/dmcn.12766

Pakula, A. T., Van Naarden Braun, K., and Yeargin-Allsopp, M. (2009). Cerebral Palsy: classification and Epidemiology. *Phys. Med. Rehabil. Clin. N. Am.* 20, 425–452.

Palisano, R. J., Rosenbaum, P., Bartlett, D., and Livingston, M. H. (2008). Content validity of the expanded and revised Gross Motor Function Classification System. *Dev. Med. Child Neurol.* 50, 744–750. doi: 10.1111/j.1469-8749.2008.03089.x

Papageorgiou, E., Simon-Martinez, C., Molenaers, G., Ortibus, E., Van Campenhout, A., and Desloovere, K. (2019). Are spasticity, weakness, selectivity, and passive range of motion related to gait deviations in children with spastic cerebral palsy? A statistical parametric mapping study. *PLoS One* 14:e0223363. doi: 10.1371/journal.pone.0223363

Pekny, S. E., Izawa, J., and Shadmehr, R. (2015). Reward-dependent modulation of movement variability. *J. Neurosci.* 35, 4015–4024. doi: 10.1523/JNEUROSCI.3244-14.2015

Picerno, P., Cereatti, A., and Cappozzo, A. (2008). Joint kinematics estimate using wearable inertial and magnetic sensing modules. *Gait Posture* 28, 588–595. doi: 10.1016/j.gaitpost.2008.04.003

Prosser, L. A., Lauer, R. T., VanSant, A. F., Barbe, M. F., and Lee, S. C. K. (2010). Variability and symmetry of gait in early walkers with and without bilateral cerebral palsy. *Gait Posture* 31, 522–526. doi: 10.1016/j.gaitpost.2010.03.001

Ross, S. A., and Engsberg, J. R. (2007). Relationships Between Spasticity, Strength, Gait, and the GMFM-66 in Persons With Spastic Diplegia Cerebral Palsy. *Arch. Phys. Med. Rehabil.* 88, 1114–1120. doi: 10.1016/j.apmr.2007.06.011

Sangeux, M., Passmore, E., Graham, H. K., and Tirosh, O. (2016). The gait standard deviation, a single measure of kinematic variability. *Gait Posture* 46, 194–200. doi: 10.1016/j.gaitpost.2016.03.015

Sangeux, M., Wolfe, R., and Graham, H. K. (2013). One side or two? *Dev. Med. Child Neurol.* 55, 786–787.

Schwartz, M. H., and Rozumalski, A. (2008). The gait deviation index: a new comprehensive index of gait pathology. *Gait Posture* 28, 351–357. doi: 10.1016/j.gaitpost.2008.05.001

Schwartz, M. H., Trost, J. P., and Wervey, R. A. (2004). Measurement and management of errors in quantitative gait data. *Gait Posture* 20, 196–203. doi: 10.1016/j.gaitpost.2003.09.011

Soucie, J. M., Wang, C., Forsyth, A., Funk, S., Denny, M., Roach, K. E., et al. (2011). Range of motion measurements: reference values and a database for comparison studies. *Haemophilia* 17, 500–507. doi: 10.1111/j.1365-2516.2010.02399.x

Stergiou, N., Buzzi, U. H., Kurz, M. J., and Heidel, J. (2004). "Nonlinear tools in human movement," in *Innovative analyses of human movement*, ed. N. Stergiou (Netherlands: Elsevier). 63–90.

Stergiou, N., Harbourne, R. T., and Cavanaugh, J. T. (2006). Optimal movement variability: a new theoretical perspective for neurologic physical therapy. *J. Neurol. Phys. Ther.* 30, 120–129. doi: 10.1097/01.npt.0000281949.48193.d9

Viehweger, E., Bérard, C., Berruyer, A., and Simeoni, M. C. (2007). Bilan articulaire des membres inférieurs d'un enfant atteint d'une infirmité motrice cérébrale. *Ann. Readapt. Med. Phys.* 50, 258–265.

Wu, H. G., Miyamoto, Y. R., Castro, L. N. G., Ölveczky, B. P., and Smith, M. A. (2014). Temporal structure of motor variability is dynamically regulated and predicts motor learning ability. *Nat. Neurosci.* 17, 312–321. doi: 10.1038/nn.3616

Zeni, J. A., Richards, J. G., and Higginson, J. S. (2008). Two simple methods for determining gait events during treadmill and overground walking using kinematic data. *Gait Posture* 27, 710–714. doi: 10.1016/j.gaitpost.2007.07.007

Conflict of Interest: The authors declare that the research was conducted in the absence of any commercial or financial relationships that could be construed as a potential conflict of interest.

frontiers in Human Neuroscience

ORIGINAL RESEARCH
published: 29 March 2022
doi: 10.3389/fnhum.2022.822205

Comparison of the Gait Biomechanical Constraints in Three Different Type of Neuromotor Damages

Silvia Minosse[1,2], Martina Favetta[1], Alberto Romano[1], Alessandra Pisano[1], Susanna Summa[1], Tommaso Schirinzi[1,3], Gessica Vasco[1], Enrico Castelli[1] and Maurizio Petrarca[1]*

[1] Department of Neurorehabilitation and Robotics, Movement Analysis and Robotics Laboratory (MARLab), "Bambino Gesù" Children's Hospital, IRCCS, Rome, Italy, [2] Department of Biomedicine and Prevention, University of Rome "Tor Vergata", Rome, Italy, [3] Department of Systems Medicine, University of Rome "Tor Vergata", Rome, Italy

OPEN ACCESS

Edited by:
Marco Iosa,
Sapienza University of Rome, Italy

Reviewed by:
Corrado Italo Angelini,
University of Padua, Italy
Ruxu Zhang,
Central South University, China

***Correspondence:**
Susanna Summa
susanna.summa@opbg.net

Specialty section:
This article was submitted to Motor Neuroscience, a section of the journal Frontiers in Human Neuroscience

Received: 25 November 2021
Accepted: 28 February 2022
Published: 29 March 2022

Citation:
Minosse S, Favetta M, Romano A, Pisano A, Summa S, Schirinzi T, Vasco G, Castelli E and Petrarca M (2022) Comparison of the Gait Biomechanical Constraints in Three Different Type of Neuromotor Damages. Front. Hum. Neurosci. 16:822205. doi: 10.3389/fnhum.2022.822205

Background and Objective: Absolute angle represents the inclination of a body segment relative to a fixed reference in space. This work compares the absolute and relative angles for exploring biomechanical gait constraints.

Methods: Gait patterns of different neuromotor conditions were analyzed using 3D gait analysis: normal gait (healthy, H), Cerebral Palsy (CP), Charcot Marie Tooth (CMT) and Duchenne Muscular Dystrophy (DMD), representing central and peripheral nervous system and muscular disorders, respectively. Forty-two children underwent gait analysis: 10 children affected by CP, 10 children by CMT, 10 children by DMD and 12 healthy children. The kinematic and kinetic parameters were collected to describe the biomechanical pattern of participants' lower limbs. The absolute angles of thigh, leg and foot were calculated using the trigonometric relationship of the tangent. For each absolute series, the mean, range, maximum, minimum and initial contact were calculated. Kinematic and kinetic gait data were studied, and the results were compared with the literature.

Results: Statistical analysis of the absolute angles showed how, at the local level, the single segments (thigh, leg and foot) behave differently depending on the pathology. However, if the lower limb is studied globally (sum of the kinematics of the three segments: thigh, leg and foot), a biomechanical constraint emerges.

Conclusion: Each segment compensates separately for the disease deficit so as to maintain a global biomechanical invariance. Using a model of inter-joint co-variation could improve the interpretation of the clinical gait pattern.

Keywords: gait, cerebral palsy, Charcot-Marie-Tooth, Duchenne Muscular Dystrophy, absolute angle, biomechanical constraints

INTRODUCTION

The introduction of gait analysis has enhanced the concept that motor behavior emerges from the body-environment coupling (Kuniyoshi and Suzuki, 2004; Abu-Faraj et al., 2015). Gait analysis is a multi-factorial analysis assessing kinematic, kinetic and electromyographic activities (EMG). These techniques are used to identify the kinematic determinants of human locomotion. Attention was focused on the relationship between the biomechanics of the human body and the brain (Lacquaniti et al., 1999) as these two elements do not work at the same logical level. The body biomechanics represents a given system of constraints, as shown by Collins et al. (2005) with his bipedal modeling of dynamic passive gait. In living creatures, the body is characterized by a redundancy of degree of freedom (DoF), raising the problem about their control during dynamic functional activities (Davies, 1968). The Central Nervous System fine-tunes the synergic actions of the muscles controlling the redundancy of the body DoF (Davies, 1968). In this perspective, the brain is the "medium" of the relationship between the organism and the environment, as explained by the ecologic approach to motor control and learning (Gibson, 1979). Although this relationship is well established, knowledge concerning the particular strategies used by the brain to mediate between body biomechanics and the environment is limited. The nature of the biomechanical constraints implies that appropriate solutions for walking are limited, and the usual bipedal walking represents a sort of final common path. However, different gait patterns that deviate from the "typical" one are frequently observed in pathologic conditions. It is possible to hypothesize that the way of walking, expressed in pathological conditions, can offer some keys for understanding the invariance rules that bind the biomechanical and neurological mechanisms. As an example, it was demonstrated that patients with hemiplegia and voluntary toe walkers shared the same kinematic, kinetic and EMG patterns (Romkes and Brunner, 2007). To explore the elements of invariance, we decided to analyze the gait pattern of children with different pathologies looking at differences and similarities. We analyzed the gait pattern that emerged from three different types of damage to the neuromotor system caused by Cerebral Palsy (CP), Charcot-Marie-Tooth (CMT) and Duchenne Muscular Dystrophy (DMD). They can be considered paradigmatic examples corresponding to damage involving the upper motor neuron, the lower motor neuron, and the muscles. CP, CMT and DMD children present complex and heterogeneous gait patterns already described using gait analysis tools (Salami et al., 2017; Wojciechowski et al., 2017; Davids et al., 2018; Goudriaan et al., 2018; Romano et al., 2019). To date, there has been no comparative study aimed at defining similarities and differences. The present study was facilitated by the fact that our gait lab is situated within a big clinical research center specialized in following children with rare diseases.

Briefly, CP is characterized by movement disorder, spasticity, muscle weakness, ataxia and rigidity (Armand et al., 2016). It has been reported that the alterations in the selective motor control are the result of failure to control reciprocal activation of the agonist and the antagonist muscles and correlate with the gait inability (Crenna, 1998; Chruscikowski et al., 2017). Their gait alterations are currently classified in literature (Rodda et al., 2004; Cioni et al., 2008) without reaching a consensus.

CMT is a peripheral nervous system disorder. Affected patients show skeletal deformities, distal muscle weakness and atrophy, and sensory impairment leading to walking impairment (Lencioni et al., 2017) which have already been classified in literature (Wojciechowski et al., 2017).

DMD is characterized by a progressive replacement of muscle fibers with fibro-fatty tissue and severe muscular weakness. Progressive muscular degeneration determines the onset of compensatory strategies during walking (Doglio et al., 2011). The gait pattern of this population has been widely described (Sienko Thomas et al., 2010; Goudriaan et al., 2018).

The present study aimed to investigate similarities and differences between the gait patterns of three different pathologic groups of children with CMT, DMD and CP compared to healthy children. The main hypothesis is that the three different gait patterns were influenced by the particular nature of the pathology (central, peripheral and muscular). However, they could also share elements of invariance. This invariance can be induced by body biomechanics and environmental physics, similarly to what identified in studies of lower limb absolute angles in healthy subjects (Borghese et al., 1996; Hamill et al., 2014). Ours is a pilot study in which, besides kinematics, the kinematic gait relative and absolute body segment configurations were compared, searching for differences and similarities, to enhance present knowledge related to the control of bipedal locomotion in pathological conditions.

MATERIALS AND METHODS

Participants

Ten children with CMT, ten children with DMD and ten children with CP were enrolled in the study. The eligibility criteria for this study were: age between 5 and 15 years and independent walking without orthosis. CP is a heterogeneous condition by definition. Consequently, both to reduce CP heterogeneity and to achieve the aims of this study, only participants with Gross Motor Function Classification System I and II were included, with a gait pattern corresponding to group IV of the Rodda et al. (2004) classification (Rodda et al., 2004) and to form IV of the Cioni et al. (2008) gait classification (Cioni et al., 2008). Exclusion criteria were: surgical treatment in the last year and administration of botulin toxin or experimental drug during the previous 6 months.

The group of children with CMT consisted of eight boys and two girls, with an average age of 12.0 (range: 7.0–15.0 years), an average weight of 46.3 (range: 25.0–79.5 kg), an average height of 1.44 (range:1.19–1.69 m) and an average leg length of 0.76 (range: 0.64–0.96 m).

The group of children with DMD consisted of 10 boys, with an average age of 7.7 (range: 5.0–11.0 years), average weight of 27.9 (range: 17.8–46.0 kg), average height of 1.23 (range: 1.04–1.63 m) and average leg length of 0.61 (range: 0.53–0.71 m).

The group of children with CP consisted of five boys and five girls, with an average age of 9.3 (range: 5.6–15.7 years), an average weight of 29.0 (range: 18.5–49.5 kg), an average height of 1.28 (range: 0.96–1.57 m) and average leg length of 0.69 (range: 0.48–0.87 m).

Reference data were collected in a group of twelve children, seven boys and five girls, without any neurological or neuromuscular problems, with an average age of 10.9 (range: 6.0–14.5), an average weight of 39.2 (range: 22.0–60.3 kg), average height 1.43 (range: 1.15–1.68 m) and average leg length 0.79 (range: 0.63–0.94 m).

All the children and their parents gave informed consent before starting the evaluation sessions. The Ethics Committee of the Hospital authorized the study. For an exhaustive clinical description of the pathologic groups see **Table 1**.

TABLE 1 | Clinical scale and six Minute Walking Test (6MWT): For Cerebral Palsy (CP) the clinical scale used is the Gross Motor Function Measure-66 (GMFM-66), for Charcot Marie Tooth (CMT) the clinical scale is the CMT Pediatric Scale (CMTPedS), and for Duchenne Muscular Dystrophy (DMD) the clinical scale is the NorthStar Ambulatory Assessment (NSAA).

CP	GMFM-66 (%)	6MWT (m)
CP1	51.85	280
CP2	78.28	335
CP3	98	501
CP4	66.69	352
CP5	70.39	375
CP6	96	443
CP7	86.52	331
CP8	75.34	390
CP9	100	414
CP10	71.22	345
CP11	86.52	395
CMT	**CMTPedS**	
CMT1	21	555
CMT2	18	562
CMT3	16	606
CMT4	25	550
CMT5	13	462
CMT6	18	512
CMT7	28	440
CMT8	31	375
CMT9	22	516
CMT10	28	464
DMD	**NorthStar Ambulatory Assessment**	
DMD1	31	564
DMD2	-	385
DMD3	28	335
DMD4	23	406
DMD5	26	364
DMD6	12	340
DMD7	31	425
DMD8	15	386
DMD9	31	464
DMD10	31	550

Gait Analysis

Gait analysis was performed using an eight-camera motion capture system (Vicon MX, United Kingdom) with sampling rates of 200 Hz and two force plates (AMTI, Or6-6, United States) with sampling rates of 1 kHz. The two force plates were situated in the middle portion of a 10 m walkway. Plug-in-Gait protocol for reconstructing a body kinematic and kinetic model was used. Participants walked barefoot at their self-selected speed. For each child, three representative gait cycles were considered. Kinematic and kinetic temporal series were normalized to the stride duration. Kinetic data were normalized to the subject's weight. In addition, we evaluated spatio-temporal parameters, walking velocity and step length were normalized to leg length.

The lower limb absolute angles (segment angles) that describe the segment's orientation in space were also calculated. Absolute angles are computed using the trigonometric relationship of the tangent. The tangent is equal to the angular coefficient obtained with a linear fit between the proximal endpoints of the segment. Schematic illustrations of the absolute angles (thigh, leg and foot) and relative angles (hip, knee and ankle) are reported in **Figure 1**. The following list of variables was selected from absolute angle curves of thigh, leg and foot: initial contact, average, range, maximum and minimum. The sum of the absolute angles (thigh, leg and foot) was then evaluated to determine the biomechanical constraints in lower limbs. The initial contact, average, range, maximum and minimum were calculated from the total absolute angle. See **Tables 2**, **3** for a detailed report of the kinematic and kinetic parameters.

Statistics

For each child, we evaluated three kinematic and three kinetic parameters for each representative gait cycle. Finally, we calculated the mean values. The Shapiro–Wilk normality test was used to verify the normal distribution. Since the data were not normally distributed, we assessed a non-parametric statistic. The Wilcoxon signed rank test for paired samples was used to compare the data obtained for the left and right limbs. Since the test was not statistically significant, the average between right and left limbs was calculated for all patients. The Kruskal–Wallis test and a post–hoc with Bonferroni correction determined significant differences in the kinematic (relative and absolute angles) and kinetic parameters between the four groups (CMT, DMD, CP and healthy). A $p < 0.05$ was considered to indicate statistical significance.

RESULTS

Spatio-temporal, kinematic (relative and absolute angles) and kinetic parameters for the variable illustrated in **Table 2** are shown in **Table 3**.

Children with DMD walked with a statistically significant higher stride velocity and a shorter stride time than those with CMT and CP. Stride width values were significantly larger in DMD and CP children compared to healthy controls. No statistically significant differences in any spatio-temporal

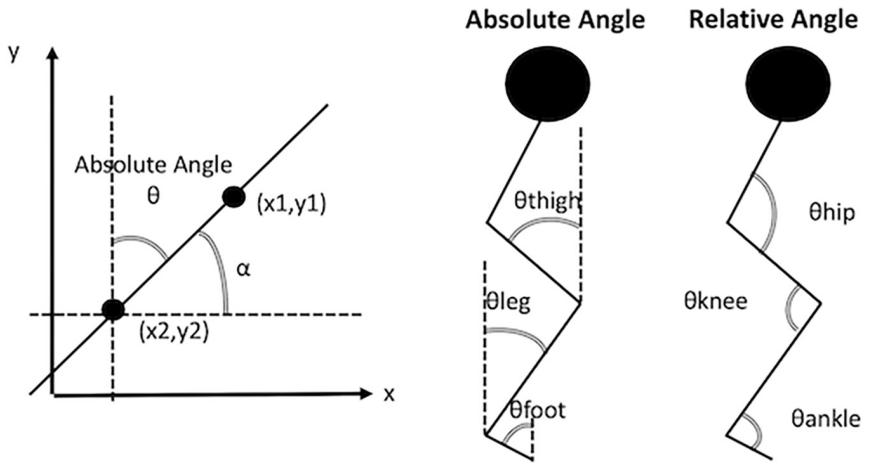

FIGURE 1 | Illustrative example of absolute angles and relative angles. In the panel (right) the absolute angle ∈ is the complementary angle of angle α. The angle α is obtained from the arctangent of the slope of the line passing through the points (x1, y1) and (x2, y2). In the panel (center) are depicted the absolute angles of thigh, leg, and foot. In the panel (left) are depicted the relative angle of the hip, the knee and the ankle.

parameters were found when comparing the children with CMT with the healthy children or those with CP (**Table 3**).

The analysis of kinematic pelvic parameters did not show statistically significant differences between healthy controls and children with CMT or DMD (**Figure 2**). The children with CP presented average and range pelvic tilt angles statistically higher than controls and children with CMT. Although we did not find any statistical significance in this sample, we observed that patients with DMD tended toward a pelvic anteversion and CMT patients toward a pelvic retroversion, as it is shown in the sagittal view of the Pelvis angle in **Figure 2** (i.e. the CMT time series angle is the lower curve).

The pelvic obliquity angle at initial contact in children affected by DMD was increased compared to those with CP. The children with CMT showed a reduction in the range of the pelvic obliquity angle compared to DMD and CP groups (**Figure 2**).

The children with CMT presented the average of the flexion/extension and maximum extension of hip angle lower compared to healthy children (**Figure 2**). The CP group showed an increase in maximum hip flexion compared to healthy patients. The children affected by CMT showed initial contact, average, and maximum and minimum flexion/extension of the hip angles statistically lower compared to CP children. For the patients affected by CP the initial contact of hip adduction/abduction angle resulted lower and statistically significant when compared to children with DMD and CMT (**Figure 2**). Patients with DMD showed a range of hip adduction/abduction angle greater than peers with CMT and CP.

The children with CMT showed decreased initial contact, average and maximum and minimum knee flexion angles compared to healthy children (**Figure 2**). However, the initial contact, average, and maximum knee flexion angles were significantly higher in children with CP than in peers with CMT and DMD.

Ankle dorsal/plantar angle at initial contact, average and maximum ankle dorsal angle during the stance phase were significantly lower in participants with CMT and DMD than in healthy children (**Figure 2**). The maximum ankle dorsal angle during swing phase values was statistically lower for all pathological groups (CMT, DMD and CP) than for healthy control groups. The ankle dorsal/plantar angle range resulted lower for children with CMT compared to participants with CP.

Increased range and maximum foot progression angles were only observed in children with CP compared with healthy children (**Figure 2**).

The children with CP presented initial contact, average, range, and maximum and minimum rotation of the foot progression angles significantly higher than children with CMT (**Figure 2**). We observed a reduction of the range of the foot progression angle for children with DMD compared to children with CP.

The absolute angle for thigh, leg and foot are shown in **Figure 3**. There are no statistically significant differences between CMT and DMD groups for absolute angle of thigh, leg and foot. However, there were differences between the children with CMT and peers in the CP and healthy groups for the thigh and leg segments but not for the foot segment. Differences between children in the DMD and CP groups were found for the thigh and leg segments. Patients in the DMD group only differ from the healthy group as regards the thigh segment (**Table 2**). However, **Figure 3** shows that the sum of the absolute angles (thigh, leg and foot) does not present statistically significant differences between these groups ($p > 0.05$).

Patients with CP showed an increase in maximum hip power generation during the stance phase when compared to peers with CMT and DMD. Maximum knee power absorbed during stance was lower in children with CP than in participants with CMT and DMD. The children with CP showed maximum ankle power generation and absorption during the stance phase statistically lower than healthy children (**Figure 4**).

TABLE 2 | The list of the kinematic and kinetic variables of the lower limb (pelvis, hip, knee and ankle) and the absolute angles of thigh, leg and foot.

Foot progression angle	
FPA_{IC}	Foot progression angle at initial contact
FPA_a	Average of foot progression angle
FPA_r	Range of foot progression angle
FPA_{max}	Maximum rotation of foot progression angle
FPA_{min}	Minimum rotation of foot progression angle
$FPA_{max.\%}$	% of Gait cycle corresponding of maximum rotation of foot progression angle
$FPA_{min.\%}$	% of Gait cycle corresponding of minimum rotation of foot progression angle
Pelvis	
P^T_{IC}	Pelvic tilt angle at initial contact
P^T_a	Average pelvic tilt angle
P^T_r	Range pelvic tilt angle
P^O_{IC}	Pelvic obliquity angle at initial contact
P^O_a	Average pelvic obliquity angle
P^O_r	Range pelvic obliquity angle
Hip	
$H^{F/E}_{IC}$	Hip flexion/extension angle at initial contact
$H^{F/E}_a$	Average hip flexion/extension angle
$H^{F/E}_r$	Range hip flexion/extension angle
H^F_{max}	Maximum hip flexion angle
H^E_{max}	Maximum hip extension angle
$H^F_{max.\%}$	% of Gait cycle corresponding of maximum hip flexion angle
$H^E_{max.\%}$	% of Gait cycle corresponding of maximum hip extension angle
$H^{Ad/Ab}_{IC}$	Hip adduction/abduction angle at initial contact
$H^{Ad/Ab}_a$	Average hip adduction/abduction angle
$H^{Ad/Ab}_r$	Range hip adduction/abduction angle
H^{Ad}_{max}	Maximum hip adduction angle
H^{Ab}_{max}	Maximum hip abduction angle
$H^{Ad}_{max.\%}$	% of Gait cycle corresponding of maximum hip adduction angle
$H^{Ab}_{max.\%}$	% of Gait cycle corresponding of maximum hip abduction angle
$HP^{G.st}_{max}$	Maximum hip power generation during stance phase
$HP^{A.st}_{max}$	Maximum hip power absorbed during stance phase
$HP^{G.sw}_{max}$	Maximum hip power generation during swing phase
Knee	
$K^{F/E}_{IC}$	Knee flexion/extension angle at initial contact
$K^{F/E}_a$	Average knee flexion/extension angle
$K^{F/E}_r$	Range knee flexion/extension angle
$K^{F.st}_{max}$	Maximum knee flexion angle during stance phase
$K^{E.st}_{max}$	Maximum knee extension angle during stance phase
$K^{F.sw}_{max}$	Maximum knee flexion angle during swing phase
$K^{F.st}_{max.\%}$	% of Gait cycle corresponding of maximum knee flexion angle during stance phase
$K^{E.st}_{max.\%}$	% of Gait cycle corresponding of maximum knee extension angle during stance phase
$K^{F.sw}_{max.\%}$	% of Gait cycle corresponding of maximum knee flexion angle during swing phase
$KP^{G.st}_{max}$	Maximum knee power generation during stance phase
$KP^{A.st}_{max}$	Maximum knee power absorbed during stance phase
$KP^{G.sw}_{max}$	Maximum knee power generation during swing phase
Ankle	
$A^{D/P}_{IC}$	Ankle dorsal/plantar angle at initial contact
$A^{D/P}_a$	Average ankle dorsal/plantar angle
$A^{D/P}_r$	Range ankle dorsal/plantar angle
(Continued)	

TABLE 2 | (Continued)

Ankle	
$A^{D.st}_{max}$	Maximum ankle dorsal angle during stance phase
$A^{P.st}_{max}$	Maximum ankle plantar angle during stance phase
$A^{D.sw}_{max}$	Maximum ankle dorsal angle during swing phase
$A^{D.st}_{max.\%}$	% of Gait cycle corresponding of maximum ankle dorsal angle during stance phase
$A^{P.st}_{max.\%}$	% of Gait cycle corresponding of maximum ankle plantar angle during stance phase
$A^{D.sw}_{max.\%}$	% of Gait cycle corresponding of maximum ankle dorsal angle during swing phase
$AP^{G.st}_{max}$	Maximum ankle power generation during stance phase
$AP^{A.st}_{max}$	Maximum ankle power absorbed during stance phase
Absolute angles	
Thigh	
T_{IC}	Absolute thigh angle at initial contact
T_a	Average of absolute thigh angle
T_r	Range of absolute thigh angle
T_{max}	Maximum of absolute thigh angle
T_{min}	Minimum of absolute thigh angle
Leg	
L_{IC}	Absolute leg angle at initial contact
L_a	Average of absolute leg angle
L_r	Range of absolute leg angle
L_{max}	Maximum of absolute leg angle
L_{min}	Minimum of absolute leg angle
Foot	
F_{IC}	Absolute foot angle at initial contact
F_a	Average of absolute foot angle
F_r	Range of absolute foot angle
F_{max}	Maximum of absolute foot angle
F_{min}	Minimum of absolute foot angle

DISCUSSION

In the present study, we conducted gait analysis on children affected by three different pathologies (CP, CMT, and DMD), representing paradigmatic examples corresponding to damage mainly involving the upper motoneuron, the lower motoneuron and the muscles, respectively. We analyzed spatial and temporal parameters, kinematics and kinetics of gait in children with CMT, DMD, and CP compared to a control group. The stride velocity of the three pathologies (CMT, DMD and CP) was not statistically significant compared to the healthy group, which allows us to underline how the three groups are comparable from the functional perspective.

We studied kinematics, analyzing lower limb relative and absolute angles with respect to the vertical axis. The study of relative angles evidenced the distinctive solutions peculiar to each pathologic group; at the same time, the study of absolute angles highlighted the crucial role of the pelvis and foot segments with respect to the typical pattern shown by the thigh and the shank.

Furthermore, it is noteworthy that standard gait analysis reports merge absolute segment orientation in space, like the pelvis or the foot progression angle, with relative joint angles of the hip, knee, and ankle. Another interesting aspect is the special

TABLE 3 | Differences between the median values of two different pathologies: Healthy (H), Cerebral Palsy (CP), Charcot Marie Tooth (CMT) and Duchenne Muscular Dystrophy (DMD).

Variables	H–CMT		H–DMD		H–CP		CMT–DMD		CMT–CP		DMD–CP	
	Δ	p	Δ	p	Δ	p	Δ	p	Δ	p	Δ	p
Foot Off (%)	−0.14	ns	0.42	ns	−1.80	ns	0.56	ns	−1.66	ns	−2.22	ns
Stride Velocity (1/s)	0.17	ns	−0.19	ns	0.15	ns	**−0.36**	**0.042**	−0.03	ns	**0.34**	**0.015**
Stride Length (-)	0.07	ns	0.00	ns	0.15	Ns	−0.08	ns	0.08	ns	0.16	ns
Stride Time (s)	−0.10	ns	0.11	ns	−0.02	ns	**0.21**	**0.002**	0.08	ns	**−0.13**	**0.036**
Stride Width (-)	−0.01	ns	**−0.06**	**0.017**	**−0.12**	**0.001**	−0.05	ns	−0.11	ns	−0.06	ns
FPA_{IC} (deg)	3.22	ns	−2.73	ns	−11.90	ns	−5.95	ns	**−15.12**	**0.002**	−9.17	ns
FPA_{a} (deg)	2.67	ns	−3.74	ns	−13.67	ns	−6.40	ns	**−16.34**	**0.002**	−9.93	ns
FPA_{r} (deg)	−1.48	ns	−0.70	ns	**−11.19**	**0.002**	0.78	ns	**−9.71**	**0.024**	**−10.49**	**0.042**
FPA_{max} (deg)	2.06	ns	−4.07	ns	**−16.84**	**0.048**	−6.12	ns	**−18.90**	**0.004**	−12.77	ns
FPA_{min} (deg)	1.88	ns	−3.11	ns	−5.22	ns	−4.99	ns	**−7.11**	**0.040**	−2.12	ns
$FPA_{max.\%}$ (%)	−5.08	ns	10.08	ns	-0.40	ns	15.16	ns	4.68	ns	−10.48	ns
$FPA_{min.\%}$ (%)	0.95	ns	0.78	ns	−4.48	ns	−0.17	ns	−5.43	ns	−5.26	ns
P_{IC}^{T} (deg)	1.60	ns	−4.33	ns	−3.92	ns	−5.92	ns	−5.51	ns	0.41	ns
P_{a}^{T} (deg)	1.55	ns	−4.09	ns	**−7.20**	**0.007**	−5.64	ns	**−8.75**	**0.005**	−3.11	ns
P_{r}^{T} (deg)	0.22	ns	−1.35	ns	**−4.63**	**<0.001**	−1.57	ns	**−4.86**	**0.008**	−3.29	ns
P_{IC}^{O} (deg)	−0.49	ns	−1.75	ns	2.08	ns	−1.25	ns	2.58	ns	**3.83**	**< 0.001**
P_{a}^{O} (deg)	0.04	ns	−0.01	ns	0.15	ns	−0.05	ns	0.11	ns	0.16	ns
P_{r}^{O} (deg)	2.60	ns	−2.18	ns	−2.56	ns	**−4.78**	**0.027**	**−5.16**	**0.018**	−0.38	ns
$H_{IC}^{F/E}$(deg)	8.74	ns	−1.96	ns	−10.85	ns	−10.70	ns	**−19.59**	**< 0.001**	−8.89	ns
$H_{a}^{F/E}$(deg)	**7.59**	**0.049**	−1.92	ns	−7.36	ns	−9.50	ns	**−14.95**	**< 0.001**	−5.45	ns
$H_{r}^{F/E}$(deg)	−0.62	ns	−0.82	ns	−5.62	ns	−0.20	ns	−5.01	ns	−4.80	ns
H_{max}^{F}(deg)	10.19	ns	−0.94	ns	**−12.61**	**0.014**	−11.14	ns	**−22.80**	**< 0.001**	−11.66	ns
H_{max}^{E}(deg)	**9.28**	**0.018**	1.01	ns	−5.76	ns	−8.27	ns	**−15.03**	**< 0.001**	−6.76	ns
$H_{max.\%}^{F}$(%)	8.73	ns	−0.29	ns	−2.20	ns	−9.02	ns	−10.93	ns	−1.91	ns
$H_{max.\%}^{E}$(%)	−0.96	ns	−0.20	ns	1.64	ns	0.76	ns	2.60	ns	1.84	ns
$H_{IC}^{Ad/Ab}$(deg)	−2.28	ns	−1.64	ns	2.66	ns	0.64	ns	**4.94**	**0.001**	**4.30**	**0.002**
$H_{a}^{Ad/Ab}$(deg)	−0.35	ns	1.08	ns	1.71	ns	1.44	ns	2.06	ns	0.63	ns
$H_{r}^{Ad/Ab}$(deg)	3.07	ns	−2.65	ns	1.74	ns	**−5.72**	**< 0.001**	−1.33	ns	**4.40**	**0.030**
H_{max}^{Ad}(deg)	1.66	ns	−2.21	ns	3.00	ns	−3.86	ns	1.35	ns	5.21	ns
H_{max}^{Ab}(deg)	−1.04	ns	3.30	ns	2.13	ns	**4.34**	**0.049**	3.17	ns	−1.16	ns
$H_{max.\%}^{Ad}$(%)	**−18.43**	**0.005**	−6.43	ns	**−12.92**	**0.012**	12.00	ns	5.51	ns	−6.49	ns
$H_{max.\%}^{Ab}$(%)	0.57	ns	0.12	ns	3.64	ns	−0.44	ns	3.07	ns	3.51	ns
$HP_{max}^{G.st}$(W/kg)	0.23	ns	0.20	ns	−0.39	ns	−0.04	ns	**−0.62**	**0.013**	**−0.58**	**0.002**
$HP_{max}^{A.st}$(W/kg)	0.13	ns	−0.06	ns	0.09	ns	−0.20	ns	−0.04	ns	0.15	ns
$HP_{max}^{G.sw}$ (W/kg)	0.48	ns	0.34	ns	0.07	ns	−0.14	ns	−0.41	ns	−0.27	ns
$K_{IC}^{F/E}$(deg)	**10.80**	**0.019**	6.22	ns	−19.68	ns	−4.58	ns	**−30.48**	**< 0.001**	**−25.91**	**< 0.001**
$K_{a}^{F/E}$(deg)	**14.01**	**<0.001**	5.92	ns	−3.43	ns	−8.09	ns	**−17.44**	**<0.001**	−9.35	ns
$K_{r}^{F/E}$(deg)	1.71	ns	−3.41	ns	3.84	ns	−5.13	ns	2.12	ns	7.25	ns
$K_{max}^{F.st}$(deg)	**11.29**	**0.004**	7.65	ns	−14.99	ns	−3.64	ns	**−26.29**	**< 0.001**	**−22.65**	**0.004**
$K_{max}^{E.st}$(deg)	**14.13**	**< 0.001**	7.61	ns	3.60	ns	−6.52	ns	**−10.54**	**0.004**	−4.01	ns
$K_{max}^{F.sw}$(deg)	**14.94**	**< 0.001**	2.57	ns	2.71	Ns	**−12.37**	**0.024**	**−12.24**	**0.019**	0.14	ns
$K_{max.\%}^{F.st}$(%)	1.71	ns	−0.33	ns	7.47	< 0.001	−2.04	ns	**5.76**	**0.042**	**7.80**	**0.009**
$K_{max.\%}^{E.st}$(%)	−7.76	ns	1.86	ns	3.40	ns	9.62	ns	11.16	ns	1.54	ns
$K_{max.\%}^{F.sw}$(%)	−0.85	ns	−0.69	ns	**−7.83**	**< 0.001**	0.15	ns	**−6.98**	**0.019**	**−7.14**	**< 0.001**
$KP_{max}^{G.st}$(W/kg)	−0.36	ns	0.03	ns	−0.53	ns	0.39	ns	−0.17	ns	−0.56	ns
$KP_{max}^{A.st}$(W/kg)	−0.41	ns	−0.33	ns	0.64	ns	0.08	ns	**1.05**	**0.006**	**0.97**	**0.010**
$KP_{max}^{G.sw}$(W/kg)	0.05	ns	0.13	ns	0.16	ns	0.08	ns	0.11	ns	0.03	ns
$A_{IC}^{D/P}$(deg)	**6.76**	**0.006**	5.58	ns	**8.26**	**0.003**	−1.18	ns	1.50	ns	2.67	ns
$A_{a}^{D/P}$(deg)	**5.66**	**0.029**	5.04	ns	**7.62**	**0.009**	−0.62	ns	1.96	ns	2.58	ns
$A_{r}^{D/P}$(deg)	7.03	ns	1.70	ns	−5.25	ns	−5.33	ns	**−12.27**	**0.014**	−6.95	ns

(Continued)

TABLE 3 | (Continued)

Variables	H–CMT		H–DMD		H–CP		CMT–DMD		CMT–CP		DMD–CP	
	Δ	p	Δ	p	Δ	p	Δ	p	Δ	p	Δ	p
$A^{D.st}_{max}$(deg)	**6.00**	**0.034**	5.85	ns	**9.03**	**0.017**	−0.15	ns	3.04	ns	3.19	ns
$A^{P.st}_{max}$(deg)	1.63	ns	6.78	ns	14.24	ns	5.15	ns	12.62	ns	7.47	ns
$A^{D.sw}_{max}$(deg)	**8.58**	**< 0.001**	**5.65**	**0.022**	**7.52**	**0.002**	−2.94	ns	−1.07	ns	1.87	ns
$A^{D.st}_{max.\%}$(%)	−1.98	ns	4.02	ns	13.75	ns	6.00	ns	15.73	ns	9.73	ns
$A^{P.st}_{max.\%}$(%)	1.44	ns	−1.88	ns	−2.78	ns	−3.32	ns	−4.22	ns	−0.90	ns
$A^{D.sw}_{max.\%}$(%)	−1.09	ns	−2.75	ns	−2.86	ns	−1.66	ns	−1.77	ns	−0.10	ns
$AP^{G.st}_{max}$(W/kg)	0.76	ns	0.75	ns	**1.23**	**< 0.001**	0.00	ns	0.47	ns	0.47	ns
$AP^{A.st}_{max}$(W/kg)	0.27	ns	0.06	ns	**0.38**	**< 0.001**	−0.21	ns	0.11	ns	0.32	ns
T_{IC} (deg)	**7.24**	**0.009**	4.59	ns	−6.95	ns	−2.65	ns	**−14.19**	**< 0.001**	**−11.54**	**0.003**
T_a (deg)	**7.37**	**< 0.001**	**5.06**	**0.016**	−2.68	ns	−2.31	ns	**−10.06**	**0.001**	**−7.74**	**0.039**
T_r (deg)	−0.01	ns	−0.11	ns	−6.60	ns	−0.10	ns	−6.58	ns	−6.48	ns
T_{max} (deg)	**7.55**	**0.013**	3.97	ns	−8.86	ns	−3.58	ns	**−16.41**	**< 0.001**	**−12.83**	**0.003**
T_{min} (deg)	**8.38**	**0.001**	**5.42**	**0.038**	−2.29	ns	−2.96	ns	**−10.67**	**0.002**	−7.71	ns
L_{IC} (deg)	−4.36	ns	−2.47	ns	**11.46**	**0.019**	1.89	ns	**15.82**	**< 0.001**	**13.93**	**0.001**
L_a (deg)	**−5.81**	**0.004**	−2.22	ns	2.59	ns	3.59	ns	**8.40**	**< 0.001**	4.81	ns
L_r (deg)	6.25	ns	1.50	ns	**16.12**	**< 0.001**	−4.75	ns	9.87	ns	**14.62**	**0.002**
L_{max}(deg)	−2.96	ns	−0.61	ns	**11.20**	**0.002**	2.35	ns	**14.16**	**< 0.001**	**11.81**	**0.005**
L_{min} (deg)	**−8.80**	**0.004**	−3.16	ns	**−4.77**	**0.025**	5.64	ns	4.04	ns	−1.61	ns
F_{IC} (deg)	−1.75	ns	−3.10	ns	**−10.99**	**0.018**	−1.35	ns	−9.23	ns	−7.88	ns
F_a (deg)	−2.31	ns	3.34	ns	8.26	ns	5.65	ns	10.57	ns	4.92	ns
F_r (deg)	5.57	ns	−5.49	ns	1.42	ns	−11.06	ns	−4.15	ns	6.91	ns
F_{max}(deg)	0.12	ns	0.13	ns	1.31	ns	0.02	ns	1.19	ns	1.17	ns
F_{min} (deg)	−6.17	ns	5.57	ns	−0.22	ns	11.73	ns	5.95	ns	−5.78	ns

*Abbreviations as **Table 1**.*

Δ, differences between the median values of two different pathologies; p, p-value corresponding; ns, not significant. Significant values are highlighted in bold characters.

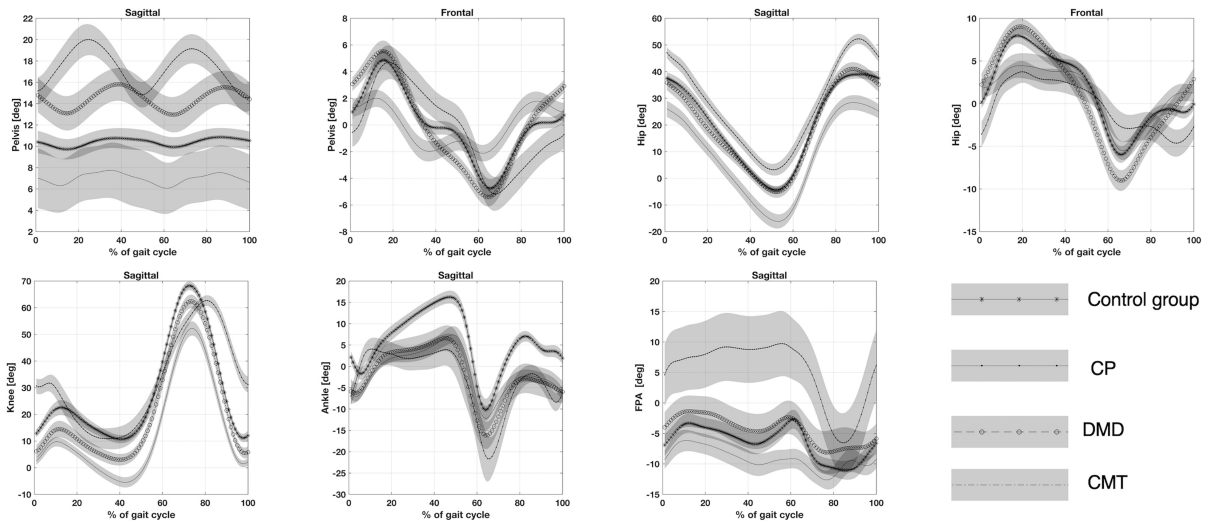

FIGURE 2 | Top panel (from left to right): Pelvis angle on the sagittal and the frontal plane. Hip angle on the sagittal and the frontal plane. Bottom panel (from left to right): Knee angle, Ankle angle on the sagittal plane and Foot progression angle (FPA) on the transversal plane. CP, participants with Cerebral Palsy; CMT, participants with Charcot Marie Tooth; DMD, participants with Duchenne Muscular Dystrophy; normal gait (healthy, H).

functional role of some body regions: the pelvis embodies the relationship between the lower limbs and the upper body (Amori et al., 2015); and the foot relates the body to the environment.

We observed increasing hip flexion with the increase of pelvis anteversion and vice versa. The absolute pelvis orientation in space and the hip angles are connected. At the same time,

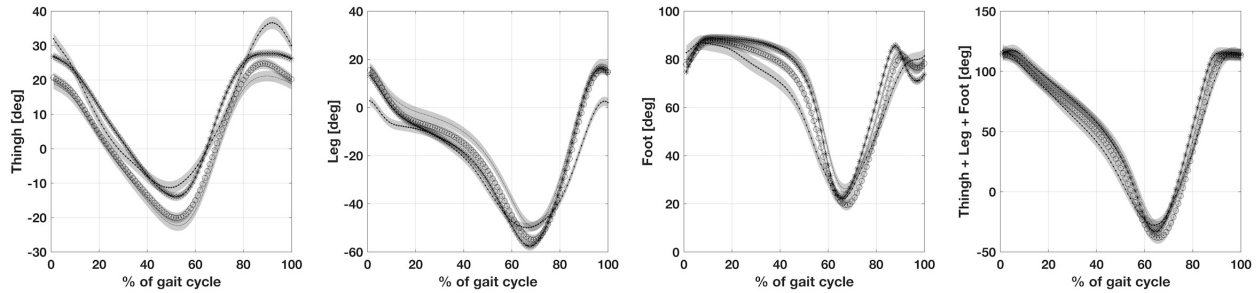

FIGURE 3 | Illustrates from left to right, the absolute angles of thigh, leg, foot and the sum of thigh, leg and foot. CP, participants with Cerebral Palsy; CMT, participants with Charcot Marie Tooth; DMD, participants with Duchenne Muscular Dystrophy; normal gait (healthy, H).

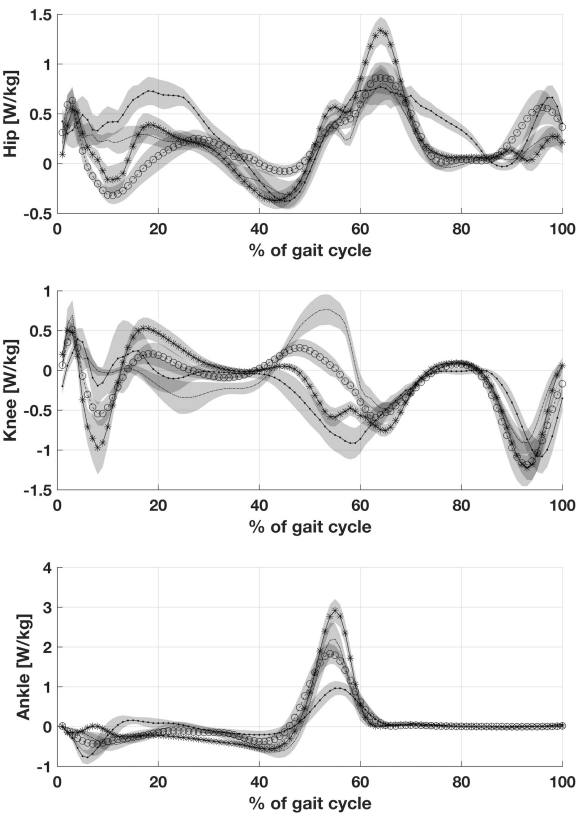

FIGURE 4 | Depicts joints power: Hip joint power, Knee joint power and Ankle joint power. CP, participants with Cerebral Palsy; CMT, participants with Charcot Marie Tooth; DMD, participants with Duchenne Muscular Dystrophy; normal gait (healthy, H).

the knee mediates the attitude of the pelvis and the foot, reducing the range of motion as in the case of reduction of ankle range in conjunction with the pelvis anteversion attitude (**Figure 2**). Furthermore, the knee angle tended to shift in flexion or extension in relation to pelvis anteversion or retroversion, respectively. The above-mentioned pathological factor restricts the biomechanical relationship to a particular path. It is impossible to distinguish the contributions of two elements: biomechanics on one side and pathological conditions on the other, in both their central and peripheral expressions (Crenna, 1998). Children with CP that are affected mainly by selective motor control deficits and muscle weakness showed a marked reduction of dorsal flexion in stance and increased plantar flexion in pre-swing. This behavior allows storage and release of the mechanical energy in the muscle structure, conserving energy on the vertical plane (Holt et al., 2000; Fonseca et al., 2001). Children with Duchenne dystrophy showed similar ankle behavior. Yet, in that case, even if the mechanism of passive mechanical energy exploitation is similar, the cause is different because it is due to the decline of contractile fiber in muscles and their relative weakness (Romano et al., 2019). In children with Charcot-Marie-Tooth, we observed a reduction of the ankle range of motion, probably linked mainly to both muscular and articular degeneration. In all the cases, the specific anatomical changes represent constraining elements for gait function.

It is possible to explain the differences in pelvis behavior if we consider the previously mentioned factors in mediation with the upper body. The balancing of the pelvis implies a fine-tuning of muscle activities to stabilize the segment on the two spherical hip joints in a dynamic equilibrium compatible with gait progression. Pelvic anteversion in children with CP could be interpreted as a simplification of the pelvis stabilization in stance phase, hanging on the hamstring muscles, reaching maximum anteversion during the monopodic support gait phase. In children with Duchenne, where the main problem is the weakness and not the deficit of fine motor control, the double bump is present, but it is in phase with the control group, a sort of boost of functional activities (Romano et al., 2019). Children with Charcot-Marie-Tooth present a tendency toward pelvic retroversion. It is possible to observe similar attitudes in the gait of children who are blind from birth (Gazzellini et al., 2016). It is an attitude linked with a cautious gait in which the dynamic aspects are restrained. The causes are dissimilar, that is, in blind children, the uncertainty stems from the reduction of exteroception information, while in the children studied here, it is due to the decrease of information from the foot engaging the terrain. What is common to the two situations is the absence of information from a specific sensory channel. We can speculate about the role of another element which may influence these gait

differences: perception. The absolute angles of thigh, leg and foot showed a more consistent behavior throughout the different pathologies. Only children with CP differentiated from the other groups during the final swing phase for the hip and during stance for the foot.

It is intriguing to note that if we sum the thigh and the leg orientation with respect to the vertical axis in the three disease groups, any differences between the three pathologies are canceled. We can hypothesize that these time series represent the invariance necessary to achieve an efficient gait, using all the peculiar available resources, both central and peripheral. When all the lower limb segments were considered together, a slight variation during stance induced by the foot orientation differentiates mainly children with CP from children with CMT. The characteristics of the foot condition in these two pathologies resulted from central and peripheral disease, respectively. The nature of these pathologies leads to opposite feet musculoskeletal abnormalities, which influence the strike of the foot on the ground: flat feet for CP and cavus feet in CMT. However, it should be noted that this work has certain limitations relating to the number of patients assessed, even though DMD and CMT diseases can be classed as rare diseases, qualifying this work as an exploratory study. Overall, our study suggests that the pelvis and the foot attitude play a crucial role in determining the biomechanical configuration for all four groups analyzed. Physical orthopaedic and rehabilitative treatment should consider the personal biomechanical configuration in terms of constrains of the gait. Each group showed a particular solution for balancing body segments, exploiting the available residual resources of the organism, both peripheral and central. Meanwhile, the spatial orientation of the thigh and leg were linked together in a sort of biomechanical invariance independent of the studied pathology. Both elements seem to contribute to a body configuration compatible with bipedal gait.

DATA AVAILABILITY STATEMENT

The raw data supporting the conclusions of this article will be made available by the authors, without undue reservation.

ETHICS STATEMENT

The studies involving human participants were reviewed and approved by "Bambino Gesù" Children's Hospital. Written informed consent to participate in this study was provided by the participants' legal guardian/next of kin.

AUTHOR CONTRIBUTIONS

SM, MF, AR, AP, SS, EC, and MP managed the overall project (conceptualization, methodology, and interpretation). SM and MP performed the data preprocessing, statistical analysis, results interpretation, and prepared the original manuscript draft. AP, MF, and AR performed the Gait Analysis data acquisition and database maintenance. GV and TS were responsible for the recruitment and clinical examinations and results interpretation. All authors critically reviewed, read, and approved the submitted version of the manuscript.

REFERENCES

Abu-Faraj, Z. O., Harris, G. F., Smith, P. A., and Hassani, S. (2015). "Human gait and clinical movement analysis," in *Wiley Encyclopedia of Electrical and Electronics Engineering*, ed. J. G. Webster (New York, NY: John Wiley & Sons, Inc.).

Amori, V., Petrarca, M., Patané, F., Castelli, E., and Cappa, P. (2015). Upper body balance control strategy during continuous 3D postural perturbation in young adults. *Gait Posture* 41, 19–25. doi: 10.1016/j.gaitpost.2014.08.003

Armand, S., Decoulon, G., and Bonnefoy-Mazure, A. (2016). Gait analysis in children with cerebral palsy. *EFORT Open Rev.* 1, 448–460. doi: 10.1302/2058-5241.1.000052

Borghese, N. A., Bianchi, L., and Lacquaniti, F. (1996). Kinematic deferminants of human locomotion. *J. Physiol.* 494, 863–879. doi: 10.1113/jphysiol.1996.sp021539

Chruscikowski, E., Fry, N. R. D., Noble, J. J., Gough, M., and Shortland, A. P. (2017). Selective motor control correlates with gait abnormality in children with cerebral palsy. *Gait Posture* 52, 107–109. doi: 10.1016/j.gaitpost.2016.11.031

Cioni, G., Lodesani, M., Pascale, R., Coluccini, M., Sassi, S., Paolicelli, P. B., et al. (2008). The term diplegia should be enhanced. Part II: contribution to validation of the new rehabilitation oriented classification. *Eur. J. Phys. Rehabil. Med.* 44, 203–211.

Collins, S., Ruina, A., Tedrake, R., and Wisse, M. (2005). Efficient bipedal robots based on passive-dynamic walkers. *Science* 307, 1082–1085. doi: 10.1126/science.1107799

Crenna, P. (1998). Spasticity and "spastic" gait in children with cerebral palsy. *Neurosci. Biobehav. Rev.* 22, 571–578. doi: 10.1016/S0149-7634(97)00046-8

Davids, J. R., Cung, N. Q., Pomeroy, R., Schultz, B., Torburn, L., Kulkarni, V. A., et al. (2018). Quantitative Assessment of Knee Progression Angle during Gait in Children with Cerebral Palsy. *J. Pediatr. Orthop.* 38, e219–e224. doi: 10.1097/BPO.0000000000001134

Davies, B. T. (1968). A review of " The Co-ordination and Regulation of Movements " By N. Bernstein. (Pergamon Press, 1967.) [Pp. xii + 196.] 505. *Ergonomics* 11, 95–97. doi: 10.1080/00140136808930945

Doglio, L., Pavan, E., Pernigotti, I., Petralia, P., Frigo, C., and Minetti, C. (2011). Early signs of gait deviation in Duchenne muscular dystrophy. *Eur. J. Phys. Rehabil. Med.* 47, 587–594. doi: 10.1016/j.gaitpost.2008.10.044

Fonseca, S. T., Holt, K. G., Saltzman, E., and Fetters, L. (2001). A dynamical model of locomotion in spastic hemiplegic cerebral palsy: influence of walking speed. *Clin. Biomech.* 16, 793–805. doi: 10.1016/S0268-0033(01)00067-5

Gazzellini, S., Lispi, M. L., Castelli, E., Trombetti, A., Carniel, S., Vasco, G., et al. (2016). The impact of vision on the dynamic characteristics of the gait: strategies in children with blindness. *Exp. Brain Res.* 234, 2619–2627. doi: 10.1007/s00221-016-4666-9

Gibson, J. J. (1979). *Gibson, James J. "The Theory of Affordances" The Ecological Approach to Visual Perception*. Boston: Houghton Mifflin.

Goudriaan, M., Van den Hauwe, M., Dekeerle, J., Verhelst, L., Molenaers, G., Goemans, N., et al. (2018). Gait deviations in Duchenne muscular dystrophy—Part 1. A systematic review. *Gait Posture* 62, 247–261. doi: 10.1016/j.gaitpost.2018.03.020

Hamill, J., Knutzen, K. M., and Derrick, T. R. (2014). *Biomechanical Basis of Human Movement*, Fourth Edn. Philadelphia: Wolters Kluwer Health.

Holt, K. G., Fonseca, S. T., and Lafiandra, M. E. (2000). The dynamics of gait in children with spastic hemiplegic cerebral palsy: theoretical and clinical

implications. *Hum. Mov. Sci.* 19, 375–405. doi: 10.1016/S0167-9457(00)00019-1

Kuniyoshi, Y., and Suzuki, S. (2004). "Dynamic emergence and adaptation of behavior through embodiment as coupled chaotic field," in *2004 IEEE/RSJ International Conference on Intelligent Robots and Systems (IROS)*, (Piscataway: IEEE).

Lacquaniti, F., Grasso, R., and Zago, M. (1999). Motor patterns in walking. *News Physiol. Sci.* 14, 168–174. doi: 10.1152/physiologyonline.1999.14.4.168

Lencioni, T., Piscosquito, G., Rabuffetti, M., Bovi, G., Di Sipio, E., Diverio, M., et al. (2017). Responsiveness of gait analysis parameters in a cohort of 71 CMT subjects. *Neuromuscul. Disord.* 27, 1029–1037. doi: 10.1016/j.nmd.2017.07.003

Rodda, J. M., Graham, H. K., Carson, L., Galea, M. P., and Wolfe, R. (2004). Sagittal gait patterns in spastic diplegia. *J. Bone Jt. Surg.* 86, 251–258. doi: 10.1302/0301-620X.86B2.13878

Romano, A., Favetta, M., Schirinzi, T., Summa, S., Minosse, S., D'Amico, A., et al. (2019). Evaluation of gait in Duchenne Muscular Dystrophy: relation of 3D gait analysis to clinical assessment. *Neuromuscul. Disord.* 29, 920–929. doi: 10.1016/j.nmd.2019.10.007

Romkes, J., and Brunner, R. (2007). An electromyographic analysis of obligatory (hemiplegic cerebral palsy) and voluntary (normal) unilateral toe-walking. *Gait Posture* 26, 577–586. doi: 10.1016/j.gaitpost.2006.12.010

Salami, F., Niklasch, M., Krautwurst, B. K., Dreher, T., and Wolf, S. I. (2017). What is the price for the Duchenne gait pattern in patients with cerebral palsy? *Gait Posture* 58, 453–456. doi: 10.1016/j.gaitpost.2017.09.006

Sienko Thomas, S., Buckon, C. E., Nicorici, A., Bagley, A., McDonald, C. M., and Sussman, M. D. (2010). Classification of the gait patterns of boys with Duchenne muscular dystrophy and their relationship to function. *J. Child Neurol.* 25, 1103–1109. doi: 10.1177/0883073810371002

Wojciechowski, E., Sman, A., Cornett, K., Raymond, J., Refshauge, K., Menezes, M. P., et al. (2017). Gait patterns of children and adolescents with Charcot-Marie-Tooth disease. *Gait Posture* 56, 89–94. doi: 10.1016/j.gaitpost.2017.05.005

Conflict of Interest: The authors declare that the research was conducted in the absence of any commercial or financial relationships that could be construed as a potential conflict of interest.

frontiers | Frontiers in Human Neuroscience

ORIGINAL RESEARCH
published: 04 April 2022
doi: 10.3389/fnhum.2022.826333

Application of the Gait Deviation Index to Study Gait Impairment in Adult Population With Spinal Cord Injury: Comparison With the Walking Index for Spinal Cord Injury Levels

Isabel Sinovas-Alonso[1,2], Diana Herrera-Valenzuela[1,2], Roberto Cano-de-la-Cuerda[3]*, Ana de los Reyes-Guzmán[2], Antonio J. del-Ama[4] and Ángel Gil-Agudo[2]*

[1] International Doctoral School, Rey Juan Carlos University, Madrid, Spain, [2] Biomechanics and Technical Aids Unit, National Hospital for Paraplegics, Toledo, Spain, [3] Faculty of Health Sciences, Department of Physical Therapy, Occupational Therapy, Physical Medicine and Rehabilitation, Rey Juan Carlos University, Alcorcón, Spain, [4] School of Science and Technology, Department of Applied Mathematics, Materials Science, Engineering and Electronic Technology, Rey Juan Carlos University, Móstoles, Spain

OPEN ACCESS

Edited by:
Carmelo Chisari,
Pisana University Hospital, Italy

Reviewed by:
Noureddin Nakhostin Ansari,
Tehran University of Medical Sciences, Iran
Marcelo Navega,
São Paulo State University, Brazil

***Correspondence:**
Isabel Sinovas-Alonso
msinovas@sescam.jccm.es
Roberto Cano-de-la-Cuerda
roberto.cano@urjc.es

Specialty section:
This article was submitted to Motor Neuroscience, a section of the journal Frontiers in Human Neuroscience

Received: 30 November 2021
Accepted: 07 March 2022
Published: 04 April 2022

Citation:
Sinovas-Alonso I, Herrera-Valenzuela D, Cano-de-la-Cuerda R, Reyes-Guzmán A, del-Ama AJ and Gil-Agudo Á (2022) Application of the Gait Deviation Index to Study Gait Impairment in Adult Population With Spinal Cord Injury: Comparison With the Walking Index for Spinal Cord Injury Levels. Front. Hum. Neurosci. 16:826333. doi: 10.3389/fnhum.2022.826333

The Gait Deviation Index (GDI) is a multivariate measure of overall gait pathology based on 15 gait features derived from three-dimensional (3D) kinematic data. GDI aims at providing a comprehensive, easy to interpret, and clinically meaningful metric of overall gait function. It has been used as an outcome measure to study gait in several conditions: cerebral palsy (CP), post-stroke hemiparetic gait, Duchenne muscular dystrophy, and Parkinson's disease, among others. Nevertheless, its use in population with Spinal Cord Injury (SCI) has not been studied yet. The aim of the present study was to investigate the applicability of the GDI to SCI through the assessment of the relationship of the GDI with the Walking Index for Spinal Cord Injury (WISCI) II. 3D gait kinematics of 34 patients with incomplete SCI (iSCI) was obtained. Besides, 3D gait kinematics of a sample of 50 healthy volunteers (HV) was also gathered with Codamotion motion capture system. A total of 302 (iSCI) and 446 (HV) strides were collected. GDI was calculated for each stride and grouped for each WISCI II level. HV data were analyzed as an additional set. Normal distribution for each group was assessed with Kolmogorov-Smirnov tests. Afterward, ANOVA tests were performed between each pair of WISCI II levels to identify differences among groups ($p < 0.05$). The results showed that the GDI was normally distributed across all WISCI II levels in both iSCI and HV groups. Furthermore, our results showed an increasing relationship between the GDI values and WISCI II levels in subjects with iSCI, but only discriminative in WISCI II levels 13, 19, and 20. The index successfully distinguished HV group from all the individuals with iSCI. Findings of this study indicated that the GDI is not an appropriate multivariate walking metric to represent the deviation of gait pattern in adult

population with iSCI from a normal gait profile when it is compared with the levels of walking impairment described by the WISCI II. Future work should aim at defining and validating an overall gait index derived from 3D kinematic gait variables appropriate for SCI, additionally taking into account other walking ability outcome measures.

Keywords: spinal cord injury (SCI), gait impairment, Gait Deviation Index (GDI), three-dimensional (3D) kinematic gait data, walking index for spinal cord injury (WISCI)

INTRODUCTION

The incidence of spinal cord injury (SCI) worldwide is between 250,000 and 500,000 individuals each year (Quadri et al., 2020). In Western European countries traumatic SCI incidence is of 16 to 19.4 new cases per million inhabitants per year (Scivoletto et al., 2017). Walking is usually affected in patients with SCI according to the lesion level and the resulting different levels of muscle paralysis, sensory impairment, spasticity, and the lack of trunk control (Bani et al., 2013). In the field of SCI research, there is an emphasis on the ability to ambulate as a functional outcome and as an indicator of quality of life (Jackson et al., 2008), particularly in individuals with incomplete SCI (iSCI) (Ditunno et al., 2008).

Walking function recovery is tackled through several therapeutic interventions such as surgery, physiotherapy, medications, orthotics, and robotics in which precise evaluation of walking function is mandatory (Scivoletto et al., 2011). Periodic gait measurements can be used to evaluate the response to these therapeutical approaches (McGinley et al., 2009), to assess changes in walking over time, and to discriminate between normal and altered gait (Baker, 2006). In this regard, three-dimensional (3D) kinematic gait analysis can provide useful information to guide rehabilitation interventions to improve walking function of people with traumatic and non-traumatic iSCI (Murphy et al., 2019). Nevertheless, isolated kinematic parameters do not provide a full picture of gait pattern impairment (Guzik and Drużbicki, 2020), and on the other hand, it may be difficult to describe objectively the heterogeneity of the different gait abnormalities present in iSCI and to quantify the degree by which they deviate from normal gait patterns. The Gait Deviation Index (GDI) is a multivariate measure of overall gait pathology based on 15 gait features built upon 3D kinematic data originally designed from a sample of children with cerebral palsy (CP) (Schwartz and Rozumalski, 2008). The GDI is a dimensionless parameter represented as a single score for an individual gait deviation from a normative reference group, which aims at providing a comprehensive, easy to interpret, and clinically meaningful metric of overall gait function.

The usefulness of GDI has been assessed through correlations with clinically-validated gait scales. Concurrent and face validity of GDI was firstly carried out by comparison with the Gillette Functional Assessment Questionnaire walking scale (FAQ) and topographic classifications of CP in children population (Schwartz and Rozumalski, 2008). Later, the relationship between the GDI, Gross Motor Function Measure (GMFM), and Gross Motor Function Classification System (GMFCS) in a representative sample of ambulatory children with CP provided greater validity to the GDI (Molloy et al., 2010). The ability of the GDI to distinguish between GMFCS levels in children with CP in the study developed by (Massaad et al., 2014) concurred with those found by Molloy et al. (2010) and by Schwartz and Rozumalski (2008) for the FAQ. Furthermore, face validity of the GDI in adults with CP was demonstrated by comparing with GMFCS (Maanum et al., 2012), which showed similar distributional properties as those reported in children with CP. The GDI was able to distinguish different levels of gait impairment in adults (Maanum et al., 2012) and children (Schwartz and Rozumalski, 2008; Molloy et al., 2010; Massaad et al., 2014) with CP. However, no correlations have been published between the GDI and other valid walking ability outcome measures commonly used in clinical settings to assess gait variability in adult population with SCI.

The Walking Index for Spinal Cord Injury (WISCI) II is a walking scale specifically developed for iSCI population composed of 21 levels (Dittuno et al., 2001), in which levels are ordered by degree of an individual's walking impairment, from most impaired to least impaired (Ditunno et al., 2007), integrating a hierarchical order for the use of ambulatory assistive devices (AADs), orthoses, and the physical assistance needed to complete a 10 m walking distance. WISCI II levels differs from self-selected (SS) WISCI, defined as patient's preferential condition to walk in the community or the household, and maximum WISCI, which is related to the highest level at which a person can safely walk 10 m (Burns et al., 2011). The WISCI II is a valid (Morganti et al., 2005; Ditunno et al., 2007), reliable (Marino et al., 2010; Scivoletto et al., 2014), and responsive (van Hedel et al., 2006) outcome measure to assess walking ability in people with SCI. In our best knowledge, there is no scientific literature which have studied the relationship between the GDI and the WISCI II in adult population with SCI.

The GDI has been used as an outcome measure to study gait in several conditions such as: CP (Schwartz and Rozumalski, 2008; Molloy et al., 2010; Cimolin et al., 2011; Sagawa et al., 2013; Massaad et al., 2014; Wilson et al., 2015; Malt et al., 2016; Ito et al., 2019; Rasmussen et al., 2019), post-stroke hemiparetic gait (Correa et al., 2017; Guzik and Drużbicki, 2020), Duchenne muscular dystrophy (Sienko Thomas et al., 2010), Parkinson's disease (Galli et al., 2012; Speciali et al., 2013), arthritis (Broström et al., 2013; Esbjörnsson et al., 2014; Rosenlund et al., 2016; Kobsar et al., 2019; Bazarnik-Mucha et al., 2020), lower limb amputations (Eshraghi et al., 2014; Kark et al., 2016), degenerative spinal pathologies (Mar et al., 2019; Trivedi et al., 2021; Zhou et al., 2021), diverse genetic (Ito et al., 2020; Mindler et al., 2020) and congenital disorders (Eriksson et al., 2015; Garman et al., 2019), and even the effect of the COVID-19 on physical function (Ito et al., 2021), among others. A recently published article by

Hwang et al. (2021) used the GDI as a way to quantify and characterize gait patterns in ambulatory children and adolescents with transverse myelitis, whose gait showed moderate kinematic deviations from normal gait pattern. Nevertheless, to date, no work has been published regarding the validity of the GDI in population with SCI.

Joint kinematics and spatiotemporal gait parameters differ between adult and child population due to the maturation and aging processes of the gait, associated to the neuromuscular development and the changes in strength that occur during adolescence and adulthood (Cupp et al., 1999; Ganley and Powers, 2005). In this regard, it is necessary to consider the functional differences of the gait pattern in relation to the mature stage in people with SCI.

The aim of the present study was to evaluate the relationship between the GDI and WISCI II levels in adult population with iSCI. Our hypothesis was that the most altered gait kinematics of people with iSCI, reflected by GDI values below 100, would be associated with lower scores of the WISCI II.

MATERIALS AND METHODS

Study Design

An observational retrospective study was conducted on a database of 3D kinematic gait analysis of adult population composed by patients with iSCI and healthy volunteers (HV) gathered between August 2019 and July 2021 at the Biomechanics and Technical Aids Unit of the National Hospital for Paraplegics of Toledo (Spain). All the individuals recruited for the study signed informed consent to participate in the study. According to the Declaration of Helsinki, all participants were informed about the purpose and course of the study, and about their rights to withdraw from the study. The study protocol was reviewed and approved by the Local Ethics Committee of University Hospital Complex of Toledo, Spain.

Participants

Patients included in the study met the following inclusion criteria: (i) subjects aged 16 years or over; (ii) having suffered a SCI regardless of the etiology (traumatic or non-traumatic), time since injury onset, and neurological level of injury (NLI); (iii) classified as C, D, or E by the American Spinal Injury Association (ASIA) Impairment Scale (AIS) (Kirshblum et al., 2011); (iv) with the ability of walking 10 m independently with any type of external assistance required (orthoses, crutches or canes); (v) with SS WISCI II levels collected; and (vi) capacity to be informed and give consent to participate in the study. Patients from the database were excluded of the study if they followed one of the different conditions: (i) having suffered from rheumatic, orthopedic, or other neurological disorders outside of SCI that affected gait; (ii) need for support in parallel bars, walker and/or physical assistance required of one or two people to walk 10 m safely; (iii) psychiatric or cognitive conditions that may have interfered with the performance of the gait analysis.

Based on the medical history reported by HV in the recruitment process, they were excluded if they experienced musculoskeletal or neurological disorders that affected gait. 3D kinematic data acquired from HV were used to calculate an average normal value of gait kinematics and hence to calculate the deviation from normal gait pattern for each patient, in essence, the GDI.

FIGURE 1 | Placement of the 22 active markers of Codamotion motion capture system on the lower limbs of an individual from HV group.

Experimental Protocol

3D kinematic gait data were obtained with Codamotion motion capture system (Charnwood Dynamics, Ltd., United Kingdom), comprised of 22 active markers placed on the lower limbs (**Figure 1**), three scanners, and two Kistler force platforms embedded in a 10-m walkway. Markers were positioned on the following anatomical references: sacrum (two lateral markers), anterior superior iliac spines (ASIS), posterior superior iliac spines (PSIS), lateral surface of the thighs (anterior and posterior femur markers), lateral femoral condyles, lateral surface of the legs (anterior and posterior tibia markers), lateral malleoli, calcaneus (posterior lateral heels), and fifth metatarsal heads. Marker trajectories were collected at a sampling frequency of 200 Hz. A 3D skeletal model was created for each individual based on markers placement and anthropometric measures taken for each subject, which included: weight, height, pelvis width and depth, knees and ankles width. Subjects were informed to walk naturally at their SS speed with the minimum external assistance required -canes, crutches, and/or orthoses-. A valid stride was

TABLE 1 | Characteristics of individuals recruited for the study.

	HV	iSCI
N	50	34
Gender (M/F)	19/31	26/8
Age (years)	34.6 (15.2)	34.6 (18.0)
Height (cm)	166.6 (8.7)	169.7 (10.7)
Weight (Kg)	69.6 (15.0)	70.0 (15.2)
BMI (kg/m^2)	24.9 (4.0)	24.2 (4.2)

Parameters reported as mean (SD). HV, healthy volunteers; iSCI, incomplete spinal cord injury; M, male; F, female; SD, standard deviation; BMI, body mass index.

TABLE 2 | Clinical characteristics of individuals with iSCI.

Clinical characteristics	iSCI (*n* = 34)	
NLI	C1-C7	16
	T1-T6	3
	T7-L1	11
	L2-L5	4
AIS	C	4
	D	28
	E	2
Etiology (T/NT)	19T/15NT	
Time since injury (years)	5.7 (7.8)	
SS WISCI II level	17.8 (2.4)	

Parameters reported as mean (SD). NLI, neurological level of injury; AIS, American spinal injury association impairment scale; T, traumatic; NT, non-traumatic; SS WISCI II, self-selected walking index for spinal cord injury II.

TABLE 3 | Descriptive statistics of GDI values (mean and range) within each WISCI II level.

WISCI II levels	*n* strides	Mean (SD)	Range
12 $_{(13,\ 19,\ 20,HV)}$	2	57.6 (2.9)	55.5-59.6
13 $_{(12,\ 15,\ 16,\ 18,\ 19,\ 20,HV)}$	6	47.1 (1.8)	45.0-49.2
15 $_{(13,\ 19,\ 20,HV)}$	18	58.6 (7.2)	49.6-70.7
16 $_{(13,\ 19,\ 20,HV)}$	65	63.7 (11.0)	46.6-88.2
18 $_{(13,\ 19,\ 20,HV)}$	12	59.3 (4.4)	49.9-62.6
19 $_{(12,\ 13,\ 15,\ 16,\ 18,\ 20,HV)}$	87	70.2 (8.1)	52.2-95.3
20 $_{(12,\ 13,\ 15,\ 16,\ 18,\ 19,HV)}$	112	80.4 (15.2)	60.0-126.0
HV $_{(12,\ 13,\ 15,\ 16,\ 18,\ 19,\ 20)}$	446	100.0 (10.0)	73.1-127.9

Groups in parentheses indicate statistically significant differences ($p < 0.05$).

considered as the one in which each foot was on a different force platform. Five complete gait cycles or three complete cycles in those individuals with SCI who were not able to get five valid cycles were collected, time-normalized and averaged. A total of 302 and 446 strides were collected for the group with iSCI and the HV group, respectively. The complete records were then processed using the software for data analysis ODIN v.2.02 (Codamotion Ltd., United Kingdom) to calculate the mean values of 3D kinematic parameters for the gait cycle of the right and left leg, for pelvis, and hip, knee, and ankle joints.

Data Analysis

The GDI is calculated upon the procedure described in Schwartz and Rozumalski (2008). The index is derived from a set of nine kinematic curves of a single stride: i) pelvic orientation and hip angles in the three planes of space (sagittal, frontal and transversal), (ii) knee flexion and extension, (iii) ankle dorsiflexion and plantar flexion, and (iv) foot progression angle.

In the original study (Schwartz and Rozumalski, 2008), a dataset with more than 6,000 strides of patients with CP was used to calculate a 15-feature basis to account for 98% of the total variation of the whole dataset and to allow to reconstruct the kinematic gait curves with a 98% fidelity on average. This basis allowed to calculate the representation of any kinematic gait curve, by multiplying the basis with the kinematic curves of a stride. Afterward, the Euclidean distance between this kinematic gait curve and the average of a set of healthy control strides were calculated, so that the deviation of a gait pattern from a normal gait profile was represented. Lastly, this value was scaled to improve the interpretability of the index, so that every 10 points of GDI below 100 corresponded to 1 standard deviation (SD) away from the typical gait kinematics, whereas a score ≥ 100 represented a normal gait profile.

The GDI for our sample population was calculated for each stride in both groups, subjects with iSCI and HV group, using the orthonormal basis provided in Schwartz and Rozumalski (2008). HV group data, used as the reference gait pattern to compute the gait deviation, were collected following the same procedure used with the individuals with iSCI. Each 3D kinematic gait analysis was associated to a SS WISCI II level according to the preferential condition to walk declared by the participants with iSCI. GDI data were grouped according to the corresponding WISCI II level and HV group data were considered as an additional set. Normal distribution for each group was assessed with Kolmogorov-Smirnov tests. To facilitate the analysis, a histogram of the GDI data comprised within each WISCI II level was calculated with a normal distribution curve fitted to its mean and SD. Afterward, one-way ANOVA tests were performed between the GDI values of each pair of WISCI II levels to identify differences among groups. *P*-value was set to $p < 0.05$ for all statistical procedures. All the data analysis was performed with Matlab R2019a (The MathWorks, Inc., Natick, MA, United States).

RESULTS

Thirty-four ($n = 34$) adults with iSCI and fifty ($n = 50$) HV met the inclusion criteria (**Table 1**). Clinical characteristics of individuals with iSCI are shown in **Table 2**. The dataset of iSCI sample included the following WISCI II levels: 12, 13, 15, 16, 18, 19, and 20.

The analysis showed that GDI data were normally distributed across all WISCI II levels and also in the HV group. **Table 3** presents the number of strides, the range, the mean, and the SD of GDI values comprised in each WISCI II level. Results showed a trend of increasing average GDI values with decreasing level of walking impairment in WISCI II levels 13 to 20 and the HV group, except in level 18, whose average GDI was lower than the average on level 16. This can be easily seen in **Figure 2**, that shows the histograms of the GDI values stratified by WISCI II levels. Statistically significant differences were found between HV group and all WISCI II levels. Nevertheless, they were only found

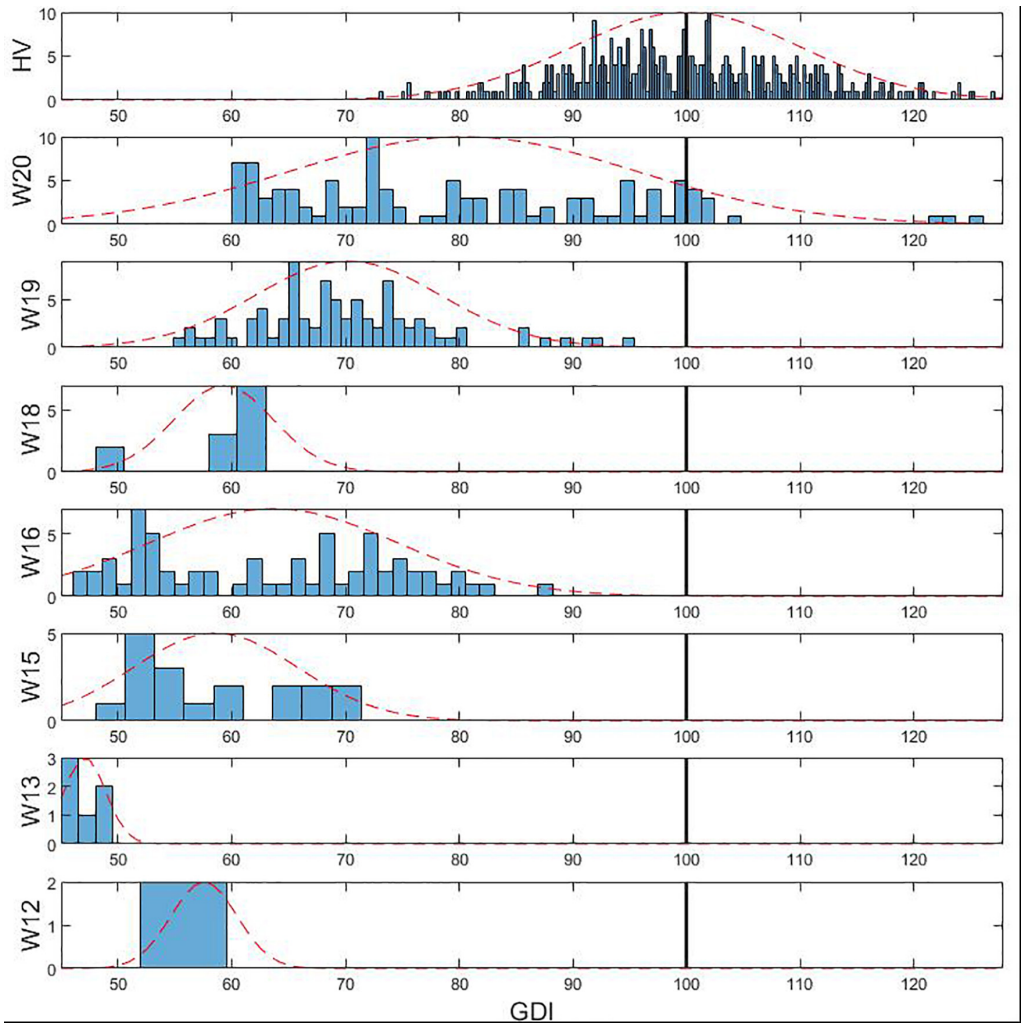

FIGURE 2 | Histograms of GDI values stratified by WISCI II levels in population with iSCI. The dotted line represents the normal distribution curve fitted to the data wihtin each WISCI II level. The vertical black line indicates the HV mean.

between WISCI II levels 13, 19, and 20. No statistically significant differences were found between levels under 18 (inclusive), except by level 13. Therefore, the increasing relationship between the GDI values and WISCI II levels was only discriminative in the highest levels in subjects with iSCI (WISCI II 19: 70.2 ± 8.1; WISCI II 20: 80.4 ± 15.2), but not in the lower levels, except in WISCI II level 13 (47.1 ± 1.8).

DISCUSSION

Our results showed an increasing relationship between the GDI values and WISCI II levels from 13 to 20, and the HV group, except for level 18. Nevertheless, results of the study showed that the application of the GDI only distinguished WISCI II levels 13 (gait assisted with a walker), 19 (gait assisted with a cane), and 20 (no assistance required) from all the other WISCI II levels in adult population with iSCI. The index successfully distinguished all the individuals with iSCI from HV group. For those with WISCI II level 20, GDI values were able to discriminate successfully an impaired gait, even if it did not required any external assistance, from a normal gait pattern. These results does not support previous studies in which WISCI II showed a ceiling effect (Lemay and Nadeau, 2010; Wirz et al., 2010) and a better sensitivity to change in spinal cord injured subjects with more impaired gait compared to those with higher levels of walking function (van Hedel et al., 2006). Regarding ranges of GDI values below WISCI II level 19, except for level 13, results showed an overlap between the different levels, which indicates that the GDI compresses into a small range all WISCI II levels.

Altogether, our results indicate that the GDI was not able to discriminate the functional diversity of adult population with iSCI related to walking impairment defined by WISCI II levels. Therefore, results do not support our hypothesis, built upon the previous correlation analysis of the GDI with other clinical scales used in CP (Schwartz and Rozumalski, 2008; Molloy et al., 2010; Maanum et al., 2012; Massaad et al., 2014). Although more impaired gait patterns, lower GDI values,

are associated with lower WISCI II levels, as shown by the stratification, the differences between all levels are not statistically significant. Thus, the GDI is not a valid metric to distinguish the different walking impairment levels defined by WISCI II in adult population with iSCI. These results may be explained by several reasons. First, because GDI gait features were originally obtained from 3D kinematic data of children with CP (Schwartz and Rozumalski, 2008), GDI could not be an appropriate index to study gait functionality in adult population with SCI. Therefore, application of the GDI in other pathologies different from CP should be done with caution. Second, WISCI II considers gait impairment in terms of physical assistance, AADs, and orthoses required to walk 10 m, but without providing information concerning joint kinematics related to limb coordination. Thus, other walking ability outcome measures different from WISCI II are necessary to cover the whole functional spectrum of walking ability in population with iSCI, such as categorical and spatiotemporal-related walking and balance measures (Sinovas-Alonso et al., 2021).

This study brings to light the existing lack of scientific literature in relation to an overall gait index that covers the functional diversity of patients with iSCI. This may be due to the fact that gait patterns in iSCI are very heterogeneous and variable depending on the level and severity of the lesion, making it difficult to establish a clear pattern for the set of functional alterations that a subject with iSCI may present. Knowledge of the most commonly altered kinematic variables in iSCI would allow the creation of an overall gait index that could cover the diversity of functional alterations involved in iSCI patients' gait. This multivariate walking metric would allow a more accurate assessment of the evolution of patients with iSCI by quantifying the changes and, thus, assessing the quality of the therapeutic interventions carried out. Therefore, future work should aim at defining an overall gait index derived from 3D kinematic gait variables appropriate and specific for population with iSCI, focusing on its validation with other walking ability outcome measures.

There are several limitations in our work. The main one is related to the sample size in group with iSCI, which is reduced in some WISCI II levels and not homogeneous between the different levels and neither between iSCI and HV group. This reduced sample is related to the fact that funding lasted for one year of data gathering and we were not able to continue experimentation after July 2021. Sample size was also reduced due to the health situation associated with the COVID-19 pandemic. Furthermore, this research has considered gait maturation at the age of 16 years to ensure that young individuals with iSCI had reach a stable kinematics (Bleyenheuft and Detrembleur, 2012), which restricts the sample size of adults with iSCI included in the study. Another limitation of this study is related to the fact that during 3D kinematic gait analysis individuals with iSCI walked with the minimum external assistance required to walk safely. It means that some of the patients who usually wore orthoses or used canes to walk more comfortably did not use them since the context of the measure was to analyze gait with the least external interferences under medical prescription. It is highly likely that GDI values have been affected by this fact and, consequently, the relationship with the SS WISCI II levels, which were sometimes different from those at the moment of the test. Finally, due to the retrospective design of the study there is a lack of registration of other walking ability outcome measures, what has limited the study to the analysis of the relationship between the GDI and the WISCI II.

The findings of this study indicated that the GDI is not an appropriate multivariate walking metric to represent the deviation of gait pattern in adult population with iSCI from a normal gait profile when it is compared with the levels of walking impairment described by the WISCI II. It is necessary to conduct further research into the development of a new overall gait index derived from SCI-specific 3D kinematic gait variables, involving a larger population, and validating it against other walking ability outcome measures such as categorical and spatiotemporal-related walking and balance measures.

DATA AVAILABILITY STATEMENT

The raw data supporting the conclusions of this article will be made available by the authors, without undue reservation.

ETHICS STATEMENT

The studies involving human participants were reviewed and approved by Local Ethics Committee of University Hospital Complex of Toledo, Spain. Written informed consent to participate in this study was provided by the participants' legal guardian/next of kin. Written informed consent was obtained from the individual(s) for the publication of any potentially identifiable images or data included in this article.

AUTHOR CONTRIBUTIONS

DH-V, ÁG-A, and IS-A conceived the study. IS-A and AR-G registered data. DH-V analyzed data. IS-A and DH-V wrote the manuscript. RC-d-l-C and AJd-A contributed to the interpretation and discussion of study results. AJd-A obtained funding. All authors revised and approved the final version of the manuscript, read and agreed to the published version of the manuscript.

FUNDING

This research was supported by the TAILOR project: "Modular robotic and neuroprosthetic customizable systems for the assistance of pathological gait," funded by MICIN/AEI/10.13039/501100011033 and by "ERDF A way of making Europe" (Grant No. RTI2018-097290-B-C31).

ACKNOWLEDGMENTS

We acknowledge all participants (hospital staff, students and patients) who accepted voluntarily to be part of this study.

REFERENCES

Baker, R. (2006). Gait analysis methods in rehabilitation. *J. Neuroeng. Rehabil.* 3:4. doi: 10.1186/1743-0003-3-4

Bani, M. A., Arazpour, M., Ghomshe, F. T., Mousavi, M. E., and Hutchins, S. W. (2013). Gait evaluation of the advanced reciprocating gait orthosis with solid versus dorsi flexion assist ankle foot orthoses in paraplegic patients. *Prosthet. Orthot. Int.* 37, 161–167. doi: 10.1177/0309364612457704

Bazarnik-Mucha, K., Snela, S.Ł, Szczepanik, M., Jarmuziewicz, A., Guzik, A., WoliŃska, O., et al. (2020). Three-dimensional analysis of gait in children and adolescents with juvenile idiopathic arthritis. *Acta Bioeng. Biomech.* 22, 35–45.

Bleyenheuft, C., and Detrembleur, C. (2012). Kinematic covariation in pediatric, adult and elderly subjects: is gait control influenced by age? *Clin. Biomech.* 27, 568–572. doi: 10.1016/j.clinbiomech.2012.01.010

Broström, E. W., Esbjörnsson, A.-C., von Heideken, J., Larsson, P., Wretenberg, P., and Iversen, M. (2013). Change in Gait Deviation Index after anti-tumour necrosis factor-α treatment in individuals with rheumatoid arthritis: a pilot study. *Scand. J. Rheumatol.* 42, 356–361. doi: 10.3109/03009742.2013.776102

Burns, A. S., Delparte, J. J., Patrick, M., Marino, R. J., and Ditunno, J. F. (2011). The reproducibility and convergent validity of the walking index for spinal cord injury (WISCI) in chronic spinal cord injury. *Neurorehabil. Neural Repair* 25, 149–157. doi: 10.1177/1545968310376756

Cimolin, V., Galli, M., Vimercati, S. L., and Albertini, G. (2011). Use of the Gait Deviation Index for the assessment of gastrocnemius fascia lengthening in children with Cerebral Palsy. *Res. Dev. Disabil.* 32, 377–381. doi: 10.1016/j.ridd.2010.10.017

Correa, K. P., Devetak, G. F., Martello, S. K., de Almeida, J. C., Pauleto, A. C., and Manffra, E. F. (2017). Reliability and Minimum Detectable Change of the Gait Deviation Index (GDI) in post-stroke patients. *Gait Posture* 53, 29–34. doi: 10.1016/j.gaitpost.2016.12.012

Cupp, T., Oeffinger, D., Tylkowski, C., and Augsburger, S. (1999). Age-related kinetic changes in normal pediatrics. *J. Pediatr. Orthop.* 19, 475–478. doi: 10.1097/00004694-199907000-00010

Dittuno, P. L., Ditunno, J. F., and Dittuno, J. F. (2001). Walking index for spinal cord injury (WISCI II): scale revision. *Spinal Cord* 39, 654–656. doi: 10.1038/sj.sc.3101223

Ditunno, J. F., Barbeau, H., Dobkin, B. H., Elashoff, R., Harkema, S., Marino, R. J., et al. (2007). Validity of the walking scale for spinal cord injury and other domains of function in a multicenter clinical trial. *Neurorehabil. Neural Repair* 21, 539–550. doi: 10.1177/1545968307301880

Ditunno, P. L., Patrick, M., Stineman, M., and Ditunno, J. F. (2008). Who wants to walk? Preferences for recovery after SCI: a longitudinal and cross-sectional study. *Spinal Cord* 46, 500–506. doi: 10.1038/sj.sc.3102172

Eriksson, M., Bartonek, Å, Pontén, E., and Gutierrez-Farewik, E. M. (2015). Gait dynamics in the wide spectrum of children with arthrogryposis: a descriptive study. *BMC Musculoskelet. Disord.* 16:384. doi: 10.1186/s12891-015-0834-5

Esbjörnsson, A.-C., Rozumalski, A., Iversen, M. D., Schwartz, M. H., Wretenberg, P., and Broström, E. W. (2014). Quantifying gait deviations in individuals with rheumatoid arthritis using the Gait Deviation Index. *Scand. J. Rheumatol.* 43, 124–131. doi: 10.3109/03009742.2013.822095

Eshraghi, A., Osman, N. A. A., Karimi, M., Gholizadeh, H., Soodmand, E., and Abas, W. A. B. W. (2014). Gait Biomechanics of Individuals with Transtibial Amputation: effect of Suspension System. *PLoS One* 9:e96988. doi: 10.1371/journal.pone.0096988

Galli, M., Cimolin, V., De Pandis, M. F., Schwartz, M. H., and Albertini, G. (2012). Use of the Gait Deviation index for the evaluation of patients with Parkinson's disease. *J. Mot. Behav.* 44, 161–167. doi: 10.1080/00222895.2012.664180

Ganley, K. J., and Powers, C. M. (2005). Gait kinematics and kinetics of 7-year-old children: a comparison to adults using age-specific anthropometric data. *Gait Posture* 21, 141–145. doi: 10.1016/j.gaitpost.2004.01.007

Garman, C. R., Graf, A., Krzak, J., Caudill, A., Smith, P., and Harris, G. (2019). Gait Deviations in Children With Osteogenesis Imperfecta Type I. *J. Pediatr. Orthop.* 39, e641–e646. doi: 10.1097/BPO.0000000000001062

Guzik, A., and Drużbicki, M. (2020). Application of the Gait Deviation Index in the analysis of post-stroke hemiparetic gait. *J. Biomech.* 99:109575. doi: 10.1016/j.jbiomech.2019.109575

Hwang, M., Flanagan, A., Graf, A., Kruger, K. M., Scullion, N., Tayne, S., et al. (2021). Gait Characteristics in Youth With Transverse Myelitis. *Top Spinal Cord Inj. Rehabil.* 27, 38–48. doi: 10.46292/sci20-00048

Ito, T., Noritake, K., Sugiura, H., Kamiya, Y., Tomita, H., Ito, Y., et al. (2019). Association between Gait Deviation Index and Physical Function in Children with Bilateral Spastic Cerebral Palsy: a Cross-Sectional Study. *J. Clin. Med.* 9:E28. doi: 10.3390/jcm9010028

Ito, T., Sugiura, H., Ito, Y., Noritake, K., and Ochi, N. (2021). Effect of the COVID-19 Emergency on Physical Function among School-Aged Children. *Int. J. Environ. Res. Public Health* 18:9620. doi: 10.3390/ijerph18189620

Ito, Y., Ito, T., Kurahashi, N., Ochi, N., Noritake, K., Sugiura, H., et al. (2020). Gait characteristics of children with Williams syndrome with impaired visuospatial recognition: a three-dimensional gait analysis study. *Exp. Brain Res.* 238, 2887–2895. doi: 10.1007/s00221-020-05946-0

Jackson, A. B., Carnel, C. T., Ditunno, J. F., Read, M. S., Boninger, M. L., Schmeler, M. R., et al. (2008). Outcome measures for gait and ambulation in the spinal cord injury population. *J. Spinal Cord Med.* 31, 487–499. doi: 10.1080/10790268.2008.11753644

Kark, L., Odell, R., McIntosh, A. S., and Simmons, A. (2016). Quantifying prosthetic gait deviation using simple outcome measures. *World J. Orthop.* 7, 383–391. doi: 10.5312/wjo.v7.i6.383

Kirshblum, S. C., Burns, S. P., Biering-Sorensen, F., Donovan, W., Graves, D. E., Jha, A., et al. (2011). International standards for neurological classification of spinal cord injury (Revised 2011). *J. Spinal Cord Med.* 34, 535–546. doi: 10.1179/204577211X13207446293695

Kobsar, D., Charlton, J. M., and Hunt, M. A. (2019). Individuals with knee osteoarthritis present increased gait pattern deviations as measured by a knee-specific gait deviation index. *Gait Posture* 72, 82–88. doi: 10.1016/j.gaitpost.2019.05.020

Lemay, J.-F., and Nadeau, S. (2010). Standing balance assessment in ASIA D paraplegic and tetraplegic participants: concurrent validity of the Berg Balance Scale. *Spinal Cord* 48, 245–250. doi: 10.1038/sc.2009.119

Maanum, G., Jahnsen, R., Stanghelle, J. K., Sandvik, L., Larsen, K. L., and Keller, A. (2012). Face and construct validity of the Gait Deviation Index in adults with spastic cerebral palsy. *J. Rehabil. Med.* 44, 272–275. doi: 10.2340/16501977-0930

Malt, M. A., Aarli, Å, Bogen, B., and Fevang, J. M. (2016). Correlation between the Gait Deviation Index and gross motor function (GMFCS level) in children with cerebral palsy. *J. Child Orthop.* 10, 261–266. doi: 10.1007/s11832-016-0738-4

Mar, D., Lieberman, I., and Haddas, R. (2019). The Gait Deviation Index as an indicator of gait abnormality among degenerative spinal pathologies. *Eur. Spine J.* 29, 2591–2599. doi: 10.1007/s00586-019-06252-2

Marino, R. J., Scivoletto, G., Patrick, M., Tamburella, F., Read, M. S., Burns, A. S., et al. (2010). Walking index for spinal cord injury version 2 (WISCI-II) with repeatability of the 10-m walk time: inter- and intrarater reliabilities. *Am. J. Phys. Med. Rehabil.* 89, 7–15. doi: 10.1097/PHM.0b013e3181c560eb

Massaad, A., Assi, A., Skalli, W., and Ghanem, I. (2014). Repeatability and validation of Gait Deviation Index in children: typically developing and cerebral palsy. *Gait Posture* 39, 354–358. doi: 10.1016/j.gaitpost.2013.08.001

McGinley, J. L., Baker, R., Wolfe, R., and Morris, M. E. (2009). The reliability of three-dimensional kinematic gait measurements: a systematic review. *Gait Posture* 29, 360–369. doi: 10.1016/j.gaitpost.2008.09.003

Mindler, G. T., Kranzl, A., Stauffer, A., Haeusler, G., Ganger, R., and Raimann, A. (2020). Disease-specific gait deviations in pediatric patients with X-linked hypophosphatemia. *Gait Posture* 81, 78–84. doi: 10.1016/j.gaitpost.2020.07.007

Molloy, M., McDowell, B. C., Kerr, C., and Cosgrove, A. P. (2010). Further evidence of validity of the Gait Deviation Index. *Gait Posture* 31, 479–482. doi: 10.1016/j.gaitpost.2010.01.025

Morganti, B., Scivoletto, G., Ditunno, P., Ditunno, J. F., and Molinari, M. (2005). Walking index for spinal cord injury (WISCI): criterion validation. *Spinal Cord* 43, 27–33. doi: 10.1038/sj.sc.3101658

Murphy, A. T., Kravtsov, S., Sangeux, M., Rawicki, B., and New, P. W. (2019). Utilizing three dimensional clinical gait analysis to optimize mobility outcomes in incomplete spinal cord damage. *Gait Posture* 74, 53–59. doi: 10.1016/j.gaitpost.2019.08.001

Quadri, S. A., Farooqui, M., Ikram, A., Zafar, A., Khan, M. A., Suriya, S. S., et al. (2020). Recent update on basic mechanisms of spinal cord injury. *Neurosurg. Rev.* 43, 425–441. doi: 10.1007/s10143-018-1008-3

Rasmussen, H. M., Pedersen, N. W., Overgaard, S., Hansen, L. K., Dunkhase-Heinl, U., Petkov, Y., et al. (2019). Gait analysis for individually tailored interdisciplinary interventions in children with cerebral palsy: a randomized controlled trial. *Dev. Med. Child Neurol.* 61, 1189–1195. doi: 10.1111/dmcn.14178

Rosenlund, S., Holsgaard-Larsen, A., Overgaard, S., and Jensen, C. (2016). The Gait Deviation Index Is Associated with Hip Muscle Strength and Patient-Reported Outcome in Patients with Severe Hip Osteoarthritis-A Cross-Sectional Study. *PLoS One* 11:e0153177. doi: 10.1371/journal.pone.0153177

Sagawa, Y., Watelain, E., De Coulon, G., Kaelin, A., Gorce, P., and Armand, S. (2013). Are clinical measurements linked to the Gait Deviation Index in cerebral palsy patients? *Gait Posture* 38, 276–280. doi: 10.1016/j.gaitpost.2012.11.026

Schwartz, M. H., and Rozumalski, A. (2008). The Gait Deviation Index: a new comprehensive index of gait pathology. *Gait Posture* 28, 351–357. doi: 10.1016/j.gaitpost.2008.05.001

Scivoletto, G., Miscusi, M., Forcato, S., Ricciardi, L., Serrao, M., Bellitti, R., et al. (2017). The Rehabilitation of Spinal Cord Injury Patients in Europe. *Acta Neurochir. Suppl.* 124, 203–210. doi: 10.1007/978-3-319-39546-3_31

Scivoletto, G., Tamburella, F., Laurenza, L., Foti, C., Ditunno, J. F., and Molinari, M. (2011). Validity and reliability of the 10-m walk test and the 6-min walk test in spinal cord injury patients. *Spinal Cord* 49, 736–740. doi: 10.1038/sc.2010.180

Scivoletto, G., Tamburella, F., Laurenza, L., Torre, M., Molinari, M., and Ditunno, J. F. (2014). Walking Index for Spinal Cord Injury version II in acute spinal cord injury: reliability and reproducibility. *Spinal Cord* 52, 65–69. doi: 10.1038/sc.2013.127

Sienko Thomas, S., Buckon, C. E., Nicorici, A., Bagley, A., McDonald, C. M., and Sussman, M. D. (2010). Classification of the gait patterns of boys with Duchenne muscular dystrophy and their relationship to function. *J. Child Neurol.* 25, 1103–1109. doi: 10.1177/0883073810371002

Sinovas-Alonso, I., Gil-Agudo, Á, Cano-de-la-Cuerda, R., and del-Ama, A. J. (2021). Walking Ability Outcome Measures in Individuals with Spinal Cord Injury: a Systematic Review. *Int. J. Environ. Res. Public Health* 18:9517. doi: 10.3390/ijerph18189517

Speciali, D. S., de Oliveira, E. M., dos Santos, N. M., Pereira, F. V., Fracini, A. C., Fukuda, T. Y., et al. (2013). Use of the Gait Deviation Index and spatiotemporal variables for the assessment of dual task interference paradigm. *J. Bodyw. Mov. Ther.* 17, 19–27. doi: 10.1016/j.jbmt.2012.03.001

Trivedi, J., Srinivas, S., Trivedi, R., Davidson, N., Munigangaiah, S., Bruce, C., et al. (2021). Preoperative and Postoperative, Three-dimensional Gait Analysis in Surgically Treated Patients With High-grade Spondylolisthesis. *J. Pediatr. Orthop.* 41, 111–118. doi: 10.1097/BPO.0000000000001721

van Hedel, H. J. A., Wirz, M., and Curt, A. (2006). Improving walking assessment in subjects with an incomplete spinal cord injury: responsiveness. *Spinal Cord* 44, 352–356. doi: 10.1038/sj.sc.3101853

Wilson, N. C., Signal, N., Naude, Y., Taylor, D., and Stott, N. S. (2015). Gait Deviation Index Correlates With Daily Step Activity in Children With Cerebral Palsy. *Arch. Phys. Med. Rehabil.* 96, 1924–1927. doi: 10.1016/j.apmr.2015.05.024

Wirz, M., Müller, R., and Bastiaenen, C. (2010). Falls in persons with spinal cord injury: validity and reliability of the Berg Balance Scale. *Neurorehabil. Neural Repair* 24, 70–77. doi: 10.1177/1545968309341059

Zhou, C., Xia, H., Yin, J., and Zheng, Y. (2021). Three-dimensional gait quantitative analysis in postoperative rehabilitation of lumbar degenerative diseases: a self-controlled before-after study. *Am. J. Transl. Res.* 13, 6913–6920.

Conflict of Interest: The authors declare that the research was conducted in the absence of any commercial or financial relationships that could be construed as a potential conflict of interest.

Publisher's Note: All claims expressed in this article are solely those of the authors and do not necessarily represent those of their affiliated organizations, or those of the publisher, the editors and the reviewers. Any product that may be evaluated in this article, or claim that may be made by its manufacturer, is not guaranteed or endorsed by the publisher.

frontiers | Frontiers in Human Neuroscience

ORIGINAL RESEARCH
published: 19 May 2022
doi: 10.3389/fnhum.2022.826376

Machine Learning Classifiers to Evaluate Data From Gait Analysis With Depth Cameras in Patients With Parkinson's Disease

Beatriz Muñoz-Ospina[1], Daniela Alvarez-Garcia[2,3], Hugo Juan Camilo Clavijo-Moran[4], Jaime Andrés Valderrama-Chaparro[5], Melisa García-Peña[3], Carlos Alfonso Herrán[3], Christian Camilo Urcuqui[3], Andrés Navarro-Cadavid[3] and Jorge Orozco[1]*

[1]Fundación Valle del Lili, Departamento de Neurología, Cali, Colombia, [2]Fundación Valle del Lili, Departamento de Neurocirugía, Cali, Colombia, [3]Universidad Icesi, Lab i2t/CENIT, Cali, Colombia, [4]Fundación Valle del Lili, Centro de investigaciones clínicas, Cali, Colombia, [5]Universidad Icesi, Facultad de ciencias de la salud, Cali, Colombia

OPEN ACCESS

Edited by:
Marco Iosa,
Sapienza University of Rome, Italy

Reviewed by:
Stefano Filippo Castiglia,
Sapienza University of Rome, Italy
Jean Meunier,
Université de Montréal, Canada
Tomoko Arakaki,
Hospital Ramos Mejía, Argentina

***Correspondence:**
Beatriz Muñoz-Ospina
beatriz.munoz@fvl.org.co

Specialty section:
This article was submitted to Motor Neuroscience, a section of the journal Frontiers in Human Neuroscience

Received: *30 November 2021*
Accepted: *13 April 2022*
Published: *19 May 2022*

Citation:
Muñoz-Ospina B, Alvarez-Garcia D, Clavijo-Moran HJC, Valderrama-Chaparro JA, García-Peña M, Herrán CA, Urcuqui CC, Navarro-Cadavid A and Orozco J (2022) Machine Learning Classifiers to Evaluate Data From Gait Analysis With Depth Cameras in Patients With Parkinson's Disease. Front. Hum. Neurosci. 16:826376. doi: 10.3389/fnhum.2022.826376

Introduction: The assessments of the motor symptoms in Parkinson's disease (PD) are usually limited to clinical rating scales (MDS UPDRS III), and it depends on the clinician's experience. This study aims to propose a machine learning technique algorithm using the variables from upper and lower limbs, to classify people with PD from healthy people, using data from a portable low-cost device (RGB-D camera). And can be used to support the diagnosis and follow-up of patients in developing countries and remote areas.

Methods: We used Kinect®eMotion system to capture the spatiotemporal gait data from 30 patients with PD and 30 healthy age-matched controls in three walking trials. First, a correlation matrix was made using the variables of upper and lower limbs. After this, we applied a backward feature selection model using R and Python to determine the most relevant variables. Three further analyses were done using variables selected from backward feature selection model (Dataset A), movement disorders specialist (Dataset B), and all the variables from the dataset (Dataset C). We ran seven machine learning models for each model. Dataset was divided 80% for algorithm training and 20% for evaluation. Finally, a causal inference model (CIM) using the DoWhy library was performed on Dataset B due to its accuracy and simplicity.

Results: The Random Forest model is the most accurate for all three variable Datasets (Dataset A: 81.8%; Dataset B: 83.6%; Dataset C: 84.5%) followed by the support vector machine. The CIM shows a relation between leg variables and the arms swing asymmetry (ASA) and a proportional relationship between ASA and the diagnosis of PD with a robust estimator (1,537).

Conclusions: Machine learning techniques based on objective measures using portable low-cost devices (Kinect®eMotion) are useful and accurate to classify patients with Parkinson's disease. This method can be used to evaluate patients remotely and help clinicians make decisions regarding follow-up and treatment.

Keywords: Parkinson's disease, gait, biomechanics, kinect, depth camera, machine learning

INTRODUCTION

Parkinson's disease (PD) represents the second most prevalent neurodegenerative disease in the world with an alarming growth rate in the number of affected individuals estimating that the number of cases will double between 2015 and 2040 (de Lau and Breteler, 2006; Tysnes and Storstein, 2017; Dorsey and Bloem, 2018). PD is clinically characterized by motor symptoms such as bradykinesia, rigidity, tremor, gait disturbance, and impaired postural instability (Schneider and Obeso, 2014; Postuma et al., 2015; Deb et al., 2021). Diagnosis and follow-up are based on several scales and questionnaires to assess severity including Movement Disorder Society-Sponsored Revision of the Unified Parkinson's Disease Rating Scale (MDS-UPDRS; Goetz et al., 2008). However, these clinical scales are subjective with high inter-rater variability between clinicians. Furthermore, follow-up is also based on self-report questionnaires that imply recall bias (Deb et al., 2021). In the last 20 years, there has been great interest in developing objective measurement focused on early diagnosis, accurate follow-up, evaluation of motor fluctuations, and prognosis in PD, from which has arisen technology-based objective measurements (TOMs) as a complement for clinical assessment (Urcuqui et al., 2018; Deb et al., 2021).

In PD, changes in gait kinematics and spatiotemporal features are hallmarks of the disease. Gait analysis is complex and usually requires a gait and biomechanics laboratory which is expensive and not globally available for medical consultation (Urcuqui et al., 2018). Recently, several cost-effective instruments have been used to assess PD motor symptoms such as RGB-D cameras (Kinect®). Despite the large number of TOMs studies and available data, such as inertial measurement units (IMUS) that do not need a specialized laboratory, the RGB-D cameras are the most accessible technology in remote areas for its cost and its simplicity. However, the data processing and classification methods are still variable upon the studies.

Machine learning (ML) techniques have been studied in several medical areas including PD (Sidey-Gibbons and Sidey-Gibbons, 2019) in order to classify healthy volunteers from patients using voice analysis (Ozkan, 2016), feet pressure systems (Abdulhay et al., 2018), RGB-D cameras (Buongiorno et al., 2019; Jaggy Castaño-Pino et al., 2019), optoelectronic motion analysis system (Varrecchia et al., 2021), wearable sensors such as accelerometers or inertial measurement units (IMU; Yoneyama et al., 2013; Caramia et al., 2018), walkway pressure analysis (Wahid et al., 2015), and variables associated with knee and trunk rotation (Varrecchia et al., 2021). Other studies have been using unsupervised learning to extract features in the initial stages of the disease (Singh and Samavedham, 2015), propose a method to obtain informative correlation-aware signals (Zhang et al., 2021), and evaluate clustering algorithms to support the prediction of the disease (Sherly Puspha Annabel et al., 2021). Most of the studies that aimed to classify healthy people from PD patients focused solely on leg variables or arm variables or axial trunk and knee rotation even though the disease involves all four limbs and the first affected are the arms (Ospina et al., 2018; Monje et al., 2021).

With the rise of telemedicine in recent years, particularly after the beginning of the SARS-CoV2 pandemic, never has it been so important to develop simple assessment methods that do not require high costs or specialized equipment, particularly in developing countries where access to specialized medicine is limited. In addition, telemedicine programs in Parkinson's disease are a growing field and gait measurement demands many challenges to evaluate patients in rural regions and developing countries in order to ensure quality evaluation. Remote monitoring with synchronous and asynchronous assessments included the use of specialized devices and recorded and uploaded videos, for motor evaluation such as bradykinesia, gait, and falls (Shalash et al., 2021).

In this work, our aim is to study the causal relationship between gait features from upper and lower extremities and assess the performance of a machine learning model to classify people with PD from healthy subjects using data from a portable low-cost device (Depth Camera) called Kinect®eMotion system in order to support diagnosis and follow-up to patients with PD in remote areas.

MATERIALS AND METHODS

Design and Participants

The dataset was extracted from a single-center study carried out between June and December 2016, by the Neurology Service at the Fundación Valle del Lili academic Hospital in Cali—Colombia (Muñoz Ospina et al., 2019). We included spatiotemporal gait data from 30 patients with PD and 30 healthy age-matched controls. Each patient was evaluated by a movement disorder specialist and met the criteria from the UK Parkinson's Disease Society Brain Bank diagnostic criteria. No participants had major features that affected their gait (major orthopedic surgeries, osteoarthritis, other neuromuscular disorders, or walking aids) All participants with PD were treated with dopaminergic agonists and were evaluated in the "on" state. Institutional review board approval was obtained prior to starting the study and all participants provided written informed consent before participation.

Gait data were obtained from previous studies using an RGB-D camera (Kinect®eMotion) coupled with a signal processing software. Subjects underwent a single gait evaluation session during which each subject was asked to walk at their preferred speed during three consecutive walking trials. The measurements were made in a corridor 4 m long and 1.5 m wide free of interference. The distance allowed for Kinect® to record a minimum of one full gait cycle per limb. **Figure 1** shows the setup during a measurement campaign in a rural area in the southwest of the country.

As indicated in previous studies we used wavelet techniques to extract gait phases and generate several spatio/temporal variables (see **Table 1**). These variables were obtained based on a wavelet decomposition using a Daubechies wavelet (Db8; Jaggy Castaño-Pino et al., 2019).

FIGURE 1 | RGB-D camera setup and gait evaluation zone.

TABLE 1 | Gait variables definition.

Arms variables	
Swing magnitude (left/right)	Distance taken by the wrist from the maximum anterior to the maximum posterior point during an arm swing cycle.
Swing time (left/right)	Time taken by the wrist to travel the distance between the maximum anterior and maximum posterior points during an arm swing cycle.
Swing speed (left/right)	Calculated as the distance traveled by the arm (arm swing) per unit of time (arm time)
Arm swing asymmetry (ASA; Zifchock et al., 2008)	$ASA = \frac{\left[45° - arct\left(\frac{Arm\ swing\ more}{Arm\ swing\ less}\right)\right]}{90°} \times 100$
Leg variables	
Global gait speed	Calculated as the distance traveled (test distance) per unit of time (test time)
Total time (left/right)	Time during which the ankle (left/right) was in the motion capture area.
Total distance (left/right)	Distance during which the ankle (left/right) was in the motion capture area.
Total swing time (left/right)	Total time while the foot (left/right) was in the swing phase.
Total stance time (left/right)	Total time while the foot (left/right) was in the stance phase.
Swing time (left/right)	Time, while one foot left/right, was on swing phase during 1 leg gait cycle.
Stance time(left/right)	Time while one foot (left/right) was on stance phase during 1 leg gait cycle.
Number of steps (left/right)	Number of steps taken by one foot (left/right) during the test.
Step length (left/right)	Distance traveled by one foot (left/right) during 1 step.

ASA: arm swing more is the value of the arm's swing magnitude with the highest value. It is expressed in percentages.

Preprocessing Features

As we aimed to study arms and legs variables (one dataset for each set of features), the integration of all the data was made using a unique ID for each patient and the result was a dataset of 620 records and 28 features. The join presented 96 records without values that were excluded during the study. After the

filtering process, the dataset had a shape of 554 × 28; 37% of the dataset corresponded to healthy controls and 63% to PD patients.

Two datasets were generated with the same shape for further analysis: one with normalized information because this is a prerequisite for some machine learning algorithms and the other set of information without normalizing technique. For normalization we used the open library ClusterSim (Walesiak and Dudek, 2020) which uses the following formula: $\frac{(x-mean)}{\sqrt{(sum(x-mean)^2}}$.

Exploratory Analysis

The data exploration included an evaluation between gait variables using a correlation matrix; three thresholds (0.35, 0.4, and 0.9) were selected randomly from a range of 0–1. Each value was analyzed, the correlations higher than the threshold 0.9 did not show similarity in the variables related to arms and legs. Using the value of 0.4 the features presented a similarity; the highest similarities between upper and lower extremities were obtained using 0.35 as the correlation threshold. Scatter plots were created using the correlation matrix. Backward and forward feature selection models were applied using R and Python to determine the most important variables for further analysis, especially to perform a partial correlation analysis with different sets of features. The significance level selected was 5% for all the variables in the backward feature selection process.

Machine Learning and Evaluation

Three further analyses were done using variables selected from: Backward models (Dataset A), movement disorders specialist (Dataset B), and all the variables from the dataset (Dataset C).

Dataset A: In order to find the most important variables, a backward elimination process for all the models used in this research was run for the full set of variables and the results were: Left-arm magnitude, arm swing asymmetry (ASA; Zifchock et al., 2008), left swing time, left length of step.

Dataset B: Eight variables were selected (Swing magnitude of both arms, swing time of both legs, step length of both feet, ASA, and global gait speed) by a movement disorder specialist according to their clinical relevance to PD diagnosis and follow-up.

Dataset C: All variables were included in this dataset.

Seven machine learning algorithms were chosen based on the results of previous studies (Urcuqui et al., 2018; Reyes et al., 2019; Alzubaidi et al., 2021). Six of the selected algorithms were trained using R statistical software (logistic regression, decision tree without processing, pre-pruning decision tree, post-pruning decision tree, naive Bayes, and random forest). Using Python, a support vector machine model was trained (see **Table 2**: machine learning parameters and commands for execution).

The experiments applied hold-out (a train set, validation set, and testing set were made) and K-fold cross-validation to reduce overfitting. The dataset was divided into: 10 records for final validation, 80% for algorithm training, and 20% for testing. The cross-validation used k iterations equal to 5 to include different sets of information during the training and validation phases. Classification metrics used in this study for the testing phase were accuracy, false-positive ratio, false negative ratio, and Cohen's Kappa, the latter as an evaluation metric to evaluate the model's performance against the imbalance of the values from the dependent variables.

Causal Inference Model

We decided to find if there was some causal relationship between the variables. For this task, we used the DoWhy library (Sharma and Kiciman, 2020) and applied the causal inference model (CIM). The causal model was applied to each relevant variable of the selected dataset.

The DoWhy library is a Python library developed by Microsoft with the aim to spark causal thinking and analysis. The main idea of the DoWhy library is to model and validate causal assumptions testing these assumptions for any estimation method. The library is based on the Structural Causal Model theory proposed by Pearl (1995) and implements a refutation API to simplify the analysis for non-experts in this area (see **Supplementary Material** for details on the procedure).

TABLE 2 | Machine learning parameters and commands for execution.

Model	Dataset C	Dataset B	Dataset A
Logistic regression	method="glmStepAIC" Direction= "forward" preprocess = c ("center", "scale") trace = TRUE, AIC = 607.49	method="glmStepAIC" Direction= "forward" preprocess = c ("center", "scale") trace = TRUE, AIC = 621.4	method="glmStepAIC" Direction= "forward" preprocess = c ("center", "scale") trace = TRUE, AIC = 620.67
Support Vector Machine	Kernel = rbf C = 5 Gamma = 0.05	Kernel = rbf C = 10 Gamma = 0.05	Kernel = rbf C = 10 Gamma = 0.05
Decision tree without processing	CP = 0.042	CP = 0.036	CP = 0.027
Decision tree pre-pruning	Depth = 5	Depth = 8	Depth = 7
Decision tree post-pruning	CP = 0.042	CP = 0.036	CP = 0.054
Naïve Bayes	Laplace = 0 UserKernel = TRUE Adjust = 1	Laplace = 0 UserKernel = TRUE Adjust = 1	Laplace = 0 UserKernel = TRUE Adjust = 1
Random Forest	Mtry = 3 nTree = 1500	Mtry = 2 nTree = 1500	Mtry = 2 nTree = 1500

RESULTS

We included data from 30 patients with PD, 17 (57%) men, and 30 healthy age-matched controls. Both groups had a median age of 66 years (IQR 59–75). The median duration of the disease was 5 years (IQR 1–7). Hoehn and Yahr stage classification was stage I for 17% of the patients, stage II for 73%, and stage III for the remaining 10%. The mean of MDS-UPDRS part III was 39.06 (±13.74; see **Table 3**). We retained a dataset with 554 records and 28 variables, we did not exclude outliers to simulate real clinical situations.

First, we conducted an exploratory analysis using a correlation matrix to identify the most relevant variables. We reduced data based on the degree of correlation, retaining only variables with a correlation greater than 0.35 (see **Figure 2**).

Based on the correlation matrix we obtained several scatter plots (see **Figure 3**).

Variable Selection

Using the Backward feature selection model, the most relevant variables were: (1) swing magnitude of left arm; (2) swing time of left leg; (3) left step length; and (4) arm swing asymmetry (ASA). Based on previous studies and clinical expertise, a dataset was created (B) to perform further analysis with some selected variables: swing magnitude of both arms, swing time of both legs, step length of both feet, arm swing asymmetry (ASA), and global gait speed.

Machine Learning Results

Results from the coefficient of concordance Kappa and accuracy for each model using each set of variables for the test dataset are shown in **Table 4**.

As we can see, the Random Forest model is the most accurate for all three variable Datasets (Dataset A: 81.8%; Dataset B: 83.6%; Dataset C: 84.5%) followed by the support vector machine for both, A and B datasets, and decision tree pre-pruning for dataset C. Results showing the degree of false positive and false negative are shown for each model and each set of variables in **Table 4**.

In order to verify the accuracy of the model we selected 10 aleatory data from the sample (validation records), we compared the classification between patient and control that the algorithm was able to predict vs. the real diagnosis. The accuracy was 90% with only one false positive case.

TABLE 3 | Clinical features of the sample.

	PD patients	Healthy controls	*p*-value
Age	66 (IQR 59–75)	66 (IQR 59–75)	0.88
Sex:	17 (57%)	19 (63%)	0.60
Male	13 (43%)	11 (36%)	
Female			
Disease duration (years)	5 (IQR 1–7)	-	
Hoehn and Yahr		-	
I	5 (17%)		
II	22 (73%)		
III	3 (10%)		
MoCA	22 (IQR 16–26)	22.5 (IQR 21–24)	0.57
Left side symptoms	17/30 (57%)		
Right side symptoms	11/30 (37%)		
Symmetrical	2/30 (7%)		
MDS-UPDRS III	39.06 (±13.74)	-	
FOG-Q	6.73 (± 4.95)	-	

MoCA, Montréal cognitive Assessment; FOG-Q, Freezing of gait questionnaire. MDS-UPDRS part III: movement disorder society sponsored revision of the Unified Parkinson's Disease Rating Scale. The laterality of the symptoms was obtained based on the MDS-UPDRS part III.

Relationship Between Arms and Legs Variables

Due to its accuracy (83.6%) and simplicity (eight variables), dataset B was chosen to run the CIM. Using this model and the DoWhy library relationships between leg gait variables and arm swing variables were analyzed (**Figure 4**).

Causal inference estimator results show that there is a proportional relationship between ASA and the diagnosis of PD (estimator: 1,536). This can be interpreted as every time the classifier goes up 1 unit (the subject is diagnosed with PD), ASA goes up 1,536 units. To verify the robustness of this estimation three refuters tests were calculated. When "random common cause refuter" is applied to this estimator the results do not significantly vary (1,520), the same happens with "data subset refuter" (1,531) which implies the result is robust. In the placebo treatment refuter, the result for ASA is 0.00436 which is very close to 0. This also means the estimator is robust (see **Table 5**). That is why based on the DoWhy library, ASA is the most representative variable in the causal inference model.

DISCUSSION

The main objective of this study was to propose a machine learning-based algorithm to classify the patients with PD from the healthy controls, using a portable RGB-D camera (Kinect® eMotion capture system). These results are in line with our attempt to explore other ways to assess the gait variables using a low-cost system that can be used during medical consultation in a developing country. According to our previous results, this machine learning-based algorithm will improve the data analytical and clinical efforts to analyze disease-relevant information for physicians and patients.

Correlations and Variable Exploration

As expected there is a positive strong correlation between arm speed and arm swing magnitude which represents that some of the normal dynamics of human gait is preserved even in PD patients. Despite the correlation of magnitude between both arms being weak and positive, this could be explained by the limb movement asymmetry secondary to the motor symptoms of the disease (increased rigidity and bradykinesia) predominantly affecting only one body side in the PD group. This pathological asymmetry between left and right arm swing magnitudes is represented by the ASA coefficient which is one of the earliest clinical manifestations of PD (Mirelman et al., 2016).

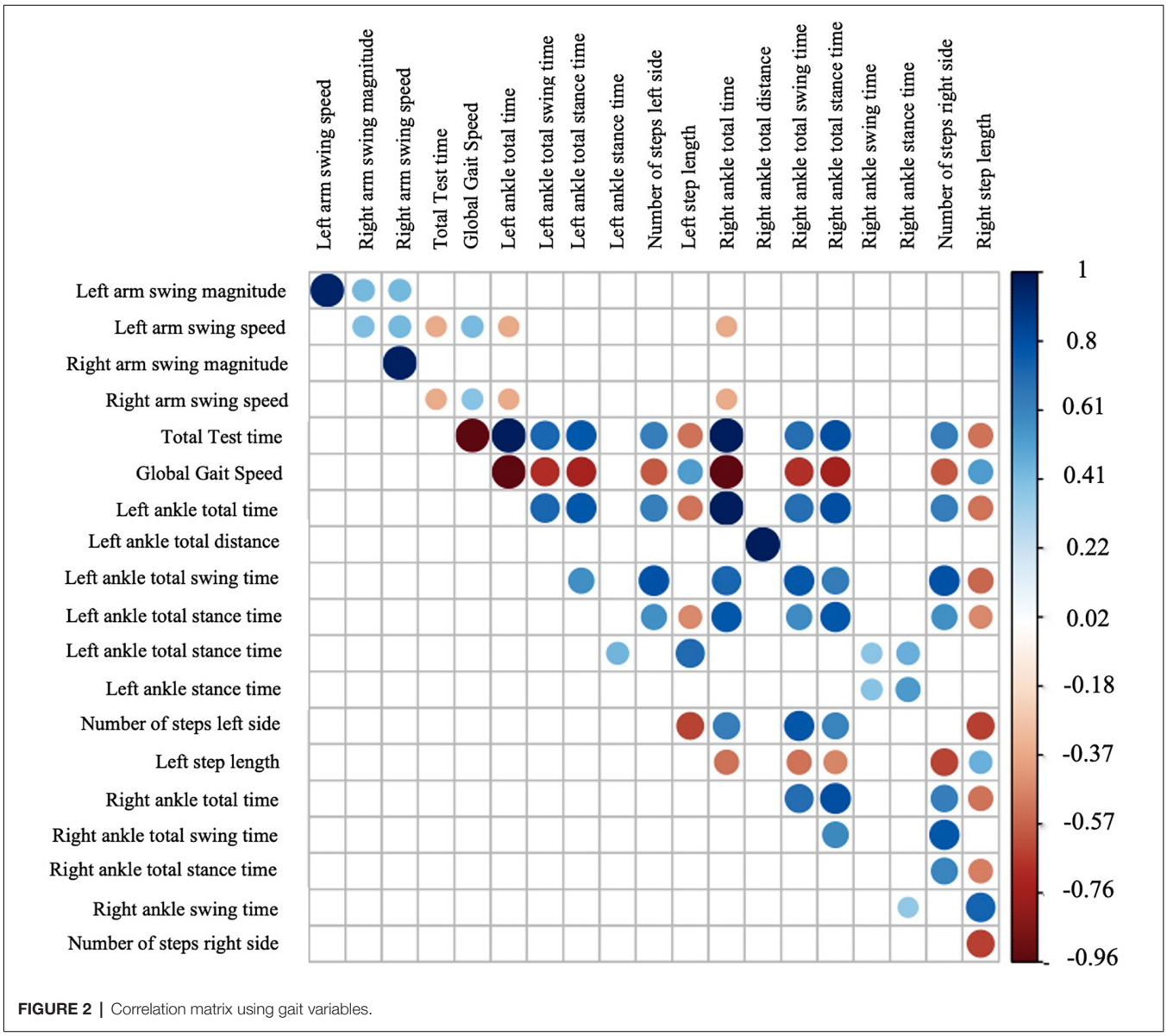

FIGURE 2 | Correlation matrix using gait variables.

Regarding the results of the non-PD group, controls exhibit a similar speed in both upper limbs, which could be related to the normal pattern of gait unaffected by the disease (see **Figure 3**).

Variable Selection and Dataset Construction

Variables were selected according to different criteria into three datasets. When the backward technique was applied predominantly left variables (arm swing magnitude, step length, and swing time) were selected, which could be related to the prevalence of left-sided motor symptoms in our sample of PD patients (17/30; 57%).

Also, the gait variables selected by the backward feature selection model are related to the clinical changes expected in PD and features needed to fulfill diagnostic criteria: PD patients move their arms and legs more slowly (bradykinesia) and stiffy (rigidity) than controls, for this reason, the magnitude of the arm swing, the time of the leg swing and the step length differ significantly from the healthy-controls.

Furthermore, the selection of both arm and leg variables suggests alterations in the motor pattern of upper and lower limbs. These complex changes in the gait dynamics indicate that objective examination of gait should consider multiple motor variables of each limb. This consideration is consistent with clinical environments where the patient diagnosis and follow-up are based on a full-body examination using the MDS-UPDRS part III (Goetz et al., 2008; Postuma et al., 2015).

Machine Learning Algorithm

Our results show that it is possible to classify patients from controls using different datasets processed by multiple machine learning techniques with different accuracy levels.

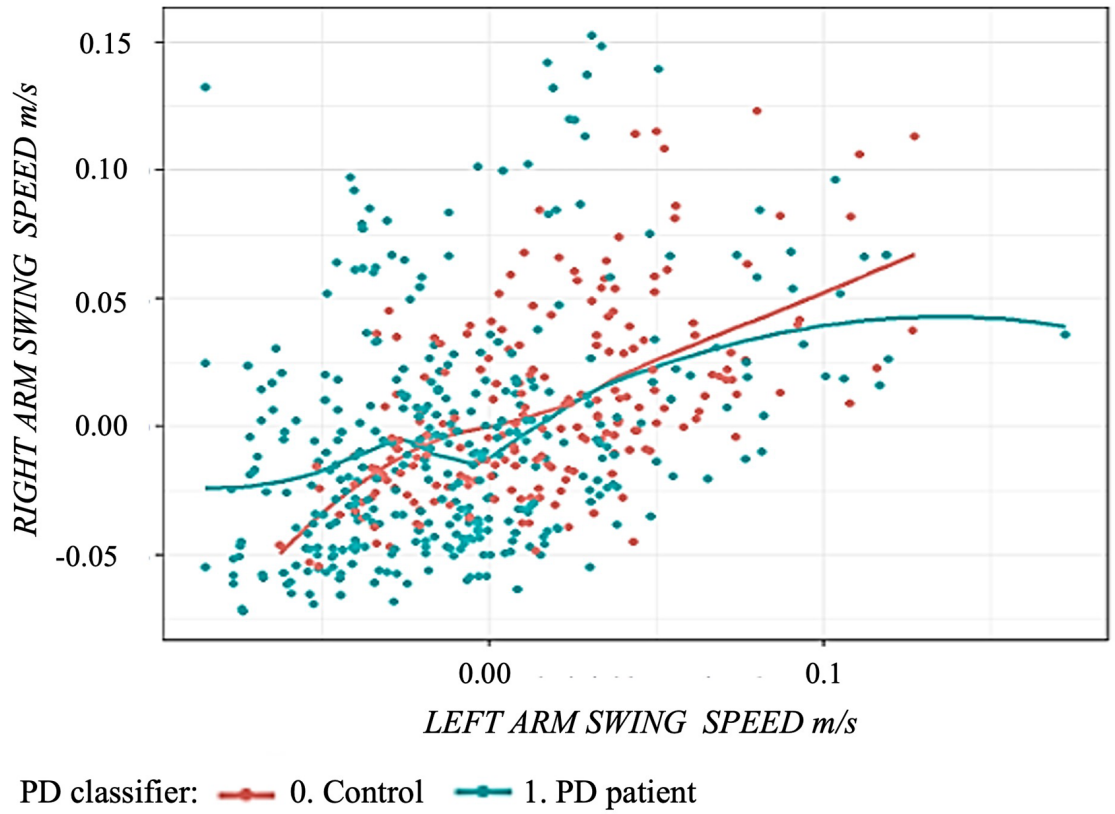

FIGURE 3 | Scatter plot using arm swing speed comparing controls and Parkinson's disease patients: green curve represents the regression curve of the left and right arms swing speed in Parkinson's disease patients. The red curve represents the regression curve of the left and right arms swing speed in healthy subjects.

TABLE 4 | Confusion matrix results showing kappa, accuracy, false positive, and false negative rate for each machine learning model using the test dataset.

	Kappa			Accuracy			False positive			False negative		
	A	B	C	A	B	C	A	B	C	A	B	C
Logistic regression	0.433	0.415	0.400	0.745	0.736	0.718	0.304	0.324	0.381	0.234	0.237	0.221
Support vector machine	0.487	0.572	0.347	0.766	0.802	0.706	0.301	0.204	0.259	0.432	0.323	0.373
Decision tree without processing	0.404	0.388	0.268	0.727	0.718	0.654	0.352	0.369	0.466	0.233	0.237	0.269
Decision tree pre-pruning	0.404	0.471	0.476	0.727	0.745	0.745	0.37	0.362	0.368	0.188	0.175	0.164
Decision tree post-pruning	0.449	0.388	0.268	0.681	0.718	0.654	0.429	0.369	0.466	0.25	0.237	0.269
Naïve Bayes	0.466	0.423	0.414	0.745	0.718	0.690	0.356	0.4	0.448	0.185	0.184	0.094
Random Forest	0.611	0.650	0.661	0.818	0.836	0.845	0.244	0.22	0.167	0.25	0.131	0.149

A = model using backward selected variables; B = model using expertise selected variables; C = model using all gait variables.

Although dataset C had the best performance, dataset B was chosen for having a high accuracy with a low number of variables, which facilitates the data acquisition and processing.

The clinician accuracy for the diagnosis of Parkinson's disease varies upon studies, however a systematic review showed that clinical diagnosis for PD in non-experts is 73.8% (67.8%–79.6%); for a movement disorder expert at first consult is 79.6% (46%–95.1%) and 83.9% at follow-up (69.7%–92.6%). Also, the accuracy for the UK Parkinson's Disease Society Brain Bank diagnostic criteria is 82.7% (62.6%–93%; Rizzo et al., 2016) with a high sensibility (90%) but a low specificity (30%–40%; Marsili et al., 2018). With an accuracy of 83.3%, the selected random forest machine learning algorithm is not far from the clinical reality in the ideal settings. These selected variables are closely related to the PD diagnostic criteria because they represent surrogate measures of the slowness of movement (bradykinesia), asymmetry of arm swing, and rigidity.

The Gait Is Intricate: The Causal Inference Estimator

Although much is known about the gait pattern, asymmetry of arm swing (ASA) is a clinical characteristic that has been widely used in the last decade to describe the affected motor central pattern in PD patients (Lewek et al., 2010; Huang et al., 2012; Roggendorf et al., 2012; Mirelman et al., 2016). According to

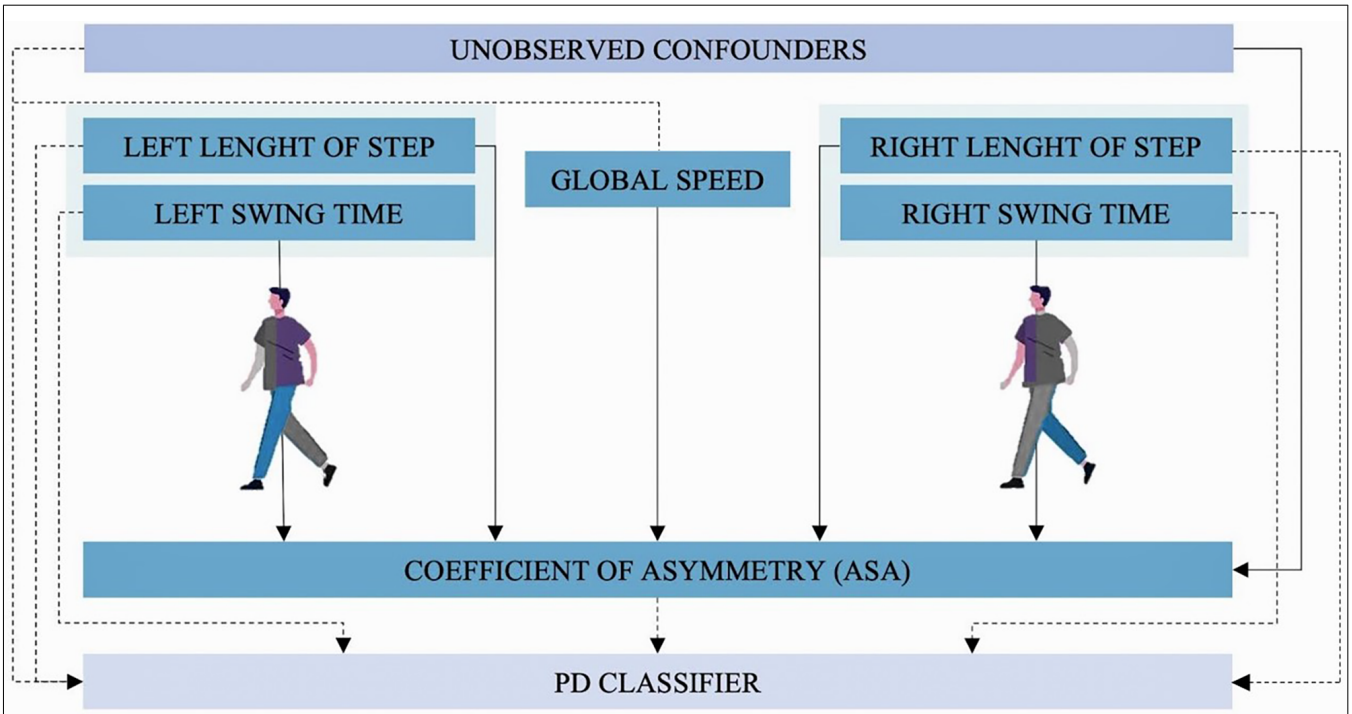

FIGURE 4 | Causal inference model. Dashed arrows show the causal relation identified by the model between leg and arms gait variables with the diagnosis of PD (PD-Classifier). Continued lines show the causal relations identified by the model between arms and legs gait variables.

TABLE 5 | Causal inference model estimators and refuters.

	Estimator	Refuter		
		Random common	Placebo treatment	Data subset
Left arm swing magnitude	−1.403	−1.397	0.011	1.415
Right arm swing magnitude	−1.791	−1.732	0.045	−1.812
Arm swing asymmetry	1.537	1.521	0.005	1.531
Global Gait speed	−0.637	−0.638	−0.021	−0.638
Left foot swing time	−0.109	−0.103	−0.008	−0.110
Left foot step length	−0.464	−0.464	0.010	−0.464
Right foot swing time	−0.120	−0.124	−0.003	−0.111
Right foot step length	−0.386	−0.390	−0.015	−0.389

our causal inference estimator, there is a relation between leg variables and the symmetry of the arms which represents a new opportunity in the research of these dynamics, particularly in pathological conditions such as PD.

Finding Differences Between PD Patients and Controls

As seen in the causal inference estimator, there are some unobserved confounders and other variables that could explain some of the changes secondary to PD, as seen in other neurodegenerative diseases, its complexity, and inter-patient variability difficulties to obtain higher accuracy levels. The challenge of new methods of signal processing and machine learning in clinical research is helping clinicians to achieve clinically meaningful technology-based objective measures (TOMs; Espay et al., 2016).

Related Work

Prior works were made using RBG-D cameras to classify PD patients, the variables selected included stride length, age, gait speed, stance time, step length, distance, cycle time, and swing time. The model that had the best accuracy (82%) was Random Forest. This includes a larger number of variables and not all of them are related to the clinical reality, also no further analysis was made (Urcuqui et al., 2018).

As reported in the literature other studies used RBG-D cameras to classify PD patients, but they used other methods. One of them used neural networks and cross-validation using the variables of gait velocity and stride length with an accuracy of 97.2% (Ťupa et al., 2015) or another classification method (the Bayesian), with a maximum accuracy of 94.1% using the stride length and age (Procházka et al., 2015). Differences could be also due to different preprocessing, filtering and exploration of the data. However,

other models reported in the literature used only variables from legs.

Other studies used foot pressure sensors and selected the variables of stride time, stance time, swing time, and foot strike profile to classify the controls from the PD patients with an accuracy of 92.7% (Abdulhay et al., 2018). Similar accuracy (92.6%) was found with a normalized multiple regression and Random forest using stance time, stride length, time of total stance, and cadence with the same type of device (Wahid et al., 2015).

The arm swing analysis has been a point of interest in the study of PD. Previous studies confirm that the arms swing magnitude and speed are significantly reduced in the PD for both limbs (Jaggy Castaño-Pino et al., 2019). On the other hand, several studies have been made with wearable technology (Inertial movement unit (IMU), accelerometers). An arm swing asymmetry (ASA) can also be extracted with accelerometers, it is calculated with the root mean square (RMS) differences between arm movements. The ASA and RMS significantly differ in PD patients. This could be used in future studies (Rincón et al., 2020).

Advantages, Limitations, and Future Work

The Kinect® eMotion system is a portable RGB Camera that can be used in different scenarios (**Figure 1**) and does not require a specialized gait laboratory. For that reason, this technology can be used as a complement to telemedicine in places without specialized medicine to support the diagnosis and management of patients' PD. Our findings suggest that in the future it could be considered to employ these measures and algorithms to complement Parkinson's disease diagnosis as well as to adapt the algorithms to evaluate disease progression, clinical subtypes, follow-up, response to treatment and correlate with clinical rating scales such as MDS-UPDRS.

Some limitations of the study were the sample size which limited the training of the algorithms to create a more accurate and robust model and only one dataset was used for training the algorithms which could also limit the results. Also, no gait speed matching procedure was implemented, however, some spatio-temporal gait parameters are speed-dependent which may have led to overrepresenting some of the gait variables in the backward feature selection model. Furthermore, some machine learning algorithms described in previous studies for classification between PD and healthy controls were not implemented such as artificial neural networks (ANN) and K-nearest neighbor (K-NN). The first was implemented in the first stages of the study, however, their results were similar to simple statistical methods with no machine learning and no further analysis was performed. The latter is a different machine learning algorithm because it does not save information, it cannot be trained. These limitations will be considered in the development of future studies.

Further studies are needed to explore the use of RGB-D cameras and machine learning algorithms for follow-up and treatment response and more data is needed to improve the machine learning training which will allow to achieve higher accuracy.

CONCLUSIONS

This study shows how machine learning techniques based on objective measures using portable low-cost devices (Kinect® eMotion) are useful to classify patients with Parkinson's disease. This proposed method can be used to evaluate patients remotely and help clinicians make decisions regarding follow-up and treatment.

DATA AVAILABILITY STATEMENT

The data analyzed in this study is subject to the following licenses/restrictions: the raw data supporting the conclusions of this article can be made available by the authors on request, prior approval by the institutional ethics committee. Requests to access these datasets should be directed to beatriz.munoz@fvl.org.co.

ETHICS STATEMENT

The studies involving human participants were reviewed and approved by Comité de ética en investigación biomédica (CEIB), Fundación Valle Del Lili. The patients/participants provided their written informed consent to participate in this study.

AUTHOR CONTRIBUTIONS

JO, AN-C, BM-O, and CU participated in the design of the study, interpretation and revision of data. JV-C organized the database. MG-P, CH, and CU contributed with data processing, statistical analysis, machine learning data processing, and interpretation of the work. JV-C, HC-M, and DA-G participated with data analysis and its interpretation as well as the writing of the first draft of the manuscript. AN-C and BM-O wrote sections of the manuscript. All authors contributed to the article and approved the submitted version.

FUNDING

This study was financed by Minciencias Grant #38-2021.

ACKNOWLEDGMENTS

This work was possible thanks to support from Universidad Icesi, Minciencias, and Fundación Valle del Lili.

SUPPLEMENTARY MATERIAL

The Supplementary Material for this article can be found online at: https://www.frontiersin.org/articles/10.3389/fnhum.2022.826376/full#supplementary-material.

REFERENCES

Abdulhay, E., Arunkumar, N., Narasimhan, K., Vellaiappan, E., and Venkatraman, V. (2018). Gait and tremor investigation using machine learning techniques for the diagnosis of Parkinson disease. *Future Gener. Comput. Syst.* 83, 366–373. doi: 10.1016/j.future.2018.02.009

Alzubaidi, M. S., Shah, U., Dhia Zubaydi, H., Dolaat, K., Abd-Alrazaq, A. A., Ahmed, A., et al. (2021). The role of neural network for the detection of Parkinson's disease: a scoping review. *Healthcare (Basel)* 9:740. doi: 10.3390/healthcare9060740

Buongiorno, D., Bortone, I., Cascarano, G. D., Trotta, G. F., Brunetti, A., and Bevilacqua, V. (2019). A low-cost vision system based on the analysis of motor features for recognition and severity rating of Parkinson's disease. *BMC Med. Inform. Decis. Mak.* 19:243. doi: 10.1186/s12911-019-0987-5

Caramia, C., Torricelli, D., Schmid, M., Munoz-Gonzalez, A., Gonzalez-Vargas, J., Grandas, F., et al. (2018). IMU-based classification of Parkinson's disease from gait: a sensitivity analysis on sensor location and feature selection. *IEEE J. Biomed. Health Inform.* 22, 1765–1774. doi: 10.1109/JBHI.2018.2865218

de Lau, L. M., and Breteler, M. M. (2006). Epidemiology of Parkinson's disease. *Lancet Neurol.* 5, 525–535. doi: 10.1016/S1474-4422(06)70471-9

Deb, R., Bhat, G., An, S., Shill, H., and Ogras, U. Y. (2021). Trends in technology usage for Parkinson's disease assessment: a systematic review. *medRxiv* [Preprint]. doi: 10.1101/2021.02.01.21250939

Dorsey, E. R., and Bloem, B. R. (2018). The Parkinson pandemic—a call to action. *JAMA Neurol.* 75, 9–10. doi: 10.1001/jamaneurol.2017.3299

Espay, A. J., Bonato, P., Nahab, F. B., Maetzler, W., Dean, J. M., Klucken, J., et al. (2016). Technology in Parkinson's disease: challenges and opportunities: technology in PD. *Mov. Disord.* 31, 1272–1282. doi: 10.1002/mds.26642

Goetz, C. G., Tilley, B. C., Shaftman, S. R., Stebbins, G. T., Fahn, S., Martinez-Martin, P., et al. (2008). Movement disorder society-sponsored revision of the unified Parkinson's disease rating scale (MDS-UPDRS): scale presentation and clinimetric testing results: MDS-UPDRS: clinimetric assessment. *Mov. Disord.* 23, 2129–2170. doi: 10.1002/mds.22340

Huang, X., Mahoney, J. M., Lewis, M. M., Guangwei, D. U., Piazza, S. J., and Cusumano, J. P. (2012). Both coordination and symmetry of arm swing are reduced in Parkinson's disease. *Gait Posture* 35, 373–377. doi: 10.1016/j.gaitpost.2011.10.180

Jaggy Castaño-Pino, Y., Navarro, A., Muñoz, B., and Luis Orozco, J. (2019). "Using wavelets for gait and arm swing analysis," in *Wavelet Transform and Complexity*, ed D. Baleanu (London: IntechOpen), 1–16. doi: 10.5772/intechopen.84962

Lewek, M. D., Poole, R., Johnson, J., Halawa, O., and Huang, X. (2010). Arm swing magnitude and asymmetry during gait in the early stages of Parkinson's disease. *Gait Posture* 31, 256–260. doi: 10.1016/j.gaitpost.2009.10.013

Marsili, L., Rizzo, G., and Colosimo, C. (2018). Diagnostic criteria for Parkinson's disease: from james parkinson to the concept of prodromal disease. *Front. Neurol.* 9:156. doi: 10.3389/fneur.2018.00156

Mirelman, A., Bernad-Elazari, H., Thaler, A., Giladi-Yacobi, E., Gurevich, T., Gana-Weisz, M., et al. (2016). Arm swing as a potential new prodromal marker of Parkinson's disease: arm swing as a new prodromal marker of PD. *Mov. Disord.* 31, 1527–1534. doi: 10.1002/mds.26720

Monje, M. H. G., Sánchez-Ferro, Á., Pineda-Pardo, J. A., Vela-Desojo, L., Alonso-Frech, F., and Obeso, J. A. (2021). Motor onset topography and progression in Parkinson's disease: the upper limb is first. *Mov. Disord.* 36, 905–915. doi: 10.1002/mds.28462

Muñoz Ospina, B., Valderrama Chaparro, J. A., Arango Paredes, J. D., Castaño Pino, Y. J., Navarro, A., and Orozco, J. L. (2019). Age matters: objective gait assessment in early Parkinson's disease using an RGB-D camera. *Parkinsons Dis.* 2019:5050182. doi: 10.1155/2019/5050182

Ospina, B. M., Chaparro, J. A. V., Paredes, J. D. A., Pino, Y. J. C., Navarro, A., and Orozco, J. L. (2018). Objective arm swing analysis in early-stage Parkinson's disease using an RGB-D camera (Kinect®). *J. Parkinsons Dis.* 8, 563–570. doi: 10.3233/JPD-181401

Ozkan, H. (2016). A comparison of classification methods for telediagnosis of Parkinson's disease. *Entropy* 18:115. doi: 10.3390/e18040115

Pearl, J. (1995). Causal diagrams for empirical research. *Biometrika* 82, 669–688. doi: 10.2307/2337329

Postuma, R. B., Berg, D., Stern, M., Poewe, W., Olanow, C. W., Oertel, W., et al. (2015). MDS clinical diagnostic criteria for Parkinson's disease: MDS-PD clinical diagnostic criteria. *Mov. Disord.* 30, 1591–1601. doi: 10.1002/mds.26424

Procházka, A., Vyšata, O., Vališ, M., Ťupa, O., Schätz, M., and Mařík, V. (2015). Bayesian classification and analysis of gait disorders using image and depth sensors of Microsoft Kinect. *Digit. Signal Process.* 47, 169–177. doi: 10.1016/j.dsp.2015.05.011

Reyes, J. F., Steven Montealegre, J., Castano, Y. J., Urcuqui, C., and Navarro, A. (2019). "LSTM and convolution networks exploration for Parkinson's diagnosis," in *2019 IEEE Colombian Conference on Communications and Computing (COLCOM)* (Barranquilla, Colombia: IEEE), 1–4. doi: 10.1109/ColComCon.2019.8809160

Rincón, D., Valderrama, J., González, M. C., Muñoz, B., Orozco, J., Montilla, L., et al. (2020). Wristbands containing accelerometers for objective arm swing analysis in patients with Parkinson's disease. *Sensors (Basel)* 20:4339. doi: 10.3390/s20154339

Rizzo, G., Copetti, M., Arcuti, S., Martino, D., Fontana, A., and Logroscino, G. (2016). Accuracy of clinical diagnosis of Parkinson disease: a systematic review and meta-analysis. *Neurology* 86, 566–576. doi: 10.1212/WNL.0000000000002350

Roggendorf, J., Chen, S., Baudrexel, S., van de Loo, S., Seifried, C., and Hilker, R. (2012). Arm swing asymmetry in Parkinson's disease measured with ultrasound based motion analysis during treadmill gait. *Gait Posture* 35, 116–120. doi: 10.1016/j.gaitpost.2011.08.020

Schneider, S. A., and Obeso, J. A. (2014). "Clinical and pathological features of Parkinson's disease," in *Behavioral Neurobiology of Huntington's Disease and Parkinson's Disease*, Vol. 22, eds H. H. P. Nguyen, and M. A. Cenci (Berlin, Heidelberg: Springer Berlin Heidelberg), 205–220. doi: 10.1007/7854_2014_317

Shalash, A., Spindler, M., and Cubo, E. (2021). Global perspective on telemedicine for Parkinson's disease. *J. Parkinsons Dis.* 11, S11–S18. doi: 10.3233/JPD-202411

Sharma, A., and Kiciman, E. (2020). DoWhy: an end-to-end library for causal inference. *ArXiv* [Preprint]. doi: 10.48550/arXiv.2011.04216

Sherly Puspha Annabel, L., Sreenidhi, S., and Vishali, N. (2021). "A novel diagnosis system for Parkinson's disease using K-means clustering and decision tree," in *Communication and Intelligent Systems*, Vol. 204, eds H. Sharma, M. K. Gupta, G. S. Tomar, and W. Lipo (Singapore: Springer Singapore), 607–615. doi: 10.1007/978-981-16-1089-9_48

Sidey-Gibbons, J. A. M., and Sidey-Gibbons, C. J. (2019). Machine learning in medicine: a practical introduction. *BMC Med. Res. Methodol.* 19:64. doi: 10.1186/s12874-019-0681-4

Singh, G., and Samavedham, L. (2015). Unsupervised learning based feature extraction for differential diagnosis of neurodegenerative diseases: a case study on early-stage diagnosis of Parkinson disease. *J. Neurosci. Methods* 256, 30–40. doi: 10.1016/j.jneumeth.2015.08.011

Ťupa, O., Procházka, A., Vyšata, O., Schätz, M., Mareš, J., Vališ, M., et al. (2015). Motion tracking and gait feature estimation for recognising Parkinson's disease using MS Kinect. *Biomed. Eng. Online* 14:97. doi: 10.1186/s12938-015-0092-7

Tysnes, O.-B., and Storstein, A. (2017). Epidemiology of Parkinson's disease. *J. Neural Transm. (Vienna)* 124, 901–905. doi: 10.1007/s00702-017-1686-y

Urcuqui, C., Castano, Y., Delgado, J., Navarro, A., Diaz, J., Munoz, B., et al. (2018). "Exploring machine learning to analyze Parkinson's disease patients," in *2018 14th International Conference on Semantics, Knowledge and Grids (SKG)*, (Guangzhou, China: IEEE), 160–166. doi: 10.1109/SKG.2018.00029

Varrecchia, T., Castiglia, S. F., Ranavolo, A., Conte, C., Tatarelli, A., Coppola, G., et al. (2021). An artificial neural network approach to detect presence and severity of Parkinson's disease via gait parameters. *PLoS One* 16:e0244396. doi: 10.1371/journal.pone.0244396

Wahid, F., Begg, R. K., Hass, C. J., Halgamuge, S., and Ackland, D. C. (2015). Classification of Parkinson's disease gait using spatial-temporal gait features. *IEEE J. Biomed. Health Inform.* 19, 1794–1802. doi: 10.1109/JBHI.2015.2450232

Walesiak, M., and Dudek, A. (2020). "The choice of variable normalization method in cluster analysis," in *Education Excellence and Innovation Management: A 2025 Vision to Sustain Economic Development During Global Challenges* (Sevilla: International Business Information Management Association (IBIMA)), 325–340. Available online at: https://rdrr.io/cran/clusterSim/man/data.Normalization.html#heading-5.

Yoneyama, M., Kurihara, Y., Watanabe, K., and Mitoma, H. (2013). Accelerometry-based gait analysis and its application to Parkinson's disease assessment—part 2: a new measure for quantifying walking behavior. *IEEE Trans. Neural Syst. Rehabil. Eng.* 21, 999–1005. doi: 10.1109/TNSRE.2013.2268251

Zhang, X., Wang, Y., Zhang, L., Jin, B., and Zhang, H. (2021). Exploring unsupervised multivariate time series representation learning for chronic disease diagnosis. *Int. J. Data Sci. Anal.* doi: 10.1007/s41060-021-00290-0

Zifchock, R. A., Davis, I., Higginson, J., and Royer, T. (2008). The symmetry angle: a novel, robust method of quantifying asymmetry. *Gait Posture* 27, 622–627. doi: 10.1016/j.gaitpost.2007.08.006

Conflict of Interest: The authors declare that the research was conducted in the absence of any commercial or financial relationships that could be construed as a potential conflict of interest.

frontiers | Frontiers in Human Neuroscience

ORIGINAL RESEARCH
published: 02 June 2022
doi: 10.3389/fnhum.2022.861136

Longitudinal Alterations in Gait Features in Growing Children With Duchenne Muscular Dystrophy

*Ines Vandekerckhove[1], Marleen Van den Hauwe[1,2], Nathalie De Beukelaer[1], Elze Stoop[1,3], Marije Goudriaan[4], Margaux Delporte[5], Geert Molenberghs[5,6], Anja Van Campenhout[3,7,8], Liesbeth De Waele[2,7], Nathalie Goemans[2,7], Friedl De Groote[9] and Kaat Desloovere[1,3]**

[1] Department of Rehabilitation Sciences, KU Leuven, Leuven, Belgium, [2] Department of Child Neurology, University Hospitals Leuven, Leuven, Belgium, [3] Clinical Motion Analysis Laboratory, University Hospitals Leuven, Leuven, Belgium, [4] Department of Human Movement Sciences, Vrije Universiteit Amsterdam, Amsterdam, Netherlands, [5] Interuniversity Institute for Biostatistics and Statistical Bioinformatics (I-BIOSTAT), KU Leuven, Leuven, Belgium, [6] Interuniversity Institute for Biostatistics and Statistical Bioinformatics (I-BIOSTAT), Data Science Institute, Hasselt University, Hasselt, Belgium, [7] Department of Development and Regeneration, KU Leuven, Leuven, Belgium, [8] Department of Orthopedics, University Hospitals Leuven, Leuven, Belgium, [9] Department of Movement Sciences, KU Leuven, Leuven, Belgium

OPEN ACCESS

Edited by:
Simone Carozzo, Sant'Anna Crotone Institute, Italy

Reviewed by:
Paul Horn, Cincinnati Children's Hospital Medical Center, United States
Andrew Geronimo, Penn State Milton S. Hershey Medical Center, United States

***Correspondence:**
Kaat Desloovere
kaat.desloovere@kuleuven.be

Specialty section:
This article was submitted to Motor Neuroscience, a section of the journal Frontiers in Human Neuroscience

Received: *24 January 2022*
Accepted: *12 April 2022*
Published: *02 June 2022*

Citation:
Vandekerckhove I, Van den Hauwe M, De Beukelaer N, Stoop E, Goudriaan M, Delporte M, Molenberghs G, Van Campenhout A, De Waele L, Goemans N, De Groote F and Desloovere K (2022) Longitudinal Alterations in Gait Features in Growing Children With Duchenne Muscular Dystrophy. Front. Hum. Neurosci. 16:861136. doi: 10.3389/fnhum.2022.861136

Prolonging ambulation is an important treatment goal in children with Duchenne muscular dystrophy (DMD). Three-dimensional gait analysis (3DGA) could provide sensitive parameters to study the efficacy of clinical trials aiming to preserve ambulation. However, quantitative descriptions of the natural history of gait features in DMD are first required. The overall goal was to provide a full delineation of the progressive gait pathology in children with DMD, covering the entire period of ambulation, by performing a so-called mixed cross-sectional longitudinal study. Firstly, to make our results comparable with previous literature, we aimed to cross-sectionally compare 31 predefined gait features between children with DMD and a typically developing (TD) database (1). Secondly, we aimed to explore the longitudinal changes in the 31 predefined gait features in growing boys with DMD using follow-up 3DGA sessions (2). 3DGA-sessions (n = 124) at self-selected speed were collected in 27 boys with DMD (baseline age: 4.6–15 years). They were repeatedly measured over a varying follow-up period (range: 6 months–5 years). The TD group consisted of 27 children (age: 5.4–15.6 years). Per measurement session, the spatiotemporal parameters, and the kinematic and kinetic waveforms were averaged over the selected gait cycles. From the averaged waveforms, discrete gait features (e.g., maxima and minima) were extracted. Mann-Whitney U tests were performed to cross-sectionally analyze the differences between DMD at baseline and TD (1). Linear mixed effect models were performed to assess the changes in gait features in the same group of children with DMD from both a longitudinal (i.e., increasing time) as well as a cross-sectional perspective (i.e., increasing baseline age) (2). At baseline, the boys with DMD differed from the TD children in 17 gait features. Additionally, 21 gait features evolved longitudinally when following-up the same boys with DMD and 25 gait features presented a significant cross-sectional baseline age-effect. The current study quantitatively described the longitudinal alterations in

gait features in boys with DMD, thereby providing detailed insight into how DMD gait deteriorates. Additionally, our results highlight that gait features extracted from 3DGA are promising outcome measures for future clinical trials to quantify the efficacy of novel therapeutic strategies.

Keywords: Duchenne muscular dystrophy, typically developing children, three-dimensional gait analysis, gait pattern, longitudinal study, mixed models for repeated measures

INTRODUCTION

Duchenne muscular dystrophy (DMD) is an X-linked degenerative muscular disorder and is the most common muscular dystrophy in children, affecting one in 3,500–6,000 new-born boys (Sutherland et al., 1981; Emery and Eh, 1991; Sussman, 2002). DMD is caused by mutations in the gene encoding dystrophin (Sussman, 2002). Subsequently, the dystrophin protein, which is important for ensuring the stability of the muscle cell membrane and protecting the muscles from contraction-induced damage (Petrof et al., 1993; Moens et al., 1994; Lindsay et al., 2020), is deficient. Therefore, the muscles progressively degenerate as children with DMD get older (Sussman, 2002). This degeneration is characterized by progressive loss of contractile tissue, which is replaced by fat and fibrotic tissue (Sussman, 2002; Jones et al., 2010). The primary clinical symptom due to muscle damage is progressive muscle weakness (Sussman, 2002). Secondary symptoms include increasing muscle stiffness (i.e., increased resistance to muscle lengthening) and contractures (i.e., reduced range of motion) (Sussman, 2002; Bushby et al., 2010; Skalsky and McDonald, 2012). These muscle impairments contribute to a decline in motor function, such as rising from the floor and climbing stairs, eventually resulting in loss of ambulation (Sutherland et al., 1981; Sussman, 2002). To date, no curative treatment for DMD is available (Sussman, 2002). If untreated, these children become wheelchair-bound around the age of nine years and die at a mean age of 19 years due to cardiac or pulmonary failure (Bushby et al., 2005, 2010). However, multidisciplinary symptomatic medical, surgical, and rehabilitative treatment, including long-term use of corticosteroids, and ventilatory support, have altered the natural disease course and have increased life expectancy until approximately the age of 30 years (Bushby et al., 2010).

Even with the current state-of-the-art medical care, children with DMD lose ambulation at a mean age of 12 years (Ryder et al., 2017). Promising novel therapeutic strategies might alter the natural history of the disease such that the most affected children remain ambulant until 12 years of age (Yiu and Kornberg, 2015) and some children even remain ambulant over 15 years of age (Goemans et al., 2017). However, it has been difficult to transfer these new therapeutic interventions from clinical trials into clinical practice, as it has been very challenging to prove the efficacy of novel drugs in DMD (Goemans, 2013). Clinical trials often use the 6-min walk test (6MWT), the North Star Ambulatory Assessment (NSAA) and timed tests as evaluation tools (Mazzone et al., 2010; Goemans, 2013; Goudriaan et al., 2018a). These assessments reflect clinically meaningful aspects of daily life and have been proven reliable, valid, and feasible (Kierkegaard and Tollbäck, 2007; Frosini et al., 2009; McDonald et al., 2010). Therefore, clinicians have accepted these tools as standard clinical assessments to track the long-term progression of the disease and to predict loss of ambulation in children with DMD (McDonald et al., 1995; Mazzone et al., 2010). However, the 6MWT, the NSAA, and the timed tests measure global gross motor function and might not be sensitive enough to detect significant changes in the gait pattern of individuals with DMD. This might especially be true in the early disease stages, where compensation strategies are still successful (Kirschner et al., 2010; Lu et al., 2014; Lynn et al., 2015). Hence, there is an urgent need for sensitive, suitable, and clinically meaningful outcome measures to prove the successes of emergent therapeutic strategies (Goemans, 2013).

Three-dimensional gait analysis (3DGA) is proposed as an alternative evaluation method that can be used in clinical trials (Romano et al., 2019; Wren et al., 2020). It allows for a detailed analysis of gait pathology, including altered joint kinematics, kinetics and muscle activity patterns. The assessment of these parameters might be beneficial when evaluating the efficacy of novel therapeutic strategies (Heberer et al., 2016). While 3DGA is part of the standard clinical care in children with cerebral palsy (Bregou Bourgeois et al., 2014; Shin et al., 2016), this method is not implemented in the clinical follow-up of children with DMD (Bushby et al., 2010). Even though several gait features measured with 3DGA correlated strongly with clinical assessments, the correlation coefficients (ρ) ranged substantially, from -0.032 (range of ankle dorsiflexion/plantar flexion motion) to 0.858 (maximal dorsiflexion angle during swing) for the NSAA and from -0.022 (range of hip flexion/extension motion) to 0.850 (hip adduction/abduction mean angle) for the 6MWT (Romano et al., 2019). This stresses the added value of 3DGA to monitor the functional ability in children with DMD (Romano et al., 2019). Furthermore, previous studies indicated that 3DGA could provide detailed insight into disease progression and treatment response in children with DMD that may otherwise go undetected when only global function is studied (D'Angelo et al., 2009; Heberer et al., 2016). Lastly, to maintain a certain level of functionality and to postpone spinal deformities and muscle contractures, prolonging the ambulation is considered the most important treatment goal in children with DMD (Sussman, 2002). Measuring the progressive alterations in the gait pattern of boys with DMD in detail by means of 3DGA could provide sensitive outcome measures to evaluate the efficacy of novel therapeutic strategies (Heberer et al., 2016).

However, before 3DGA can be used as an assessment method in clinical trials, a full delineation of the progressive gait pathology in children with DMD is required.

Goudriaan et al. (2018a) summarized previous studies that applied 3DGA to objectively quantify gait deviations in children with DMD (Goudriaan et al., 2018a). Due to insufficient description of the study population and measurement devices, small sample sizes, and wide age ranges contributing to heterogeneous groups, generalization of the findings is challenging. From the 79 gait parameters reported in literature, the studies only agreed on an increase in knee range of motion (D'Angelo et al., 2009; Doglio et al., 2011), a decrease in walking speed, stride length, step length, dorsiflexion angle in swing (Sutherland et al., 1981; D'Angelo et al., 2009; Gaudreault et al., 2010; Doglio et al., 2011), maximal knee extension moment (Khodadadeh et al., 1986; Gaudreault et al., 2010; Doglio et al., 2011), maximal dorsiflexion moment (Gaudreault et al., 2007, 2010; Doglio et al., 2011), maximal hip power generation (D'Angelo et al., 2009; Gaudreault et al., 2010), and maximal ankle power generation (D'Angelo et al., 2009; Gaudreault et al., 2010; Doglio et al., 2011) in the children with DMD when compared to typically developing (TD) children. Furthermore, even though DMD is a progressive disorder (Sussman, 2002), mostly cross-sectional studies including participants with a wide age range have been performed to investigate the differences in gait features between DMD and TD. While these studies give insight into the characteristics of DMD gait, they do not provide the complete picture of how their gait pattern deteriorates over time nor which gait features might be predictive for the loss of ambulation.

Sutherland et al. (1981) were one of the few to describe the progression of the gait pathology in children with DMD by introducing three stages, namely the early, transitional and late stage (Sutherland et al., 1981). A subtle effect of disease progression (e.g., muscle weakness) was already apparent in the early stage. This included slight backward leaning of the trunk with lumbar lordosis to compensate for weak hip extensors, and posterior tilt of the pelvis in combination with hip hyperextension. During swing, increased hip flexion probably compensated for the drop foot. Consequently, a flat foot strike at initial contact was seen in the young boys with DMD. Furthermore, an increased external foot progression was measured throughout the entire gait cycle. In the transitional stage, the early posterior tilt changed toward increased pelvic anterior tilt in combination with increased hip flexion, which represented the most remarkable characteristic. Sutherland et al. (1981) indicated this as a compensation mechanism for increased weakness in the knee extensors. Furthermore, boys with DMD walked with increased base of support, shoulder sway and lateral trunk leaning to compensate for weak hip abductors. In addition to the drop foot in swing, children in the transitional stage showed characteristics of equinus gait, namely forefoot strike at initial contact and reduced dorsiflexion in stance. Furthermore, a transition from external to internal foot progression occurred. Due to the progressive muscle weakness, the aforementioned compensation mechanisms became more pronounced in the late stage and therefore, the gait features in boys deviated even more from TD children (Sienko Thomas et al., 2010). The equinus gait at this late stage was also more evident, as the ankle joint was constantly in plantar flexion throughout the gait cycle (Sutherland et al., 1981). However, the classification of Sutherland et al. (1981) was introduced approximately 40 years ago (Sutherland et al., 1981). Meanwhile, the state-of-the-art medical care has altered the natural history of DMD, resulting in a longer ambulation period for boys with DMD (Sussman, 2002; Bushby et al., 2010). A later study from 2010 (Sienko Thomas et al., 2010), which classified the gait pattern in children with DMD based on the gait deviation index, could only partially confirm the stages of Sutherland et al. (1981). While these differences could to some extent be the result of different analysis methods, they emphasize a strong need for updated longitudinal 3DGA assessments in the same cohort of children with DMD.

The overall goal was to provide a full delineation of the progressive gait pathology in children with DMD, covering the entire period of ambulation, by performing a so-called mixed cross-sectional longitudinal study. To make our results comparable with previous literature, our first aim was to cross-sectionally compare 31 predefined gait features that were defined based on previous literature (Sutherland et al., 1981; Sienko Thomas et al., 2010; Goudriaan et al., 2018a) and case discussions in a clinical specialist team, between children with DMD and a TD database. We hypothesized that the gait features would be significantly different between the two groups, specifically when looking at the pelvis. The second aim was to explore the longitudinal changes in the 31 predefined gait features in growing boys with DMD using follow-up 3DGA sessions. We hypothesized that the gait features would change significantly over time as children with DMD grow older and the disease progresses.

MATERIALS AND METHODS

Participants

Thirty children with DMD were recruited at the multidisciplinary clinic of the Neuro-Muscular Reference Centre (NMRC) in the University Hospitals Leuven. The following inclusion criteria were used: (1) diagnosed with DMD *via* immunohistochemistry, muscle biopsy and/or mutation of the dystrophin gene; (2) between three and 16 years old, (3) able to walk independently for at least 100 meters. Chronic treatment with corticosteroids and participation in clinical trials were permitted. Exclusion criteria were: cognitive and behavioral disorders preventing accurate measurements (1), history of lower limb surgery (2), clinical picture of Becker muscular dystrophy and genetic diagnosis predicting a milder phenotype, such as in-frame deletions (3). Twenty-seven TD boys of a similar age as the children with DMD, and without the presence of any neurological or neuromuscular disorder, were selected out of the reference database from the Clinical Motion Analysis Laboratory of the University Hospitals Leuven (Pellenberg).

All children were measured at the Clinical Motion Analysis Laboratory. This study was approved by the local ethics committee (Ethical Committee UZ Leuven/KU Leuven; S55867, S56041, and S61324) under the Declaration of Helsinki. Participants' parents or caretakers signed a written informed

consent after agreeing to participate in the study. Children of 12 years or older also signed an assent.

Study Design

We performed a so-called mixed cross-sectional longitudinal study, with a cross-sectional component (children measured only once) and a longitudinal component (children with repeated measures over time) (**Figure 1**). The children with DMD enrolled in the study at different ages (range: 4.6–15 years) and were repeatedly measured over variable time intervals, establishing a longitudinal database. 3DGA's were collected at multiple time points, with a frequency of two to nine times at a variable time interval of 5–35 months, covering a varying follow-up period ranging from 6 months to 5 years (average follow-up period: 2.5 years) in the boys with DMD. This resulted in an unbalanced dataset of 124 3DGA-sessions. The TD children (n = 27) were only measured at one time point, resulting in a cross-sectional database consisting of 27 3DGA sessions.

To achieve the first aim, we used a cross-sectional comparison to assess the differences in 31 predefined gait features between the children with DMD at the time of baseline assessment and the TD children (**Figure 2A**). To achieve the second aim, the changes in 31 predefined gait features in the same group of children with DMD were assessed from both a longitudinal as well as a cross-sectional perspective (**Figure 2B**). The time course of the measurements (time) represented the longitudinal effect. The effect of increasing age at the time of the first measurement (baseline age), represented the cross-sectional effect. This design was chosen, since the boys with DMD enrolled in the study at different ages resulting in the mixed longitudinal dataset.

Data Collection

The 3DGA's were conducted in barefoot condition, at self-selected walking speed on a 10-m walkway. Reflective markers with a diameter of 14 mm were attached to the skin according to the Plug-In Gait Full-Body model and a 10-15 Vicon camera system (Vicon-UK, Oxford, United Kingdom) sampled at 100 Hz recorded the marker trajectories. These trajectories were filtered with a built-in Woltring filter (mode: MSE; smoothing: 15 mm^2). Two force plates (AMTI, Watertown, MA, United States) embedded in the walkway registered ground reaction forces at 1,500 Hz to calculate internal joint moments. Gait cycles were defined through manually indicating the gait events, with the support of force plate data if available, i.e., initial contacts and toe offs, in the Nexus software (Nexus 2.10. Vicon-UK, Oxford, United Kingdom). Subsequently, pelvis kinematic and lower limb joint kinematic and kinetic waveforms were estimated. For both sides, ten gait cycles with kinematic data, of which three to five gait cycles with kinetic data, were collected.

Data Analysis

The quality of the collected gait cycles was checked with a custom-made software in MATLAB (The Mathworks Inc., Natick, M.A., 2016). Kinematic and kinetic waveforms were resampled to 101 data points per gait cycle. Kinematic waveforms were expressed in degrees. Kinetic waveforms were normalized to bodyweight and therefore, internal joint moments were expressed in Newton meters per kilogram bodyweight (Nm/kg), and power waveforms in Watt per kilogram bodyweight (W/kg). Per measurement session, the spatiotemporal parameters, and the kinematic and kinetic waveforms were averaged over the selected gait cycles with good quality for each side. Four spatiotemporal parameters were included: cadence (steps/s), walking velocity (WV), step length (SL), and step width (SW). Using the equations (Eq.) of Hof (Hof, 1996), WV, SL and SW were converted into non-dimensional quantities. WV was normalized to leg length and gravitational acceleration (Eq. 1). SL and SW were normalized to leg length (Eq. 2 and 3). Equations:

$$WV_{norm} = \frac{WV}{\sqrt{l * g}} \quad (1)$$

$$SL_{norm} = \frac{SL}{l} \quad (2)$$

$$SW_{norm} = \frac{SW}{l} \quad (3)$$

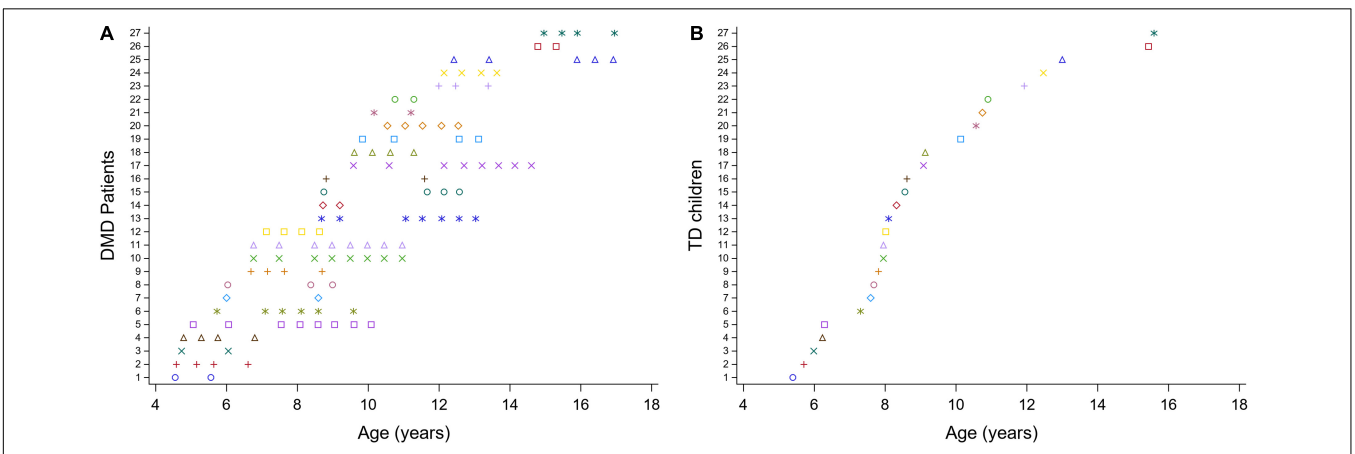

FIGURE 1 | Mixed cross-sectional longitudinal dataset. Overview of the ages at the included measurements for the children with DMD **(A)** and for the TD database **(B)**. Each color represents one patient. DMD, Duchenne muscular dystrophy; TD, typically developing.

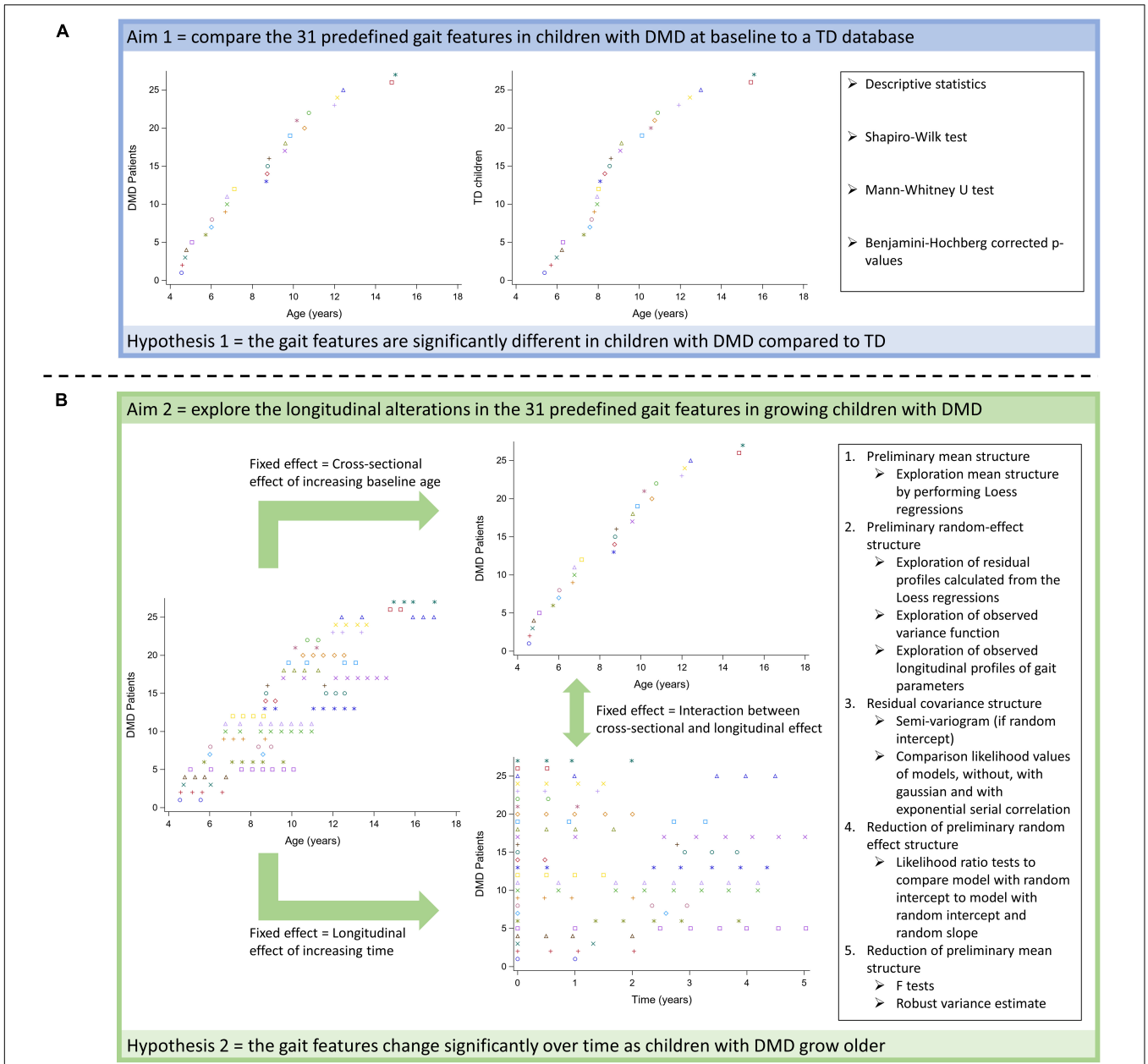

FIGURE 2 | Schematic overview of statistical analyses to achieve the first **(A)** and the second aim **(B)**.

with WV_{norm}, SL_{norm}, SW_{norm}, l, and g representing normalized walking velocity, normalized step length, normalized step width, leg length, and gravitational acceleration, respectively.

From the average continuous kinematic and kinetic waveforms, minima, maxima, range of motions, and values at specific events in the gait cycle were calculated using the previously mentioned custom-made software, to obtain 16 predefined kinematic and 10 kinetic parameters. The TD database from the Clinical Motion Analysis Laboratory (n = 86) served as a reference to calculate one additional kinematic parameter, i.e., the gait profile score (GPS), for the DMD and TD group (Baker et al., 2009). The GPS is an overall gait index representing the difference in kinematics between an individual subject and a control group. In total, the dataset contained 31 predefined gait features (i.e., 4 spatiotemporal, 17 kinematic, and 10 kinetic parameters), which were selected based on previous literature (Sutherland et al., 1981; Sienko Thomas et al., 2010; Goudriaan et al., 2018a) and clinical expertise.

Since children with DMD may present an asymmetric gait pattern, gait features of the right and the left side were not averaged. To avoid a complex dataset with the inclusion of both sides on each time point per patient, only the gait features of the weakest side for the children with DMD were used in

further analyses. This side was determined based on the strength outcomes of the clinical exam (manual muscle testing). For the TD children and in case no weakest side could be determined for the children with DMD, a random number generator was used to define the evaluated side.

Statistical Analysis

An overview of all statistical analyses per research aim is provided in **Figure 2**.

We used descriptive statistics to provide an overview of the studied gait features in both groups (DMD and TD) for the first aim (**Figure 2A**). Depending on the distribution of the data, means and standard deviations or medians and interquartile ranges were reported.

To verify our hypotheses related to the first aim, we first checked the normality of the data by inspecting the distribution plots and *via* the Shapiro-Wilk test. Since most of the parameters were not normally distributed, a Mann-Whitney *U* test was performed to investigate differences in subject characteristics and gait features between the children with DMD at baseline and the TD children. The *p*-values were corrected according to the stepwise Benjamini-Hochberg procedure with a false discovery rate of 5% to correct for the comparison of 36 parameters (Benjamini and Hochberg, 1995).

To investigate the longitudinal evolution of the pathological gait pattern in the children with DMD (second aim; **Figure 2B**), linear mixed effect models (LMM) were used. These methods were required to handle the unbalanced mixed longitudinal dataset, as the number of repeated measurements and the time interval between measurements varied among the children with DMD (Verbeke and Molenberghs, 2000). LMM take the correlation between repeated measurements into account by modeling the variance both between and within the patients. Therefore, fitting LMM requires specification of a mean structure and a covariance structure (Verbeke and Molenberghs, 1997, 2000). The mean structure consists of fixed effects, i.e., time effects, covariates, and interaction effects, while the covariance structure consists of random effects and serial correlation (Verbeke and Molenberghs, 2000). The time course of the measurements within the patients (time), which represented the longitudinal effect was selected as the time effect (Eq. 4). In case of a quadratic relationship between time and the gait feature, the higher-order term of time, i.e., time squared (time^2), was added in the LMM. Baseline age, which represented the cross-sectional effect of increasing age was selected as a covariate (Eq. 4). The higher-order terms of baseline age, i.e., baseline age squared (baseline age^2) and baseline age cubed (baseline age^3), were added in the LMM, when a quadratic and cubic relationship between baseline age and the gait feature were observed, respectively. In addition, the longitudinal effect may depend on the baseline age. Therefore, the interaction between time and baseline age (time × baseline age) was also included as a fixed effect in the LMM (Eq. 4). To model the variability among the boys with DMD, random effects consisting of a random intercept and a random slope for the time effect, were added (Eq. 4). A random intercept and slope account for the variability in starting point and progression rate between patients, respectively (Verbeke and Molenberghs, 2000). To model the variability within the participants, measurement error, and serial correlation were added in the LMM (Eq. 4). Serial correlation is needed when the error term is not fully described by the constant variance of the measurement error and there is still, after adding random effects, a certain correlation between serial measurements (Verbeke and Molenberghs, 2000). This correlation usually decreases in function of the time separation between the repeated measurements. Serial correlation represents the belief that part of an individual's observed profile is a response to time-varying stochastic processes operating within that patient. The gait features were defined as the responses.

$$\begin{aligned} Responses = {} & \beta_0+\beta_1\times Time+\beta_2\times Time^2+\beta_3\times Baseline\ age+\beta_4 \\ & \times Baseline\ age^2+\beta_5\times Baseline\ age^3+\beta_6\times Time \\ & \times Baseline\ age+b_{1i}+b_{2i}\times Time+\varepsilon_{(1)ij}+\varepsilon_{(2)ij} \end{aligned} \quad (4)$$

with β_0, β_1, β_2, β_3, β_4, β_5, β_6, b_{1i}, b_{2i}, $\varepsilon_{(1)ij}$, $\varepsilon_{(2)ij}$, representing intercept, regression coefficient for Time, regression coefficient for Time^2, regression coefficient for Baseline age, regression coefficient for Baseline age^2, regression coefficient for Baseline age^3, regression coefficient for the interaction between Time and Baseline age, random intercept, random slope for Time, measurement error, and serial correlation, respectively. Both time and baseline age were expressed in years. From baseline age the smallest value was subtracted. Therefore, the intercept represents the response's value at baseline age 4.6 and time zero.

We used the following workflow to construct the LMM (**Figure 2B**; Verbeke and Molenberghs, 1997, 2000). First, the average trend was explored by performing Loess regressions (point 1, **Figure 2B**). Based on visual inspection of the smoothed line resulting from the Loess regression, the higher-order terms of the fixed effects were selected to build a comprehensive preliminary mean structure (Verbeke and Molenberghs, 2000; Diggle et al., 2002). Second, the preliminary random-effect structure was defined based on the exploration of the residual profiles calculated from the Loess regressions and the observed variance function, i.e., the change of the squared residuals over time (point 2, **Figure 2B**). In addition, it was informally checked if the observed longitudinal profiles could be well-explained by a specific linear regression function with a SAS® macro (metagof.sas online available at https://ibiostat.be/online-resources) (Verbeke and Molenberghs, 1997). Based on the data exploration, a random-effect structure with solely a random intercept, i.e., assuming a constant variance, or a random intercept and slope, i.e., allowing the variance to change over time, was selected. Third, the residual covariance structure was selected (point 3, **Figure 2B**). The semi-variogram (Diggle, 1988) was used to explore the presence and the nature of serial correlation only when a random intercept was included. The random intercept captures child-specific characteristics, whereas serial correlation accounts for the fact that measurements closer to each other in time are typically more strongly correlated than measurements farther apart within the measurement sequence of a given child. The likelihood values of three models with the preliminary mean and random-effect structures, one without,

one with Gaussian, and one with exponential serial correlation were compared to define the residual covariance structure. Precisely, they are based on so-called restricted maximum likelihood, a modification of classical maximum likelihood to alleviate small-sample biases. Fourth, it was checked if the number of random effects in the preliminary random-effects structure could be reduced by performing the likelihood ratio test to compare a model with a random intercept vs. a model with a random intercept and slope (point 4, **Figure 2B**). For technical reasons, i.e., because the variance components need to form a positive-definite matrix, these likelihood ratios follow a mixture of χ^2 distributions ($\chi^2_{1:2}$) needed to be used to detect significance in the results. Fifth, the reduction of the number of fixed effects was checked by performing F tests (point 5, **Figure 2B**). To correct for possible misspecification of the covariance matrix, the robust variance estimate, also called sandwich estimate, was calculated. This way, robust inference of the F test could be obtained. Due to the explorative nature of the second aim, the *p*-values were not corrected for multiple comparisons.

After formulating the LMM, so-called empirical Bayes estimates were calculated and used to detect outliers, i.e., patients with an "exceptional" starting point and evolution over time. The data of the outliers were checked. If data were removed, the previous five steps were repeated to define the final LMM.

All statistical analyses were performed using SAS®, version 9.4 (Statistical Analysis Software 9.4, SAS Institute Inc., Cary, NC, United States).

RESULTS

In total, 27 boys with DMD aged between 4.6 and 15 years old at baseline [median age (interquartile range): 8.7 (4.5) years] and repeatedly measured (range: two to nine measurements) over a varying follow-up period (range: 6 months–5 years) were included in the study. The control group consisted of 27 TD children aged between 5.4 and 15.6 years old [median age (interquartile range): 8.3 (3.1) years] (**Table 1**).

All the collected 3DGA sessions of three patients and only one follow-up session for four patients were excluded due to obvious marker misplacement, inconsistent walking and/or behavioral disturbances leading to inaccurate measurements. The measurements with marker misplacement (n = 2) were only included for the spatiotemporal parameters, but excluded for the kinematic and kinetic parameters. This resulted in a final dataset of 115 and 113 measurements for the spatiotemporal and kinematic/kinetic data, respectively.

TABLE 1 | Subject characteristics of boys with DMD at baseline and TD children, and results from MWU-test.

	Median (Q1-Q3)		MWU-test
Variables	**DMD**	**TD**	**BH corrected *p*-value**
Gender	Boys: 27	Boys: 27	
Age (years)	8.7 (6.0–10.5)	8.3 (7.6–10.7)	0.5500
Weight (kg)	23.7 (19.7–36.0)	27.2 (23.3–37.0)	0.2437
Height (m)	1.21 (1.08–1.31)	1.33 (1.24–1.49)	0.0033*
BMI (kg/m^2)	17.6 (16.3–21.9)	15.6 (15.0–17.8)	0.0070*
Leg length (m)	0.58 (0.50–0.65)	0.65 (0.61–0.78)	0.0024*

The asterisks (*) indicate significance level at BH corrected p-value < 0.05. BH, Benjamini-Hochberg procedure; BMI, Body Mass Index; DMD, Duchenne muscular dystrophy; MWU, Mann-Whitney U; TD, typically developing.

Aim 1: Gait Features in Children With Duchenne Muscular Dystrophy at Baseline Compared to Typically Developing Children

Spatiotemporal Parameters

At baseline, the boys with DMD presented a lower WV_{norm} (p = 0.0036) and smaller SL_{norm} (p = 0.0281) compared to TD (**Table 2**). The SW_{norm} was significantly broader in DMD compared to TD (p = 0.0036).

Kinematic and Kinetic Parameters

The maximal anterior pelvic tilt angle was larger in DMD compared to TD (p = 0.0047) (**Table 2**). The minimal and maximal hip flexion angles during stance (p = 0.0006) and swing (p = 0.0018), respectively, were larger in the children with DMD compared to TD. The maximal hip extension moment was smaller (p = 0.0012), while the minimal hip extension moment was larger (p = 0.0009) in DMD compared to TD. The boys with DMD presented a smaller minimal hip adduction angle during swing (p = 0.0018) than TD children. The boys with DMD walked with a larger minimal knee flexion angle during stance than TD children (p = 0.0070). The range of knee flexion/extension motion during the stance phase was smaller in DMD compared to TD (p = 0.0070). Boys with DMD walked with a larger maximal knee flexion angle during swing than TD children (p = 0.0038). The minimal knee extension moment was larger in DMD compared to TD (p = 0.0007). Minimal plantar flexion moment during loading response was larger (p = 0.0012), while the maximal plantar flexion moment (p = 0.0009) and ankle power (p = 0.0020) during push-off were smaller in the children with DMD compared to TD. Lastly, boys with DMD walked with a smaller maximal internal foot progression angle than TD children (p = 0.0005).

Aim 2: Longitudinal Evolution of Gait Features in Growing Boys With Duchenne Muscular Dystrophy

The results of the LMM are presented in **Tables 3–7**. Per gait feature (i.e., each row in a table), the estimates of the fixed effects with the corresponding p-values are presented. For example, in **Table 3**, for the outcome SW_{norm}, 0.262 ($p < 0.05$), -0.027 (p = 0.0006), 0.005 (p = 0.0016), 0.003 (p = 0.3895), 0.005 ($p < 0.0001$) are the estimates of the intercept, the regression coefficient of the linear time effect, the regression coefficient of the quadratic time effect, the regression coefficient of the baseline age effect, and the regression coefficient of the interaction effect between time and baseline age, respectively. The 95% confidence interval of the fixed effects' estimates, and the random-effect and

TABLE 2 | Group differences in gait features between DMD at baseline and TD, and results from MWU-test.

	Median (Q1-Q3)		MWU-test
Variables	**DMD**	**TD**	**BH corrected *p*-value**
Cadence (steps/s)	2.25 (2.01–2.40)	2.21 (1.97–2.47)	0.4639
WVnorm (/)	0.40 (0.37–0.43)	0.46 (0.43–0.51)	0.0036*
SWnorm (/)	0.28 (0.24–0.30)	0.16 (0.11–0.19)	0.0036*
SLnorm (/)	0.74 (0.70–0.79)	0.77 (0.74–0.85)	0.0281*
Gait profile score (°)	6.81 (5.13–8.37)	5.21 (4.87–6.57)	0.0924
Max anterior pelvic tilt (°)	16.36 (14.30–19.03)	11.64 (8.69–15.26)	0.0047*
ROM pelvic obliquity (°)	9.62 (7.50–13.32)	7.42 (6.97–9.20)	0.0502
ROM pelvic rotation (°)	14.41 (9.96–17.18)	14.93 (11.21–17.49)	0.7535
Min hip flex angle stance (°)	−3.08 (−7.68 to 3.77)	−10.13 (−13.32 to −6.84)	0.0006*
Max hip flex angle swing (°)	41.81 (34.67–49.01)	34.12 (29.19–37.89)	0.0018*
ROM hip sagittal plane (°)	42.70 (38.90–46.95)	45.42 (41.02–47.77)	0.2578
Max hip ext mom stance (Nm/kg)	0.507 (0.388–0.688)	1.098 (0.699–1.319)	0.0012*
Min hip ext mom stance (Nm/kg)	−0.698 (−0.789 to −0.516)	−0.904 (−1.068 to −0.772)	0.0009*
Max hip power stance (W/kg)	0.440 (0.334–0.775)	0.665 (0.445–1.094)	0.0554
Min hip add angle stance (°)	−6.79 (−8.36 to −3.96)	−4.92 (−6.29 to −2.92)	0.0501
Min hip add angle swing (°)	−9.45 (−11.38 to −8.03)	−6.50 (−7.14 to −5.34)	0.0018*
Max hip abd mom stance (Nm/kg)	0.559 (0.443–0.735)	0.648 (0.581–0.723)	0.0582
Max knee flex angle stance (°)	35.02 (33.16–39.36)	35.55 (28.03–40.28)	0.7722
Min knee flex angle stance (°)	9.06 (3.86–12.31)	3.65 (−2.54–7.62)	0.0070*
ROM knee sagittal plane stance (°)	28.01 (24.31–30.70)	30.72 (28.06–33.23)	0.0070*
Max knee flex angle swing (°)	69.48 (64.38–74.45)	64.75 (60.05–67.84)	0.0038*
Max knee ext mom stance (Nm/kg)	0.414 (0.337–0.490)	0.512 (0.325–0.663)	0.1263
Min knee ext mom stance (Nm/kg)	−0.049 (−0.120 to 0.022)	−0.207 (−0.334 to −0.157)	0.0007*
Dorsiflex angle IC (°)	0.80 (−3.61 to 4.07)	0.77 (−1.70 to 3.77)	0.9586
Max dorsiflex angle stance (°)	15.09 (11.34–17.20)	12.53 (9.47–16.55)	0.3147
Max dorsiflex angle swing (°)	5.31 (0.02–6.95)	5.27 (2.56–8.35)	0.4202
Min plantar flex mom LR (Nm/kg)	−0.050 (−0.088 to −0.008)	−0.127 (−0.184 to −0.069)	0.0012*
Max plantar flex mom PO (Nm/kg)	0.976 (0.864–1.185)	1.318 (1.141–1.446)	0.0009*
Min ankle power LR (W/kg)	−0.501 (−0.941 to −0.265)	−0.467 (−0.605 to −0.349)	0.9128
Max ankle power PO (W/kg)	3.022 (2.271–3.384)	3.973 (3.100–4.386)	0.0020*
Max int foot prog angle stance (°)	−7.96 (−11.96 to −3.13)	0.11 (−4.16 to 4.22)	0.0005*

The asterisks (*) indicate significance level at BH corrected p-value < 0.05.
abd, abduction; add, adduction; BH, Benjamini-Hochberg procedure; DMD, Duchenne muscular dystrophy; dorsiflex, dorsiflexion; ext, extension; flex, flexion; IC, initial contact; int, internal; LR, loading response; Max, maximal; Min, minimal; mom, moment; MWU, Mann-Whitney U; PO, push-off; prog, progression; ROM, range of motion; SLnorm, normalized step length; SWnorm, normalized step width; TD, typically developing; WVnorm, normalized walking velocity.

TABLE 3 | Results of linear mixed effect models with spatiotemporal parameters as responses in children with DMD.

	Fixed effects										
	Intercept	**Regression coefficients**									
		Longitudinal effects				**Cross-sectional effects**				**Interaction effects**	
		Time		**Time^2**		**Baseline age**		**Baseline age^2**		**Time × Baseline age**	
Variables	β_0	β_1	***p*-value**	β_2	***p*-value**	β_3	***p*-value**	β_4	***p*-value**	β_6	***p*-value**
Cadence (steps/s)	2.617*	−0.058	0.0019*			−0.124	0.0001*	0.006	0.0266*		
WVnorm (/)	0.457*	−0.012	0.0613			−0.011	<0.0001*				
SLnorm (/)	0.785*	−0.016	0.0214*			−0.009	0.0026*				
SWnorm (/)	0.262*	−0.027	0.0006*	0.005	0.0016*	0.003	0.3895			0.005	<0.0001*

The asterisks (*) indicate significance level at p < 0.05.
DMD, Duchenne muscular dystrophy; SLnorm, normalized step length; SWnorm, normalized step width; WVnorm, normalized walking velocity.

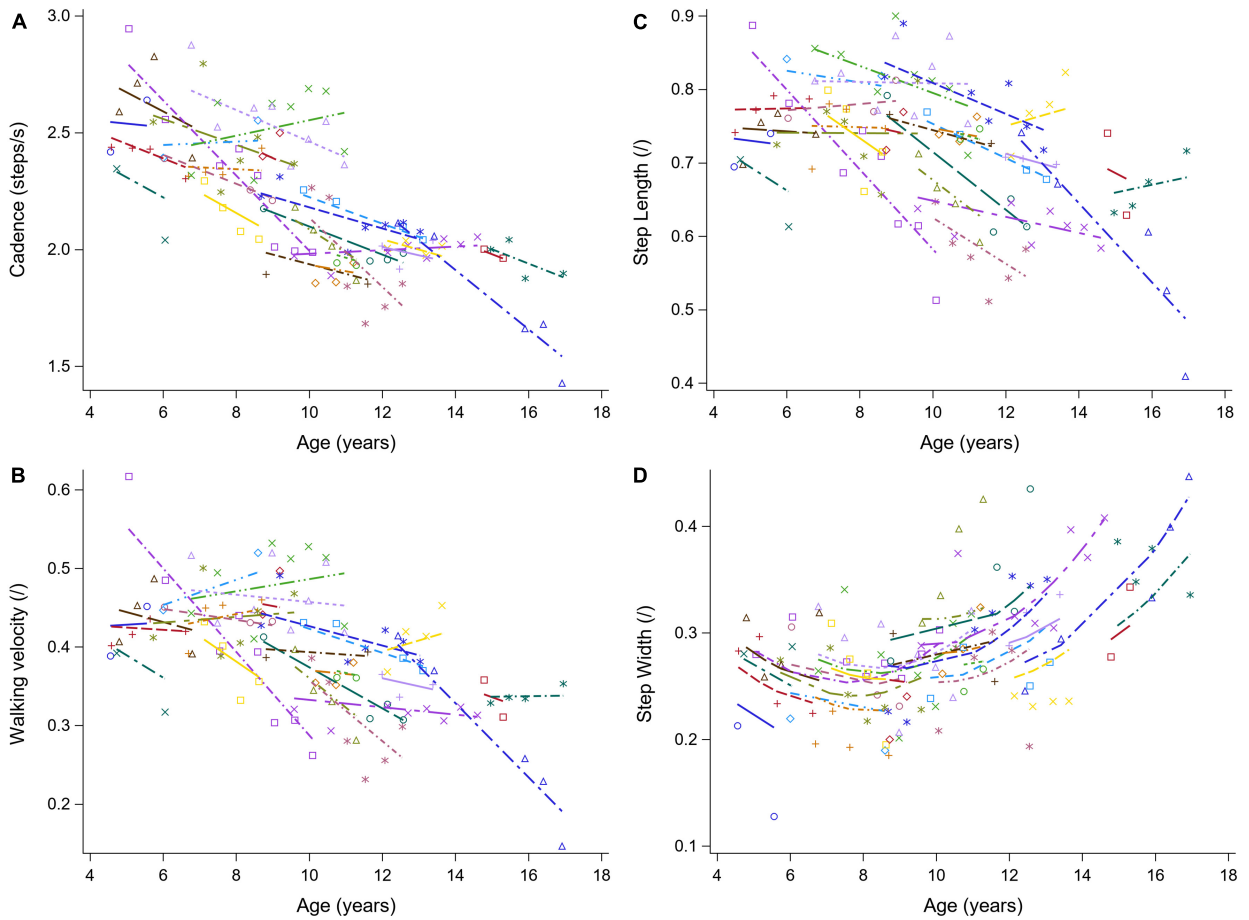

FIGURE 3 | The individual predicted profiles (dashed lines) for cadence **(A)**, normalized walking velocity **(B)**, normalized step length **(C)**, and normalized step width **(D)**. The actual observed values are visualized by the symbols. Each color represents one patient with DMD. The regression coefficients of the fixed effects are given in **Table 3**. DMD, Duchenne muscular dystrophy.

residual covariance structures are presented in **Supplementary Tables 1, 2**, respectively. Additionally, the individual predicted profiles are visualized in **Figures 3–7**.

Spatiotemporal Parameters

The results of the LMM for the spatiotemporal parameters are given in **Table 3**. A longitudinal decrease in cadence of 0.058 steps/s per year was observed (**Figure 3A**). In addition, cadence decreased with baseline age, with a larger decrease before the age of nine and a smaller decrease after the age of nine. Only a small baseline age-effect was detected for WV_{norm}, resulting in a decrease of 0.011 per year (**Figure 3B**). SL_{norm} decreased significantly longitudinally and with baseline age, with 0.016 and 0.009 per year, respectively (**Figure 3C**). For SW_{norm}, the longitudinal change was related to baseline age, i.e., a slow decrease and a rapid increase were detected before and after the baseline age of nine, respectively (**Figure 3D**).

Kinematic and Kinetic Parameters

The results of the LMM for the GPS and the pelvis kinematics are given in **Table 4**. The longitudinal change in GPS was related to age, i.e., the GPS increased more rapidly with increasing age (**Figure 4A**). A baseline age-effect resulted in a small decrease in GPS before the age of nine and a large increase in GPS after the age of nine. A longitudinal increase of 1.33 degrees per year in the maximal anterior pelvic tilt was found (**Figure 4B**). In addition, a small baseline age-effect resulted in a decreasing maximal anterior pelvic tilt before the age of nine, while above the age of nine, a larger baseline age-effect resulted in an increasing maximal anterior pelvic tilt. Furthermore, the pelvis range of motion (i.e., obliquity and rotation) increased longitudinally and with baseline age (**Figures 4C,D**). For pelvic obliquity, the range of motion increased 0.58 and 0.74 degrees, longitudinally and with baseline age, respectively. The pelvis rotation range of motion increased longitudinally with 1.35 degrees per year. With increasing baseline age, the pelvis rotation range of motion decreased until the age of seven and increased after the age of nine.

The results of the LMM for the hip kinematics and kinetics are given in **Table 5**. A longitudinal increase in the minimal hip flexion angle during stance of 1.88 degrees per year was found (**Figure 5A**). In addition, this angle increased progressively with

TABLE 4 | Results of linear mixed effect models with the gait profile score and pelvis kinematics as responses in children with DMD.

	Fixed effects								
	Intercept	Regression coefficients							
		Longitudinal effects		Cross-sectional effects				Interaction effects	
		Time		Baseline age		Baseline age^2		Time × Baseline age	
Variables	β_0	β_1	*p*-value	β_3	*p*-value	β_4	*p*-value	β_6	*p*-value
Gait profile score (°)	6.69*	0.19	0.4649	−0.57	0.0797	0.09	0.0134*	0.10	0.0362*
Max anterior pelvic tilt (°)	15.71*	1.33	0.0004*	−1.42	0.0853	0.26	0.0003*		
ROM pelvic obliquity (°)	7.60*	0.58	0.0012*	0.74	0.0004*				
ROM pelvic rotation (°)	13.32*	1.35	0.0296*	−1.27	0.1577	0.25	0.0067*		

The asterisks (*) indicate significance level at $p < 0.05$.
DMD, Duchenne muscular dystrophy; Max, maximal; ROM, range of motion.

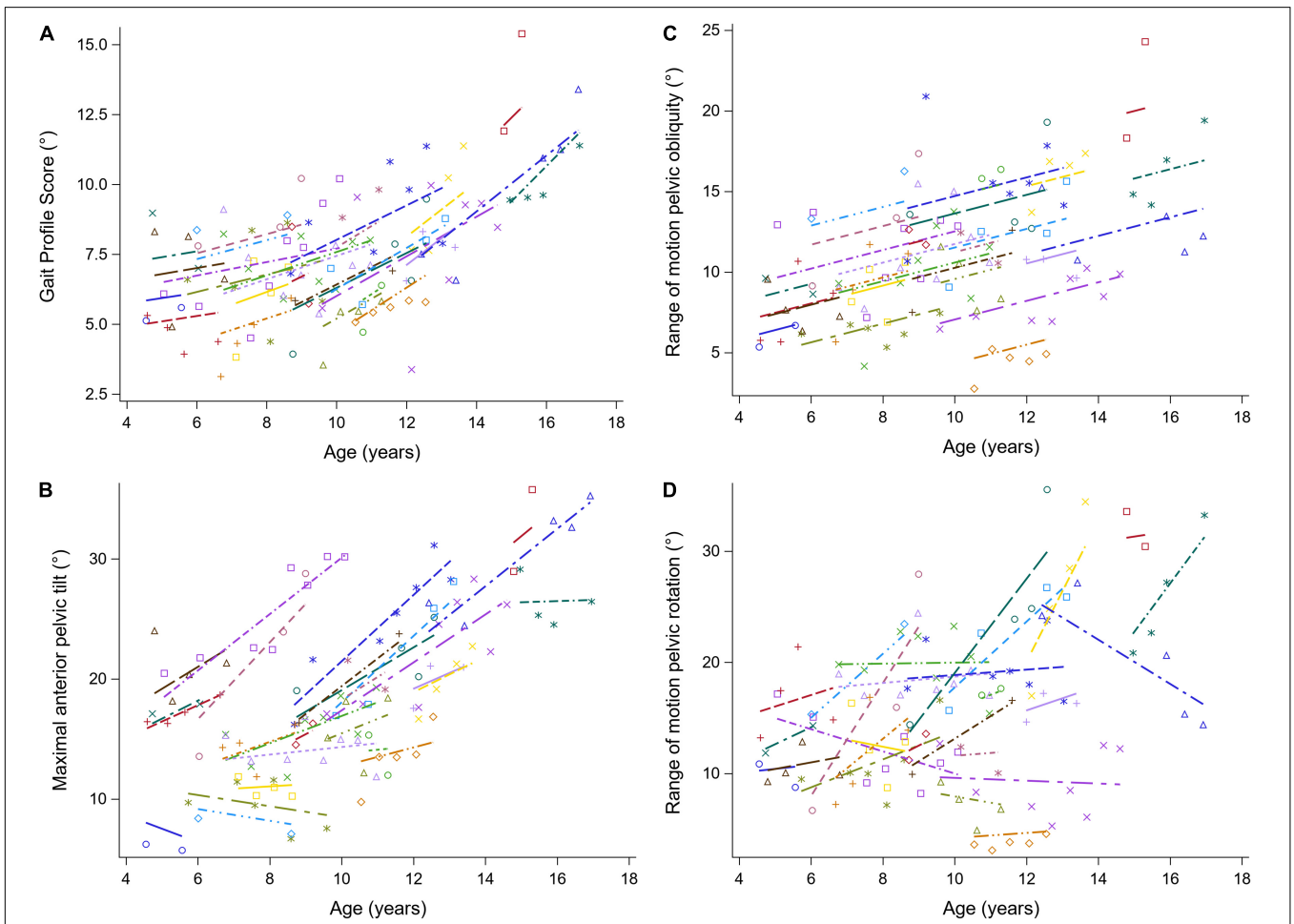

FIGURE 4 | The individual predicted profiles (dashed lines) for the GPS **(A)**, the maximal anterior pelvic tilt **(B)**, range of motion pelvic obliquity **(C)**, and range of motion pelvic rotation **(D)**. The actual observed values are visualized by the symbols. Each color represents one patient with DMD. The regression coefficients of the fixed effects are given in **Table 4**. DMD, Duchenne muscular dystrophy; GPS, Gait Profile Score.

baseline age. The longitudinal increase in the maximal hip flexion angle during swing was related to increasing baseline age, i.e., this angle increased more rapidly with baseline age (**Figure 5B**). The maximal hip flexion angle during swing also increased with baseline age. The range of hip flexion/extension motion decreased with baseline age (**Figure 5C**). Similar patterns, i.e.,

TABLE 5 | Results of linear mixed effect models with the hip kinematics and kinetics as responses in children with DMD.

	Fixed effects									
	Intercept	Regression coefficients								
		Longitudinal effects		Cross-sectional effects					Interaction effects	
		Time		$Time^2$		Baseline age		$Baseline\ age^2$		Time*Baseline age	
Variables	β_0	β_1	*p*-value	β_2	*p*-value	β_3	*p*-value	β_4	*p*-value	β_6	*p*-value
Min hip flex angle stance (°)	−7.63*	1.88	0.0022*			−0.22	0.8131	0.23	0.0133*		
Max hip flex angle swing (°)	37.10*	−0.22	0.7167			1.08	0.0075*			0.30	0.0049*
ROM hip sagittal plane (°)	47.10*	−0.60	0.2100			−0.76	0.0267*				
Max hip ext mom stance (Nm/kg)	0.502*	0.035	0.3421	−0.020	0.0104*	0.065	0.0141*	−0.010	< 0.0001*		
Max hip power stance (W/kg)	0.475*	0.066	0.3015	−0.030	0.0484*	0.061	0.0927	−0.008	0.0166*		
Min hip add angle stance (°)	−3.32*	−0.42	0.0250*			−1.24	0.0026*	0.094	0.0110*		
Min hip add angle swing (°)	−6.92*	−0.48	0.0930			−1.42	0.0013*	0.12	0.0009*		
Max hip abd mom stance (Nm/kg)	0.537*	0.029	0.0166*			0.017	0.0238*			−0.010	0.0024*

The asterisks (*) indicate significance level at $p < 0.05$.
abd, abduction; add, adduction; DMD, Duchenne muscular dystrophy; ext, extension; flex, flexion; Max, maximal; Min, minimal; mom, moment; ROM, range of motion.

an increase followed by a decrease, were detected longitudinally for the maximal hip extension moment and the maximal hip power (**Figures 5D,E**). In addition, before the age of nine, the maximal hip extension moment and the maximal hip power increased with baseline age, while after the age of nine these gait features decreased. A longitudinal decrease in the minimal hip adduction angle during stance was detected (**Figure 5F**). Before the age of ten, the minimal hip adduction angles during stance and swing (**Figure 5G**) decreased with baseline age, while these gait features increased above the age of ten. The longitudinal change in the maximal hip abduction moment was related to baseline age, i.e., a longitudinal increase and decrease were detected before and after the baseline age of nine, respectively (**Figure 5H**). Additionally, the maximal hip abduction moment increased with baseline age.

The results of the LMM for the knee kinematics and kinetics are given in **Table 6**. The maximal knee flexion angle during stance decreased longitudinally with 0.85 degrees per year (**Figure 6A**). With increasing baseline age, the maximal and minimal knee flexion angles during stance increased with 0.73 and 1.00 degrees per year, respectively (**Figures 6A,B**). A longitudinal pattern, i.e., an increase followed by a decrease, was visible in the range of knee flexion/extension motion (**Figure 6C**). Before and after the age of nine, the range of knee flexion/extension motion increased and decreased with baseline age, respectively. The maximal knee flexion angle during swing decreased longitudinally with 1.25 degrees per year (**Figure 6D**). Longitudinally, a slow decrease followed by a rapid increase in the minimal knee extension moment was observed (**Figure 6F**). In contrast, the minimal knee extension moment showed an alternating pattern with increasing baseline age, i.e., firstly a decrease, secondly an increase, lastly another decrease.

The results of the LMM for the ankle kinematics and kinetics are given in **Table 7**. A longitudinal decrease of 1.20 degrees in the dorsiflexion angle at initial contact per year was found (**Figure 7A**). Additionally, this angle decreased progressively with baseline age. During swing, the longitudinal change in the maximal dorsiflexion angle was related to age, i.e., this angle decreased more rapidly with baseline age (**Figure 7B**). Before the age of nine, the maximal dorsiflexion angle in stance and swing increased, while after the age of nine, these gait features decreased with baseline age (**Figures 7B,C**). The minimal plantar flexion moment during loading response increased longitudinally with 0.010 Nm/kg per year (**Figure 7D**). The increasing baseline age resulted in an increase of 0.037 Nm/kg per year in the maximal plantar flexion moment during push-off (**Figure 7E**). The minimal ankle power during loading response decreased progressively with baseline age (**Figure 7F**). Longitudinally, a progression toward an internal foot progression angle was visible (**Figure 7H**). Before the age of nine, the foot progression angle increased externally with baseline age, while above the age of nine this angle increased internally.

DISCUSSION

This mixed cross-sectional longitudinal study aimed at providing a full description of the progressive gait pathology in children with DMD. First, 31 predefined gait features were cross-sectionally compared between children with DMD at baseline and a TD database. This allowed for a comparison of our results with previous literature. We hypothesized that the predefined gait features of children with DMD would deviate from TD children already at baseline, since the children with DMD enrolled at different ages, ranging from 4.6 to 15 years old, and therefore, presented different stages of the disease progression. Second, the longitudinal changes in the 31 predefined gait features in the same cohort of boys with DMD were explored in a follow-up study over a period of 5 years. We hypothesized that the predefined

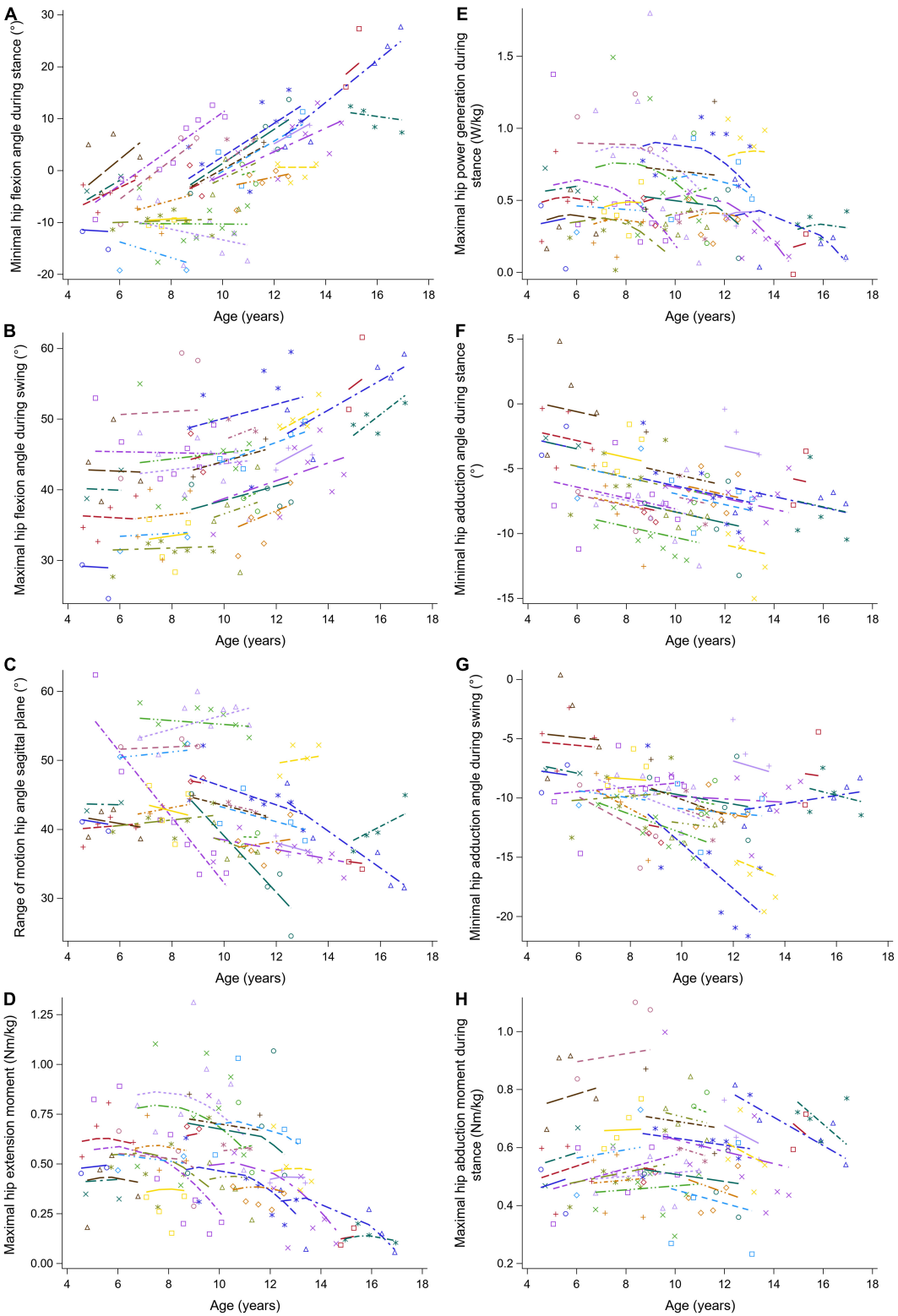

FIGURE 5 | The individual predicted profiles (dashed lines) for the minimal hip flexion angle during stance **(A)**, maximal hip flexion angle during swing **(B)**, range of hip motion in the sagittal plane **(C)**, maximal hip extension moment **(D)**, maximal hip power generation during stance **(E)**, minimal hip adduction angle during stance **(F)**, minimal hip adduction angle during swing **(G)**, and maximal hip abduction moment during stance **(H)**. The actual observed values are visualized by the symbols. Each color represents one patient with DMD. The regression coefficients of the fixed effects are given in **Table 5**. DMD, Duchenne muscular dystrophy.

TABLE 6 | Results of linear mixed effect models with knee kinematics and kinetics as responses in children with DMD.

	Fixed effects									
	Intercept	Regression coefficients								
		Longitudinal effects				Cross-sectional effects				
		Time		Time^2		Baseline age		Baseline age^2		Baseline age^3	
Variables	β_0	β_1	*p*-value	β_2	*p*-value	β_3	*p*-value	β_4	*p*-value	β_5	*p*-value
Max knee flex angle stance (°)	32.14*	−0.85	0.0010*			0.73	0.0094*				
Min knee flex angle stance (°)	3.73*	−0.49	0.3203			1.00	0.0006*				
ROM knee sagittal plane stance (°)	26.06*	0.61	0.3377	−0.36	0.0033*	1.03	0.1231	−0.12	0.0361*		
Max knee flex angle swing (°)	68.83*	−1.25	0.0029*								
Max knee ext mom stance (Nm/kg)	0.418*	−0.018	0.3034								
Min knee ext mom stance (Nm/kg)	−0.043	−0.017	0.2387	0.008	0.0111*	−0.068	0.0302*	0.020	0.0176*	−0.001	0.0229*

The asterisks (*) indicate significance level at $p < 0.05$.
DMD, Duchenne muscular dystrophy; ext, extension; flex, flexion; Max, maximal; Min, minimal; mom, moment; ROM, range of motion.

gait features would evolve significantly over time, as children with DMD grow older.

Aim 1: Gait Features of Children With Duchenne Muscular Dystrophy at Baseline Compared to Typically Developing Children

Our hypothesis concerning the first aim was only partly confirmed, since 17 out of the 31 gait features differed in the boys with DMD at baseline compared to the TD children and not all differences were in agreement with previous findings. In comparison to the most commonly reported gait features summarized in the systematic review of Goudriaan et al. (2018a), we only agreed on a reduced walking velocity, step length, maximal dorsiflexion moment, and maximal ankle power generation in children with DMD compared to TD children. In addition, we found that boys with DMD walked with an increased anterior pelvic tilt in combination with a decreased hip extension at the end of stance, which is in agreement with previous findings (Sutherland et al., 1981; Boccardi et al., 1997; Gaudreault et al., 2010; Goudriaan et al., 2018b). At the beginning of the stance phase, the maximal hip extension moment was reduced in the boys with DMD compared to the TD children. This is in line with previous literature (Boccardi et al., 1997; D'Angelo et al., 2009; Gaudreault et al., 2010) and is explained by a smaller ground reaction force and reduced lever arm due to the more posteriorly aligned ground reaction force (Gaudreault et al., 2010). This is potentially achieved by backward trunk leaning commonly observed in children with DMD and suggested to be a compensation strategy for hip extensor weakness (Sutherland et al., 1981). In contrast to Boccardi et al. (1997), we found that the maximal hip flexion moment, later in stance, was also decreased in children with DMD, probably due to the increased maximal anterior pelvic tilt and decreased maximal hip extension at terminal stance. Furthermore, the boys with DMD walked with a broader base of support, which is consistent with previous literature and is considered a compensation mechanism for the weak hip abductors (Sutherland et al., 1981; Boccardi et al., 1997; Romano et al., 2019). The increased maximal external foot progression angle found in the children with DMD also aligned the ground reaction force more laterally. However, the maximal hip abduction moment was not reduced in DMD, which is in contrast with the findings reported by Gaudreault et al. (2010). The minimal knee flexion angle at the end of the stance phase was increased, while previous research more frequently reported knee hyperextension, as a compensation mechanism for weak knee extensors (D'Angelo et al., 2009; Doglio et al., 2011). In relation to the more flexed knee position at the end of stance, the range of knee flexion/extension motion during stance was decreased in DMD compared to TD. The maximal knee flexion moment was decreased in the boys with DMD. The compensation mechanism around the hip may also indirectly affect the kinetics around the knee, as the more posteriorly directed ground reaction force is probably located more closely to the knee joint. In contrast to the equinus gait commonly seen in clinical practice, ankle kinematics did not significantly differ between DMD at baseline and TD. However, the ankle kinetics showed some significant characteristics of an equinus walking pattern as the maximal dorsiflexion moment, maximal plantar flexion moment and maximal ankle power generation were reduced in DMD. In swing, boys with DMD presented an increased maximal hip flexion, maximal hip abduction and maximal knee flexion angle, which have been reported as compensation mechanisms for a drop foot, i.e., a lack of ankle dorsiflexion in swing (Sutherland et al., 1981; D'Angelo et al., 2009; Doglio et al., 2011).

In summary, our findings are not fully consistent with previous literature. Especially, knee hyperextension and equinus gait in the ankle kinematics were not detected. Since DMD is a progressive disorder, wide age ranges result in heterogeneous groups with boys that are located in different stages of the disease progression. Consequently, it is likely that the full spectrum

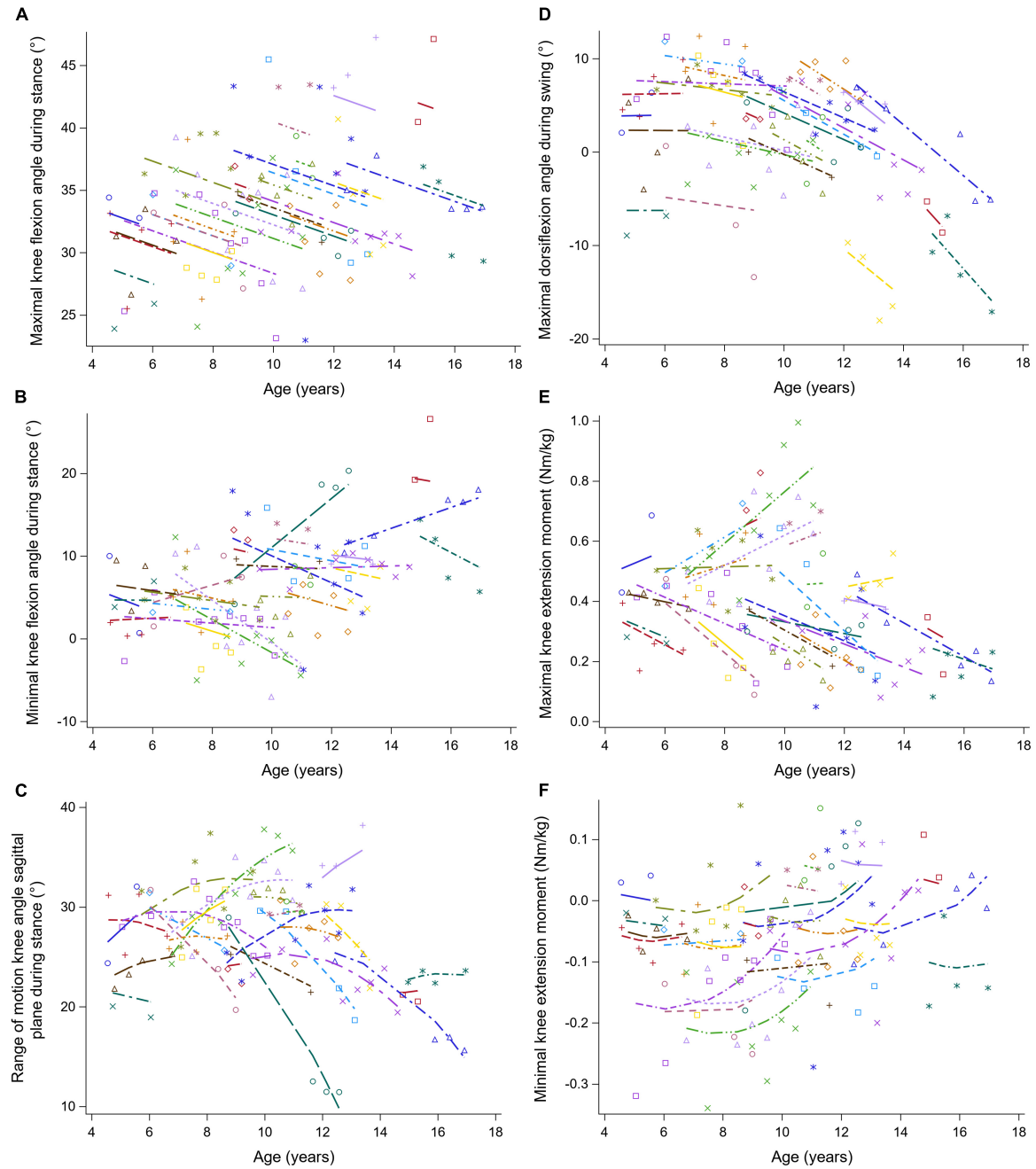

FIGURE 6 | The individual predicted profiles (dashed lines) for the maximal knee flexion angle during stance **(A)**, minimal knee flexion angle during stance **(B)**, range of knee motion in sagittal plane during stance **(C)**, maximal knee flexion angle during swing **(D)**, maximal knee extension moment **(E)**, and minimal knee extension moment **(F)**. The actual observed values are visualized by the symbols. Each color represents one patient with DMD. The regression coefficients of the fixed effects are given in **Table 6**. DMD, Duchenne muscular dystrophy.

of gait pathology is leveled out when such a heterogeneous group is compared to a TD group. Therefore, longitudinal analyses studying how gait features evolve over time in the same children with DMD are more of interest than investigating an average/mean of gait features in a heterogeneous group. This longitudinal description is also clinically relevant for treatments aiming to prolong ambulation.

Aim 2: Evolution of Gait Features in Growing Boys With Duchenne Muscular Dystrophy

Our hypothesis concerning the second aim was confirmed. Indeed, several gait features showed a significant altered evolution in the boys with DMD. To avoid confusion since the

TABLE 7 | Results of linear mixed effect models with ankle kinematics and kinetics as responses in children with DMD.

	Fixed effects								
	Intercept	Regression coefficients							
		Longitudinal effects		Cross-sectional effects				Interaction effects	
		Time		Baseline age		Baseline age^2		Time × Baseline age	
Variables	β_0	β_1	***p*-value**	β_3	***p*-value**	β_4	***p*-value**	β_6	***p*-value**
Dorsiflex angle IC (°)	1.70	−1.20	<0.0001*	0.52	0.5141	−0.15	0.0338*		
Max dorsiflex angle stance (°)	11.34*	−0.59	0.1390	2.64	0.0010*	−0.32	<0.0001*		
Max dorsiflex angle swing (°)	2.14	0.06	0.9074	2.09	0.0202*	−0.29	<0.0001*	−0.35	0.0003*
Min plantar flex mom LR (Nm/kg)	−0.060*	0.010	<0.0001*						
Max plantar flex mom PO (Nm/kg)	0.867*	−0.009	0.4905	0.037	<0.0001*				
Min ankle power LR (W/kg)	−0.533*	−0.026	0.5465	0.059	0.2426	−0.011	0.0196*		
Max ankle power PO (W/kg)	2.875*	−0.026	0.7813						
Max int foot prog angle stance (°)	−6.29*	2.10	0.0019*	−3.06	0.0021*	0.40	0.0006*		

The asterisks (*) indicate significance level at $p < 0.05$.
DMD, Duchenne muscular dystrophy; dorsiflex, dorsiflexion; flex, flexion; IC, initial contact; int, internal; LR, loading response; Max, maximal; Min, minimal; mom, moment; PO, push-off; prog, progression; ROM, range of motion.

cross-sectional baseline age-effect could be misinterpreted as a longitudinal time effect, both effects were discussed separately.

Longitudinal Effect

Twenty-one gait features evolved longitudinally. Overall, our results are in agreement with the changes summed over the three stages as reported by Sutherland et al. (1981).

Global Gait Outcome

The increase in GPS confirmed the overall progressive gait pathology seen in children with DMD. To our knowledge, the current study is the first in finding a significant progression in a global gait outcome. Previously reported differences in GPS and gait deviation index between progressive groups, which were classified based on motor abilities or the gait deviation index, did not reach significance (Sienko Thomas et al., 2010; de Souza et al., 2019). Mainly at older ages, a steep increase in GPS could be detected, while in young boys with DMD the increase in GPS was small. Therefore, the GPS might not be sensitive enough to detect altered gait pathology and thus relevant improvements in clinical trials, especially in young boys with DMD.

Sagittal and Transversal Pelvic Kinematics—Sagittal Hip Kinematics—Step Length

In agreement with Sutherland et al. (1981), the anterior pelvic tilt increased over time in the children with DMD (**Supplementary Figure 1**), potentially due to increasing stiffness and shortening of the hip flexors and/or hip extensor weakness (Boccardi et al., 1997; D'Angelo et al., 2009; Gaudreault et al., 2010). Consequently, the hip extension deficit increased by almost two degrees per year. To compensate for this and to improve step length (Doglio et al., 2011), the boys with DMD increased the motion of the pelvic rotation in the transverse plane over time. However, this compensation mechanism was not sufficient enough to prevent the decrease in step length.

Sagittal Hip Kinetics

The maximal hip extension moment and power generation decreased longitudinally in the boys with DMD, suggesting a longitudinal progression of the compensation for the weak hip extensor muscles. Unexpectedly, the steep decline in these gait features was first preceded by a small increase or stabilization in approximately the first 6–12 months of the follow-up period. Taking into account the results of Heberer et al. (2016), the start of corticosteroids or clinical trial participation may contribute to the initial improvements in the maximal hip extension moment and power generation (Heberer et al., 2016). This suggests that these two gait features may potentially monitor the effect of clinical trials that aim to prolong walking ability (Heberer et al., 2016).

Step Width—Frontal Pelvic and Hip Kinematics

Our longitudinal analysis revealed an initial small gait maturation toward a smaller step width in the boys with DMD (Sutherland, 1997; Sala and Cohen, 2013), followed by a steep longitudinal increase in step width after the age of nine (**Supplementary Figure 2**). Unexpectedly, a longitudinal increase in the maximal hip abduction was already visible from the start of the follow-up. This could be related to the observed longitudinal increase in range of motion of the pelvic obliquity, as a result of the previously reported contralateral elevation of the pelvis at the end of the stance phase (Gaudreault et al., 2010; Romano et al., 2019). In short, children with DMD present a complex progressive interaction between mechanisms to compensate for hip abductor weakness, i.e., increase in step width and pelvic obliquity.

Frontal Hip Kinetics

The longitudinal compensation mechanisms for hip abductor weakness were not reflected in a reduction of the maximal hip abduction moment. In fact, initially, the maximal hip abduction moment increased. Hip abductors have been reported as muscles that are likely to stiffen and contract in

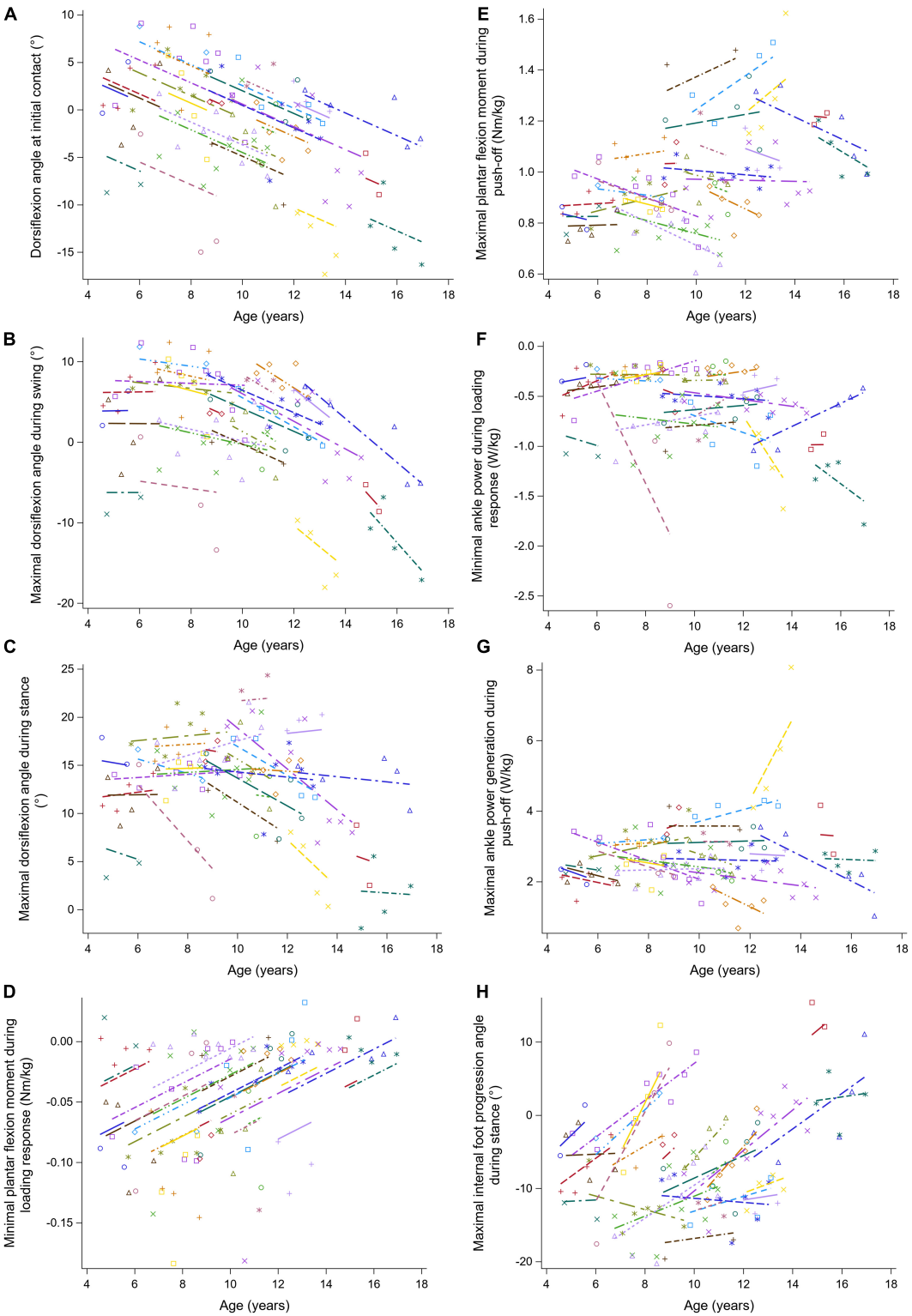

FIGURE 7 | The individual predicted profiles (dashed lines) for the dorsiflexion angle at initial contact **(A)**, maximal dorsiflexion angle during swing **(B)**, maximal dorsiflexion angle during stance **(C)**, minimal plantar flexion moment during loading response **(D)**, maximal plantar flexion moment during push-off **(E)**, minimal ankle power during loading response **(F)**, maximal ankle power generation during push-off **(G)**, and maximal internal foot progression angle during stance **(H)**. The actual observed values are visualized by the symbols. Each color represents one patient with DMD. The regression coefficients of the fixed effects are given in **Table 7**. DMD, Duchenne muscular dystrophy.

DMD (McDonald et al., 1995; Skalsky and McDonald, 2012). Therefore, it is expected that the passive forces, caused by the increased resistance to elongation of the stiff hip abductors, contribute to the net moments during gait (Gaudreault et al., 2009). Since several hip abductors also act as internal hip rotators (Neumann, 2010), stiff and contracted hip abductors may have resulted in the increasing internal foot progression. This may explain the increase in the maximal hip abduction moment, since the ground reaction force is more medially located to the hip joint with internally rotated feet. Only after the age of nine, the maximal hip abduction moment started to decrease longitudinally, suggesting that the beneficial effect of the stiffness and contracture may no longer sufficiently compensate the weak hip abductors. Therefore, boys with DMD older than nine years would need to use other compensation mechanisms, such as increasing the step width, to align the ground reaction force more laterally, which was indeed observed in the current study.

Knee Kinematics

The maximal knee flexion angle during loading response decreased longitudinally. Avoiding knee flexion to compensate for knee extensor muscle weakness has been reported in previous cross-sectional research comparing the gait features between DMD and TD (D'Angelo et al., 2009; Romano et al., 2019). The range of knee flexion/extension motion during stance first increased and then decreased longitudinally. Interestingly, Doglio et al. (2011) reported an increased knee range of motion due to knee hyperextension at the end of stance in young boys with DMD compared to TD children (Doglio et al., 2011). Furthermore, a decrease in the maximal knee extension angle at the end of stance, possibly due to the formation of knee flexion contractures in a later stage of the disease (Sussman, 2002; Choi et al., 2018), may contribute to a reduction in knee flexion/extension range of motion. In the current study, however, no significant average evolution toward knee hyperextension could be detected. Yet, looking at the individual predicted profiles, these gait features seemed to be related. In boys with DMD progressing toward an increased maximal knee extension at the end of stance, the knee range of motion increased and vice versa.

Knee Kinetics

Although the maximal knee flexion angle during loading response decreased longitudinally, there was no change in the maximal knee extension moment. Therefore, our findings could not confirm the longitudinal progression of the compensation for weakness in the knee extensors. On a patient-specific level, both increasing as well as decreasing evolutions in the maximal knee extension moment were observed. Hence, it might be that some of the boys with DMD appeared to have sufficient knee extensor strength to control the increasing maximal knee extension moment. This might have been a requirement for ambulation, since a larger knee extension moment is difficult to avoid with the previously described compensation around the hip (i.e., posterior alignment of the ground reaction force due to backward trunk leaning). Moreover, this clinical presentation of these boys with DMD matched with limited gait pathology in the early stage as described by Sutherland et al. (1981). Others, who corresponded more to the transitional stage of Sutherland et al. (1981), needed to compensate for increasing knee extensor weakness by decreasing the knee extension moment. Due to the progressive muscle weakness, a switch from an increasing toward a decreasing knee extension moment was expected. However, such a transition, from the early to the transitional stage, was not captured in the current longitudinal analyses of the same children with DMD. The maximal knee flexion moment presented first a small increase or stabilization, which was followed by a steep decline longitudinally. Therefore, the decreasing knee flexion moment may be an indirect result of the increasing compensation strategy for weak hip extensors (i.e., posterior alignment of the ground reaction force to the hip joint results in a closer alignment of the ground reaction force to the knee joint). In summary, the longitudinal evolution in the maximal knee extension and flexion moments were thus less straightforward, most likely due to the influence of the proximal compensations and the presence of different gait stages across patients.

Ankle Kinematics

The current study partly confirmed the progressive equinus gait reported by Sutherland et al. (1981). An evolution from a normal heel strike to flatfeet followed by forefoot contact was captured, which is probably caused by muscle weakness of the tibialis anterior and/or muscle contracture of the gastrocnemius (Sussman, 2002; Gaudreault et al., 2009; Yiu and Kornberg, 2015). Additionally, the observed increased plantar flexion angle resulted in a ground reaction force that was more anteriorly to the knee joint, and may serve as well as a compensation mechanism for knee extensor weakness (Sutherland et al., 1981; D'Angelo et al., 2009; Doglio et al., 2011). But, in the current study, there was no average longitudinal reduction in the maximal dorsiflexion angle during stance. The onset and worsening of a midfoot break may have contributed to a dorsiflexion overestimation in some of the boys with DMD. Yet, based on the plantar flexion angle at initial contact and the video recordings detecting a midfoot break in combination with a premature heel rise, the longitudinal increase in equinus gait in the children with DMD was evident.

Ankle Kinetics

The progressive equinus gait could only be partly confirmed. Due to the progression toward flat- or forefeet strike, the maximal dorsiflexion moment reduced longitudinally. No significant longitudinal evolution was detected for the maximal plantar flexion moment and ankle power generation. This suggests that the progressive weakness of the plantar flexors may have limited impact on the ankle kinetics during push-off. However, similar as suggested for the maximal dorsiflexion angle during stance, the presence of a midfoot break might have influenced the lever arm and thus the ankle kinetics during push-off. Therefore, characteristics of a progressive equinus gait in the ankle kinetics were mainly visible during loading response, when no midfoot break was present.

Swing Phase

During swing, the ankle progressed toward a drop foot over time in the boys with DMD (**Supplementary Figure 3**), which is in agreement with the changes over the three stages reported by Sutherland et al. (1981). Increasing the maximal hip abduction angle, the maximal knee flexion angle, and the maximal hip flexion angle have been reported as compensation mechanisms to aid foot clearance and avoid tripping (Sutherland et al., 1981; D'Angelo et al., 2009; Doglio et al., 2011). Similar longitudinal evolutions in the maximal dorsiflexion angle and the maximal hip flexion angle in swing were found, i.e., the longitudinal decrease in the maximal dorsiflexion angle seemed to be related with the longitudinal increase in the maximal hip flexion angle, both progressing more rapidly with increasing baseline age. Therefore, the current study suggests that the evolution in the maximal hip flexion angle in swing could be the main compensation for the progressive drop foot.

Cross-Sectional Baseline Age-Effect

Since DMD is a progressive disorder, an increase or decrease in the gait features with age was expected. This was confirmed by the current study, as 25 gait features presented a significant cross-sectional baseline age-effect. Regarding the age-effect, the evolution in several gait features (e.g., GPS, maximal anterior pelvic tilt, range of pelvic motion, maximal hip extension moment, maximal hip power, maximal plantar flexion angle in stance, and swing) was often preceded by an opposite trend. Since boys with DMD achieve independent walking generally at a later age compared to TD (Sussman, 2002), the younger boys with DMD may still present an immature gait pattern. Therefore, this opposite trend in the gait features may represent a maturation process. Similar to Heberer et al. (2016), it is also possible that starting the use of corticosteroids or a novel therapeutic strategy in a clinical trial may result in an improvement in the gait features. However, the effect of baseline age on the gait features is a cross-sectional analysis and therefore, the variability among patients could be misinterpreted as a maturation or treatment effect. Additionally, some of the gait features presented an opposite cross-sectional baseline age-effect to the longitudinal effect. For example, the maximal knee flexion angle decreased longitudinally, but, increased with the cross-sectional baseline age. This baseline age-effect could be explained by the absence and presence of a knee flexion contracture, which was measured during a standard clinical exam (goniometry), in the younger and older boys with DMD, respectively. However, the progression from decreasing the maximal knee flexion angle to compensate for knee extensor weakness toward increasing the maximal knee flexion angle when a knee flexion contracture starts to develop was not detected within the same patients. Therefore, the cross-sectional age-effect may reflect the heterogeneity among children with DMD instead of a longitudinal evolution.

Limitations

Although the current study investigated a unique mixed longitudinal database, the amount of 3DGA-sessions collected over the entire ambulation period in the same boys with DMD was still limited. To take into account that the children with DMD who enrolled at older ages were in more advanced stages of the disease, the effect of increasing baseline age was studied. Due to the small follow-up period in some of the children (i.e., minimal follow-up time of 6 months), the longitudinal effect was not always in agreement with the cross-sectional effect of increasing baseline age. Therefore, caution is needed with the interpretation of the baseline age-effect, since it could be partly influenced by the existing variation between patients. Additionally, the differences in clinical background such as the underlying gene mutation, clinical trial participation, corticosteroid doses, periods of serial casting, and the functional level, etc.[1] among the boys with DMD, may have contributed to the heterogeneity of our study sample. Furthermore, several gait features were solely defined based on the maximal or minimal value. Therefore, the timing of this value in the gait cycle could vary between as well as within the boys with DMD depending on how pathological the gait pattern was at a certain stage of the disease progression. Statistical analysis, such as statistical (non-)parametric mapping, could be used to take into account the time dependency. However, LMM are not yet implemented in statistical (non-)parametric mapping. Lastly, our simplistic foot model (Plug-In Gait Full-Body model) could have resulted in a dorsiflexion overestimation, if the boys with DMD presented a midfoot break.

CONCLUSION

In conclusion, we provided a quantitative description of the evolution in gait features in growing boys with DMD based on a unique mixed longitudinal dataset and therefore, our findings improved the understanding of the natural history of the progressive DMD gait pathology. Despite the limited follow-up period and the large variability between the children with DMD, we found that 21 gait features progressed longitudinally in the patients with DMD. This suggests that these gait features are promising outcome measures for future clinical trials to quantify the efficacy of novel therapeutic strategies aiming to prolong ambulation. Next steps are (1) the assessment of the sensitivity of these gait features to change (e.g., in clinical trials) and comparing them to the outcomes from standard clinical measurements (e.g., 6MWT and NSAA), (2) the confirmation of our findings and the investigation of the effect of treatments (i.e., corticosteroid use, clinical trial participation and serial casting) as well as the effect of individual characteristics (e.g., underlying gene mutation and functional level) on the gait evolution in a larger sample size with a longer follow-up per participant and a larger presentation of boys in the late stage of the disease and, (3) the exploration of how the underlying impairments, e.g., progressive muscle weakness and stiffness, contribute to the progressive gait pathology.

DATA AVAILABILITY STATEMENT

The datasets presented in this study can be found in online repositories. The names of the repository/repositories

[1] https://dx.doi.org/10.6084/m9.figshare.17313188

and accession number(s) can be found in the article/ **Supplementary Material**.

ETHICS STATEMENT

The studies involving human participants were reviewed and approved by the local ethics committee (Ethical Committee UZ Leuven/KU Leuven; S55867, S56041, and S61324). Written informed consent to participate in this study was provided by the participants' legal guardian/next of kin.

AUTHOR CONTRIBUTIONS

IV and KD: conceptualization. IV, MVdH, NDB, MG, and ES: data curation. IV, MD, and GM: formal analysis. IV, NG, LDW, and KD: funding acquisition. IV, MD, GM, and KD: methodology. KD: resources and supervision. IV: visualization and writing–original draft. MVdH, NDB, ES, MG, MD, GM, NG, LDW, AVC, FDG, and KD: writing–review and editing. All authors have read and agreed to the published version of the manuscript.

FUNDING

This work was supported by the Duchenne Parent Project NL (17.011) and by the Research Foundation - Flanders (FWO-Vlaanderen) through a research fellowship to IV (1188921N). MG was funded by the Dutch Organization for Scientific Research (NWO) VIDI grant (no. 016.156.346 FirSTeps), the European Research Council (ERC) under the European Union's Horizon 2020 Research and Innovation Program (no. 715945 Learn2Walk), and the Johanna Kinderfonds and Kinderrevalidatie Fonds Adriaanstichting (no. 20200028).

ACKNOWLEDGMENTS

We thank all the children and parents for their participation in this study and the colleagues of UZ Leuven for helping to recruit the boys with DMD.

SUPPLEMENTARY MATERIAL

The Supplementary Material for this article can be found online at: https://www.frontiersin.org/articles/10.3389/fnhum.2022.861136/full#supplementary-material

REFERENCES

Baker, R., McGinley, J. L., Schwartz, M. H., Beynon, S., Rozumalski, A., Graham, H. K., et al. (2009). The gait profile score and movement analysis profile. *Gait Posture* 30, 265–269. doi: 10.1016/j.gaitpost.2009.05.020

Benjamini, Y., and Hochberg, Y. (1995). Controlling the false discovery rate: a practical and powerful approach to multiple testing. *J. R. Stat. Soc. Ser. B* 57, 289–300. doi: 10.1111/j.2517-6161.1995.tb02031.x

Boccardi, S., Gabardi, C., Negrini, A., and Santambrogio, G. C. (1997). Locomotor and posture strategies in patients with Duchenne Muscular Dystrophy (DMD): Part I. Gait analysis. *Eur. Med. Phys.* 33, 13–22.

Bregou Bourgeois, A., Mariani, B., Aminian, K., Zambelli, P. Y., and Newman, C. J. (2014). Spatio-temporal gait analysis in children with cerebral palsy using, foot-worn inertial sensors. *Gait Posture* 39, 436–442. doi: 10.1016/j.gaitpost.2013.08.029

Bushby, K., Bourke, J., Bullock, R., Eagle, M., Gibson, M., and Quinby, J. (2005). The multidisciplinary management of Duchenne muscular dystrophy. *Curr. Paediatr.* 15, 292–300. doi: 10.1016/j.cupe.2005.04.001

Bushby, K., Finkel, R., Birnkrant, D. J., Case, L. E., Clemens, P. R., Cripe, L., et al. (2010). Diagnosis and management of Duchenne muscular dystrophy, part 1: diagnosis, and pharmacological and psychosocial management. *Lancet Neurol.* 9, 77–93. doi: 10.1016/S1474-4422(09)70271-6

Choi, Y.-A., Chun, S.-M., Kim, Y., and Shin, H.-I. (2018). Lower extremity joint contracture according to ambulatory status in children with Duchenne muscular dystrophy. *BMC Musculoskelet. Disord.* 19:287. doi: 10.1186/s12891-018-2212-6

D'Angelo, M. G., Berti, M., Piccinini, L., Romei, M., Guglieri, M., Bonato, S., et al. (2009). Gait pattern in Duchenne muscular dystrophy. *Gait Posture* 29, 36–41. doi: 10.1016/j.gaitpost.2008.06.002

de Souza, M. A., Cezarani, A., da Lizzi, E. A. S., de Davoli, G. B. Q., Mattiello, S. M., Jones, R., et al. (2019). The use of the gait profile score and gait variable score in individuals with Duchenne Muscular Dystrophy. *J. Biomech.* 98:109485. doi: 10.1016/j.jbiomech.2019.109485

Diggle, P. J. (1988). An approach to the analysis of repeated measurements. *Biometrics* 44, 959–971.

Diggle, P., Heagerty, P., Liang, K.-Y., and Zeger, S. (2002). *Analysis of Longitudinal Data*, 2nd Edn. Oxford: Oxford University Press.

Doglio, L., Pavan, E., Pernigotti, I., Petralia, P., Frigo, C., and Minetti, C. (2011). Early signs of gait deviation in Duchenne muscular dystrophy. *Eur. J. Phys. Rehabil. Med.* 47, 587–594.

Emery, A. E. H., and Eh, E. (1991). Population diseases–a of inherited world survey. *Neuromuscul. Disord.* 1, 19–29.

Frosini, S., Vita, G., Mongini, T., Politano, L., Bello, L., Astrea, G., et al. (2009). Reliability of the North Star Ambulatory Assessment in a multicentric setting. *Neuromuscul. Disord.* 19, 458–461. doi: 10.1016/j.nmd.2009.06.368

Gaudreault, N., Gravel, D., and Nadeau, S. (2009). Evaluation of plantar flexion contracture contribution during the gait of children with Duchenne muscular dystrophy. *J. Electromyogr. Kinesiol.* 19, 180–186. doi: 10.1016/j.jelekin.2007.09.004

Gaudreault, N., Gravel, D., Nadeau, S., Desjardins, P., and Brière, A. (2007). A method to evaluate contractures effects during the gait of children with Duchenne dystrophy. *Clin. Orthop. Relat. Res* 456, 51–57. doi: 10.1097/BLO.0b013e3180312bd7

Gaudreault, N., Gravel, D., Nadeau, S., Houde, S., and Gagnon, D. (2010). Gait patterns comparison of children with Duchenne muscular dystrophy to those of control subjects considering the effect of gait velocity. *Gait Posture* 32, 342–347. doi: 10.1016/j.gaitpost.2010.06.003

Goemans, N. (2013). *Therapy Development and Clinical Outcome Measures for Duchenne Muscular Dystrophy.* Ph.D. thesis. Leuven: KU Leuven.

Goemans, N., Tulinius, M., Kroksmark, A. K., Wilson, R., van den Hauwe, M., and Campion, G. (2017). Comparison of ambulatory capacity and disease progression of Duchenne muscular dystrophy subjects enrolled in the drisapersen DMD114673 study with a matched natural history cohort of subjects on daily corticosteroids. *Neuromuscul. Disord.* 27, 203–213. doi: 10.1016/j.nmd.2016.11.013

Goudriaan, M., Van den Hauwe, M., Dekeerle, J., Verhelst, L., Molenaers, G., Goemans, N., et al. (2018a). Gait deviations in Duchenne muscular dystrophy—Part 1. A systematic review. *Gait Posture* 62, 247–261. doi: 10.1016/j.gaitpost.2018.03.020

Goudriaan, M., Van den Hauwe, M., Simon-Martinez, C., Huenaerts, C., Molenaers, G., Goemans, N., et al. (2018b). Gait deviations in Duchenne muscular dystrophy—Part 2. Statistical non-parametric mapping to analyze gait deviations in children with Duchenne muscular dystrophy. *Gait Posture* 63, 159–164. doi: 10.1016/j.gaitpost.2018.04.038

Heberer, K., Fowler, E., Staudt, L., Sienko, S., Buckon, C. E., Bagley, A., et al. (2016). Hip kinetics during gait are clinically meaningful outcomes in young boys with Duchenne muscular dystrophy. *Gait Posture* 48, 159–164. doi: 10.1016/j.gaitpost.2016.05.013

Hof, A. L. (1996). Scaling gait data to body size. *Gait Posture* 4, 222–223. doi: 10.1016/0966-6362(95)01057-2

Jones, D., Round, J., and de Haan, A. (2010). *Skeletal Muscles, From Molecules to Movement. A Textbook of Muscle Physiology for Sport Exercise, Physiotherapy and Medicine*. London: Elsevier.

Khodadadeh, S., McClelland, M. R., Patrick, J. H., Edwards, R. H. T., and Evans, G. A. (1986). Knee moments in duchenne muscular dystrophy. *Lancet* 2, 544–545. doi: 10.1016/S0140-6736(86)90628-8

Kierkegaard, M., and Tollbäck, A. (2007). Reliability and feasibility of the six minute walk test in subjects with myotonic dystrophy. *Neuromuscul. Disord.* 17, 943–949. doi: 10.1016/j.nmd.2007.08.003

Kirschner, J., Schessl, J., Schara, U., Reitter, B., Stettner, G. M., Hobbiebrunken, E., et al. (2010). Treatment of Duchenne muscular dystrophy with ciclosporin A: a randomised, double-blind, placebo-controlled multicentre trial. *Lancet Neurol.* 9, 1053–1059. doi: 10.1016/S1474-4422(10)70196-4

Lindsay, A., Baumann, C. W., Rebbeck, R. T., Yuen, S. L., Southern, W. M., Hodges, J. S., et al. (2020). Mechanical factors tune the sensitivity of mdx muscle to eccentric strength loss and its protection by antioxidant and calcium modulators. *Skelet. Muscle* 10, 1–14. doi: 10.1186/s13395-020-0221-2

Lu, Q., Cirak, S., and Partridge, T. (2014). What can we learn from clinical trials of exon skipping for DMD? *Mol. Ther. Nucleic Acids* 3:e152. doi: 10.1038/mtna.2014.6

Lynn, S., Aartsma-Rus, A., Bushby, K., Furlong, P., Goemans, N., De Luca, A., et al. (2015). Measuring clinical effectiveness of medicinal products for the treatment of Duchenne muscular dystrophy. *Neuromuscul. Disord.* 25, 96–105. doi: 10.1016/j.nmd.2014.09.003

Mazzone, E., Martinelli, D., Berardinelli, A., Messina, S., D'Amico, A., Vasco, G., et al. (2010). North Star Ambulatory Assessment, 6-minute walk test and timed items in ambulant boys with Duchenne muscular dystrophy. *Neuromuscul. Disord.* 20, 712–716. doi: 10.1016/j.nmd.2010.06.014

McDonald, C. M., Henricson, E. K., Han, J. J., Abresch, R. T., Nicorici, A., Elfring, G. L., et al. (2010). The 6-minute walk test as a new outcome measure in Duchenne muscular dystrophy. *Muscle Nerve* 41, 500–510. doi: 10.1002/mus.21544

McDonald, C., Abresch, R., Carter, G., Fowler, W. J., Johnson, E., Kilmer, D., et al. (1995). Profiles of neuromuscular diseases. Duchenne muscular dystrophy. *Am. J. Phys. Med. Rehabil.* 74(Suppl. 5), S70–S92.

Moens, P., Baatsen, P. H. W. W., and Maréchal, G. (1994). Increased susceptibility of EDL muscles from mdx mice to damage induced by contraction with stretch. *J. Muscle Res. Cell Motil.* 15, 490–492.

Neumann, D. A. (2010). Kinesiology of the hip: a focus on muscular actions. *J. Orthop. Sports Phys. Ther.* 40, 82–94. doi: 10.2519/jospt.2010.3025

Petrof, B. J., Shrager, J. B., Stedman, H. H., Kelly, A. M., and Sweeney, H. L. (1993). Dystrophin protects the sarcolemma from stresses developed during muscle contraction. *Proc. Natl. Acad. Sci. U.S.A.* 90, 3710–3714. doi: 10.1073/pnas.90.8.3710

Romano, A., Favetta, M., Schirinzi, T., Summa, S., Minosse, S., Catteruccia, M., et al. (2019). Evaluation of gait in duchenne muscular dystrophy: relation of 3D gait analysis to clinical assessment. *Neuromuscul. Disord.* 29, 920–929. doi: 10.1016/j.nmd.2019.10.007

Ryder, S., Leadley, R. M., Armstrong, N., Westwood, M., De Kock, S., Butt, T., et al. (2017). The burden, epidemiology, costs and treatment for Duchenne muscular dystrophy: an evidence review. *Orphanet J. Rare Dis.* 12, 1–21. doi: 10.1186/s13023-017-0631-3

Sala, D. A., and Cohen, E. (2013). Gait component changes observed during independent ambulation in young children. *Indian J. Pediatr.* 80, 397–403. doi: 10.1007/s12098-012-0926-2

Shin, H., Sung, K. H., Chung, C. Y., Lee, K. M., Lee, S. Y., Lee, I. H., et al. (2016). Relationships between isometric muscle strength, gait parameters, and gross motor function measure in patients with cerebral palsy. *Yonsei Med. J.* 57, 217–224.

Sienko Thomas, S., Buckon, C. E., Nicorici, A., Bagley, A., McDonald, C. M., and Sussman, M. D. (2010). Classification of the gait patterns of boys with Duchenne muscular dystrophy and their relationship to function. *J. Child Neurol.* 25, 1103–1109. doi: 10.1177/0883073810371002

Skalsky, A. J., and McDonald, C. M. (2012). Prevention and management of limb contractures in neuromuscular diseases. *Phys. Med. Rehabil. Clin. N. Am.* 23, 675–687. doi: 10.1016/j.pmr.2012.06.009

Sussman, M. (2002). Duchenne muscular dystrophy. *J. Am. Acad. Orthop. Surg.* 10, 138–151. doi: 10.1016/j.clinph.2004.05.006

Sutherland, D. (1997). The development of mature gait. *Gait Posture* 6, 163–170. doi: 10.1016/S0966-6362(97)00029-5

Sutherland, D. H., Olshen, R., Cooper, L., Wyatt, M., Leach, J., Mubarak, S., et al. (1981). The pathomechanics of gait in Duchenne Muscular Dystrophy. *Dev. Med. Child Neurol.* 23, 3–22.

Verbeke, G., and Molenberghs, G. (1997). *Linear Mixed Models in Practice: A SAS-Oriented Approach*. New York, NY: Springer.

Verbeke, G., and Molenberghs, G. (2000). *Linear Mixed Models for Longitudinal Data*. Springer Series in Statistics. New York, NY: Springer-Verlag.

Wren, T. A. L., Tucker, C. A., Rethlefsen, S. A., Gorton, G. E., and Õunpuu, S. (2020). Clinical efficacy of instrumented gait analysis: systematic review 2020 update. *Gait Posture* 80, 274–279. doi: 10.1016/j.gaitpost.2020.05.031

Yiu, E. M., and Kornberg, A. J. (2015). Duchenne muscular dystrophy. *J. Paediatr. Child Health* 51, 361–367. doi: 10.1201/b13434

Conflict of Interest: The authors declare that the research was conducted in the absence of any commercial or financial relationships that could be construed as a potential conflict of interest.

frontiers | Frontiers in Human Neuroscience

ORIGINAL RESEARCH
published: 03 June 2022
doi: 10.3389/fnhum.2022.846205

Causal Effects of Motor Control on Gait Kinematics After Orthopedic Surgery in Cerebral Palsy: A Machine-Learning Approach

Katherine M. Steele[1] and Michael H. Schwartz[2,3]*

[1] Department of Mechanical Engineering, University of Washington, Seattle, WA, United States, [2] Gillette Children's Specialty Healthcare, St. Paul, MN, United States, [3] Department of Orthopedic Surgery, University of Minnesota, St. Paul, MN, United States

Background: Altered motor control is common in cerebral palsy (CP). Understanding how altered motor control affects movement and treatment outcomes is important but challenging due to complex interactions with other neuromuscular impairments. While regression can be used to examine associations between impairments and movement, causal modeling provides a mathematical framework to specify assumed causal relationships, identify covariates that may introduce bias, and test model plausibility. The goal of this research was to quantify the causal effects of altered motor control and other impairments on gait, before and after single-event multi-level orthopedic surgery (SEMLS).

Methods: We evaluated the impact of SEMLS on change in Gait Deviation Index (ΔGDI) between gait analyses. We constructed our causal model with a Directed Acyclic Graph that included the assumed causal relationships between SEMLS, ΔGDI, baseline GDI (GDI_{pre}), baseline neurologic and orthopedic impairments (Imp_{pre}), age, and surgical history. We identified the adjustment set to evaluate the causal effect of SEMLS on ΔGDI and the impact of Imp_{pre} on ΔGDI and GDI_{pre}. We used Bayesian Additive Regression Trees (BART) and accumulated local effects to assess relative effects.

Results: We prospectively recruited a cohort of children with bilateral CP undergoing SEMLS (N = 55, 35 males, age: 10.5 ± 3.1 years) and identified a control cohort with bilateral CP who did not undergo SEMLS (N = 55, 30 males, age: 10.0 ± 3.4 years). There was a small positive causal effect of SEMLS on ΔGDI (1.70 GDI points). Altered motor control (i.e., dynamic and static motor control) and strength had strong effects on GDI_{pre}, but minimal effects on ΔGDI. Spasticity and orthopedic impairments had minimal effects on GDI_{pre} or ΔGDI.

Conclusion: Altered motor control did have a strong effect on GDI_{pre}, indicating that these impairments do have a causal effect on a child's gait pattern, but minimal effect on

OPEN ACCESS

Edited by:
Marco Iosa,
Sapienza University of Rome, Italy

Reviewed by:
Kristan Leech,
University of Southern California, United States
Ye Ma,
Ningbo University, China

****Correspondence:***
Katherine M. Steele
kmsteele@uw.edu

Specialty section:
This article was submitted to Motor Neuroscience, a section of the journal Frontiers in Human Neuroscience

Received: *30 December 2021*
Accepted: *09 May 2022*
Published: *03 June 2022*

Citation:
Steele KM and Schwartz MH (2022) Causal Effects of Motor Control on Gait Kinematics After Orthopedic Surgery in Cerebral Palsy: A Machine-Learning Approach. Front. Hum. Neurosci. 16:846205. doi: 10.3389/fnhum.2022.846205

expected changes in GDI after SEMLS. Heterogeneity in outcomes suggests there are other factors contributing to changes in gait. Identifying these factors and employing causal methods to examine the complex relationships between impairments and movement will be required to advance our understanding and care of children with CP.

Keywords: cerebral palsy, machine learning, motor control, electromyography (EMG), gait, orthopedic surgery, weakness, spasticity

INTRODUCTION

Children diagnosed with cerebral palsy (CP) exhibit altered motor control due to an injury to the brain at or near the time of birth (Desloovere, 2005; Handsfield et al., 2016; O'Brien et al., 2021). Altered motor control can be observed in CP in many ways, such as increased co-contraction, decreased capacity to selectively move individual joints, spasticity, dystonia, and altered movement patterns. Prior research has suggested that quantifying motor control is important to understand function and inform treatment planning (Fowler et al., 2010; Cahill-Rowley and Rose, 2014; Schwartz et al., 2016; Shuman et al., 2018; Bekius et al., 2020). However, altered motor control occurs and interacts with many other impairments in CP, which makes quantifying and isolating the effects of altered motor control challenging. In addition to altered motor control, orthopedic impairments can also develop, including muscle contractures and altered bone morphology (Crane, 1959; Fabry et al., 1973; O'Dwyer et al., 1989; Lee et al., 2009; Mathewson and Lieber, 2015). Together, these neurologic and orthopedic impairments are associated with limitations in movement and impact the capacity of children with CP to participate in daily activities (Rose et al., 1989; Johnston et al., 2004; Bjornson et al., 2014; Kamp et al., 2014; Gross et al., 2018).

The complexity of CP makes it challenging to objectively determine the causal effects of specific impairments on gait. As a result, many children with CP undergo clinical gait analysis (CGA) (Gage et al., 2009), which provides quantitative measures of a child's gait pattern that can be tracked over time and used to inform treatment decisions (Miller et al., 1996; Steinwender et al., 2000; Gough and Shortland, 2008). In particular, CGA was historically developed to support decision making for orthopedic surgery (Gage et al., 1984; Lee et al., 1992; Sullivan et al., 1995; Gage and Novacheck, 2001). Many children's hospitals now have CGA laboratories used for pre-operative and post-operative assessments.

While CGA has been used for treatment planning for over 30 years, deciphering causal effects of impairments on gait has remained elusive. Data from CGA is traditionally used to evaluate associations between a specific impairment and an outcome measure, typically using bivariate or multivariate regression analyses applied to retrospective data (Kramer and Ann MacPhail, 1994; Damiano et al., 2000; Ross and Engsberg, 2007; Shin et al., 2015; MacWilliams et al., 2020). In cases where multivariate regression has been used, the choice of variables for inclusion has often not had a clear causal basis. Our prior work to evaluate the impact of motor control on gait and treatment outcomes have relied on these methods (Steele et al., 2015; Schwartz et al., 2016; Shuman et al., 2018). Using multivariate regression with retrospective data from multiple hospitals, we have repeatedly demonstrated that Dynamic Motor Control (DMC) during walking is associated with outcomes (i.e., Gross Motor Functional Classification System Levels, Gait Deviation Index, Walking Speed, Pediatric Outcomes Data Collection Instrument) after orthopedic surgery, rhizotomy, or botulinum toxin injections (Steele et al., 2015; Schwartz et al., 2016). Similar analyses have demonstrated that other impairments—such as strength, hamstring length, or torsional deformities—are also correlated with treatment outcomes (Chambers et al., 1998; Hicks et al., 2011; Shore et al., 2012; Galarraga et al., 2017; Rajagopal et al., 2018).

Understanding whether altered motor control and other impairments cause altered gait or treatment outcomes is nearly impossible with non-causal regression alone. Given the complexity and heterogeneity of CP, this "*implied cause by association*" approach, without regard to possible confounding, is likely to lead to confusing and even erroneous conclusions. For example, researchers may observe that strength is associated with walking speed. However, strength is also affected by other primary neurologic deficits, like poor motor control, which may have an independent causal impact on speed. Understanding causal effects is impossible without considering these causal pathways and adjusting for relevant factors.

In recent years, there has been remarkable growth in the development and successful applications of causal inference methods (Pearl, 2009; Imbens and Rubin, 2015). From a conceptual perspective, causal methods allow researchers to explicitly share assumed causal relationships and mathematically define covariates necessary for estimating causal effects (Pearl, 1995). From a computational perspective, numerous algorithms have been developed for modeling causal outcomes. Among the most successful of these are Bayesian Additive Regression Trees (BART), which have been shown to produce estimates of causal effects with low levels of bias and variance and realistic confidence intervals (Chipman et al., 2010; Hill, 2011; Dorie et al., 2019; Hahn et al., 2020). Williams et al. (2018) have highlighted the potential of causal inference for pediatrics. However, these methods have had limited application in CP or biomechanics research.

The goal of this research was to quantify the causal effects of motor control and other impairments on gait, before and after orthopedic surgery. Specifically, we prospectively recruited children with CP who were undergoing single-event multilevel orthopedic surgery (SEMLS). We also identified a cohort of controls from the same time period who were not undergoing SEMLS between gait analyses. We developed a causal model

and used BART to quantify the effects of motor control and other impairments on changes in gait kinematics after SEMLS. These methods provide a foundation for understanding the complex and interactive effects of impairments on gait for children with CP.

MATERIALS AND METHODS

Participants

We recruited children with bilateral CP who were between 6 and 18 years old at the time of baseline gait analyses and scheduled for SEMLS. The goal of our prospective recruitment was to follow a representative cohort of patients at Gillette Children's Specialty Healthcare from their baseline gait analysis through two follow-up assessments at six-months and one-year after SEMLS. The one-year analysis was our primary outcome; however, for nine participants we used the six-month follow-up visit due to pandemic and other scheduling related disruptions. We included patients whose baseline gait analysis was no more than six months before their scheduled surgery date. We defined SEMLS as surgery consisting of two or more major orthopedic procedures on a single side. One participant was scheduled for SEMLS, but only received a single procedure, bilateral femoral derotation osteotomy. We included this participant in the analysis. We also identified a cohort of controls with CP who did not undergo SEMLS. We identified children with bilateral CP who underwent multiple gait analyses with kinematic and electromyographic (EMG) recordings, with a maximum time of 2.5 years between visits during the same time period. We excluded participants who underwent prior or current rectus femoris transfer, since we were evaluating motor control from EMG recordings. This research was conducted with approval from the University of Minnesota Institutional Review Board.

Causal Model

For this analysis we focused on evaluating the impact of SEMLS on gait kinematics. We *a priori* specified our outcome measure as the Gait Deviation Index (GDI, ClinicalTrials.gov NCT02699554) as a common summary measure of walking kinematics that has been used extensively in prior studies to evaluate and predict treatment outcomes.

We constructed our causal model with a Directed Acyclic Graph (DAG) (Verma and Pearl, 1991; Shrier and Platt, 2008; Brewer et al., 2017). The logic behind our DAG is as follows (**Figure 1**):

(1) Our objective was to determine the impact of SEMLS on change in GDI (ΔGDI). Thus, SEMLS is our exposure and ΔGDI is our outcome. SEMLS induces a change in impairment (ΔImp) that causes the observed ΔGDI.
(2) The covariates we identified as common causes of both SEMLS (i.e., variables that impact the choice to undergo SEMLS) and ΔGDI included: Age and baseline impairment (Imp_{pre}). Baseline impairments represent a set of variables collected during CGA to evaluate neurologic and orthopedic impairments (**Table 1**).
(3) Baseline GDI (GDI_{pre}) and ΔGDI are related by measurement methods (i.e., noise, errors, regression to the mean) and other, unmeasured factors.
(4) Surgical treatment history (Hx) is a common cause of baseline impairment (Imp_{pre}) and whether or not SEMLS is recommended.

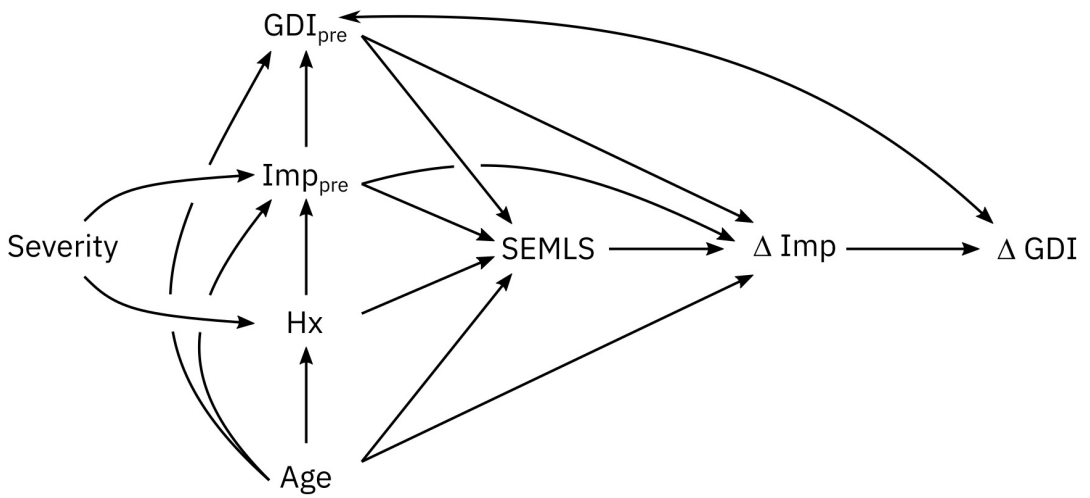

FIGURE 1 | DAG describing the assumed causal relationships between SEMLS (exposure) and ΔGDI (outcome). The causal relationship between SEMLS and ΔGDI is mediated by changes in impairments (ΔImp). Baseline GDI (GDI_{pre}) and ΔGDI are related by measurement methods and other, unmeasured factors. Baseline impairment (Imp_{pre}), surgical history (Hx), and Age are also included as causal factors. The DAG also includes unmeasured factors related to general CP severity, which impact baseline impairment and surgical history. The step-by-step process and rationale for this DAG are available in the **Supplementary Material** and an interactive version is available on dagitty (http://dagitty.net/mUCSPWo).

TABLE 1 | Variable definitions.

Variable	Description
GDI	Overall measure of the deviation in an individual's kinematics compared to non-disabled peers scaled such that mean(SD) over the non-disabled population is 100(10) (Schwartz and Rozumalski, 2008). Kinematics were evaluated using marker-based motion analysis and a modified plug-in-gait marker set
SEMLS	Binary variable indicating whether or not child had single-event multi-level orthopedic surgery, defined as a surgery with two or more orthopedic surgeries on at least one leg
Hx	Binary list of prior surgical treatments
Age	Years from birth defined as days/365.25
Impairments	**Spasticity:** Mean modified Ashworth score across plantarflexors, hamstrings, hip adductors, and rectus femoris
	Strength: Mean manual muscle strength score across hip flexors/extensors, knee flexors/extensors, and ankle dorsiflexors/plantarflexors where 1 is defined as a 'visible or palpable contraction' and 5 is defined as 'full range of motion against gravity'
	Static Motor Control (SMC): Mean static motor control score across hip abduction, hip flexion, hip extension, knee extension, and ankle plantarflexion where 0 is very little or no control of single joint movement, 1 is impaired voluntary movement at a single joint, and 2 is good voluntary movement at a joint
	Dynamic Motor Control (DMC): Measure of the complexity of muscle activity during gait evaluated from synergy analysis of EMG data. Complexity is evaluated as the total variance accounted for by one synergy of EMG data during CGA and compared to non-disabled peers scaled such that mean(sd) over the non-disabled population is 100(10) (Shuman et al., 2017, 2018)
	Torsional Deformity: Femoral anteversion and tibial torsion (bimalleolar axis angle) measured during physical exam
	Contracture: Measures of joint range of motion from physical exam including maximum ankle dorsiflexion with the knee extended, maximum knee extension, unilateral popliteal angle, and maximum hip extension measured during the Thomas Test

(5) We included a general severity (Sev) measure as an unmeasured factor that impacts baseline impairment (Imp_{pre}) and surgical treatment history (Hx).

Note that similar DAGs could be constructed for other outcome measures such as walking speed or energy cost. Similarly, other factors could be added to the DAG, if there were rational arguments that they were common causes of one of the variables in the DAG and ΔGDI. The step-by-step process we used to construct our DAG is illustrated in the **Supplementary Material**.

From the DAG we determined the variables that needed to be included in any model (e.g., regression, BART) to evaluate the total causal effect of SEMLS on ΔGDI. These variables are called the adjustment set, representing the confounding covariates that could produce bias if not included in an analysis. For this DAG, the minimal sufficient adjustment set to estimate the total causal effect of SEMLS on ΔGDI was: Age, GDI_{pre}, and Imp_{pre}. We also determined the adjustment set to evaluate the total causal effect of baseline impairment (Imp_{pre}) on ΔGDI and GDI_{pre}. The minimal sufficient adjustments sets were Age and Hx for ΔGDI and Age for GDI_{pre}. The plausibility of a DAG can be evaluated by identifying conditional independencies, variables that should be independent given the causal relationships defined in the DAG. We identified the adjustment sets and independencies with dagitty (Textor et al., 2016) and all analyses were conducted in R (version 4.1.0) (R Core Team, 2021).

Bayesian Additive Regression Trees

To assess the total causal effects of SEMLS and baseline impairment (Imp_{pre}) on change in GDI (ΔGDI) we used Bayesian Additive Regression Trees (BART), a machine learning method that uses a boosted ensemble of regression trees for non-parametric function estimation relying on a Bayesian probability model (Chipman et al., 2010). Like other tree-based regression methods, an advantage of BART is that it can handle non-linear effects and interactions (Tan and Roy, 2019). For causal modeling, recent work has demonstrated that BART-based models achieve accurate and precise causal predictions (Hill, 2011; Dorie et al., 2019).

For this analysis, we used BART models to estimate ΔGDI using the adjustment sets identified by the DAG. Thus, to identify the impact of SEMLS on ΔGDI, we included the covariates Age, GDI_{pre}, and Imp_{pre}. Baseline impairments were not available for all participants. Missing data in Imp_{pre} were imputed using multivariate imputation by chained equations (MICE) (van Buuren and Groothuis-Oudshoorn, 2011). We used the *bartMachine* package to implement the analysis (Kapelner and Bleich, 2016). We optimized the hyperparameters for each BART model using 10-fold cross-validation. We report the pseudo-R^2 (*1 – SSE/SST)* for each BART model and used k-fold cross-validation (k = 10) to determine the out-of-sample root mean square error (RMSE).

To assess the relative effects of individual variables from BART, we used accumulated local effect (ALE) analysis (Molnar et al., 2018). The ALE analysis is similar to a partial dependence plot, but the averaging is done locally to avoid including observations that are unlikely to ever be realized (e.g., someone walking three standard deviations slower than average but with a normal cadence). The ALE plots illustrate the impact of each variable over the range of values for that variable, conditioned on the other covariates in the model. Thus, ALE plots can be useful for examining non-linear effects identified by BART. For example, the ALE plot can highlight non-linear effects such as when a variable impacts GDI with a deviation from average (i.e., a U-shaped plot) or when a variable only impacts GDI above or below a certain cut-off (i.e., a step function or discontinuity).

RESULTS

Participants

We prospectively recruited 55 children with bilateral CP who underwent SEMLS (**Table 2**). During this same time period, we identified 55 children with bilateral CP who visited the gait laboratory for repeat visits and no intervening surgical procedures. The participants who underwent SEMLS were older and had more femoral anteversion, more tibial torsion, and lower GDI scores at the initial gait analysis than the participants who did not undergo SEMLS. The SEMLS participants received, on average, five procedures (**Figure 2**).

TABLE 2 | Baseline participant characteristics, average (SD).

	No SEMLS	SEMLS
N	55	55
Males N	30	35
Age (years)	10.0 (3.4)	10.5 (3.1)
GDI	69.4 (10.0)	68.8 (12.0)
GDI Post	69.2 (11.9)	71.5 (11.7)
SMC	1.24 (0.42)	1.11 (0.40)
DMC	81.1 (9.0)	80.5 (9.5)
Strength	3.37 (0.59)	3.52 (0.63)
Spasticity	1.16 (0.42)	1.29 (0.46)
Anteversion (°)	36.3 (10.4)	39.8 (11.3)
Bimalleolar (°)	12.8 (10.6)	13.4 (11.3)
Dorsiflexion (°)	0.32 (8.52)	–0.96 (7.63)
Knee extension (°)	0.52 (6.60)	0.12 (7.47)
Thomas Test (°)	0.61 (6.23)	2.21 (6.11)
Popliteal angle (°)	51.5 (15.4)	55.7 (12.8)

Effects of SEMLS

There was a small positive causal effect of SEMLS on ΔGDI. The estimated total causal effect of SEMLS on ΔGDI was 1.70 GDI points, representing the difference between the SEMLS (+0.85 GDI points) and control (–0.85 GDI points) cohorts. While the average change in GDI between visits was 2.74 ± 8.08 for the SEMLS cohort and –0.26 ± 7.44 for the control cohort, the total causal effects represents the estimated effect of SEMLS after adjusting for differences in Age, GDI_{pre}, and Imp_{pre}. The BART model explained 18% of the variance in ΔGDI, with an out-of-sample root mean square error of 7.77. The implied conditional independencies of the DAG were also evaluated and all partial correlations were less than 0.3, supporting model plausibility (**Supplementary Material**).

Effects of Impairments

Baseline values of neurologic and orthopedic impairments (Imp_{pre}) had minimal effects on ΔGDI (**Figure 3**). SMC, DMC, and strength had moderate effects on GDI_{pre}, but not ΔGDI. Greater SMC or DMC resulted in higher GDI_{pre} scores, while muscle weakness had a negative impact on GDI_{pre} scores. Orthopedic impairments had smaller effects on GDI_{pre}. Knee extension range of motion and tibial torsion (i.e., bimalleolar angle) had the largest effect among orthopedic impairments on GDI. Participants who had excessive knee range of motion (i.e., hyperextension) had worse baseline GDI scores. Contracture of the plantarflexors, hamstrings, or iliopsoas, as well as femoral anteversion had minimal impact on GDI_{pre} or ΔGDI. The BART models evaluating the effects of impairments explained 63% of the variance in GDI_{pre} and 9% of the variance in ΔGDI. The out-of-sample performance of the BART models were RMSE = 8.57 for GDI_{pre} and RMSE = 8.04 for ΔGDI.

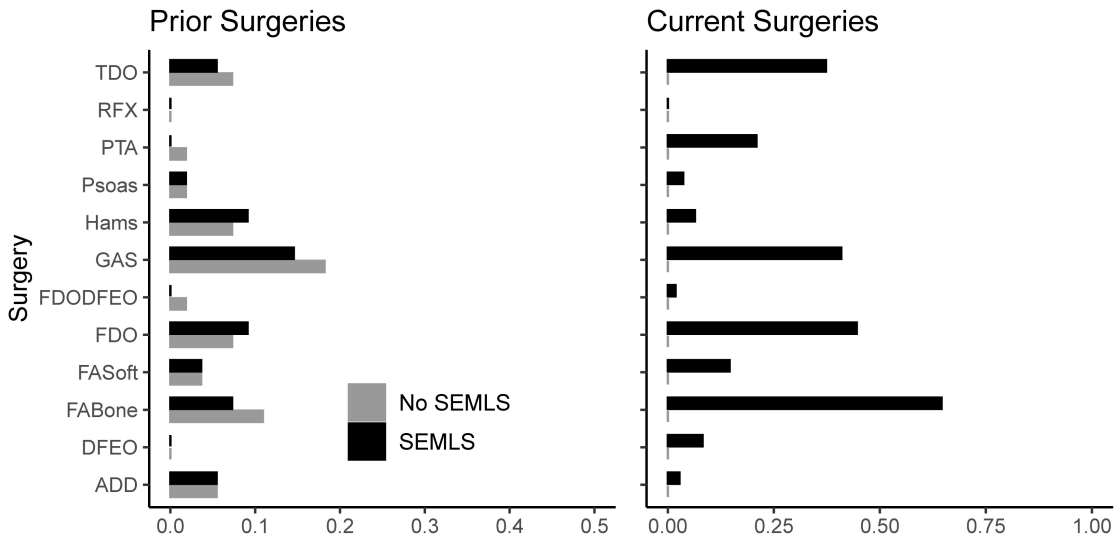

FIGURE 2 | Prior and current surgeries of participants in both cohorts. Note that we excluded potential participants who underwent rectus femors transfer. TDO, tibial derotation osteotomy; RFX, rectus femoris transfer; PTA, patellar tendon advancement; Psoas, psoas lengthening or release; Hams, hamstring lengthening; GAS, plantarflexor lengthening; FDODFEO, distal femoral derotation and extension osteotomy; FDO, femoral derotation osteotomy; FAsoft, foot/ankle soft tissue procedure; FABone, foot/ankle boney procedure; DFEO, distal femoral extension osteotomy; ADD, adductor lengthening or release.

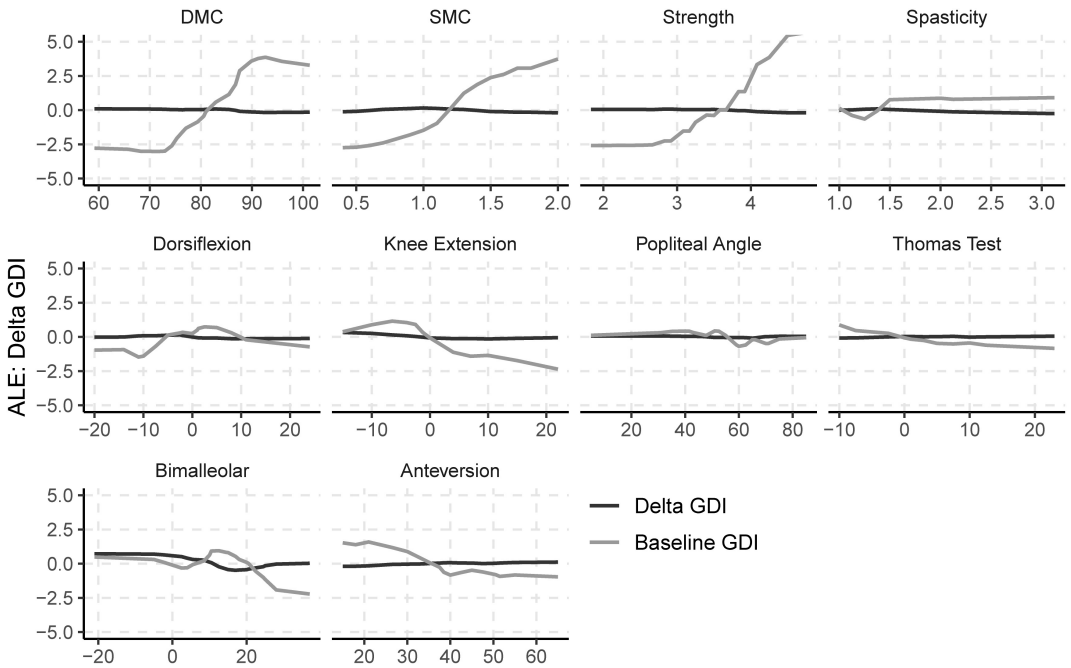

FIGURE 3 | Accumulated local effects (ALE) of baseline neurologic and orthopedic impairments on GDI_{pre} and ΔGDI.

DISCUSSION

This study showed that SEMLS has a small positive causal effect on change in GDI for children with bilateral CP. A 10-point change in GDI is generally considered a clinically significant improvement in walking function (Massaad et al., 2014). The observed change in GDI and total causal effect were far below this threshold. However, the cohorts who did not undergo SEMLS experienced a reduction in GDI between visits, resulting in a net effect of SEMLS around 1.70 GDI points. While average changes in GDI were modest, there was significant variation in outcome between participants, which could not be predicted by the model that included baseline age, impairment level, or surgical history. We found that SEMLS produced an increase in GDI larger than five points for 35% of participants, but also a decrease of more than five points in 20% of the participants. Such heterogeneous responses to SEMLS have motivated our team's investigations into patient-specific factors that can improve outcomes for children with CP. We ultimately want to be able to determine why an individual walks the way they do and anticipate their responses to treatment. We had previously hypothesized that motor control could be one such factor.

Our prior retrospective regression analyses demonstrated that DMC was associated with GDI after treatment across analyses at multiple clinical centers (Schwartz et al., 2016; Shuman et al., 2018). In this study, we used a causal model to control for and evaluate the relative effects of various impairments on change in GDI. Importantly, DMC and other impairments did have a strong effect on baseline GDI, indicating that these impairments do have a causal effect on a child's gait pattern. However, these impairments had minimal effect on ΔGDI. In other words, a child who had greater DMC at baseline was likely to have a higher GDI than a child with lower DMC, but better motor control had minimal effect on expected changes in GDI. An important point in these analyses is that the overall causal effect of SEMLS was small, which contributes to the small observed effects of impairments on ΔGDI. Despite these small treatment effects, the wide heterogeneity in outcomes suggests that there are still causal factors contributing to treatment outcomes that we are missing. These may include post-operative rehabilitation, surgeon skill, or other measures of neurologic impairment. Identifying patient-specific factors that can help us understand the causal pathways that impact gait and treatment outcomes continues to be an important area for future research.

Causal modeling provides a framework to evaluate the complex relationships between impairments and outcomes in CP. We created a DAG to identify the assumed relationships between SEMLS and GDI. The DAG used in this research could be expanded to include more detail about the assumed causal relationships between specific neurologic and orthopedic impairments or to evaluate other outcome measures. Similarly, our goal in this research was not to make outcome predictions for individual patients. Rather, we wanted to understand the impact of SEMLS and impairments on GDI. This led us toward more coarse modeling choices. As an example, we ignored details of surgical procedures and did not attempt to define the causal relationships between various neurologic and orthopedic impairments, although this is an area for future study.

The DAG we created for this research gave rise to the adjustment sets necessary to evaluate the impact of SEMLS and impairments on GDI. The DAG indicates which variables should not be included in the adjustment set. For example, changes in impairments (ΔImp) are mediators in the DAG; including these variables in the adjustment set would introduce bias. SEMLS did lead to changes in femoral anteversion and ankle contracture (see **Supplementary Material**). These adjustment sets can be used with any modeling method, including linear regression or other machine learning methods. We selected BART rather than linear regression or other models because we do not expect the impact of many impairments on gait to be linear. For example, we expect impairments like tibial torsion to reduce GDI scores with excessive internal or external rotation, producing a "U-shaped" response. Similarly, for some impairments like spasticity, there may be a threshold above or below which the impairment has an effect on gait. BART also provides a Bayesian framework that gives posterior distributions for each parameter.

A limitation in this research was that we did not recruit a prospective control group. Rather, we identified participants who were evaluated at multiple CGAs without any intervening surgical procedures. This cohort may also be subject to sample bias, but randomization is not feasible for this population. Since we were interested in evaluating DMC measured from EMG recordings, we also excluded children who underwent rectus femoris transfer, since the impact of moving the insertion of this muscle on recruitment and synergies remains unclear. Thus, this sample may not capture the impact of impairments that influence stiff-knee gait in children with CP.

CONCLUSION

The overall causal effect of SEMLS on change in GDI is modest. While motor control and strength do influence an individual's gait pattern, their effect on expected changes in GDI after SEMLS were small. It is important to consider causal frameworks when analyzing observational data to avoid bias arising from confounding. Critically evaluating current CGA practices and integrating measures such as postoperative care, surgical details, or neuroimaging into treatment planning may enhance our ability to perform casual analyses aimed at understanding and improving movement for children with CP.

DATA AVAILABILITY STATEMENT

The prospective data used for this analysis will be made available by the authors upon request.

ETHICS STATEMENT

The studies involving human participants were reviewed and approved by University of Minnesota. Written informed consent to participate in this study was provided by the participants' legal guardian/next of kin.

AUTHOR CONTRIBUTIONS

MS organized the database. KS performed the statistical analysis and wrote the first draft of the manuscript. Both authors contributed to conception and design of the study and contributed to manuscript revision, read, and approved the submitted version.

FUNDING

Research reported in this publication was supported by the National Institute of Neurological Disorders & Stroke of the National Institutes of Health under award number R01NS091056.

ACKNOWLEDGMENTS

The authors thank the staff at the James R. Gage Center for Gait & Motion Analysis at Gillette Children's Specialty Healthcare for their collaboration and insight. The authors also thank Benjamin Shuman, Alyssa Spomer, Andy Ries, and Andy Georgiadis for their valuable feedback and discussions.

SUPPLEMENTARY MATERIAL

The Supplementary Material for this article can be found online at: https://www.frontiersin.org/articles/10.3389/fnhum.2022.846205/full#supplementary-material

REFERENCES

Bekius, A., Bach, M. M., van der Krogt, M. M., de Vries, R., Buizer, A. I., and Dominici, N. (2020). Muscle synergies during walking in children with cerebral palsy: a systematic review. *Front. Physiol.* 11:632. doi: 10.3389/fphys.2020.00632

Bjornson, K. F., Zhou, C., Stevenson, R. D., and Christakis, D. (2014). Relation of stride activity and participation in mobility-based life habits among children with cerebral palsy. *Arch. Phys. Med. Rehabil.* 95, 360–368. doi: 10.1016/j.apmr.2013.10.022

Brewer, L. E., Wright, J. M., Rice, G., Neas, L., and Teuschler, L. (2017). Causal inference in cumulative risk assessment: the roles of directed acyclic graphs. *Environ. Int.* 102, 30–41. doi: 10.1016/j.envint.2016.12.005

Cahill-Rowley, K., and Rose, J. (2014). Etiology of impaired selective motor control: emerging evidence and its implications for research and treatment in cerebral palsy. *Dev. Med. Child Neurol.* 56, 522–528. doi: 10.1111/dmcn.12355

Chambers, H., Lauer, A., Kaufman, K., Cardelia, J. M., and Sutherland, D. (1998). Prediction of Outcome After Rectus Femoris Surgery in Cerebral Palsy: the role of cocontraction of the rectus femoris and vastus lateralis. *J. Pediatr. Orthop.* 18, 703–711.

Chipman, H. A., George, E. I., and McCulloch, R. E. B. A. R. T. (2010). Bayesian additive regression trees. *Ann. Appl. Stat. Insti. Math. Stat.* 4, 266–298.

Crane, L. (1959). Femoral torsion and its relation to toeing-in and toeing-out. *JBJS* 41, 421–428.

Damiano, D. L., Martellotta, T. L., Sullivan, D. J., Granata, K. P., and Abel, M. F. (2000). Muscle force production and functional performance in spastic cerebral

palsy: relationship of cocontraction. *Arch. Phys. Med. Rhabil.* 81, 895–900. doi: 10.1053/apmr.2000.5579

Desloovere, K. (2005). Pathophysiology, measurement, and treatment of spasticity in children. *Neuromodulation* 8, 187–189. doi: 10.1111/j.1525-1403.2005.05237-5.x

Dorie, V., Hill, J., Shalit, U., Scott, M., and Cervone, D. (2019). Automated versus do-it-yourself methods for causal inference: lessons learned from a data analysis competition. *Stat. Sci. Inst. Math. Stat.* 34, 43–68.

Fabry, G., Macewen, G. D., and Shands, A. Jr. (1973). Torsion of the Femur: a follow-up study in normal and abnormal conditions. *JBJS* 55, 1726–1738.

Fowler, E. G., Staudt, L. A., and Greenberg, M. B. (2010). Lower—extremity selective voluntary motor control in patients with spastic cerebral palsy: increased distal motor impairment. *Dev. Med. Child Neurol.* 52, 264–269. doi: 10.1111/j.1469-8749.2009.03586.x

Gage, J. R., Fabian, D., Hicks, R., and Tashman, S. (1984). Pre- and postoperative gait analysis in patients with spastic diplegia: a preliminary report. *J. Pediatr. Orthop.* 4, 715–725. doi: 10.1097/01241398-198411000-00012

Gage, J. R., and Novacheck, T. F. (2001). An update on the treatment of gait problems in cerebral palsy. *J. Pediatr. Orthop. B.* 10, 265–274.

Gage, J. R., Schwartz, M. H., Koop, S. E., and Novacheck, T. F. (2009). *The Identification and Treatment of Gait Problems in Cerebral Palsy*. Hoboken, NJ: John Wiley & Sons,

Galarraga, C. O. A., Vigneron, V., Dorizzi, B., Khouri, N., and Desailly, E. (2017). Predicting postoperative gait in cerebral palsy. *Gait Posture* 52, 45–51.

Gough, M., and Shortland, A. P. (2008). Can clinical gait analysis guide the management of ambulant children with bilateral spastic cerebral palsy? *J. Pediatr. Orthop.* 28, 879–883. doi: 10.1097/BPO.0b013e31818e197c

Gross, P. H., Bailes, A. F., Horn, S. D., Hurvitz, E. A., Kean, J., Shusterman, M., et al. (2018). Setting a patient—centered research agenda for cerebral palsy: a participatory action research initiative. *Dev. Med. Child Neurol.* 60, 1278–1284. doi: 10.1111/dmcn.13984

Hahn, P. R., Murray, J. S., and Carvalho, C. M. (2020). Bayesian regression tree models for causal inference: regularization, confounding, and heterogeneous effects (with Discussion). *Bayesian Anal.* 15, 965–1056.

Handsfield, G. G., Meyer, C. H., Abel, M. F., and Blemker, S. S. (2016). Heterogeneity of muscle sizes in the lower limbs of children with cerebral palsy. *Muscle Nerve Wiley Online Lib.* 53, 933–945. doi: 10.1002/mus.24972

Hicks, J. L., Delp, S. L., and Schwartz, M. H. (2011). Can biomechanical variables predict improvement in crouch gait? *Gait Posture* 34, 197–201. doi: 10.1016/j.gaitpost.2011.04.009

Hill, J. L. (2011). Bayesian nonparametric modeling for causal inference. *J. Comput. Graph. Stat. Taylor Francis* 20, 217–240.

Imbens, G. W., and Rubin, D. B. (2015). *Causal Inference in Statistics, Social, and Biomedical Sciences: an Introduction*. New York, NY: Cambridge University Press.

Johnston, T. E., Moore, S. E., Quinn, L. T., and Smith, B. T. (2004). Energy cost of walking in children with cerebral palsy: relation to the gross motor function classification system. *Dev. Med. Child Neurol.* 46, 34–38.

Kamp, F., Lennon, N., Holmes, L., Dallmeijer, A., Henley, J., and Miller, F. (2014). Energy cost of walking in children with spastic cerebral palsy: relationship with age, body composition and mobility capacity. *Gait Posture* 40, 209–214. doi: 10.1016/j.gaitpost.2014.03.187

Kapelner, A., and Bleich, J. (2016). bartMachine: Machine Learning with Bayesian Additive Regression Trees. *J. Stat. Softw.* 70, 1–40.

Kramer, J. F., and Ann MacPhail, H. E. (1994). Relationships among measures of walking efficiency, gross motor ability, and isokinetic strength in adolescents with cerebral palsy. *Pediatr. Phys. Ther.* 6, 3–9.

Lee, E. H., Goh, J. C., and Bose, K. (1992). Value of gait analysis in the assessment of surgery in cerebral palsy. *Arch Phys Med Rehabil. Elsevier* 73, 642–646.

Lee, S. H., Chung, C. Y., Park, M. S., Choi, I. H., and Cho, T.-J. (2009). Tibial torsion in cerebral palsy: validity and reliability of measurement. *Clin. Orthop. Relat. Res.* 467, 2098–2104. doi: 10.1007/s11999-009-0705-1

MacWilliams, B. A., Prasad, S., Shuckra, A. L., and Schwartz, M. H. (2020). Causal factors affecting gross motor function in children diagnosed with cerebral palsy. *medRxiv*. [Preprint] doi: 10.1101/2020.10.26.20217232

Massaad, A., Assi, A., Skalli, W., and Ghanem, I. (2014). Repeatability and validation of gait deviation index in children: typically developing and cerebral palsy. *Gait Posture.* 39, 354–358. doi: 10.1016/j.gaitpost.2013.08.001

Mathewson, M. A., and Lieber, R. L. (2015). Pathophysiology of muscle contractures in cerebral palsy. *Phys. Med. Rehabil. Clin.* 26, 57–67.

Miller, F., Castagno, P., Richards, J., Lennon, N., Quigley, E., and Niiler, T. (1996). Reliability of kinematics during clinical gait analysis: a comparison between normal and children with cerebral palsy. *Gait Posture* 4, 169–170.

Molnar, C., Bischl, B., and Casalicchio, G. (2018). iml: an R package for interpretable machine learning. *JOSS J. Open Source Softw.* 3, 786.

O'Brien, S. M., Carroll, T. J., Barber, L. A., and Lichtwark, G. A. (2021). Plantar flexor voluntary activation capacity, strength and function in cerebral palsy. *Eur. J. Appl. Physiol.* 121, 1733–1741. doi: 10.1007/s00421-021-04638-z

O'Dwyer, N. J., Neilson, P. D., and Nash, J. (1989). Mechanisms of muscle growth related to muscle contracture in cerebral palsy. *Dev. Med. Child Neurol.* 31, 543–547. doi: 10.1111/j.1469-8749.1989.tb04034.x

Pearl, J. (1995). Causal diagrams for empirical research. *Biometrika* 82, 669–688.

Pearl, J. (2009). Causal inference in statistics: an overview. *Stat. Surv.* 3, 96–146.

R Core Team (2021). *R: A Language and Environment for Statistical Computing [Internet]*. Vienna: R Foundation for Statistical Computing.

Rajagopal, A., Kidziński, Ł, McGlaughlin, A. S., Hicks, J. L., Delp, S. L., and Schwartz, M. H. (2018). Estimating the effect size of surgery to improve walking in children with cerebral palsy from retrospective observational clinical data. *Sci. Rep.* 8:16344. doi: 10.1038/s41598-018-33962-2

Rose, J., Gamble, J. G., Medeiros, J., Burgos, A., and Haskell, W. L. (1989). Energy cost of walking in normal children and in those with cerebral palsy: comparison of heart rate and oxygen uptake. *J. Pediatr. Orthop.* 9, 276–279.

Ross, S. A., and Engsberg, J. R. (2007). Relationships between spasticity, strength, gait, and the GMFM-66 in persons with spastic diplegia cerebral palsy. *Arch. Phys. Med. Rehabil.* 88, 1114–1120. doi: 10.1016/j.apmr.2007.06.011

Schwartz, M. H., and Rozumalski, A. (2008). The gait deviation index: a new comprehensive index of gait pathology. *Gait Posture* 28, 351–357. doi: 10.1016/j.gaitpost.2008.05.001

Schwartz, M. H., Rozumalski, A., and Steele, K. M. (2016). Dynamic motor control is associated with treatment outcomes for children with cerebral palsy. *Dev. Med. Child Neurol.* 58, 1139–1145. doi: 10.1111/dmcn.13126

Shin, H.-I., Sung, K. H., Chung, C. Y., Lee, K. M., Lee, S. Y., Lee, I. H., et al. (2015). Relationships between isometric muscle strength, gait parameters, and gross motor function measure in patients with cerebral palsy. *Yonsei. Med. J.* 57, 217–224.

Shore, B. J., Yu, X., Desai, S., Selber, P., Wolfe, R., and Graham, H. K. (2012). Adductor surgery to prevent hip displacement in children with cerebral palsy: the predictive role of the gross motor function classification system. *JBJS* 94, 326–334.

Shrier, I., and Platt, R. W. (2008). Reducing bias through directed acyclic graphs. *BMC Med. Res. Methodol.* 8:70. doi: 10.1186/1471-2288-8-70

Shuman, B. R., Goudriaan, M., Desloovere, K., Schwartz, M. H., and Steele, K. M. (2018). Associations between muscle synergies and treatment outcomes in cerebral palsy are robust across clinical centers. *Arch. Phys. Med. Rehabil.* 99, 2175–2182. doi: 10.1016/j.apmr.2018.03.006

Shuman, B. R., Schwartz, M. H., and Steele, K. M. (2017). Electromyography data processing impacts muscle synergies during gait for unimpaired children and children with cerebral palsy. *Front. Comput. Neurosci.* 11:50. doi: 10.3389/fncom.2017.00050

Steele, K. M., Rozumalski, A., and Schwartz, M. H. (2015). Muscle synergies and complexity of neuromuscular control during gait in cerebral palsy. *Dev. Med. Child Neurol.* 57, 1176–1182. doi: 10.1111/dmcn.12826

Steinwender, G., Saraph, V., Scheiber, S., Zwick, E. B., Uitz, C., and Hackl, K. (2000). Intrasubject repeatability of gait analysis data in normal and spastic children. *Clin. Biomech.* 15, 134–139. doi: 10.1016/s0268-0033(99)00057-1

Sullivan, K., Richards, J., Miller, F., Castagno, P., and Lennon, N. (1995). Predicting the outcome of surgery for children with cerebral palsy using pre-operative gait analysis. *Gait Posture* 2:92.

Tan, Y. V., and Roy, J. (2019). Bayesian additive regression trees and the General BART model. *ArXiv190107504 Stat* [Preprint] Available online at: http://arxiv.org/abs/1901.07504 (accessed July 27, 2021), doi: 10.1002/sim.8347

Textor, J., van der Zander, B., Gilthorpe, M. S., Liśkiewicz, M., and Ellison, G. T. (2016). Robust causal inference using directed acyclic graphs: the R package 'dagitty.'. *Int. J. Epidemiol.* 45, 1887–1894. doi: 10.1093/ije/dyw341

van Buuren, S., and Groothuis-Oudshoorn, C. G. M. (2011). mice: Multivariate imputation by chained equations in R. *J. Stat. Softw.* 45, 1–67. doi: 10.3978/j.issn.2305-5839.2015.12.63

Verma, T., and Pearl, J. (1991). *Equivalence and Synthesis of Causal Models*. Los Angeles, CA: UCLA, Computer Science Department.

Williams, T. C., Bach, C. C., Matthiesen, N. B., Henriksen, T. B., and Gagliardi, L. (2018). Directed acyclic graphs: a tool for causal studies in paediatrics. *Pediatr. Res.* 84, 487–493. doi: 10.1038/s41390-018-0071-3

Author Disclaimer: The content is solely the responsibility of the authors and does not necessarily represent the official views of the National Institutes of Health.

Conflict of Interest: The authors declare that the research was conducted in the absence of any commercial or financial relationships that could be construed as a potential conflict of interest.

frontiers | Frontiers in Human Neuroscience

TYPE Original Research
PUBLISHED 04 August 2022
DOI 10.3389/fnhum.2022.797282

OPEN ACCESS

EDITED BY
Carmelo Chisari,
Pisana University Hospital, Italy

REVIEWED BY
Keonyoung Oh,
Shirley Ryan AbilityLab, United States
Miao Yu,
Peking University Third Hospital, China

*CORRESPONDENCE
Susanna Summa
susanna.summa@opbg.net

SPECIALTY SECTION
This article was submitted to Motor Neuroscience, a section of the journal Frontiers in Human Neuroscience

RECEIVED 18 October 2021
ACCEPTED 15 July 2022
PUBLISHED 04 August 2022

CITATION
Favetta M, Romano A, Summa S, Colazza A, Minosse S, Vasco G, Castelli E and Petrarca M (2022) Influence of sagittal pelvic attitude on gait pattern in normally developed people and interactions with neurological pathologies: A pilot study. *Front. Hum. Neurosci.* 16:797282. doi: 10.3389/fnhum.2022.797282

Influence of sagittal pelvic attitude on gait pattern in normally developed people and interactions with neurological pathologies: A pilot study

Martina Favetta[1], Alberto Romano[1], Susanna Summa[1]*, Alessandra Colazza[1], Silvia Minosse[1,2], Gessica Vasco[1], Enrico Castelli[1] and Maurizio Petrarca[1]

[1]Department of Neurorehabilitation and Robotics, Movement Analysis and Robotics Laboratory (MARLab), "Bambino Gesù" Children's Hospital, IRCCS, Rome, Italy, [2]Department of Biomedicine and Prevention, University of Rome "Tor Vergata", Rome, Italy

Background: Gait Analysis of healthy people, imitating pathological conditions while walking, has increased our understanding of biomechanical factors. The influence of the pelvis as a biomechanical constraint during gait is not specifically studied. How could mimicking a pelvic attitude influence the dynamic mechanical interaction of the body segments? We proposed an investigation of the pelvic attitude role on the gait pattern of typically developed people when they mimicked pelvic anteversion and posteroversion.

Materials and methods: Seventeen healthy volunteers were enrolled in this study (mean age 24.4 ± 5.5). They simulated a pelvic anteversion and posteroversion during walking, exaggerating these postures as much as possible. 3D gait analysis was conducted using an optoelectronic system with eight cameras (Vicon MX, Oxford, United Kingdom) and two force plates (AMTI, Or-6, Watertown, MA, United States). The kinematic, kinetic, and spatio-temporal parameters were compared between the three walking conditions (anteversion, posteroversion, and normal gait).

Results: In Pelvic Anteversion gait (PA) we found: increased hip flexion ($p < 0.0001$), increased knee flexion during stance ($p = 0.02$), and reduction of ankle flexion-extension Range of Motion (RoM) compared with Pelvic Normal gait (PN). In Pelvic Posteroversion gait (PP) compared with PN, we found: decreased hip flexion-extension RoM ($p < 0.01$) with a tendency to hip extension, decreased knee maximum extension in stance ($p = 0.033$), and increased ankle maximum dorsiflexion in stance ($p = 0.002$).

Conclusion: The configuration of PA contains gait similarities and differences when compared with pathologic gait where there is an anteversion as seen in children with Cerebral Palsy (CP) or Duchenne Muscular Dystrophy (DMD). Similarly, attitudes of PP have been described in

patients with Charcot-Marie-Tooth Syndrome (CMT) or patients who have undergone Pelvic Osteotomy (PO). Understanding the dynamic biomechanical constraints is essential to the assessment of pathological behavior. The central nervous system adapts motor behavior in interaction with body constraints and available resources.

KEYWORDS

gait deviations, biomechanics, gait mimicking, pelvic anteversion, pelvic posteroversion

Introduction

The relationship between biomechanical constraints and neuromuscular systems in patients with cerebral palsy is not clear even if it is crucial knowledge in rehabilitation and surgery (Blumetti et al., 2019; Davids et al., 2019). In the simulated toe-walking, crouch, and crouch/equinus gait, Thomas et al. (1996) described a decrease in both walking velocity and stride length which correlated with the increase in the number of joints involved. This pattern is also seen in patients with Cerebral Palsy (CP) (Sutherland and Davids, 1993).

Romkes and Brunner (2007) highlighted that the Gait Analysis (GA) patterns at ankle level, in healthy subjects mimicking hemiplegic walking, are similar to those of children with hemiplegic CP. Drefus et al. (2016) underlined that the knee and ankle kinematics are linked, in the absence of hamstring spasticity or contracture. Furthermore, the study of Davids et al. (1999) showed that the decrease in walking velocity and length of stride as well as the increased pelvic anteversion are similar in voluntary and obligatory toe walking.

Holt et al. (2000) suggested that, in subjects with CP, the available dynamic resources determine the walking strategies constrained by biomechanical solutions. In this perspective, the relationship between central and peripheral resources is mutual and not discernible (Crenna, 1998). That is, it is possible that the pattern is determined by biomechanical constraints related to changes in the peripheral resources available, while muscle activities act on the fine tuning of the movement.

Romkes and Brunner (2007) described differences in EMG patterns of the rectus femoris muscle between the toe walkers and the mimicking controls, and therefore, this activity is considered an entirely pathological primary deviation. Although this muscle has a proximal insertion on the pelvis, the authors did not control the pelvis in their study and consequently, their conclusions concerning the role of the rectus femoris need more detailed study. Amori et al. (2015) reported that the pelvis can act as the reference frame to achieve body standing balance during 3D postural perturbation.

Other studies investigated the pelvic obliquity and rotational restriction using a robot walker. It altered gait dynamics reducing stride length, gait velocity, and increasing the percentage of the stance phase. Furthermore, the pelvic restrictions caused limited ankle plantarflexion at the terminal stance, knee flexion at mid-swing and hip extension at mid-stance, contributing to the reduction of RoMs in all of the joints of the lower limbs (Mun et al., 2016). Another study (Alingh et al., 2019) investigated the immediate after-effect of robot-assisted gait with pelvic support or pelvic rotational constraint on overground walking in healthy adults. These authors showed that robot-assisted gait training with pelvic constraint has an immediate negative after-effect on the overground walking pattern in healthy subjects, while the robot-assisted gait training with pelvic support better resembles the natural gait pattern. Therefore, it is known that a fixation of the pelvis severely affects gait dynamics.

The development of exoskeleton allowed the creation of systems of biomechanical constraints externally imposed. In any case, the limit of these studies is that the imposed constraints did not allow the simulation of the pathological condition nor investigated the pelvis tilt.

The influence of the pelvis tilt as a biomechanical constraint during gait using *in vivo* simulation is not specifically studied. In our study, we propose to extend the previously mentioned research objectives to include the role of pelvic tilt attitude in the gait pattern of normally developed people mimicking pelvic anteversion and posteroversion. Kinematic, kinetic, and spatio-temporal parameters were compared, using 3D gait analysis, to identify the adopted strategies in the biomechanical challenge. These observations could improve our understanding of the effect of biomechanics on pathologic gait evolution useful for rehabilitation and surgery decision making. In this study, we recruited young adults because we needed their collaboration to perform precise biomechanical simulations. The correct imitation of a gait pattern is difficult to obtain with younger children. Furthermore, the gait pattern generally stabilizes at around 7 years of age (Sutherland, 1997).

Materials and methods

Participants

Seventeen healthy volunteers were enrolled in this study (12 females, 5 males; mean age 24.4 ± 5.5, range 12-31; mean height

164.7 ± 11.9; mean mass 58.8 ± 11.8). Selection criteria included no prior cardiovascular history, neurological or musculoskeletal disorders that would influence gait. All subjects agreed to participate in the study. The study was conducted in respect of the Helsinki declaration.

Experimental set up

Seventeen healthy participants simulated a pelvic anteversion and posteroversion during walking, exaggerating the postures as much as possible. Each participant had their own time to learn and adapt. Data gathering started when they reached a stable behavior. All subjects were naïve to pathological gait characteristics. 3D gait analysis was conducted using an optoelectronic system with eight cameras (Vicon MX, Oxford, United Kingdom), two force plates (AMTI, Or-6, Watertown, MA, United States) hidden in the middle section of a 12-meter walkway and a synchronic video system to assist clinical interpretation of data. The sampling rate was set at 200 Hz for the motion capture system and at 1,000 Hz for the two force plates. The kinematic and kinetic full-body models were reconstructed using the plug-in gait protocol (Davis et al., 1991; Benedetti et al., 2017; Schirinzi et al., 2018). We asked three subjects to perform the experiment. An experienced clinician verified the feasibility and solidity of the responses before increasing the study sample. Participants were asked to walk barefoot at their natural cadence and self-selected comfortable speed. The pelvic angle was controlled ongoing using the real-time tilt plotting guaranteed by our 3D gait analysis system. The participants didn't receive any feedback or further instructions. Only when the participants reached a stable behavior we became the acquisition. Ten trials were collected after two or more familiarization tests for each of the three conditions (natural gait and gait with pelvis in anteversion and in posteroversion in a random distribution between the participants). Participants performed the test without compensation of the trunk and the upper body as shown in **Figure 1**. The analysis involved kinematic, kinetic and spatio-temporal parameters. We looked at the sagittal, frontal, and transversal plane of each lower limb joint. We extracted clinical parameters: Range of Motion (RoM), mean, Initial Contact (IC), and peak values of the angle joints, moments and powers. Furthermore, we studied the foot progress angle (FPA), i.e., the angle of the foot in respect to the direction of progression. Kinematic and kinetic temporal series were normalized to the stride duration. Kinetic data were normalized to subject's weight. Average values of three consistent trials were analyzed for each condition and each participant. The consistent trials were determined by expert operators with over 30 years of experience in clinical instrumented gait analysis. The trials were selected by watching videos and choosing the tests in which the subject was more natural in performing the motor task. All parameters were evaluated separately for the two limbs. Given the non-variability between the two body sides, we calculated the average between the two contests.

Data analysis

The extraction of clinical parameters and the determination of the significant differences between the three conditions were performed. Shapiro-Wilk and Bartlett tests were used to verify, respectively, if the parameters were normally distributed and if the variance was uniform. If the assumptions of normality and of homogeneity of variances were verified, one-way ANOVA was performed. If these assumptions were not verified, we ran the Kruskal-Wallis test. The Bonferroni *post-hoc* analysis was applied to verify which pairs of groups differ significantly. A $p < 0.05$ was considered to indicate statistical significance.

Results

Descriptive statistics for all the spatio-temporal, kinematic, and kinetic parameters for the three different evaluations and comparisons between the three walking conditions are reported in **Supplementary Table 1**. Kinematic graphs are shown in **Figure 2**. Kinetic graphs are illustrated in **Figure 3**.

Pelvic anteversion gait vs. pelvic normal gait

Walking in pelvic anteversion, subjects showed a significant decrease of the step length ($p = 0.019$), stride time ($p = 0.042$), and stride length ($p = 0.014$) compared with PN; there were no significant differences in walking velocity and double support time.

The kinematics of the lower limbs in PA showed a significant increase in the mean value of pelvic movement on the sagittal plane ($p = 0.001$) and a significant increase of pelvic tilt RoM ($p < 0.0001$). The pelvic obliquity RoM was reduced ($p = 0.009$). The hip showed a significant increase of flexion ($p < 0.001$) throughout the gait cycle. At knee level, we observed a reduction of flexion-extension RoM ($p = 0.005$) and increased maximum knee flexion during stance ($p = 0.02$). The ankle showed a decrease of flexion-extension RoM ($p = 0.009$) compared to PN. In PA, kinetic data showed a significant reduction of hip maximum extension moment ($p = 0.007$), an increase of hip maximum flexion moment ($p < 0.001$) and an increase of hip positive work ($p = 0.008$).

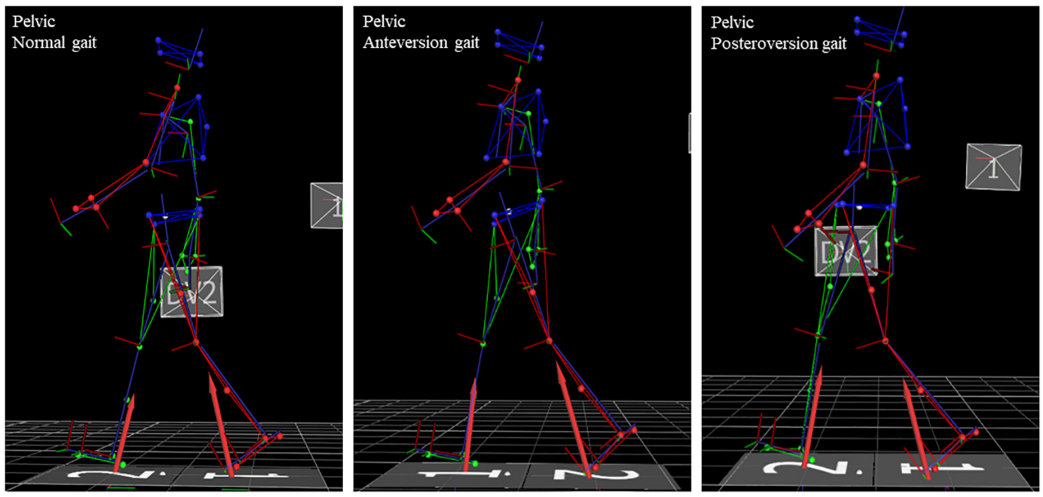

FIGURE 1
Full body reconstruction 3D gait analysis of the three conditions of experiment.

Pelvic posteroversion gait vs. pelvic normal gait

Walking in pelvic posteroversion, subjects showed a significant decrease of velocity ($p = 0.032$), step length ($p < 0.001$), and stride length ($p < 0.0001$) compared with PN; there were no significant differences in double support time.

With respect to the kinematic lower limb values, in PP we found a significant increase of pelvic tilt RoM ($p = 0.004$) with reduction of the mean value ($p = 0.013$). At hip level, we observed a significant decrease of flexion at the initial contact ($p = 0.001$) and during the entire gait cycle ($p < 0.0001$), and a reduction of flexion-extension RoM ($p < 0.01$). The knee showed a significant decrease of the maximum extension in stance ($p = 0.033$), which is also anticipated ($p = 0.002$) compared to PN. At ankle level, we observed an increase of the maximum dorsiflexion in stance ($p = 0.002$). The kinetic data in PP showed a reduction of knee extension moment value ($p = 0.001$) and an increase of ankle positive work ($p < 0.001$; $p < 0.05$) compared with PN.

Pelvic anteversion gait vs. pelvic posteroversion gait

For subjects simulating pelvic anteversion we observed: a decrease of the stance time percentage in the gait cycle ($p = 0.025$), a higher gait velocity ($p = 0.033$), and a decrease of the double support ($p = 0.006$) compared to PP. There were no significant changes in the step and stride length.

With respect to the kinematic lower limb values, in PA we found: an increase of the pelvic tilt mean ($p < 0.0001$), a decrease of pelvis obliquity at IC ($p = 0.047$), an increase of hip flexion during the gait cycle ($p < 0.0001$) and also at the IC ($p < 0.0001$), a reduction of hip abduction/adduction RoM ($p < 0.001$), an increase of hip maximum flexion ($p < 0.0001$), a decrease of hip maximum extension ($p < 0.0001$), and a decrease of maximum abduction ($p = 0.01$) compared with PP. There were no significant differences in knee kinematics between the two walking conditions. The ankle in PA showed a reduction of ankle flexion-extension RoM ($p < 0.001$) and a reduction of the ankle maximum dorsiflexion in stance ($p < 0.01$) compared to PP. Finally, PA is characterized by a greater intrarotation of foot progression angle (FPA) ($p < 0.001$), while in PP we observed a greater extrarotation. The kinetic data in PA showed a decrease of hip maximum extension moment in stance ($p < 0.0001$), an increase of hip maximum flexion moment ($p < 0.001$), an increase of hip positive work ($p < 0.01$), and a decrease of the ankle peak value of power generated ($p < 0.01$) with the reduction of ankle positive work ($p < 0.01$) compared to PP.

Discussion

Pelvic anteversion

The results reveal that the configuration of gait pattern induced by mimicking pelvic anteversion contains certain gait similarities and differences when compared with the pathological gait seen in children with Cerebral Palsy (Johnson et al., 1997; Bell et al., 2002; Petrarca et al., 2006; Armand et al., 2016) or with Duchenne Muscular Dystrophy (D'Angelo et al., 2009; Sienko Thomas et al., 2010; Goudriaan et al., 2018).

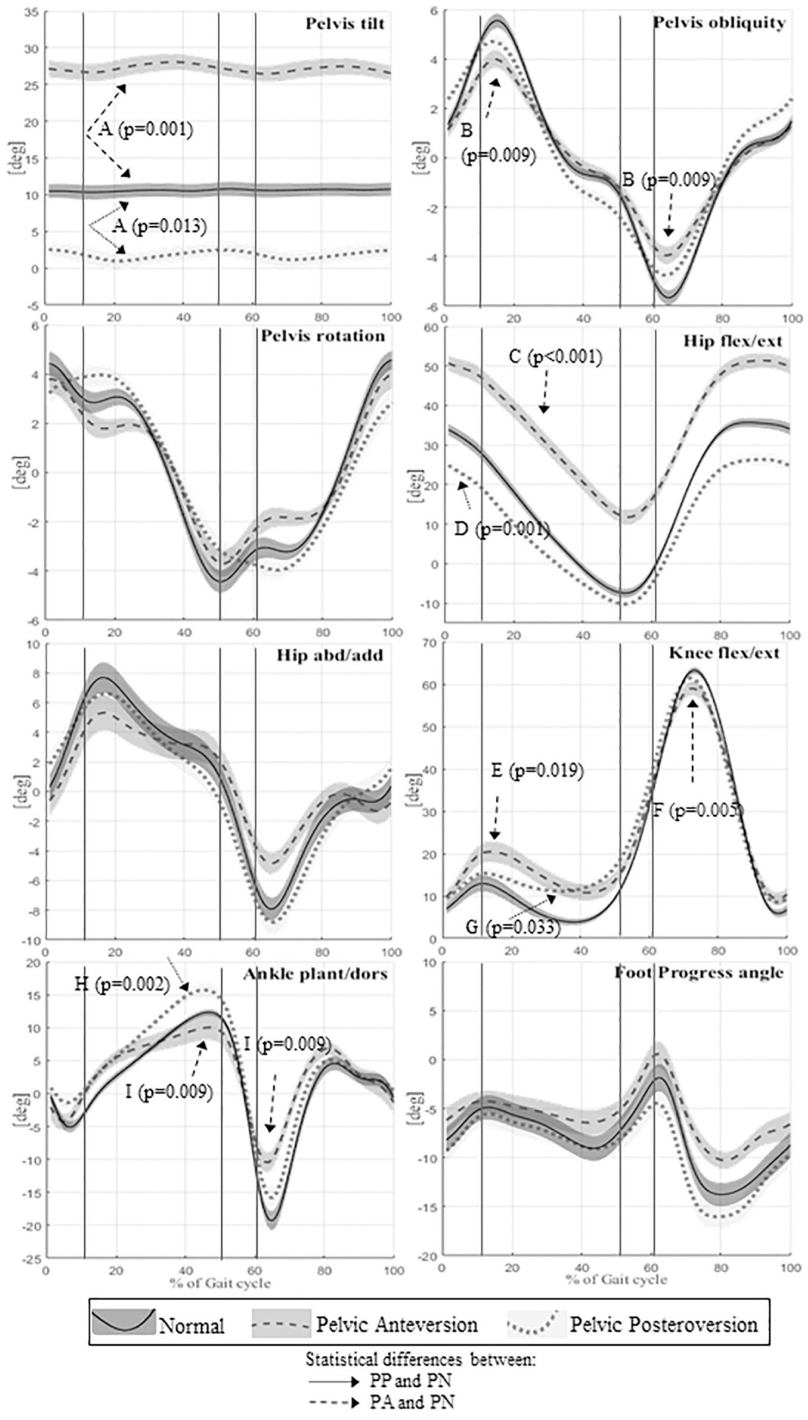

FIGURE 2
Means and standard deviation of kinematics angles of lower limb joint movements on the sagittal plane of the whole sample; the angles of the pelvic tilt, rotation and obliquity; the angles on frontal plane of hip and ankle. The angles of joint rotation in degrees are reported on the vertical axis, the time of the gait cycle in percentage is reported on the horizontal axis. Continuous lines represent averaged group value of Normal gait (PN), dashed lines represent averaged group value of Pelvic Anteversion gait (PA), dotted lines represent averaged group value of Pelvic Posteroversion gait (PP). The shaded areas denote the standard deviation (SD), dark gray, normal gray, and light gray stand respectively for Normal, Anteversion, and Posteroversion. The three lines separate the first double support phase (first line), the single support phase (second line), and the second double support phase (third line). Dashed arrows represent statistical differences between PA and PN, dotted arrows represent statistical differences between PP and PN. A (Pelvis tilt mean), B (Pelvis obliquity RoM), C (Hip flexion/extension mean), D (Hip flexion/extension IC), E (Knee max flexion in stance), F (Knee flexion/extension RoM), G (Knee max extension in stance), H (Ankle max dorsiflexion instance), I (Ankle flexion/extension RoM).

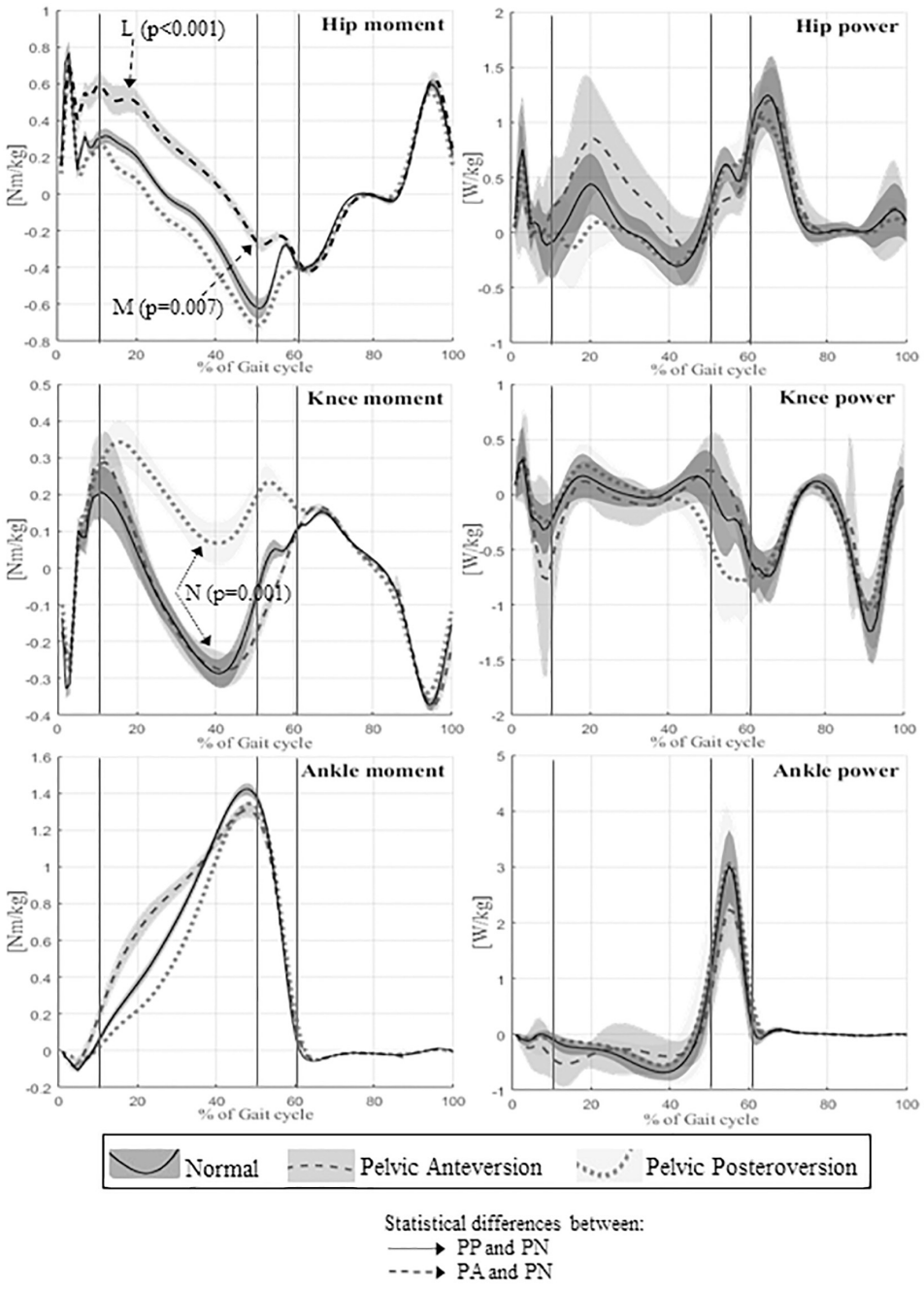

FIGURE 3
Means and standard deviation of kinetics of lower limbs joints of the whole sample (on the left panel: hip, knee, ankle moments; on the right panel: hip, knee, and ankle powers). The units of measure are reported on vertical axis, the time of gait cycle in percentage on the horizontal axis. Continuous lines represent averaged group value of Normal gait, dashed lines represent averaged group value of Pelvic Anteversion gait, and dotted lines represent averaged group value of Pelvic Posteroversion gait. The shaded areas denote the standard deviation (SD), dark gray, normal gray, and light gray stand respectively for Normal, Anteversion, and Posteroversion. The three lines separate the first double support phase (first line), the single support phase (second line), and the second double support phase (third line). Dashed arrows represent statistical differences between PA and PN, dotted arrows represent statistical differences between PP and PN. L (Hip maximum flexion moment), M (Hip max extension moment), N (Knee extension moment).

Cerebral palsy gait vs. pelvic anteversion gait

Similarities: shorter stride and step length (Johnson et al., 1997), increase of anterior pelvic tilt, increase of hip flexion, increase of knee flexion during stance (Armand et al., 2016), reduction of knee sagittal RoM, reduction of ankle sagittal RoM (Bell et al., 2002).

Differences: in healthy subjects mimicking gait with anteversion we did not find: reduction of gait velocity (Johnson et al., 1997), decrease of knee flexion during swing phase, loss of the first heel rocker at initial contact, increased plantarflexion in stance and swing (Bell et al., 2002; Armand et al., 2016). However, even if these parameters differ from those of subjects with CP, it is interesting to observe that they show a tendency, not statistically significant, toward the pathologic gait. Similarly, the PA shows a tendency to increased ankle dorsiflexion moment and to decreased ankle dorsiflexion in late stance.

Duchenne muscular dystrophy gait vs. pelvic anteversion gait

Similarities: decrease of walking speed, reduction of step and stride length, and more evident hip flexion in terminal swing (D'Angelo et al., 2009).

Differences: the gait of patients with DMD also presents increased knee extension in stance, absence of extensor knee moment (D'Angelo et al., 2009), increased knee flexion in swing. This variability of movement in the kinematics of the knee contributed to the increase in total knee range of motion (Goudriaan et al., 2018). There is an increase in ankle dorsiflexion during early stance, a decrease in dorsiflexion during late stance, and an increase in plantarflexion during swing. The kinetics of the DMD gait shows a lower power generation at the hip (Goudriaan et al., 2018).

Pelvic posteroversion

Similarly, the gait pattern induced by mimicking pelvic posteroversion presented gait similarities and differences when compared with the gait of patients exhibiting posteroversion as seen in children with Charcot-Marie-Tooth Syndrome (Don et al., 2007; Newman et al., 2007; Ferrarin et al., 2012) or in children who have undergone pelvic osteotomy (Petrarca et al., 2014).

Charcot-marie-tooth gait vs. pelvic posteroversion gait

Similarities: lower gait velocity, decrease of step length, increased hip extension during stance, reduction of hip flexion during swing, increased knee flexion during stance, and greater ankle dorsiflexion during stance (Don et al., 2007). The increase in ankle dorsiflexion needs to be coordinated with a greater hip extension in order to preserve progression and balance.

Differences: CMT gait also presents an increase of hip RoM (Ferrarin et al., 2012), while an increase of the peak knee flexion in swing is only seen in some sub-clusters of CMT. Moreover, there is usually greater ankle plantar flexion at initial contact, a foot drop in swing phase (Ferrarin et al., 2012) and a low value of the ankle plantar flexion during final stance (Don et al., 2007); our sample however showed only a tendency of no statistical significance. Ankle power production is higher at mid-stance, and again intriguingly, our sample showed a tendency of no statistical significance. The hip extensor moment and power production during stance are increased (Ferrarin et al., 2012).

Pelvic osteotomy vs. pelvic posteroversion gait

Similarities: reduced gait velocity, reduced pelvic anteversion, increased knee flexion during stance phase, and reduction of knee extensor moment during stance (Petrarca et al., 2014).

Differences: reduced dorsal moment at the ankle (Petrarca et al., 2014), although, in our sample, it is only a tendency with no statistical significance.

Assessing pathological behavior through dynamic biomechanical constraints

We can hypothesize that the similarities found between CP/PA-DMD/PA and CMT/PP-PO/PP are due to the biomechanical constraints of the body, while the differences are related to the pathological condition. Indeed, in CP excessive plantar flexion is caused by spasticity or deficits in selective motor control (Johnson et al., 1997; Crenna, 1998). In DMD the knee extension in stance compensates for the weakness of the quadriceps in order to improve balance and maintain body stability, the increased knee flexion in swing is required for the clearance of the foot to avoid tripping or falling due to excessive plantar flexion during swing (D'Angelo et al., 2009; Goudriaan et al., 2018). Muscle weakness of the dorsiflexors could cause the ankle kinematics described (Goudriaan et al., 2018). Weakness of the hip extensor could explain the lower power generation at the hip, resulting in a pelvic anterior tilt and a more flexed position of the hip (Goudriaan et al., 2018).

In CMT gait, the hip extensor moment and power production during stance are related to a greater activation of hip extensor muscles (Ferrarin et al., 2012). The mechanism used to prevent tripping is increased hip abduction and pelvic elevation at the swing time which prolongs activation of the gluteus medium muscle (Don et al., 2007).

Previous studies evaluated toe walker patients affected by CP and healthy subjects simulating toe walking (Davids et al., 1999; Romkes and Brunner, 2007; Rezgui et al., 2013). These researchers focused on examining descriptors of CP gait deviations that may be considered as primary or compensatory deviations.

The results of our study would seem to indicate an inseparable link between the kinematic gait deviations and the underlying neuromuscular pathology, which needs to be considered in a framework of continuous interactions. These interactions seem to induce a central nervous system reorganization producing new strategies

during a process of searching for the best adaptive solution. The tools at our disposal do not allow us to distinguish the impact of damage to the nervous system from the contribution of biomechanical adaptations (Crenna, 1998; Holt et al., 2000). In addition to this limitation of our knowledge, there is also the lack of a universally accepted theoretical framework concerning bipedal gait (Vaughan, 2003).

This study could support the hypothesis that the pelvis plays a key role in linking the locomotor system and the upper body (Amori et al., 2015). Furthermore, it is also known that the pelvis attitude can play a role in the foot-terrain coupling, especially in pathological condition when the control on the foot is limited by the neurological lesion. In that case, a little adjustment in retroversion of the pelvis can compensate a reduced dorsiflexion of the foot allowing the recovery of the three rockers of the foot during the stance phase (Petrarca et al., 2011). Exploiting the reciprocal influence described, seems to face new clinical opportunities during assessment and training of the function. Changing its attitude in the sagittal plane, we modified the biomechanical configuration of the body, stopping the exploitation of the body's degree of freedom in an interaction between the biomechanical configurations and the solutions of motor control. In fact, although the pathological conditions open a process of function redefinition, it is clear from this study that PA leads toward an increase of hip work and PP toward an increase of ankle work.

These two gait conditions showed some motor behaviors that resemble some characteristics of the pathological gait, even if they were not statistically significant. We speculated that specific configurations need time to emerge. Therefore, a possible limitation of this paper is the sudden collection of gait data, not giving the subject enough time to adapt to the new motor configuration; with time and training the tendency could become a new stable solution. Furthermore, these findings can be considered as preliminary data resulting from limited size of participants.

Finally, we can hypothesize that the pathological condition stops the full exploitation of the body's degrees of freedom that contribute to limit the process of research of adaptive solutions. The process of recovering the function could reopen the exploitation of new adaptive solutions by including new biomechanical configurations in a personalized trial-and-error learning method.

Data availability statement

The original contributions presented in this study are included in the article/**Supplementary material**, further inquiries can be directed to the corresponding author.

Ethics statement

The studies involving human participants were reviewed and approved by Bambino Gesù Children's Hospital Ethical Committee. The patients/participants provided their written informed consent to participate in this study.

Author contributions

MF performed acquisition and interpretation of data, organized database, and wrote the first draft of the manuscript. AR contributed to acquisition and interpretation of data. SS performed data analysis and statistical analysis. AC contributed to acquisition of data. SM contributed to data analysis. GV and EC revised the manuscript critically for intellectual content. MP achieved conception and design of the study, interpretation of data, drafting the work, and review and editing. All authors contributed to manuscript revision, read, and approved the submitted version.

Acknowledgments

We thank the subjects for their time and willingness to participate in this study. We are grateful to the Grant Office of Bambino Gesù Children's Hospital.

Conflict of interest

The authors declare that the research was conducted in the absence of any commercial or financial relationships that could be construed as a potential conflict of interest.

Publisher's note

Supplementary material

The Supplementary Material for this article can be found online at: https://www.frontiersin.org/articles/10.3389/fnhum.2022.797282/full#supplementary-material

References

Alingh, J. F., Weerdesteyn, V., Nienhuis, B., Van Asseldonk, E. H. F., Geurts, A. C. H., and Groen, B. E. (2019). Immediate after-effects of robot-assisted gait with pelvic support or pelvic constraint on overground walking in healthy subjects. *J. Neuroeng. Rehabil.* 16, 1–10. doi: 10.1186/s12984-019-0506-z

Amori, V., Petrarca, M., Patané, F., Castelli, E., and Cappa, P. (2015). Upper body balance control strategy during continuous 3D postural perturbation in young adults. *Gait Posture* 41, 19–25. doi: 10.1016/j.gaitpost.2014.08.003

Armand, S., Decoulon, G., and Bonnefoy-Mazure, A. (2016). Gait analysis in children with cerebral palsy. *EFORT Open Rev.* 1, 448–460. doi: 10.1302/2058-5241.1.000052

Bell, K. J., Õunpuu, S., DeLuca, P. A., and Romness, M. J. (2002). Natural progression of gait in children with cerebral palsy. *J. Pediatr. Orthop.* 22, 677–682. doi: 10.1097/01241398-200209000-00020

Benedetti, M. G., Beghi, E., De Tanti, A., Cappozzo, A., Basaglia, N., Cutti, A. G., et al. (2017). SIAMOC position paper on gait analysis in clinical practice: general requirements, methods and appropriateness. Results of an Italian consensus conference. *Gait Posture* 58, 252–260. doi: 10.1016/j.gaitpost.2017.08.003

Blumetti, F. C., Wu, J. C. N., Barzi, F., Axt, M. W., Waugh, M. C., and Selber, P. (2019). Orthopaedic surgery in dystonic cerebral palsy. *J. Pediatr. Orthop.* 39, 209–216. doi: 10.1097/BPO.0000000000000919

Crenna, P. (1998). Spasticity andspastic'gait in children with cerebral palsy. *Neurosci. Biobehav. Rev.* 22, 571–578.

D'Angelo, M. G., Berti, M., Piccinini, L., Romei, M., Guglieri, M., Bonato, S., et al. (2009). Gait pattern in Duchenne muscular dystrophy. *Gait Posture* 29, 36–41. doi: 10.1016/j.gaitpost.2008.06.002

Davids, J. R., Cung, N. Q., Chen, S., Sison-Williamson, M., and Bagley, A. M. (2019). Control of walking speed in children with cerebral palsy. *J. Pediatr. Orthop.* 39, 429–435. doi: 10.1097/BPO.0000000000000978

Davids, J. R., Foti, T., Dabelstein, J., and Bagley, A. (1999). Voluntary (normal) versus obligatory (cerebral palsy) toe-walking in children: a kinematic, kinetic, and electromyographic analysis. *J. Pediatr. Orthop.* 19, 461–469. doi: 10.1097/01241398-199907000-00008

Davis, R. B., Ounpuu, S., Tyburski, D., and Gage, J. R. (1991). A gait analysis data collection and reduction technique.pdf. *Hum. Mov. Sci.* 10, 575–597. doi: 10.1016/0167-9457(91)90046-Z

Don, R., Serrao, M., Vinci, P., Ranavolo, A., Cacchio, A., Ioppolo, F., et al. (2007). Foot drop and plantar flexion failure determine different gait strategies in Charcot-Marie-Tooth patients. *Clin. Biomech.* 22, 905–916. doi: 10.1016/j.clinbiomech.2007.06.002

Drefus, L. C., Hafer, J. F., and Scher, D. M. (2016). Simulated ankle equinus affects knee kinematics during gait. *HSS J.* 12, 39–43. doi: 10.1007/s11420-015-9474-4

Ferrarin, M., Bovi, G., Rabuffetti, M., Mazzoleni, P., Montesano, A., Pagliano, E., et al. (2012). Gait pattern classification in children with Charcot-Marie-Tooth disease type 1A. *Gait Posture* 35, 131–137. doi: 10.1016/j.gaitpost.2011.08.023

Goudriaan, M., Van den Hauwe, M., Dekeerle, J., Verhelst, L., Molenaers, G., Goemans, N., et al. (2018). Gait deviations in Duchenne muscular dystrophy—Part 1. A systematic review. *Gait Posture* 62, 247–261. doi: 10.1016/j.gaitpost.2018.03.020

Holt, K. G., Fonseca, S. T., and Lafiandra, M. E. (2000). The dynamics of gait in children with spastic hemiplegic cerebral palsy: theoretical and clinical implications. *Hum. Mov. Sci.* 19, 375–405. doi: 10.1016/S0167-9457(00)00019-1

Johnson, D. C., Damiano, D. L., and Abel, M. F. (1997). The evolution of gait in childhood and adolescent cerebral palsy. *J. Pediatr. Orthop.* 17, 392–396.

Mun, K. R., Guo, Z., and Yu, H. (2016). Restriction of pelvic lateral and rotational motions alters lower limb kinematics and muscle activation pattern during over-ground walking. *Med. Biol. Eng. Comput.* 54, 1621–1629. doi: 10.1007/s11517-016-1450-8

Newman, C. J., Walsh, M., O'Sullivan, R., Jenkinson, A., Bennett, D., Lynch, B., et al. (2007). The characteristics of gait in charcot-marie-tooth disease types I and II. *Gait Posture* 26, 120–127. doi: 10.1016/j.gaitpost.2006.08.006

Petrarca, M., Rosa, G., Di Cappa, P., and Patanè, F. (2006). Stepping over obstacles of different heights: kinematic and kinetic strategies of leading limb in hemiplegic children. *Gait Posture* 24, 331–341. doi: 10.1016/j.gaitpost.2005.10.010

Petrarca, M., Rossi, S., Bollea, L., Cappa, P., and Castelli, E. (2011). Patient-centered rehabilitation, three years of gait recovery in a child affected by hemiplegia: case report. *Eur. J. Phys. Rehabil. Med.* 47, 35–47.

Petrarca, M., Zaccara, A., Marciano, A., Della Bella, G., Mosiello, G., Carniel, S., et al. (2014). Gait analysis in bladder exstrophy patients with and without pelvic osteotomy: a controlled experimental study. *Eur. J. Phys. Rehabil. Med.* 50, 265–274.

Rezgui, T., Megrot, F., Fradet, L., and Marin, F. (2013). On the imitation of CP gait patterns by healthy subjects. *Gait Posture* 38, 576–581. doi: 10.1016/j.gaitpost.2013.01.022

Romkes, J., and Brunner, R. (2007). An electromyographic analysis of obligatory (hemiplegic cerebral palsy) and voluntary (normal) unilateral toe-walking. *Gait Posture* 26, 577–586. doi: 10.1016/j.gaitpost.2006.12.010

Schirinzi, T., Sancesario, A., Romano, A., Favetta, M., Gobbi, M., Valeriani, M., et al. (2018). Longitudinal gait assessment in a stiff person syndrome. *Int. J. Rehabil. Res.* 41, 377–379. doi: 10.1097/MRR.0000000000000304

Sienko Thomas, S., Buckon, C. E., Nicorici, A., Bagley, A., McDonald, C. M., and Sussman, M. D. (2010). Classification of the gait patterns of boys with Duchenne muscular dystrophy and their relationship to function. *J. Child Neurol.* 25, 1103–1109. doi: 10.1177/0883073810371002

Sutherland, D. (1997). The development of mature gait. *Gait Posture* 6, 163–170. doi: 10.1016/S0966-6362(97)00029-5

Sutherland, D. H., and Davids, J. R. (1993). Common gait abnormalities of the knee in cerebral palsy. *Clin. Orthop. Relat. Res.* 288, 139–147. doi: 10.1097/00003086-199303000-00018

Thomas, S. S., Moore, C., Kelp-Lenane, C., and Norris, C. (1996). Simulated gait patterns: the resulting effects on gait parameters, dynamic electromyography, joint moments, and physiological cost index. *Gait Posture* 4, 100–107. doi: 10.1016/0966-6362(95)01039-4

Vaughan, C. L. (2003). Theories of bipedal walking: an odyssey. *J. Biomech.* 36, 513–523. doi: 10.1016/S0021-9290(02)00419-0

frontiers | Frontiers in Human Neuroscience

TYPE Brief Research Report
PUBLISHED 20 October 2022
DOI 10.3389/fnhum.2022.907565

OPEN ACCESS

EDITED BY
Carmelo Chisari,
Pisana University Hospital, Italy

REVIEWED BY
Stephane Armand,
Université de Genève, Switzerland
Simone Carozzo,
Sant'Anna Crotone Institute, Italy

*CORRESPONDENCE
Marjolein M. van der Krogt
m.vanderkrogt@amsterdamumc.nl

SPECIALTY SECTION
This article was submitted to Motor Neuroscience, a section of the journal Frontiers in Human Neuroscience

RECEIVED 29 March 2022
ACCEPTED 23 September 2022
PUBLISHED 20 October 2022

CITATION
van der Krogt MM, Houdijk H, Wishaupt K, van Hutten K, Dekker S and Buizer AI (2022) Development of a core set of gait features and their potential underlying impairments to assist gait data interpretation in children with cerebral palsy. *Front. Hum. Neurosci.* 16:907565. doi: 10.3389/fnhum.2022.907565

Development of a core set of gait features and their potential underlying impairments to assist gait data interpretation in children with cerebral palsy

Marjolein M. van der Krogt[1,2]*, Han Houdijk[3,4,5], Koen Wishaupt[1,2], Kim van Hutten[1,5,6], Sarah Dekker[1] and Annemieke I. Buizer[1,2,7] on behalf of the GAIT.SCRIPT study group

[1]Department of Rehabilitation Medicine, Amsterdam UMC, Vrije Universiteit Amsterdam, Amsterdam, Netherlands, [2]Amsterdam Movement Sciences, Rehabilitation & Development, Amsterdam, Netherlands, [3]Department of Human Movement Sciences, Faculty of Behavioral and Movement Sciences, Vrije Universiteit Amsterdam, Amsterdam, Netherlands, [4]Department of Human Movement Sciences, University Medical Center Groningen, University of Groningen, Groningen, Netherlands, [5]Heliomare Rehabilitation Centre, Wijk aan Zee, Netherlands, [6]Basalt Rehabilitation Centre, The Hague, Netherlands, [7]Emma Children's Hospital, Amsterdam University Medical Center, Vrije Universiteit Amsterdam, Amsterdam, Netherlands

Background: The interpretation of clinical gait data in children with cerebral palsy (CP) is time-consuming, requires extensive expertise and often lacks transparency. Here we aimed to develop a set of look-up tables to support this process, linking typical gait features as present in CP to their potential underlying impairments.

Methods: We developed an initial core set of gait features and their potential underlying impairments based on biomechanical reasoning, literature and clinical experience. This core set was further specified through a Delphi process in a multidisciplinary group of experts in gait analysis of children with CP and evaluated on 20 patient cases. The likelihood of the listed gait feature–impairment relationships was scored by the expert panel on a five-point scale.

Results: The final core set included 120 relevant gait feature–impairment relations including likelihood scores. This set was presented in the form of look-up tables in both directions, i.e., sorted by gait features with potential underlying impairment, and sorted by impairments with potential related gait features. The average likelihood score for the relations was 3.5 ± 0.6 (range 2.1–4.6).

Conclusion: The developed set of look-up tables linking gait features and impairments, can assist gait analysts and clinicians in standardized biomechanical reasoning, to support treatment decision-making for gait impairments in children with CP.

KEYWORDS

clinical gait analysis, gait interpretation, impairment focused interpretation, clinical reasoning, interpretation tool, cerebral palsy, rehabilitation, biomechanics

Introduction

Gait analysis is often performed in children with cerebral palsy (CP) to diagnose gait problems, assist in treatment decision making, and to evaluate treatment outcomes, with the goal to improve walking function in daily life. Walking problems occur frequently in children with CP, and gait can be affected in various ways by a multitude of underlying neural and mechanical impairments such as spasticity, muscle weakness, joint or muscle contractures, or bony deformities.

The interpretation of gait analysis data is complex, as it comprises a large amount of information, including qualitative information from videos, quantitative data on kinematics, kinetics and electromyography (EMG), and complimentary data from physical exam and imaging. Gait analysis is a multifaceted and multidisciplinary process, in which all available elements are taken into account and interrelated to understand the origin of the gait problems and decide on the targets for treatment. In literature, there is much focus on gait data acquisition methods such as marker models (Leardini et al., 2017) and reproducibility (McGinley et al., 2009), but the process of interpretation of gait data has deserved far less attention. It has been shown that interpretation can differ substantially between centers, leading to inconsistent treatment recommendations for the same subject (Skaggs et al., 2000; Wright, 2003). Therefore, using standardized methods for data interpretation is important to ensure complete, consistent, transparent and reproducible conclusions from gait analysis (Simon, 2004).

"Impairment focused interpretation" is one standardized way of gait data interpretation (Baker, 2013). This method focuses on identifying neuromechanical impairments underlying gait deviations, which, combined with environmental and personal factors as well as other aspects that may affect walking, are used by the clinician to come to a treatment decision. The suggested process starts with making a complete list of deviating kinematic gait features in a systematic manner, typically done for each leg separately. The next step is to relate these features to each other and to underlying neural or mechanical impairments that explain the gait deviations present. Although this method standardizes the process of neuromechanical reasoning, the second step of combining gait features and linking these to underlying impairments is challenging. Gait features can be related to multiple impairments and the selection of relevant underlying impairments by the assessor is often not explicit, making interpretation subjective and not transparent.

Nevertheless, it is evident that with experience, it becomes easier to identity patterns of gait features that can be caused by a certain impairment, and to identify different potential causes for certain gait deviations. It would be worthwhile to make this expert knowledge more explicit and, combined with literature data, explicitly formulate the potential relationships between gait features and potential impairments. This would not only help novices in acquiring the skill of gait data interpretation, but also allow for better standardization, more transparency, and validation of this process. Therefore, the aim of this study was to develop an explicit core set of gait features and their potential underlying impairments as present in CP, based on literature, biomechanical reasoning and clinical expertise, to support an impairment-focused interpretation approach.

Methods

For this study we chose a modified Delphi approach (Boulkedid et al., 2011), to systematically seek consensus on potential relations between gait features and their possible underlying impairments. The whole process is shown in **Figure 1**.

First, an initial set of gait features and potential underlying impairments was created, based on a combination of literature, own clinical expertise (i.e., a preliminary set drafted for clinical use within Amsterdam UMC) and biomechanical reasoning. Literature was searched for publications that included lists of gait feature–impairment relations, which yielded two papers that contained a substantial number of relations (Armand et al., 2016, Zhou et al., 2017). Furthermore, unpublished course material was used that included a number of possible relations. The gait features included were restricted to kinematic data typically collected in gait laboratories, including 3D motion capture and video gait data of trunk, pelvis, hip, knee and ankle joint and basic foot motion, excluding for instance head and arm motions and more detailed (internal) foot motions. Possible underlying impairments were restricted to

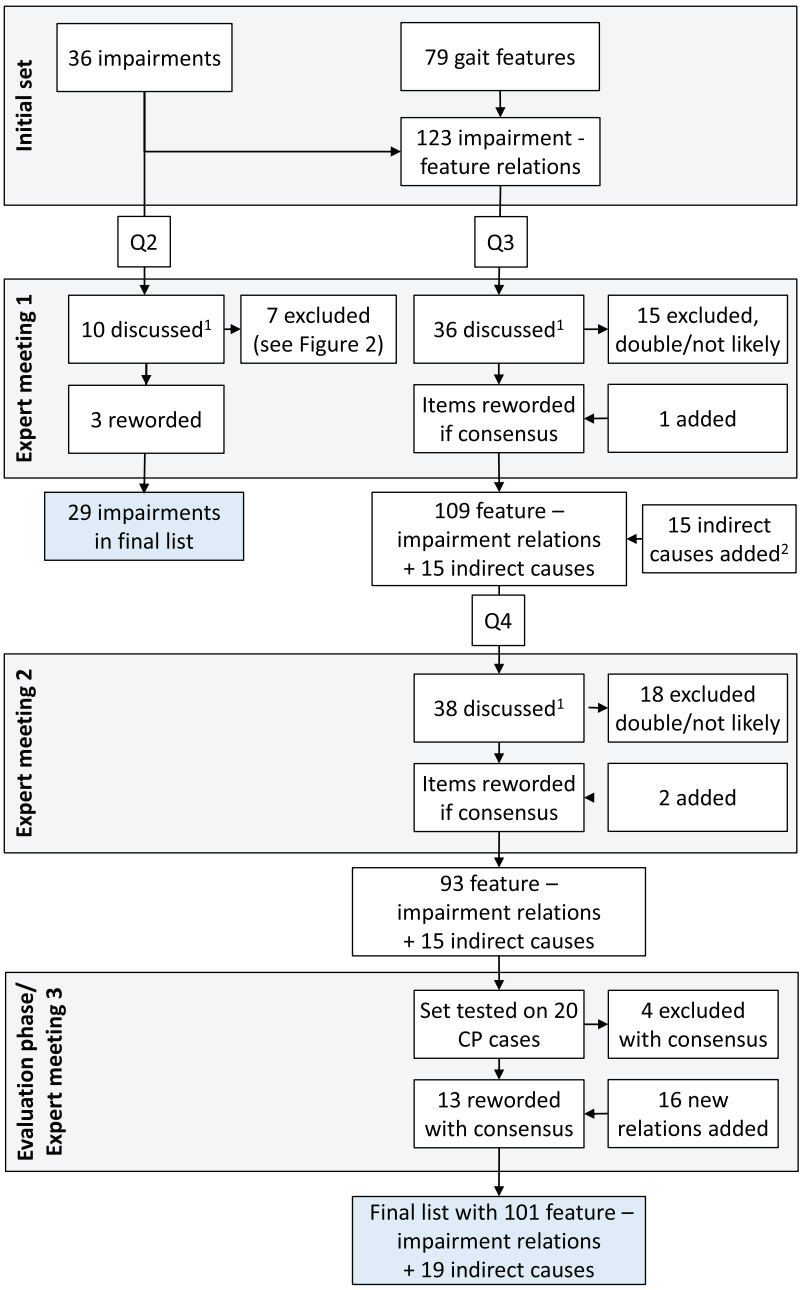

FIGURE 1
Flow chart of the process of questionnaires (Q2-4) and expert meetings. Q1 is not included, as this questionnaire only asked for background and expertise of the panelists. [1]All items with low likelihood scores (< 2, likely not relevant), a large difference between panelists (range > 3, possibly unclear), or that received many comments were discussed. [2]In the list of gait deviations with potential underlying causes, several "indirect causes" were also added, such as secondary effects or compensations (see **Supplementary Appendix A**).

neural and musculoskeletal impairments as often present in CP (i.e., spasticity, contracture, weakness, limited selective motor control, and bony deformities), excluding aspects such as pain, sensory deficits and motivational or psychological factors. Spasticity and contracture of the same muscle were combined into one item, as their effect on gait is difficult to distinguish based on kinematics alone. Feature–impairment relations were mostly defined within the ipsilateral leg, as gait analysis interpretation is typically done for each leg individually. However, clear causes of gait features related to the contralateral leg were included as well. Gait phases were defined following Harlaar (2014), as these include systematic phases and events (instances) in the gait cycle and are most commonly used throughout the Netherlands (see **Supplementary Appendix A**).

Next, a Dutch expert panel was formed for the Delphi process, in which the initial set of gait feature–impairment relations was evaluated and further specified. A total of 24 (pediatric) physiatrists, human movement scientists, physical therapists and gait analysts, with extensive knowledge and experience in pediatric clinical gait analysis, were asked to participate. They came from 10 different centers all experienced in clinical gait analysis. Panelists were selected for being renowned in the field, and/or member of the Dutch/Belgian Society for Movement Analysis Laboratories in the Low Lands (SMALLL) and/or the Netherlands Society of Rehabilitation Medicine (NSRM). For practical reasons, and to ensure all participants were familiar with the impairment focused interpretation approach, all experts were recruited from Dutch clinical centers.

All experts that were willing to participate filled in five digital questionnaires (Q1-5) and participated in three expert meetings (see **Figure 1**). In Q1, experts were asked about their background and experience in clinical gait analysis. In Q2, experts indicated on a 5-point scale how often they thought each impairment from the preliminary set would be present in children with CP (1 = almost never, 5 = very often). In Q3, experts indicated, using the same scale, how often each impairment would coincide with each possible related gait feature from the preliminary gait feature–impairment list. Furthermore, experts could comment in free-text comment fields on the wording or other aspects of each impairment, gait feature and their relation. In expert meeting 1, the results of Q1-3 were discussed, and items were either removed, reworded, or added, based on the consensus (> 70%) of the group.

A few weeks later, experts filled in Q4, in which they were again asked to score the likelihood of the updated gait feature–impairment relations, but now with the order reversed, i.e., grouped by feature. In expert meeting 2, the results of Q4 were discussed, and items removed, reworded or added based on consensus. In case large changes were made in meeting 2, the panelists were asked to score the likelihood of these updated relations.

The resulting set of gait feature–impairment relations was then evaluated for clarity and completeness, using a retrospective data set of 20 children with spastic CP. The children were aged 8.9 ± 3.2 years (range 5–14) and classified as gross motor function classification system (GMFCS) level I (N = 5), II (N = 12), or III (N = 3). For each child, the most affected leg was analyzed. 2D video recordings and 3D gait report were available for all children, as well as EMG and physical examination data. Children had not undergone an orthopedic or neurosurgical procedure in the year before the gait analysis. Written permission for the use of their data for scientific research was given. All cases were interpreted using the developed set of gait features and underlying impairments by an expert pediatric physiatrist and two students educated in clinical movement analysis.

All missing or unclear relations as gathered in this evaluation were discussed with the expert panel in expert meeting 3, held online. Finally, the resulting additional relations were presented to the panel in online questionnaire Q5 to be scored for their likelihood. This procedure resulted in a final set of gait feature–impairment relations, including their likelihood scores based on expert opinions. For each gait feature–impairment relation, the mean, standard deviation, median and range of the likelihood scores were calculated and presented.

Results

Seventeen experts filled in all questionnaires. The final panel consisted of seven physicians, five researchers, and five therapists/gait analysts. Their average age was 48.8 ± 9.0 years (range 32–60), and their experience in clinical gait analysis was 12.4 ± 4.7 years (range 4–18). Nine panelists had experience in performing gait analysis measurements (12.1 ± 4.6 years), while all panelists had experience in gait analysis interpretation (11.8 ± 4.8 years). Fourteen panelists participated in expert meeting 1, 13 in expert meeting 2, and 16 in expert meeting 3.

Figure 1 shows the flow chart describing how items were discussed, reworded, excluded, or added in the expert meetings. **Figure 2** lists the likelihood of all impairments presented in Q2. For the 123 impairment-gait feature relations in Q3, the average likelihood was 3.6 ± 0.8 (median 3.6). The final set as based on Q4 and Q5 consisted of 120 gait feature–impairment relations. These items received an average likelihood score of 3.5 ± 0.6 points (median 3.6, range 2.1–4.6). This final set of all relevant gait feature–impairment relations is presented in **Supplementary Appendix A**, while **Supplementary Appendix B** contains the reversed set with impairment gait feature relations.

Discussion

This study presents the development of a core set of gait features and potential underlying impairments to assist gait analysts and clinicians in standardized clinical reasoning in gait analysis for children with CP. A total of 120 gait feature–impairment relations received consensus on being likely in CP and were included. A unique aspect is that the tables are presented in both directions, e.g., to assist in searching for possible causes for a gait deviation (**Supplementary Appendix A**), or to help find potential gait features related to a specific impairment (**Supplementary Appendix B**).

The developed look-up tables can be used to assist the clinical reasoning process, following the impairment focused interpretation approach (Baker, 2013). After systematically listing all relevant kinematic gait features, the process of relating features to each other and linking these to underlying

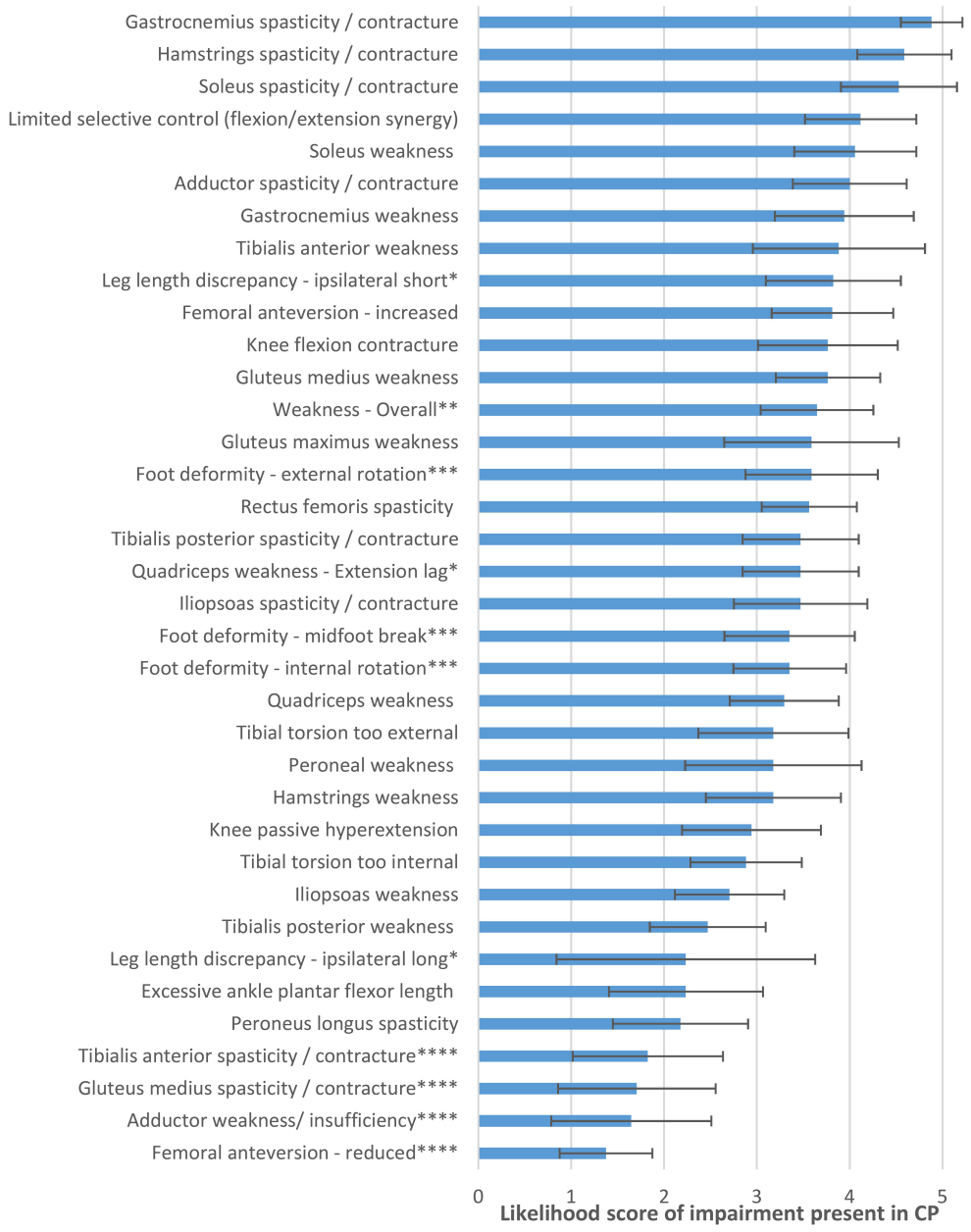

FIGURE 2
Likelihood of impairments being present in CP, as judged by the expert panel in questionnaire 2. *Reworded in final list to "Leg length discrepancy, shortest/longest leg." **Excluded in final list, as too general to be coupled with specific gait features. ***Reworded/combined in final list, to "Foot deformity" only. ****Excluded in final list, as very unlikely in CP.

impairments could take the following stepwise approach, as exemplified in **Figure 3**:

1) From the list of kinematic gait features, one feature is chosen, preferably related to the clinical problem of the patient;
2) Potential underlying impairments for this feature are identified using the table in **Supplementary Appendix A**. One of these is chosen for further consideration (the choice of which is trivial, as all potential impairments will be checked throughout the process);
3) Physical exam data is checked to see whether this impairment was observed in clinical testing;
4) All other gait features that are related to this impairment are looked up using the table in **Supplementary Appendix B**; the more of these features are present in the patient's gait, the likelier it is that the impairment has a large and relevant effect on gait;

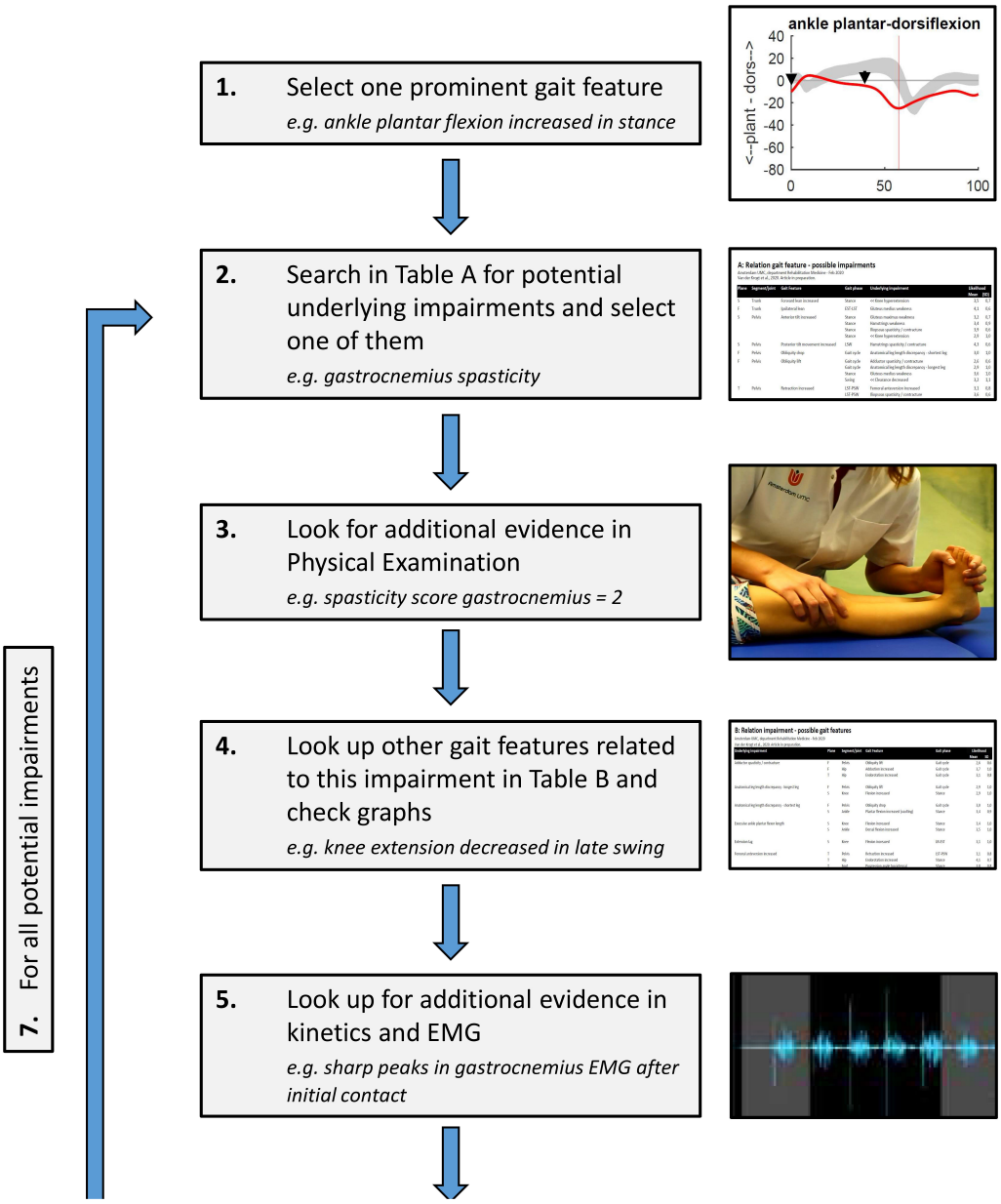

FIGURE 3
Stepwise process of clinical reasoning using the developed look-up tables in **Supplementary Appendixes A**, **B**: (1) One kinematic gait feature is chosen, preferably related to the clinical problem of the patient; (2) A potential underlying impairment is identified using the table in **Supplementary Appendix A**; (3) Physical exam data is checked to see whether this impairment was observed in clinical testing; (4) All other related gait features for this impairment are looked up using the table in **Supplementary Appendix B**; the more of these features are present in the patient's gait, the likelier it is that the impairment has a large and relevant effect on gait; (5) Additional evidence for the role of the impairment during gait is searched in EMG, kinetics, etc. (6) If, based on steps 3–5, the impairment is considered likely, it can be added to the list of impairments affecting gait for the gait report; (7) The process is repeated in an iterative process from step (2) until all possible likely impairments for the selected gait feature are identified. After this, the process is repeated from step (1) for other relevant gait features, until all are solved.

5) Additional evidence for the role of the impairment during gait is searched in EMG data, kinetics, etc.;
6) If, based on steps 3–5 (i.e., the combination of gait features, physical exam data, EMG, kinetics and other supporting data), the impairment is considered likely, it can be added to the list of impairments affecting gait for the gait report.
7) This process is repeated in an iterative process from step (2) until all possible likely impairments for the selected gait feature are identified.

After this, the process can be repeated from step (1) for other relevant gait features, until all are solved. This process results in

an overview of the most likely underlying impairments related to the patient's walking problem, and how these impairments explain the combined features of the abnormal gait pattern.

Clearly, this suggested process is restricted to the neuromechanical approach of gait analysis interpretation. It aims to disentangle potential underlying neuromechanical impairments using a combination of biomechanical gait data with clinical findings, to arrive at potential targets for intervention to enhance walking ability. The initial evaluation on 20 patient cases indicated that the main features and impairments as present in CP were included, helping to perform the impairment-focused interpretation approach in a more systematic manner. Nevertheless, medical decision making can never be fully based on such an interpretation tool only. The decision on which identified underlying impairments are most relevant for the patient's functional walking problems, and which should be treated, is still up to the expert clinician. Moreover other factors beyond the neuromechanical domain should be considered, including environmental and personal factors, as well as factors such as musculoskeletal pain, cognitive impairments, and visual or sensory deficits, that may also play an important role in walking problems.

This proposed process to identify all relevant impairments is intended to improve standardization and transparency of gait analysis interpretation. This opens up possibilities for more automated, computerized identification of features, and the development of software tools that can help to automatically relate these features to all potential underlying impairments. It is an explicit way of reasoning, where all decisions are consciously made by the clinician based on suggestions from the presented core set. This is in contrast to several more "black-box" machine learning approaches as recently proposed (e.g., Lai et al., 2009, Chia et al., 2020; Kidzinski et al., 2020). In future research, it would be interesting to compare the flow of reasoning and outcome of these different approaches, and potentially combine both approaches taking the user decisions into account when training a decision support system using artificial intelligence systems.

Although the look-up tables in this study were developed through a careful systematic process, several specific assumptions and simplifications had to be made throughout. First, it was chosen to combine the impairments spasticity and contractures into one item, as their effect on gait is difficult to disentangle based on kinematics alone. Hence, describing their related gait features separately would merely double the length of the tables with many repetitions. The clinically important distinction which of the two is most prevalent, should be made based on physical examination and/or EMG data. Nevertheless, subtle differences in effects on kinematics may exist between spasticity or contracture of the same muscle, which could be further specified in future studies. Second, although clinically important, more detailed (within-)foot and ankle deviations were not included in the present list to limit the scope, as they can be quite diverse and complex. An extension of the same approach, focusing specifically on foot and ankle deviations, would be a relevant future addition to this core set. Third, gait features were described in a qualitative manner, sometimes with quite broad phases of gait (e.g., all of stance or swing), in order to include all potential deviations over this period. Whether or not a gait feature should be considered abnormal and incorporated in the clinical reasoning process, is still up to the subjective expert view of the assessor. Finally, specific to the Delphi approach taken, the validity of the individual feature–impairment relationship was supported in this study by expert group consensus. For practical reasons and to ensure a somewhat similar tradition of gait data interpretation, it was chosen to perform the Delphi process with a national expert group. Next steps therefore include extension of the expert panel to international experts and include their views on data interpretation, as well as assessing the reliability of the proposed approach, and further validation of individual relationships based on experimental or simulation-based studies.

Conclusion

This study was one of the first that aimed specifically to standardize and support the interpretation process of gait data in children with CP. The developed look-up tables, linking a core set of gait features and impairments based on literature, biomechanical reasoning and expert consensus, supports an impairment focused interpretation approach in a systematic and transparent manner. Future study can build on the developed set of look-up tables, by further assessing their validity and reliability, and by automating the process of gait feature selection and of linking these features to potential underlying impairments.

Data availability statement

The raw data supporting the conclusions of this article will be made available by the authors after request.

Ethics statement

For this study we used video footage and 3D gait reports of clinical gait analysis of children with CP performed during regular medical care. This study design was reviewed and approved by Medical Ethics Committee of Amsterdam UMC, The Netherlands. Written informed consent for their data to be

used in scientific studies was provided by the participants' legal guardians and all children above 11 years of age.

The GAIT.SCRIPT study group

Barbara van Beeten, Christian Greve, Francisca Meuzelaar-Kiezebrink, Henrike van Proosdij, Herwin Horemans, Hurnet Dekkers, Katinka Folmer, Kenneth Meijer, Lenneke van Kats, Lucianne Speth, Marc Nederhand, Marie-Anne Kuiper, Peter Jongerius, and Yvonne Janssen-Potten.

Author contributions

MK, HH, KW, KH, SD, and AB contributed to the conception and design of the study. SD and KW processed and organized the data and performed the statistical analysis. MK and SD wrote the final draft of the manuscript. All authors contributed to manuscript revision, read, and approved the submitted version.

Acknowledgments

We thank Lieke Mulder and Justine Jacobs for their help in interpreting the retrospective patient cases and the GAIT.SCRIPT study group for their contribution throughout the Delphi process.

Conflict of interest

The authors declare that the research was conducted in the absence of any commercial or financial relationships that could be construed as a potential conflict of interest.

Publisher's note

All claims expressed in this article are solely those of the authors and do not necessarily represent those of their affiliated organizations, or those of the publisher, the editors and the reviewers. Any product that may be evaluated in this article, or claim that may be made by its manufacturer, is not guaranteed or endorsed by the publisher.

Supplementary material

The Supplementary Material for this article can be found online at: https://www.frontiersin.org/articles/10.3389/fnhum.2022.907565/full#supplementary-material

References

Armand, S., Decoulon, G., and Bonnefoy-Mazure, A. (2016). Gait analysis in children with cerebral palsy. *EFORT Open Rev.* 1, 448–460. doi: 10.1302/2058-5241.1.000052

Baker, R. W. (2013). *Measuring Walking: A Handbook of Clinical Gait Analysis*. London: Mac Keith Press.

Boulkedid, R., Abdoul, H., Loustau, M., Sibony, O., and Alberti, C. (2011). Using and reporting the Delphi method for selecting healthcare quality indicators: a systematic review. *PLoS One* 6:e20476. doi: 10.1371/journal.pone.0020476

Chia, K., Fischer, I., Thomason, P., Graham, H. K., and Sangeux, M. (2020). A decision support system to facilitate identification of musculoskeletal impairments and propose recommendations using gait analysis in children with cerebral palsy. *Front. Bioeng. Biotechnol.* 8:529415. doi: 10.3389/fbioe.2020.529415

Harlaar, J. (2014). Phases of gait and gait events: some redefining. *Gait Posture* 39, S100–S101. doi: 10.1016/j.gaitpost.2014.04.138

Kidzinski, L., Yang, B., Hicks, J. L., Rajagopal, A., Delp, S. L., and Schwartz, M. H. (2020). Deep neural networks enable quantitative movement analysis using single-camera videos. *Nat. Commun.* 11:4054. doi: 10.1038/s41467-020-17807-z

Lai, D. T., Begg, R. K., and Palaniswami, M. (2009). Computational intelligence in gait research: a perspective on current applications and future challenges. *IEEE Trans. Inf. Technol. Biomed.* 13, 687–702. doi: 10.1109/TITB.2009.2022913

Leardini, A., Belvedere, C., Nardini, F., Sancisi, N., Conconi, M., and Parenti-Castelli, V. (2017). Kinematic models of lower limb joints for musculo-skeletal modelling and optimization in gait analysis. *J. Biomech.* 62, 77–86. doi: 10.1016/j.jbiomech.2017.04.029

McGinley, J. L., Baker, R., Wolfe, R., and Morris, M. E. (2009). The reliability of three-dimensional kinematic gait measurements: a systematic review. *Gait Posture* 29, 360–369. doi: 10.1016/j.gaitpost.2008.09.003

Simon, S. R. (2004). Quantification of human motion: gait analysis-benefits and limitations to its application to clinical problems. *J. Biomech.* 37, 1869–1880. doi: 10.1016/j.jbiomech.2004.02.047

Skaggs, D. L., Rethlefsen, S. A., Kay, R. M., Dennis, S. W., Reynolds, R. A., and Tolo, V. T. (2000). Variability in gait analysis interpretation. *J. Pediatr. Orthop.* 20, 759–764. doi: 10.1097/01241398-200011000-00012

Wright, J. G. (2003). Pro: interobserver variability of gait analysis. *J. Pediatr. Orthop.* 23, 288–289. doi: 10.1097/01241398-200305000-00002

Zhou, J., Butler, E. E., and Rose, J. (2017). Neurologic correlates of gait abnormalities in cerebral palsy: implications for treatment. *Front. Hum. Neurosci.* 11:103. doi: 10.3389/fnhum.2017.00103

Frontiers in
Human Neuroscience

Bridges neuroscience and psychology to understand the human brain

The second most-cited journal in the field of psychology, that bridges research in psychology and neuroscience to advance our understanding of the human brain in both healthy and diseased states.

Discover the latest Research Topics

See more →

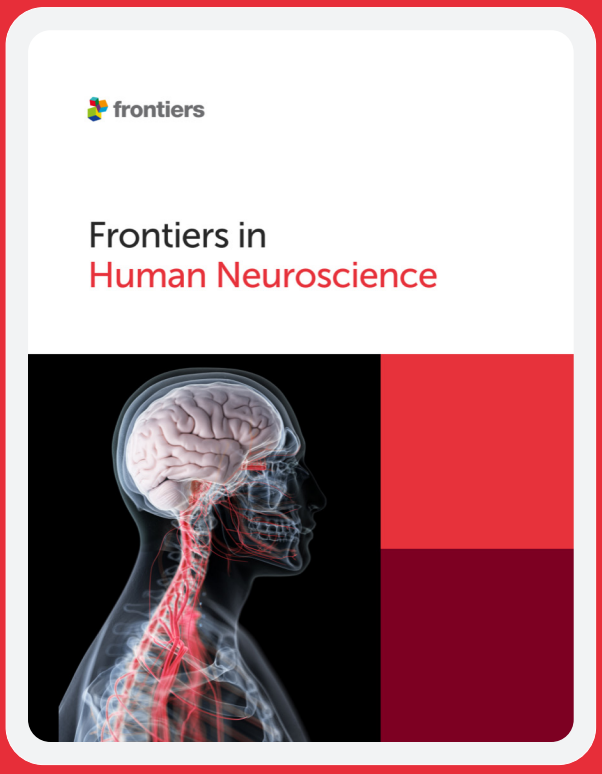

Frontiers

Avenue du Tribunal-Fédéral 34
1005 Lausanne, Switzerland
frontiersin.org

Contact us

+41 (0)21 510 17 00
frontiersin.org/about/contact